SCALE-UP IN EMULSION POLYMERISATION

Alan James Merry

This thesis is submitted for the degree of

Doctor of Philosophy

The University of Aston in Birmingham

September 1980

TO

MY

MUM AND DAD

Acknowledgements

I am indebted to the following;

The British tax payers who through the Ministry of Defence provided financial support,

The technicians and staff of the Department of Chemical Engineering of the University of Aston for their invaluable assistance,

Mr. G. Bagg of the Ministry of Defence for his helpful advice,

Ms. C. Hollings for her patience,

And last but not least Ms. P. Howson for typing the manuscript.

Summary

The procedure for successful scale-up of batchwise emulsion polymerisation has been studied. The relevant literature on liquid-liquid dispersion, on scale-up and on emulsion polymerisation has been critically reviewed.

Batchwise emulsion polymerisation of styrene in a specially built 3 litre, unbaffled, reactor confirmed that impeller speed had a direct effect on the latex particle size and on the reaction rate. This was noted to be more significant at low soap concentrations and the phenomenon was related to the depletion of micelle forming soap by soap adsorption onto the monomer emulsion surface.

The scale-up procedure necessary to maintain constant monomer emulsion surface area in an unbaffled batch reactor was therefore investigated. Three geometrically similar vessels of 152, 229 and 305 mm internal diameter, and a range of impeller speeds (190 to 960 r.p.m.) were employed. The droplet sizes were measured either through photomicroscopy or via a Coulter Counter. The power input to the impeller was also measured. A scale-up procedure was proposed based on the governing relationship between droplet diameter, impeller speed and impeller diameter.

The relationships between impeller speed, soap concentration, latex particle size and reaction rate were investigated in a series of polymerisations employing an amended commercial recipe for polystyrene. The particle size was determined via a light transmission technique.

Two computer models, based on the Smith and Ewart approach but taking into account the adsorption/desorption of soap at the monomer surface, were successful in predicting the particle size and the progress of the reaction up to the end of stage II, i.e. to the end of the period of constant reaction rate.

Key words: Emulsion, Polymerisation, Dispersion , Scale-up.

CONTENTS

FIGURES

CHAPTER 2

CHAPTER 3

CHAPTER 4

TABLES

APPENDICES

1.0 INTRODUCTION

1.0 INTRODUCTION

This project was part of a commercial development programme for the production via batchwise emulsion polymerisation of a styrene-butadiene rubber latex. The recipe for this SBR was fixed by specification and the product was required to meet certain physical property criteria amongst which was latex particle size. Thus there was a requirement to study a commercial non-ideal system and procedure, an approach which is atypical of much of the published research in this field which commonly adopts simple systems and high purity reagents.

Emulsion polymerisation is a process which has been used commercially for many years in the production of synthetic rubber latices. Such latices find a variety of uses in, for example, adhesives, tyre manufacture, foamed rubbers, paint and paper.

As a commercial process emulsion polymerisation offers a number of advantages over the alternative processes of bulk, solution and suspension polymerisation. For example, emulsion polymerisation is unique amongst these in allowing the formation of high molecular weight polymers whilst requiring short reaction time. The emulsion polymerisation process also offers operational advantages owing to the normally low viscosity of the process fluid which clearly leads to easier handling of the product fluid, and better control of heat transfer during reaction.

Often, particularly for specialist materials or for small-scale production, emulsion polymerisation is carried out batchwise in jacketed reactors which are either stainless steel or glass lined. To assist the mixing and heat transfer characteristics of the vessel it is normal to include baffles in the design of a batch reactor. One problem with emulsion polymerisation, however, is the tendency for internal surfaces including heat transfer surfaces to become coated with polymer and the presence of baffles clearly would heighten cleaning problems. There has developed an

interest, therefore, in the carrying out of emulsion polymerisation in unbaffled vessels. This leads to a problem in design owing to the fact that unbaffled vessels have in the past received scant attention from workers in the field of scale-up. Even without this added complication, scale-up of emulsion polymerisation plant entails considerable difficulty and areas of inconsistency, and indeed the normal procedure for scale-up of such plant in the past appears to have been one of trial and error with alterations being made to the composition of the recipe to compensate for inadequacies in the scale-up procedure.

The basic components in a typical recipe for emulsion polymerisation are: monomer or monomers, soap and a water soluble initiator (although many commercial recipes contain electrolytes as well). These are charged into the vessel which is then purged with an inert gas (when there are gaseous monomers, they are charged after purging) before the contents are agitated and brought to the reaction temperature. The agitation results in the emulsification of the monomer forming an emulsion which is stabilised by the adsorption of soap molecules onto the monomer/aqueous phase interface. Of the soap not adsorbed, a proportion exists in aqueous solution in a monomolecular form whilst the rest exists as uniform aggregates of soap molecules, known as micelles, which are also in aqueous solution. The classical theory for the mechanism of emulsion polymerisation suggests that the micelles solubilise by concentrating dissolved monomer at their centres. Entry of initiator radicals into the micelles initiates polymerisation of the monomer therein. More monomer diffuses from the emulsified monomer droplets, which merely act as a monomer store, to sustain the reaction. Eventually the monomer/polymer mixture in the micelle increases in volume to the point where the micelle identity is destroyed and a polymer particle emerges. Beyond the point at which all available micelles have been initiated no further polymer particles are

formed, nor are any destroyed. Polymerisation continues at a constant rate, which is proportional to the number of polymer particles, until the monomer reservoir in the droplets is exhausted and the rate then falls progressively to zero at total conversion.

Obviously there are a number of aspects relating to the scale-up of a batch process such as emulsion polymerisation. For example, the most obvious are, perhaps, heat transfer and power requirements for agitation. The key aspect of scale-up, that is the aspect that directly affects the reaction time and latex particle size for emulsion polymerisation, has, however, remained undefined.

Inspection of the classical theory of emulsion polymerisation suggests that control of the initial monomer emulsion surface area should be the key to successful scale-up. The reason for this is that by adsorbing soap onto its surface, the degree of monomer dispersion clearly will affect the number of soap molecules available in solution to form micelles. The number of micelles, of course, will determine the number of polymer particles formed, and hence the reaction rate. Thus the initial degree of monomer dispersion dictates the reaction rate and final latex particle size. The requirement, therefore, of this project was to study the control of the degree of initial monomer dispersion and its relevance to the number and final size of the latex particles and to the progress of the reaction and to scale-up.

2.0 LITERATURE SURVEY.

2.1 An introduction to emulsion polymerisation.

2.2 Droplet size studies.

2.3 Scale-up.

2.0 LITERATURE SURVEY

At the centre of this study of scale-up in emulsion polymerisation is the investigation of the effect that the initial degree of monomer dispersion, i.e. formation of the monomer emulsion, has upon the progress of the emulsion polymerisation reaction. Accordingly, in order to gain an insight into the phenomenon of dispersion the literature pertinent to emulsification has been reviewed.

Clearly, in order to investigate the effect that the degree of monomer dispersion has upon the progress of the reaction it is also necessary to gain an appreciation of the general emulsion polymerisation process. Literature relating to the basic mechanisms and mathematical models which have been proposed for emulsion polymerisation have, therefore, been reveiwed.

It is apparent that a successful scale-up of an emulsion polymerisation process must include the appropriate scale-up of the monomer dispersion process. The complete emulsion polymerisation scale-up procedure, however, is many faceted with scale-up of the monomer dispersion process being but one aspect of it. The complete scale-up procedure must provide appropriate measures to account for a variety of specific phenomena relating to heat transfer, mass transfer and power input requirements. Clearly a full study of scale-up is beyond the scope of this study alone and the literature survey has reflected this approach and has, therefore, concentrated upon topics in scale-up which are of particular interest to the study of scale-up of the monomer dispersion process.

The chapter is concluded with a survey of the few papers directly relevant to scale-up in emulsion polymerisation.

2.1 An introduction to emulsion polymerisation

The commercial production of a synthetic polymer may be performed by any of four basic processes; bulk polymerisation, solution polymerisation, suspension polymerisation and emulsion polymerisation. These processes differ in terms of the physical form in which the monomer is held during the polymerisation and although the loci of polymerisation may differ, the chemistry of polymerisation is common to all four processes[1]. Before describing these processes, therefore, it is perhaps useful to briefly discuss the general chemical mechanism of polymerisation.

Classically, polymerisation occurs in three distinct steps; initiation, propagation and termination.

i) Initiation

In order to initiate polymerisation a source of free radicals is required. This source may take the form of an inorganic salt such as potassium persulphate in aqueous solution, or organic compounds, for example organic peroxides. In the general case, if the monomer molecule is designated M and the free radical $R^{\cdot}$, then initiation is represented by

$$M + R^{\cdot} \rightarrow MR^{\cdot}$$

ii) Propagation

During propagation the polymer molecule grows by the addition of further monomer molecules.

$$(nM)R^{\cdot} + M \rightarrow ((n+1)M)R^{\cdot}$$

Due to the asymmetric nature of some monomer molecules, for example styrene ($C_6H_5CH = CH_2$), the polymer chain has the option[2] either to grow in a head to tail fashion:-

$$(C_6H_5CH - CH_2 - R)^{\cdot} + C_6H_5CH = CH_2$$

$$\rightarrow (C_6H_5CH - CH_2 - CH(C_6H_5) - CH_2 - R)^{\cdot}$$

or in a head to head fashion:-

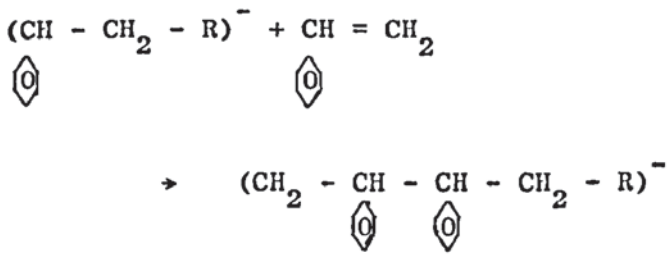

iii) Termination

Termination occurs upon the interaction of two growing polymer chains. Two forms of termination are thought possible[2], recombination and disproportionation.

Recombination results when two growing polymer chains combine to form one inactive polymer molecule.

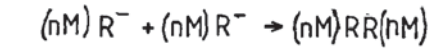

Disproportionation occurs when two growing polymer chains combine to form two inactive polymer molecules.

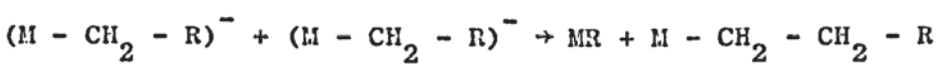

A further method of termination is possible, this being known as chain transfer. This is effected by the use of a chain transfer agent such as tertiary dodecylmercaptan (TDM). The chain transfer agents, on terminating growth of a polymer chain, form a new free radical. If the chain transfer agent is designated T, then

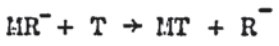

It is now possible to proceed to a description of the major polymerisation processes.

Bulk Polymerisation[1]

As the name suggests, this process involves the addition of initiator to a volume of monomer. The reaction is generally exothermic which obviously suggests that the temperature must be controlled and

typically the reaction is carried out in a batch vessel. Major problems associated with heat transfer and agitation may occur due to the high viscosities encountered as the polymerisation proceeds.

An additional drawback of bulk polymerisation, which is shared with solution and suspension polymerisation, is that the molecular weight of the polymer is an inverse function of the initiator concentration. If, therefore, a high molecular weight product is required, then a low initiator concentration would be required, which would also result in a low rate of polymerisation.

Solution Polymerisation[1]

In solution polymerisation, the monomer is dissolved in a suitable solvent, which will often be an organic liquid. A major advantage of this technique is the reduction of the very high viscosities encountered in bulk polymerisation and hence there is a considerable improvement in heat transfer.

Suspension Polymerisation[1]

Suspension polymerisation involves the dispersion of monomer in an aqueous phase which usually contains a soap in solution. The soap allows easy dispersion of the monomer, into a fine dispersion of droplets, under the influence of agitation. The soap also stabilises this dispersion. The initiator is soluble in the organic monomer and polymerisation, therefore, occurs within the droplets and the polymer is produced in particle form in aqueous suspension. The size of the polymer particles depends, of course, upon the size of the monomer droplets. The great advantage of this type of polymerisation is the extremely efficient heat transfer medium offered by the aqueous phase.

Emulsion Polymerisation

Again, emulsion polymerisation involves the dispersion of the

monomer into an aqueous phase which is usually a soap solution. In this case, however, the initiator is water soluble and generally the polymerisation occurs in loci remote from the monomer droplets. There is considerable debate concerning the true mechanism involved here and this is discussed in further detail in the following sections.

In addition to good heat transfer characteristics offered by the aqueous phase, it is also possible to obtain both a high molecular weight product and a high reaction rate simultaneously.

2.1.1. A physical picture of emulsion polymerisation

Although patents for emulsion polymerisation processes had been filed as early as 1927[3], it was not until the Second World War, when there was a need for synthetic rubber, that emulsion polymerisation was studied in any detail. The immediate post war years saw the publication by Harkins[4] of the first qualitative model for the mechanism of emulsion polymerisation, closely followed by the first quantitative model published by Smith and Ewart[5]. Refinements to these models and alternative ones were to follow but the models of Harkins[4] and Smith and Ewart[5] are still widely recognised as fundamentally valid, and it is considered useful here to firstly outline this commonly held picture of emulsion polymerisation.

A typical basic recipe[6] for emulsion polymerisation consists of one or more monomers, water, soaps and a water soluble initiator. The soap is usually present in concentrations exceeding a critical concentration, which is dependent upon the type of soap and is known as the critical micelle concentration (c.m.c.). Soap molecules added in excess of this concentration form aggregates[7], called micelles, which have the ability to solubilise, or concentrate the dissolved monomer at their centres, and thus increase the apparent solubility of the monomer. The reaction is generally recognised to proceed through

three stages[8], as shown in figure 2.1. Sometimes before the initiation of stage I, an induction period, where no apparent polymerisation occurs, is observed. This is believed to be due to oxygen contamination.

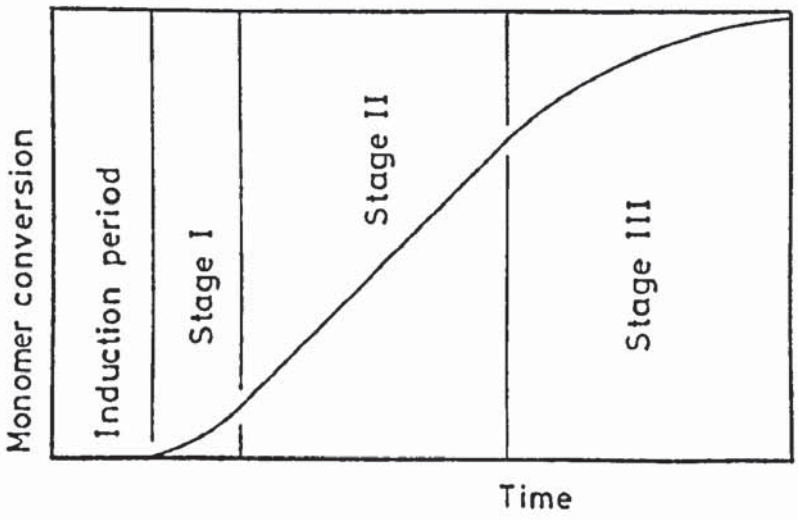

Fig 2·1 An expected typical emulsion polymerisation reaction rate curve. The stages through which the reaction passes are shown

Stage I

This is the period during which polymer particles are generated. The reaction suggested to occur during this stage are represented by figure 2.2a.

Harkins[4] suggested that the micelles are the principle loci of particle generation but the exact loci has been the subject of a number of theories and these will be discussed in detail in section 2.1.2.

At the end of stage I, the rate of particle generation falls to zero, as according to Harkins, all the original micelles have now either become the loci of polymerisation or their constituent molecules have been adsorbed onto the growing polymer particles. When the micelles

are totally depleted, the loci for further particle generation is lost and thus, at this point, the particle population reaches a maximum. The particle population is assumed to remain constant, at this maximum, for the remainder of the reaction[5].

Stage II

This stage is characterised by a constant conversion rate and, as indicated in figure 2.2b, three phases exist; the aqueous phase, the monomer drops and the growing polymer particles which are swollen by monomer dissolved in the polymer. During this stage monomer diffuses from the monomer droplets, through the aqueous phase to the polymer particles, to replace monomer used in the polymerisation. The ratio of monomer/polymer in the particles remains constant whilst a free monomer reservoir exists in droplet form, hence the end of Stage II is characterised by the total depletion of the monomer drops.

Stage III

The physical representation of the system in the final stage, stage III, is shown in figure 2.2c. Here only the monomer swollen polymer particles exist and the reaction proceeds until the total monomer is polymerised. A characteristic of stage III is a falling reaction rate as the monomer/polymer ratio decreases.

2.1.2. Loci of particle generation

With the general description of the emulsion polymerisation process in mind it is useful to proceed to a discussion of the various theories regarding the loci of particle generation. Two main theories on the loci of particle generation have been put forward; the micellar theory and the oligomeric theory.

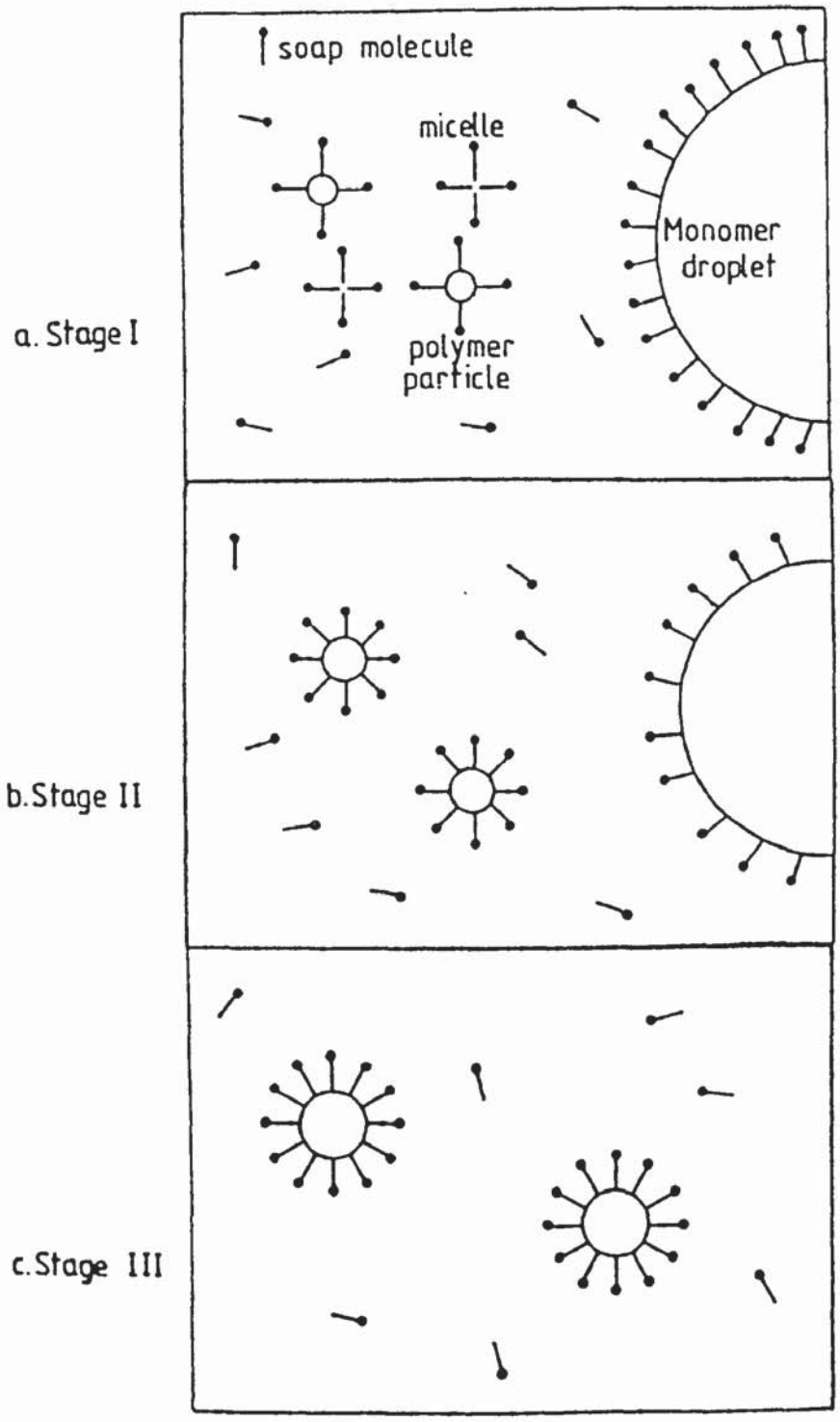

Fig 2·2 Pictorial representation of an emulsion polymerisation system during the three reaction stages.

Harkins[4] first formulated the micellar theory which was developed during his involvement in the wartime interest in emulsion polymerisation. Harkins[4] based his model on the experimental observations that the concentration of soap in the aqueous phase reduced rapidly as the polymer yield increased and that increasing the initial soap concentration decreased the final particle size. The model proposes that during stage I of the reaction, the principal loci of the particle generation are micelles. It is assumed that initiator radicals enter micelles and initiate polymerisation of the monomer therein. More monomer diffuses into the micelles to continue the growth of the polymer chain. Eventually the micelles lose their identity as the polymer mass grows into microscopic polymer particles stabilised by a monomolecular layer of soap adsorbed into their surface. There comes a point at which the total particle surface area becomes large enough to adsorb all the soap of the uninitiated micelles. Micelles, therefore, completely disappear. At this point, generation of particles ceases and the reaction proceeds to stage II. It is implicit, in Harkins'[4] model, that the final particle population is a function of the micelle population which in itself is a function of the initial soap concentration and the critical micelle concentration.

The micellar mechanism of particle generation can not, of course, explain the observations that polymerisation can occur with soap concentrations below c.m.c. or even in the total absence of soap. In explanation of this, Harkins[4] recognised the possibility of particles being generated in the aqueous phase as well as in the micelles. He claimed, however, that the number of particles generated in this way is negligible in the presence of soap in the concentrations employed for commercial polymerisations at that time (0.2 molar). Harkins gave

no detailed description of this alternative mechanism of particle generation. Roe[9], however, suggested such a mechanism for particle generation in the aqueous phase and, in contradiction of Harkins[4], he claimed that his mechanism was the principal one for particle generation even in the presence of soap. In Roe's[9] model, particle generation is assumed to result from the interaction of monomer molecules and initator radicals in free solution, rather than within the micelles. The active monomer radicals so formed react with further dissolved monomer molecules until the growing polymer chain, the oligomer, becomes too large to remain in solution. At this point, the growing polymer chain precipitates from solution forming a polymer particle. To explain the experimental observation of the effect of soap concentration on the particle population, Roe[9] proposed that when a particle is precipitated, it must, in order to retain its identity, be stabilised by soap molecules. Hence, increasing the soap concentration would mean that a greater number of particles are able to retain their identity and thus the final particle population would decrease. In this case the particle population is a function of the initial soap concentration and the monomer surface area only. The value of the c.m.c. and the presence of micelles are incidental.

In contrast to Roe[9], Goodhall et al[10] agreed with Harkins'[4] micellar model for particle generation in the presence of a soap. To explain the case of polymerisation where soap is absent, however, they suggested two possible mechanisms. The first applies to relatively soluble monomers, such as methyl methacrylate, and the second to relatively insoluble monomers, such as styrene. The first model is similar to that model presented by Roe[9], except that the ability of particles to retain their identity is no longer a function of the soap present, as the soap concentration in this case is zero. The second

mechanism involved the proposal of a considerably different model. In this case, it was suggested that oligomers once formed, assume an increasingly surfactant role until a point is reached at which the oligomers themselves form micelles. From this stage onwards, normal micellar generation occurs.

2.1.3. Kinetics of emulsion polymerisation

With regard to the kinetics of the reaction, stage I and stage II have received the most attention, there having been a number of kinetic models published. Without exception, the kinetics of stage I and stage II have been treated separately, the emphasis in stage I being on the number of particles generated whilst the rate of conversion is the subject of kinetic study in stage II.

2.1.3.1. Stage I

Smith and Ewart's[5] treatment of stage I involved prediction of the number of polymer particles generated. Two idealised situations were considered, one of which was anticipated to present an overestimate of the number of particles formed, and the other an underestimate. The first case assumed simply that all the free radicals generated were captured by micelles, leading to the equation:

$$\frac{dNp}{dt} = \rho' \qquad (2.1)$$

where ρ' = rate of radical generation per cm^3 of water ($s^{-1}.cm^{-3}_{H_2O}$)

Np = number of polymer particles per cm^3 of water ($cm^{-3}_{H_2O}$)

t = time (s)

Equation 2.1 was integrated and solved for time t_I, the time at which the micelles disappear. This yielded the following equation.

$$N_p = \rho' t_I = 0.53\ (\rho'/\mu)^{2/5}\ (a_s S)^{3/5} \qquad (2.2)$$

where μ = volumetric growth rate of a particle ($cm^3 . s^{-1}$)

a_s = specific adsorption area of a soap molecule ($cm^2 . molecule^{-1}$)

S = the total amount of soap per cm^3 of water ($molecules . cm^{-3}$)

The second situation is "that in which a given interfacial area always has the same effectiveness in collecting free radicals regardless of the size of the particle on which it is situated"[5]. This is expressed by:

$$\frac{dN_p}{dt} = \rho' \frac{A_m}{A} \qquad (2.3)$$

where A_m = surface area presented by the micelles ($cm^2 . cm^{-3}_{H_2O}$)

A = total interfacial area ($cm^2 . cm^{-3}_{H_2O}$)

Integration of equation 2.3, and evaluation of $t = t_I$ yielded the following equation.

$$N_p = 0.37\ (\rho'/\mu)^{2/5}\ (a_s S)^{3/5} \qquad (2.4)$$

Equation 2.4 is directly comparable to equation 2.2 except that the constants differ. Equation 2.2 was thought by Smith and Ewart[5] to predict a larger number of particles than would actually be formed and equation 2.4 to predict fewer. In later work, in fact, Gardon[11] developed a model based on similar assumpions as equation 2.4 and found that rather than it being an under estimate, it gave particle numbers in good agreement with experimental values.

Gardon's[12] notation was slightly different to Smith and Ewart's[5], and for stage I he presented the following expression which is mathemat-

ically similar to equation 2.4 presented by Smith and Ewart[5].

$$N_p = 0.208\ S_1^{0.6}\ (\rho'/k)^{0.4} \qquad (2.5)$$

where $S_1 = a_s\ S$

$k = 3\mu/4\Pi$

Another expression presented by Harada et al[13] shows a different dependence of N_p on initiator and soap concentrations.

$$N_p \propto (\rho/\mu)^{2/7}\ S_m^{5/7} \qquad (2.6)$$

where S_m is the emulsifier concentration available to form micelles.

Equation 2.6 is a condensation of the latter of two equations presented by Harada et al[13] for two limiting conditions.

1) When initiator radicals generated in the aqueous phase enter preferentially into micelles rather than into polymer particles. This is equivalent to the first idealised situation considered by Smith and Ewart[5]. For this case Harada et al[13] presented;

$$N_p = \left(\frac{2\rho'}{M_o k}\right)^{2/5} \left(\frac{Sm}{k_v}\right)^{3/5} \qquad (2.7)$$

where $k_v = (36\Pi/(1-\phi_w)^2\ a_s^3\ \rho_p^2)^{1/3}$

$$k_H = \frac{k_p\ M_{pc}\ M_w}{M_o\ N_A}$$

M_o = initial monomer concentration

M_{pc} = concentration of monomer in polymer particles at saturation.

M_w = molecular weight of monomer

ρ_p = density of polymer

ϕ_w = weight fraction of monomer in polymer particles

2) In this case, the radicals are considered to preferentially diffuse into polymer particles rather than into micelles. The equation presented was;

$$N_p = K_v^{-3/7} \left(\frac{\Pi K_H M_o}{8}\right)^{2/7} (\rho'/E)^{2/7} \delta_o^{5/7} \qquad (2.8)$$

where $E = k_2 M_m / k_1$

k_1 = Rate of constant of formation of polymer particles

k_2 = "Rate constant"

M_m = Aggregation number of micelles.

As may be seen, a number of complexities have been introduced by Harada et al[13] in order to model more closely the kinetic behaviour in stage I of the reaction.

Smith and Ewart[5], Gardon[11] and Harada et al[13] each claimed that their particular kinetic model for stage I was in reasonable agreement, and in the case of Harada et al[13], "excellent", agreement with experimental data. Although Smith[14] claimed that the Smith and Ewart models gave a reasonable prediction of the number of particles generated in stage I, examination of his results indicate that Smith[14] was obviously working to lower standards of accuracy than Harada et al[13]. For example, using equation 2.4, which was anticipated to give an underestimate, Smith[14] predicted the number of particles generated to be 10^{15} per cubic centimetre of water. The corresponding experimental results were in the range 5×10^{14} to 10^{15} per cubic centimetre of water. It is interesting to note that equation 2.2, anticipated to yield an overestimate, predicts for the same conditions a value of 1.43×10^{15} for the number of particles generated.

Gardon[12] was a little vague in his claims of accuracy for his model, which it was claimed predicted the number of particles generated

to be in the range 10^{12} to 10^{15} particles per cubic centimetre of water. He concluded that this was in reasonable agreement with experimental values. Experimental values were not, however, published for comparison although Gordon[12] did comment on the difficulties of measuring the diameter of very small particles, and the resultant lack of accuracy of experimentally determined values of the number of particles generated.

Harada et al[13] claimed that the Smith and Ewart[5] model when applied to the system used in Harada et al's[13] study over predicted the number of particles formed by a factor of two. The data presented by Smith[14], however, clearly shows that for that particular case at least, the Smith and Ewart prediction of N_p could be claimed to predict exactly the value, or to overestimate it by a factor of up to two. Obviously the accuracy of the experimental data renders claims of exact agreement, or even agreement to within a factor of two, unrealistic.

Harada et al[13] have presented sparse experimental data but they appear to have worked to remarkable degrees of accuracy. Indeed, agreement between their experimental data and model predictions for the number of particles generated are excellent, whilst the predictions of the Smith and Ewart model are shown to be a factor of two larger. As, however, the methods used by Harada et al[13] and Smith[14] appears to have varied only in the definition of the mean diameter used, this is no reason to expect Harada et al[13] to have significantly greater accuracy in their results.

Each of the above three groups of workers used similar methods to determine the number of particles present in a latex. From electron micrographs of the latex a value of the mean particle diameter was obtained. From this, the volume of the particles was calculated and from a knowledge of the total volume of polymer present, the value

of N_p was calculated. However, each worker used a different definition of the mean particle diameter.

Smith[14] it appears, used the linear mean diameter, i.e.

$$\bar{d}p_L = \frac{\Sigma n_i d_i}{\Sigma n_i} \qquad (2.9)$$

Gardon[12], however, claimed that the root mean cube diameter should be used, i.e.

$$\bar{d}p_{r.m.c} = \left(\frac{\Sigma n_i d_i^3}{\Sigma n_i}\right)^{1/3} \qquad (2.10)$$

Harada et al[13] used the volume mean diameter, i.e.

$$\bar{d}p_v = \frac{\Sigma n_i d_i^4}{\Sigma n_i d_i^3} \qquad (2.11)$$

If it is assumed, however, that latices prepared by emulsion polymerisation are largely monodisperse, as has been reported[14] [15], then each of the three different definitions for mean droplet diameter should yield similar results. It is only when a polydisperse sample is analysed that the way in which mean particle diameter is defined would become significant.

2.1.3.2. Stage II

Smith and Ewart[5] considered three theoretical cases in the development of the kinetics of stage II. Each of these cases, as indeed do all the general models for stage II, make the fundamental assumption that particle population remains constant after the end of stage I.

Case One

In this case the situation for which the average number of radicals per particle is small compared to unity is considered. The physical picture represented by this

assumption is that radicals may diffuse freely out of as well as into the particles.

Case Two

Here, the situation where the average number of radicals per polymer particle is approximately 0.5 is considered. This represents the physical picture in which radicals cannot leave the particles once they have entered and that termination of chain growth only occurs when a second radical enters. Termination is assumed instantaneous on entry of the second radical.

Case Three

Finally, the situation where the average number of radicals is large compared with unity was considered. This represents the case for which termination is not instantaneous on entry of the second radical and a particle may thus contain any number of radicals.

Smith and Ewart[5] claimed that the case two model gave the best agreement with experimental data. Indeed, it was the case two model that was to become generally accepted as describing stage II kinetics[2].

As already outlined, the basic concept behind the case two model is that each successive radical that enters a polymer particle either initiates polymerisation or, if there is an active growing chain already within the particle, it terminates polymerisation. This termination is assumed to be instantaneous on entry of the second radical. Hence over a period of random radical entry into a particle, that particle will have contained a growing radical for fifty per cent of the time. At any one time it may be assumed that fifty per cent of the radicals are active or that each particle contains 0.5 radicals. The validity of this assumption has not been universally accepted. Gardon[11], for instance, indicated that it was only valid whilst the polymer particle

remained small. Van der Hoff[16] proposed that when particle diameter exceeded 0.12 μm then the termination of polymerisation is not instantaneous on the entry of the second radical and thus the average radical concentration exceeds 0.5.

A further assumption in the Smith and Ewart[5] model is that the monomer concentration in each particle remains constant during stage II of the reaction. This assumption is based upon the theory that as monomer in the particles polymerises, monomer from the droplets diffuses through the aqueous phase to be dissolved in the polymer particles. The quantity of monomer dissolved in the polymer is maintained at saturation, thus maintaining a constant monomer/polymer ratio, so long as monomer droplets exist to supply monomer to the reaction sites. This assumption has been supported experimentally[12].

The reaction rate per unit volume of aqueous phase was presented by Smith and Ewart for case II as:

$$\frac{dM}{dt} = k_p M_{pc} N_p \left(\frac{1}{2}\right) \qquad (2.12)$$

where $\left(\frac{1}{2}\right)$ is the average number of radicals per particle.

Gardon[11] developed a rate equation for stage II that was effectively the same as the Smith and Ewart model although Gardon[11] used volumetric rather than molecular concentrations, i.e.:

$$\frac{dp}{dt} = \left(\frac{kp}{N_A}\right) \cdot \left(\frac{\rho m}{\rho p}\right) N_p \, \phi_v \, Q \qquad (2.13)$$

where p = volume of polymer per unit volume of water

ρ_m = density of monomer

ϕ_v = monomer volume fraction

Q = average number of radicals per particle

The presence of the parameter Q in equation 2.13 should be noted.

This parameter was used by Gardon[11] as he concluded that a value of 0.5 for the average radical concentration per particle was valid only for the case of small particles.

2.1.3.3. Stage III

The kinetics of Stage III have, to some extent, been overlooked by many researchers in the field of emulsion polymerisation. Gardon[11] [17] however, discussed the limitations of applying the assumptions of the Smith and Ewart model to a kinetic model of Stage III.

In Stage III, the monomer concentration within the particles falls and termination is "known to be a diffusion controlled process"[11]. As conversion increases a gel is reported to form within the particles slowing diffusion and hence slowing the rate of termination. It would be expected, therefore, that the rate of reaction during stage III, would, in practice, decrease less rapidly than as would be predicted by applying an incremental solution of the Smith and Ewart Stage II model.

2.1.3.4. Oligomeric Model

Roe[9] theoretically considered the kinetics of the oligomeric particle generation with surfactant present, postulating that the Smith and Ewart kinetics for micellar particle generation would suitably model polymerisation in a system where the soap had a low c.m.c. In such cases, Roe[9] reasoned, the point at which newly generated particles failed to find sufficient soap molecules to stabilise them, a point which marked the end of stage I, tended to coincide with the disappearance of the micelles. However, for cases where the concentration of soap was below c.m.c. and the c.m.c. of that soap was large, experimental results did not agree with the Smith and Ewart[5] kinetics. Roe[9] did not postulate kinetics for this case but merely suggested that it would probably be necessary to

introduce some account of the relationship between soap adsorption and stability.

2.1.3.5. Min and Ray[8] Model

Min and Ray[8] have developed a complex kinetic model for emulsion polymerisation which takes into account a number of factors that other models have disregarded. For example, such factors as:

1) The formation of polymer particles by both micellar and oligomeric generation.
2) The possibility that radicals may desorb from the polymer particles.
3) The fact that polymer particles may be stabilised by both emulsifier and polymer chain ends.
4) The existence of a mechanism for particle coagulation and breakage.
5) The gel effect within the polymer particle.
6) A polymer particle structure that may be non uniform.
7) Modelling of aqueous phase polymerisation (i.e. oligomer formation in aqueous solution) as a contribution to the total polymerisation rate.
8) Modelling of the particle size distribution and its influence on the behaviour of the polymerisations.

The complete model is complex, necessitating the use of a computer for solution of the component equations. This model will, therefore, not be reproduced here.

Min and Ray[8], however, claim that by making a number of assumptions, their model may be simplified to various levels until by applying enough assumptions their model becomes, effectively, the Smith and Ewart model. There have been no published comparisons between the Min and Ray[8] model, at any level

of complexity, and experimental results. It is, therefore, impossible to say if their model is able to predict, with any greater accuracy than existing models, the progress of an emulsion polymerisation reaction.

2.1.4. Droplet Polymerisation

The models described in the preceding section are based upon the assumption that the mechanism for particle generation is that involving micelle or oligomer generation and this is assumed to be complete at the end of stage I of the reaction. It is then assumed that the main loci of polymerisation during Stage II of the reaction are the polymer particles. A further possibility exists, however, that alongside this mechanism, polymerisation may occur within the original monomer droplets. Ugelstad et al[18] [19], for instance, claimed that under particular circumstances the droplets could become the major loci of polymerisation. They noted that for a suitable emulsifier system (in their case a mixture of sodiumhexadecylsulphate and hexadecanol was used) the initial monomer emulsion would be very fine, with droplet sizes of 1.8 μm to 0.7 μm being mentioned. It was also observed that a combination of fine dispersions and high monomer to aqueous phase ratios, such as 0.5, resulted in adsorption of most of the soap onto the surface of the drops. For example[18] under conditions as described above, of an initial soap concentration of 2.13 $g.dm^{-3}$, 2.06 grams of this soap were adsorbed onto the monomer droplets. Thus, Ugelstad et al[19] claimed that the droplets presented a sufficiently large surface area to become competitive in initiator radical capture, and hence it was possible for the droplets to become the principal loci of polymerisation.

Ugelstad et al[19] presented convincing photomicrographic evidence in support of the above theory. The photomicrographs of latices

prepared over a range of degrees of initial monomer dispersion clearly show;

1) Monodisperse latices of relatively small particle diameter as would be expected from emulsion polymerisation.

2) Relatively coarse polydisperse latices with particles of a similar size to the initial monomer dispersions.

3) A number of intermediate mixtures of 1 and 2.

In attempting to model this polymerisation Ugelstad et al[19] suggested that the kinetics of polymerisations where the principal loci of polymerisation is in the droplets, are similar to the Smith and Ewart[5] case 3, i.e.,

$$\frac{dM}{dt} = K_p M_p \rho'^{1/2} \left(\frac{V}{2 k_t}\right)^{1/2} \qquad (2.14)$$

where k_t = termination rate constant

V = droplet volume

M_p = monomer concentration at reaction site (i.e. within droplets)

This was suggested as Ugelstad et al[19] concluded from their work that the number of radicals per droplet would be greater than one. as in case three.

An obvious difference between emulsion polymerisation and droplet polymerisation is that the former exhibits a constant rate period (stage II) when the monomer concentration at the reaction site remains constant. This assumption of constant monomer concentration does not hold for droplet polymerisation, as the monomer concentration falls continuously throughout the course of the reaction owing to the build up of polymer within the droplet. Although theoretically a difference would be expected between the reaction rate curves for droplet and

emulsion polymerisation, it is difficult in practice to say purely from observation of kinetic data, which type of polymerisation has occurred. An examination of both the initial monomer dispersion and the final particle size distribution would be required.

2.1.5. Effect of Stirring on Emulsion Polymerisation

A full appreciation of the effects of agitation speed on the progress of and the product from emulsion polymerisation has been largely overlooked in studies of emulsion polymerisation. The need for some form of agitation in order to disperse the monomer, and to aid heat transfer and diffusion has always been recognised but the view of many workers is that the degree and indeed type of agitation was not significant. In small-scale laboratory preparation, for instance, a common method employed in emulsion polymerisation is that of charging the ingredients into a bottle and then tumbling this bottle end-over-end in a water bath. Obviously, this process has little, if anything, in common with commercial scale polymerisation which is generally carried out in reactors agitated by an impeller.

A few workers have, however, recognised the important role of stirring. For example, Shunmukhan et al[24] noted that by increasing the agitation they decreased the polymerisation rate and increased the induction time (i.e. the time lag before polymerisation is perceived to occur). Schoot et al[25], in a letter commenting on Shunmukhan et al's[24] paper suggested that the increased induction time may have been a result of inhibition by traces of oxygen in the nitrogen atmosphere used. The increase in the inhibition, it was suggested was due to better mass transfer between the gas and liquid phases at higher levels of agitation.

Further to this, Evans et al[26], after carrying out a number of

polymerisations at different impeller speeds, noted that the rate of polymerisation of vinylidene chloride decreased with increased agitation. They assumed the micellar model for particle initiation and from it they deduced that the micelle population was a function not only of the original soap concentration but also of the amount of soap adsorbed onto the surface of the monomer droplets, which, of course, is a function of the surface area of the monomer dispersion which is itself dependent upon the degree of agitation.

Omi et al[27] appeared to support this conclusion in that they showed that it was the level of agitation at the start of the reaction which affected the reaction rate during the later stages, suggesting that once the initial monomer dispersion had been formed, the impeller speed could be altered without any noticeable effect on the reaction rate. This appears to support Evans et al's[26] proposal that the reaction rate is affected by the amount of soap lost to the reaction by adsorption onto the monomer/aqueous interface.

The most recent and comprehensive study of the effect of stirring on emulsion polymerisation appears to be that of Nomura et al[28] who studied the effect of stirring on both reaction rate and inhibition.

The studies of inhibition of styrene polymerisations were carried out under nitrogen atmospheres of differing purity, of which the most impure was commercial grade nitrogen of 99.9% purity. The results, Nomura et al[28] concluded, indicated that the degree of inhibition was influenced by two factors, the purity of the nitrogen and the degree of agitation. The induction period was seen to increase as the stirring rate was increased or as the purity of the nitrogen was decreased.

Studies of the effects of stirring on the reaction rate were carried out under the more pure nitrogen atmosphere, and it was particularly noted that, for low initial soap concentrations, (near

the c.m.c.) the reaction rate decreased with increased stirring rates, a conclusion which is consistent with the observations of Evans et al[26] and Omi et al[27]. As initial soap concentrations were increased, however, the effect of stirring generally became less marked, within certain limits of impeller speed.

The work of Nomura et al[28] is of particular interest in that, as well as noting the previous effects of stirring, they observed a number of other effects of changing impeller speed on the progress of the polymerisation reaction which were not associated with soap adsorption or inhibition. Omi et al[27] had noted that impeller speed affected the early stages of the reaction, but once the generation of particles was complete the impeller speed had little or no effect on the progress of the reaction. Nomura et al[28] agreed with this observation but showed that this was only true if the impeller speed was retained within certain limits. Outside this given range of impeller speeds a reduced reaction rate was experienced. The upper and lower limits of this range were explained via two different phenomena.

In explanation of the lower limit of this range, it was suggested that at low impeller speeds the free soap concentration reduced during the reaction owing to adsorption onto the ever growing polymer particle surface. The dispersion of monomer droplets thus became unstable, which led to droplets coalescing and a reduction in the surface area of the monomer dispersion. The reaction rate under these conditions would, below a critical monomer interfacial area, become area controlled, i.e. it would become controlled by the rate which monomer could diffuse from the droplets.

The upper limit of the range was explained by the suggestion that at high impeller speeds the high levels of shear break down the stabilising monomolecular soap layer on some of the polymer particles

which then coagulate, thus reducing the number of particles and consequently the number of reaction sites.

As may be judged by the preceding survey, in contrast to the debate on reaction mechanisms there appears to have been a general consensus, among the papers reviewed, that the level of agitation can, under certain conditions, significantly affect the rate of polymerisation and the polymer particle population.

2.1.6. Latex Particle Size Analysis

An important characterisation of a latex is its particle size. It is a significant latex property in its own right but it is also closely linked with the reaction rate. It was this characteristic, therefore, that was central to the current investigation.

As part of their investigations into emulsion polymerisation a number of workers have measured the diameters of submicromic final latex particles using a variety of techniques including electron microscopy, light scattering, light transmission and soap titration. These techniques are outlined below.

Soap Titration[25]

This technique is based upon the concept that in the presence of sufficient soap, an interface (specifically the surface of the polymer particles in the application to latices) would become saturated with a monolayer of soap molecules, each of which would occupy a specific area. The procedure, therefore, involves firstly ensuring that the soap concentration in the latex is less than that required to saturate the surface of the particles. Soap is then titrated until the c.m.c. is reached. This point may be recognised by measuring, for example, the conductivity of the latex or its surface tension. The difference between the c.m.c. with particles present and the c.m.c. in the absence of the particles is thus recorded as the amount of soap adsorbed onto the surface of the polymer particles. Knowledge of the specific

surface area of the soap molecule and the total volume of polymer would allow calculation of the mean particle diameter.

Electron Microscopy

Size analysis is carried out by measuring the diameter of images of the polymer particles formed on an electron micrograph. Though this seems a simple and obvious technique of analysis problems have been encountered in its use owing to the deformation of the polymer particles in the electron beam[21], but methods of overcoming this problem have been suggested. It is possible, for example, to harden the particles by bromination although this can lead to an increase of apparent diameter of up to nine per cent[21]. Gold shadowing[20] is another technique used to improve the quality of electron micrographs. Obviously, it is not possible to take direct electron micrographs of the latex; samples have to be carefully prepared by drying, washing and redrying as well as the coating and mounting of the sample.

Light Scattering[20]

Light scattering is based upon the measurement of the angle between a beam of incident light and either the angle of maximum or minimum intensity of scattered light. The angular dependence of intensity depends upon the relative refractive indices of the polymer particles and the solution in which they are suspended, and upon the size of the particles and the wavelength of the light.

Light Transmission

This technique is based upon measuring the turbidity of a dilute latex[22] [23]. A typical and useful approach is that of Barnes and La Mer[23] who presented a technique for measuring the particle size and concentration of colloidal dispersions based upon the Mie theory of light transmission. The technique involves calculation of a theoretical scattering coefficient, K, for various values of the

parameter α ($\alpha = 2\pi r/\lambda$, where r is the particle radius and λ the wavelength of light). Calculation of K involves knowledge of the complex refractive indices of both the particles and the suspending medium.

The particle radius and concentration are estimated by comparing a theoretical curve with an experimental curve. Firstly the theoretical curve of log K against log $\alpha/2$ is plotted and then measured values of log (log I_o/I) against log $1/\lambda$ (I_o = incident light, I = transmitted light) are plotted on the same axis as the theoretical curve. The particle size is estimated from the displacement along the abscissa required to superimpose the maxima on the experimental curve onto the corresponding maxima on the theoretical curve as;

$$\log \alpha - \log 1/\lambda = \log 2\pi r \qquad (2.15)$$

The particle concentration is estimated from the ordinate required for superposition of the maxima, viz;

$$\log K - \log (\log I_o/I) = -\log \left(\frac{2\pi r^2 n l}{2.3}\right) \qquad (2.16)$$

where l = cell length

n = particle number concentrations

Barnes and La Mer[28] applied their technique to the measurement of the particle size and concentration of a number of sulphur sols. The accuracy of their results were not discussed nor were the results obtained compared with those from any other technique. One significant effect was, however, discussed. It was reported that the time taken to obtain a complete set of data was of the order of two hours due to the number of transmission readings taken at different wavelengths. During this time, the transmission reading fluctuated, due, it was presumed, to sedimentation of the sample. Hence, a number of rapid

key readings were made over the full range of wavelengths to be used. When all the data had been collected the resulting curve was corrected to fit the key readings.

Of more direct use to the current study is the approach followed by Bateman et al[27] who presented a similar technique, but in this case the subjects of their analysis were polystyrene latices. A table of the theoretical values of K at eight selected values of λ and over a range of particle radii was presented for polystyrene latices. A comparison of results obtained by light extinction and electron microscopy showed good agreement with deviations of two to four per cent.

As this technique had been developed specifically on polystyrene, it was the obvious choice for polymer particle size analysis in this project. The application of this technique is described further in section 3.8.

2.2 Droplet Size Studies

Emulsion droplet size is a signficant factor in emulsion polymerisation owing to the fact that the initial step in any emulsion polymerisation is the dispersion of the organic monomer into the inorganic continuous phase. It is a premise of this thesis that the initial degree of dispersion will affect the final polymer particle size, by virtue of the amount of soap adsorbed onto the droplet/aqueous interface which would thus be removed from the soap available for micelle formation. As micelles are considered to be the loci for latex particle initiation it follows that a high specific surface area of the monomer may well lead to a reduced number of initiated particles. In order, therefore, to reproduce particle population, and thus particle size, during scale-up it is vital to successfully reproduce the degree

of dispersion. In order, therefore, to assist the identification of the appropriate scale-up factors for dispersion the literature pertinent to the prediction of emulsion droplet size has been reviewed.

The majority of published literature in the field of droplet size prediction, whether presenting empirical or theoretical correlations, relate specifically to baffled vessels and surfactant free systems. Only two studies of systems containing surfactant[24] [29] appear to have been published. Studies of unbaffled vessels appear in one paper only[30] and even in this system the effect of swirl, and the vortex were suppressed by the absence of a gas/liquid interface.

A great deal of work has been reported for baffled vessels and much of this work, and the most important correlations relating to it, are discussed in the following sections. Though these may not be of direct use to the current study it is clear that problems relating to the analysis technique and reproducibility of the results apply equally well to unbaffled systems as they do to baffled systems.

2.2.1. Theoretical Considerations

In 1941, Kolmogoroff[31] [32] presented his theory of isotropic turbulence which was to become a cornerstone in the field of liquid/liquid dispersions. The original papers have since been reviewed by a number of workers, of which Batchelor[33] appears to have been the first.

Batchelor[33] carried out a full mathematical treatise on Kolmogoroff's theory, but it is perhaps better to refer to his description of "Kolmogroff's basic notion" in order to obtain an understanding of the theory.

The theory of isotropic turbulence suggests that when considering the smallest eddies, within a turbulent field at high Reynolds numbers, the structure of the turbulence is independent of the type of flow.

The motion due to these eddies of limited size is conceived to be totally random, showing no preference for any particular direction, that is, the motion is isotropic.

Two limiting processes are recognised within this range of eddies. Providing the Reynolds number is large the influence of viscosity on the larger eddies of the range is negligible, their motion being determined solely by the amount of energy which they continually pass on to smaller eddies. This quantity of energy is the local mean energy dissipation due to turbulence. The smaller eddies continually dissipate a considerable proportion of the energy they receive through the action of viscosity, the motion of the very smallest eddies being entirely laminar. This leads to the deduction that the motion due to eddies of less than a certain limiting size in an arbitrary field of turbulence is determined uniquely by two quantities, the kinematic viscosity and the local mean energy dissipation per unit mass of fluid.

Shinnar and Church[34] applied the Kolmogoroff theory to the analysis of liquid/liquid dispersion in agitated vessels and developed expressions relating to droplet breakup and coalescence. The following expression was derived, by Shinnar and Church[34], for the case of droplet breakup where the drop diameter is greater than the microscale of turbulence (η), and where, therefore, breakup is caused mainly by inertial effects.

$$\rho \varepsilon^{2/3} d^{5/3} / \sigma_i = \text{constant} \qquad (2.17)$$

where ρ = the fluid density

ε = the local energy dissipation per unit mass of fluid

d = the droplet diameter

σ_i = the interfacial tension.

The microscale of turbulence is defined as

$$\eta = \nu^{3/4} \varepsilon^{-1/4} \tag{2.18}$$

where ν = the kinematic viscosity

Hinze[35] also applied Kolmogoroff's theory to emulsification in turbulent flow and derived an expression identical to equation 2.17, thus supporting Shinnar and Church[34].

Shinnar[36] also presented an expression for the droplet breakup for the case where the drop diameter is less than the microscale of turbulence. Such a condition prevails if "σ_i is very small or ν is rather large", and in this case viscous shear is the predominant cause of droplet breakup. The expression presented was:

$$\frac{\mu_c \varepsilon^{-1/2} d}{\nu_c^{1/2} \sigma_c} = \phi\left(\frac{\mu_d}{\mu_c}\right) \tag{2.19}$$

where μ_c = the viscosity of the continuous phase

μ_d = the viscosity of the dispersed phase

ν_c = the kinetic viscosity of the continuous phase

ϕ = a "certain function"

No further expansion of equation 2.19 was presented and it may only be assumed that the function ϕ is dependent on the properties of the system.

For coalescence of drops Shinnar and Church[34] developed the following general expression.

$$\varepsilon^{-1/4} d \rho^{3/8} / A(h_o)^{3/8} = \text{constant} \tag{2.20}$$

$A(h_o)$ is a dimensionless force with a numerical value equal to the energy of adhesion between two spheres of unit diameter separated by a distance h_o.

Shinnar and Church[34] suggested that for "high Reynolds numbers" the local energy dissipated may be approximated by the average energy dissipation per unit mass for the entire vessel, $\bar{\varepsilon}$. Shinnar and Church[34] did not define further the limits of their high Reynolds number range, later experimentation by other workers[37] [38] [39], however, has shown this assumption of homogeneous energy dissipation to be invalid for Reynolds numbers up to 1×10^5 in baffled vessels. There appears, however, to be no published evidence for homogeneity of energy dissipation at higher Reynolds numbers, and thus Shinnar and Church's[34] hypothesis can not be ratified.

Based on the assumption of homogeneity Shinnar[36] developed special cases of equation 2.17 and 2.20 for baffled vessels by use of an equation developed by Rushton[40] (equation 2.21) relating energy dissipation to impeller characteristics.

$$\bar{\varepsilon} = k_1 N^3 D^2 \tag{2.21}$$

Hence on combination of equation 2.21 with equation 2.17 for breakup and 2.20 for coalescence the following equations were obtained:

Droplet breakup;

$$\left(\frac{d}{D}\right) = k_2 \left(\frac{N^2 D^3 \rho}{\sigma_i}\right)^{-0.6} \tag{2.22}$$

Droplet coalescence;

$$d = k_3 N^{-0.75} D^{-0.5} \rho^{-3/8} A(h_o)^{3/8} \tag{2.23}$$

The above equations are valid only at Reynolds numbers greater than 1×10^5. These two equations bear comparison with published experimental results for baffled vessel systems as may be noted in figure 2.3.

No special cases of equations 2.17 and 2.20 have been developed for unbaffled vessels.

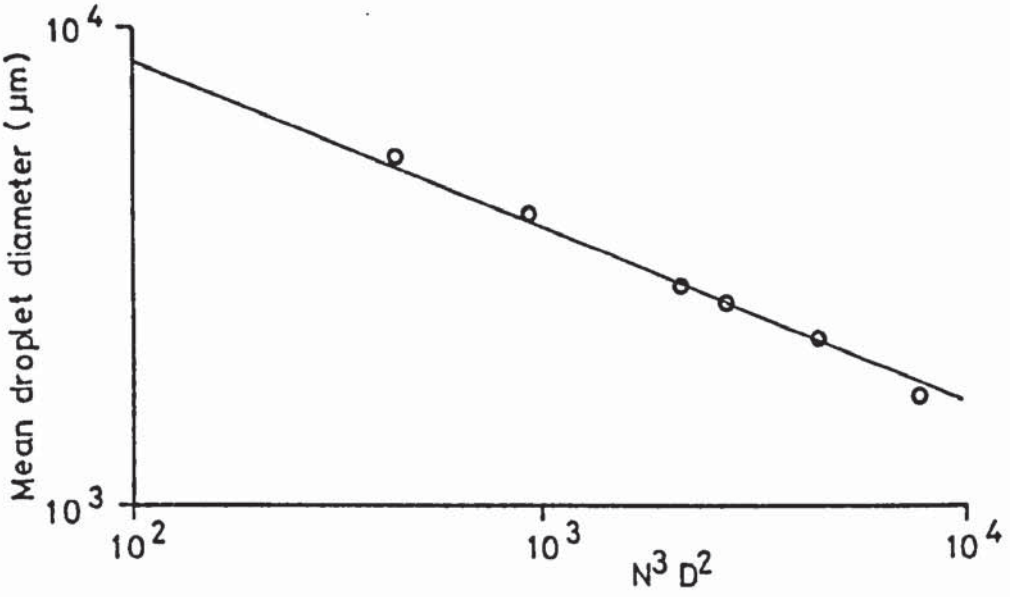

Fig 2·3 Logarithmic plot of Vermeulen's data for the case where droplet break-up controls droplet size. Gradient = -0·4

2.2.2. Empirical Relationships: Baffled Systems

In the past twenty five years a number of workers have studied liquid/liquid dispersions in either baffled vessels or in vessels where the vortex has been suppressed by eliminating the gas/liquid interface. The correlations stemming from this work can, in the main, be represented by one common form which was first presented by Vermeulen et al[41].

$$\frac{\bar{d}_s}{D} = \text{const. } f(\phi). \left(\frac{N^2 D^3 \rho}{\sigma_i}\right)^{-0.6} \qquad (2.24)$$

where $f(\phi)$ is a function of the dispersed phase hold up

$\bar{d}_s$ is the surface mean diameter (or Sauter mean) which is defined by

$$\bar{d}_s = \frac{\Sigma n_i d_i^3}{\Sigma n_i d_i^2} \qquad (2.25)$$

Table 2.1 shows the values of the constant and $f(\phi)$ presented by various workers. This equation (2.24) is directly comparable with the theoretically derived equation for droplet breakup (equation 2.22).

Worker	$f(\phi)$
Calderbank[47]	$1+3.75\phi$ (for $D/D_t = 2/3$)
	$1+9\phi$ (for $D/D_t = 1/3$)
Scully [58]	$1+3.3\phi$
Brown and Pitt[45]	$1+3.14\phi$
Mylnek and Resnik[49]	$1+5.4\phi$
Coulaloglou[37]	$1+4.47\phi$

Table 2.1 Functions of ϕ

The exponent presented in equation 2.24, i.e. -0.6, was not generally the exact exponent obtained by regression analysis but as these results were close to the theoretical value of -0.6, and the mean errors involved ranged from 5 to 15% all the final correlations were presented in the form of equation 2.24. The systems used, upon which equation 2.24 was based, were of low organic/water phase ratios, less than 0.4, but generally less than 0.3 and in some cases as low as 0.05. These conditions were employed to avoid excessive coalescence.

Roger et al[42], however, correlated data for a baffled system with an organic/water phase ratio of 0.5, conditions for which

coalescence is thought to control the mean drop size. They presented an equation of the form

$$a = \frac{k}{D} \left(\frac{D^3 N^2 \rho_c}{\sigma_i}\right)^{0.36} \left(\frac{D}{D_T}\right)^{k_1} \left(\frac{\nu_d}{\nu_c}\right)^{1/5} \left(\frac{t}{t_o}\right)^{1/6} \exp\left(3.6\frac{\Delta\rho}{\rho c}\right) \phi \quad (2.26)$$

where a = the specific interfacial area

D = the impeller diameter

D_T = the vessel diameter

t = the settling time

t_o = a reference settling time (usually unity)

By substituting $a = 6\phi/\bar{d}_s$ the above equation may be rewritten as

$$\bar{d}_s = \frac{D}{k_2} \left(\frac{D^3 N^2 \rho_c}{\sigma_i}\right)^{0.36} \left(\frac{D}{D_T}\right)^{k_1} \left(\frac{\gamma}{\gamma_c}\right)^{1/5} \left(\frac{t}{t_o}\right)^{1/6} \exp\left(\frac{3.6\Delta\rho}{\rho c}\right)^{-1} \quad (2.27)$$

where k_1 is a function of the Weber number and was found by Roger et al[42] to lie in the range 0.75 to 1.4.

Shinnar and Church[34] compared their theoretically derived equation for predicting droplet size under conditions of coalescence (equation 2.23) with the correlation presented by Roger et al[42]. However, Shinnar and Church reported Roger et al's correlation as,

$$\bar{d}_s = \frac{1}{k} N^{-0.72} D^{-0.08} \rho c^{-0.36} \sigma_i^{0.36} \left(\frac{\gamma_d}{\gamma_c}\right)^{1/5} \left(\frac{t}{t_o}\right)^{1/6} \exp\left(\frac{3.6\Delta\rho}{\rho_c}\right) 0.71 \exp\left(0.35\frac{D}{D_o}\right)^{-1} \quad (2.28)$$

where D_o is the diameter of a reference impeller.

As presented, equation 2.28 relates specifically to geometrically similar vessels, that is, vessel geometry is not a variable of the correlation, as it is in the form presented as equation 2.27 and thus the term $(D/D_T)^{k_1}$ is absorbed into the constant. The notable

difference between equation 2.27 and 2.28 is that the latter has an additional term, 0.71 exp (0.35 D/D_o), the reason for which Shinnar and Church[34] failed to explain.

In comparing equation 2.28 with the theoretical equation 2.23, Shinnar and Church[34] suggested that a number of terms were comparable, as shown in table 2.2.

2.23 (Theoretical)	2.28 (Empirical)
$N^{-0.75}$	$N^{-0.72}$
$A\ (h_o)^{3/8}$	$(\frac{\gamma_d}{\gamma_c})^{1/5}\ (\frac{t}{t_o})^{1/6}\ \sigma_i^{3.6}$
$D^{-0.5}$	$D^{-0.08}\ 0.71 \exp (0.35\ D/D_o)$

Table 2.2. Comparison of terms in the equations of Shinnar and Church, and Roger et al (After Shinnar and Church)

The comparisons were not discussed in detail, but graphical evidence, in the form of a plot of $\bar{d}_s$ against $N^3\ D^2$ showing data from Roger et al was used as supporting evidence that the two equations were comparable. (see Figure 2.4).

The difference between the correlation of Roger et al[42] and equations presented by other workers, of which Vermeulen et al's[41] is an example (equation 2.24) may be explained in terms of the balance between droplet breakup and coalescence. Equations of the Vermeulen type are consistent with the theoretical equation for the case where drop size is governed by droplet breakup., and therefore apply to poorly coalescing systems. The equation of Roger et al[42] however, has been compared with the theoretical equation for the

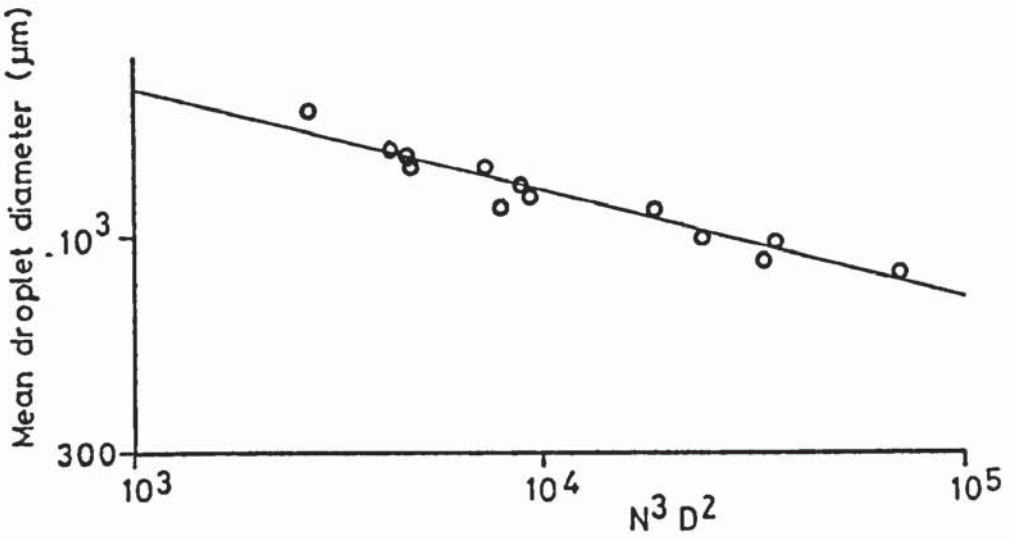

Fig 2·4 Logarithmic plot of Roger et al's data for the case where droplet coalescence controls droplet size. Gradient = -0·25 (After Shinnar and Church)

case where droplet size is controlled by coalescence, and therefore applies to strongly coalescing systems.

2.2.3. Empirical Relationships: Unbaffled Vessels

Although a number of papers have been published on studies of emulsification in baffled vessels, unbaffled vessels have been severely neglected. Weinstein and Trebal [30] appear to be the only workers who have published results of studies on emulsification under unbaffled conditions, although in their case the vortex was suppressed by exclusion of a gas/liquid interface to eliminate the effects of swirl. Their correlation was based on a modification of the general theoretical equation for the case of droplet breakup (equation 2.17) as was presented by Hinze[35] and takes the form

$$\bar{d}_s = 10^{c_1+c_2\phi}\ \nu_c^{c_3}\ \bar{\epsilon}^{c_4}\ \left(\frac{\sigma}{\rho_c}\right)^{c_5} \qquad (2.29)$$

Values of $\bar{\epsilon}$, the energy dissipated per unit mass, were calculated from power input correlations published by Laity and Treybal[43], which

showed the following relationship for vortex free unbaffled systems:

$$\bar{\varepsilon} = N^3 D^2 \cdot \text{const} \qquad (2.30)$$

Equation 2.30 is directly comparable to the relationship for baffled vessels presented as equation 2.31. Therefore, on substitution of equation 2.30 into equation 2.29, the following expression is obtained.

$$\bar{d}_s = f(\phi)\ \nu_c^{c_3}\ (N^3 D^2)^{c_4}\ \left(\frac{\sigma}{\rho_c}\right)^{c_5} \qquad (2.31)$$

The general form of equation 2.31 is similar to equation 2.27 for baffled vessels, except that the latter does not have a kinematic viscosity term. It appears, therefore, that suppressing the vortex by removing the influence of a gas/liquid interface has similar effects, with regards to emulsification, as does the presence of baffles.

Published work on the system that is of particular interest to the subject of this research problem, i.e., emulsification of an organic monomer stabilised by a surfactant in an unbaffled vessel with vortex formation, does not appear to be available. The marked lack of interest in such systems probably stems from the work of Rushton[40] which showed that it was impossible to maintain dynamic and kinematic similarity on scale-up in unbaffled systems. Dynamic similarity requires the ratio of all corresponding forces in two geometrically similar systems to be equal whilst kinematic similarity requires the ratios of velocities at corresponding points to be equal. For successful scale-up, with respect to power consumption, it is necessary to maintain geometrical, kinematic and dynamic similarity.

Regardless of the reasons, study of emulsification in unbaffled vessels with vortex formation has been out of favour as a subject for publication.

2.2.4. The Effect of Surfactants on Dispersion

All systems studied in relation to the correlations in the previous sections were free of surfactants. The addition of surfactants, however, has been noted to lead to a reduction in the mean drop size[44]. Only two workers appear to have published correlations formulated from studies of systems containing surfactants and both of these were for baffled vessels. Nomura et al[24], for instance, working with styrene dispersed in a sodium lauryl sulphate (s.l.s.) solution in excess of 3.13 $g.dm^{-3}$ formulated an empirical correlation which they claimed agreed with the theoretical equation of Shinnar and Church[34] (equation 2.23) and the empirical equation of Roger et al[42] (equation 2.27) which had been developed for surfactant free systems. The correlation of Nomura et al[24] is:

$$\bar{d}_s = 1.05\ (0.15 + 1.4S^{-3/2})\ (N^3D^2)^{-1/4} \qquad (2.32)$$

Where S is the surfactant concentration. The value of the term $(0.15 + 1.4S^{-3/2})$, was thought by Nomura et al[28] to represent the effect of a preventative action of the surfactant against coalescence. The notable comparison between equation 2.32, and the theoretical equation 2.23 is the agreement of the indices on the N and D terms. The term $(0.15 + 1.43^{-3/2})$ may also be looked upon as an empirical equivalent of $A(h_o)^{3/8}$, from the theoretical equation. As the equation of Nomura et al[24] is in agreement with the theoretical equation of Shinnar and Church[34], it would also be in agreement with the empirical equation of Roger et al[42] as this is also claimed to be in agreement with the theoretical equation (see section 2.2.2.).

Tsukiyama and Takamura[29] also presented correlations for droplet size predictions in surfactant solutions, using Tween 20 as the surfactant. However, rather than present a single general

equation with impeller diameter as a variable, three correlations were presented, one for each vessel studied.

$$\log a_1 = 0.399 \log P + 3.376 \quad (2.33)$$

$$\log a_2 = 0.386 \log P + 3.318 \quad (2.34)$$

$$\log a_3 = 0.385 \log P + 3.262 \quad (2.35)$$

where the subscripts 1, 2 and 3 refer to vessel of 150 mm, 200 mm and 250 mm diameter respectively and P is the power dissipated by the impeller. On taking antilogs and making the substitution $a = 6\phi/\bar{d}_s$, the above three equations may be represented by the general form

$$\bar{d}_s = k_1 P^{-x} \quad (2.36)$$

The term for power dissipated, P, may then be expanded, as Tsukiyama and Takamura[29] showed, to:

$$\bar{d}_s = k_2 (N^3 D^5)^{-x} \quad (2.37)$$

where $x = 0.399$, 0.386 or 0.385 for vessel diameters 150, 200, 255 mm respectively.

The most obvious difference between equation 2.38 and previous correlations relating to droplet size prediction, is the inclusion of a total power dissipated term rather than a power dissipated per unit mass, or volume, term as is the case in all previously presented equations. As, however, three separate equations were developed, one for each vessel size studied, the vessel volume term (V_T) present in the substitution, $\bar{\epsilon} = P/V_T$, would be absorbed into the constants. It is interesting to note that a log/log plot of Tsukiyama and Takamura's[29] data for mean dropsize in geometrically similar vessels (see figure 2.5) shows a linear relationship between the mean drop size and the power input per unit volume ($N^3 D^2$), with a gradient of -0.41. This gives the relationship:

$$\bar{d}_s = \text{const } (N^3 D^2)^{-0.41} \qquad (2.39)$$

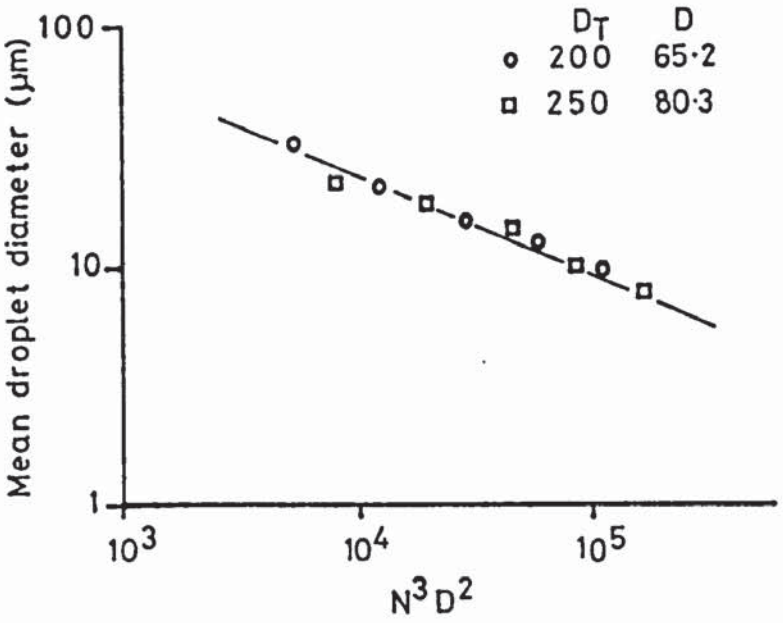

Fig 2·5 Logarithmic plot of data of Tsukiyama and Takamura. S = 0·1% w/w (Tween 20)

It appears, therefore, that the data of Tsukiyama and Takamura[29] conforms to the general correlations derived for the case of droplet breakup in surfactant free systems. The reason that the correlations actually presented by them (equations 2.33 to 2.35) varied from preceding correlations probably stemmed from the fact that Tsukiyama and Takamura[29] correlated data for a variety of impeller diameters in each vessel. Hence, overall, geometrical similarity was not maintained, thus forcing the data for each vessel to be correlated independently of data from the other vessels .

In general conclusion, therefore, it appears that the drop size in emulsions containing a surfactant may be correlated by equations of the type developed for surfactant free systems but such correlations will always be specific to the surfactant type and concentration.

2.2.5. Droplet Size Analysis Techniques

A variety of techniques have been used to analyse emulsion droplet size, falling into four basic categories; 1) photography and light transmisiion, 2) photomicroscopy, 3) Coulter Counter, 4) soap titration, of which the first was the most popular method employed.

1) Photography and light transmission

These two techniques are presented and discussed together as they were generally used in conjunction[30][41][42][45][46][47], the photographic technique commonly being used as a check or calibration for the light transmission technique.

Vermeulen et al[41] were the first to use light transmission to measure interfacial area. The apparatus consisted of a probe, containing a light source and a photoelectric cell, which was introduced into the dispersion. The smaller of the two vessels used by Vermeulen et al[41] was equipped with a window through which the emulsion in the vicinity of the probe was photographed. The theory behind the light transmission technique was based on the concept that a plot of the extinction ratio (I_o/I) against interfacial area was linear with an intercept of unity, corresponding to the equation

$$\frac{I_o}{I} = \beta_a + 1 \qquad (2.40)$$

β_a was found empirically, by Vermeulen et al[41], to depend upon the ratio (m) of the refractive index of the dispersed phase to that of the continuous phase. Photographs of the emulsions were used to calibrate the light transmission technique.

Roger et al[42] apparently used a technique similar to Vermeulen et al[41] although details of the probe and correlation between the light transmission measurements and the interfacial

area are absent from their paper. It is clear, however, that photographs were taken of each emulsion, through the base of the vessel, which was flat, thus avoiding the optical distortion that may occur when photographing through curved vessel walls. It does not, however, overcome the problems of droplets distorting under the effects of fluid motion.

Brown and Pitt[45] used techniques similar to Roger et al[42], photographing the emulsion through the vessel base. However, an additional method of calibrating the light transmission technique was employed, whereby the light transmitted by a suspension of polystyrene beads of a known diameter was measured.

Calderbank[47] also used the technique of light transmission but based it upon a different theoretical foundation, which was based upon the observation that the scattering cross section of a droplet is equal to its projected area provided the droplet is large compared with the wavelength of the light. Calderbank[47] reported that Couchy[48] had demonstrated that in an assembly of irregular randomly dispersed droplets the total interfacial area per unit volume of dispersion equals four times the projected area. Calderbank[47] gave the final relationship, therefore, as

$$\log \left(\frac{I_o}{I}\right) = \frac{al}{9.210} \qquad (2\cdot40a)$$

where l is the optical path length.

The light transmission technique was tested on polystyrene spheres of known diameter. In addition, the construction of the probe allowed photographs to be taken of the emulsion at the point where the light transmission measurements were made.

Chen and Middleman[46] also used a combination of light transmission and photography to study emulsion droplet size. But in this case

photography was the method used to analyse the droplet population, the light transmission was used only to indicate when the emulsion had reached equilibrium. This was indicated when the transmission readings ceased to fluctuate. To avoid optical distortion when photographing through the curved vessel wall, the vessel was immersed in a square Plexiglass box filled with water. The camera was focussed on an arbitrary plane midway between the vessel axis and its wall. Finally the droplets' diameters were measured directly from negatives using a travelling microscope.

Mlynek and Resnick[49] used photography alone in their study, although two techniques were used. One was the direct photography of the emulsion in the vessel via a probe. The other involved removing samples of the emulsion for photography outside the vessel. In order to prevent coalescence of the drops, when removed from the flow field, novel use of interfacial polymerisation was made. One monomer was dissolved in the organic dispersed phase, the other was present in a specially designed sampling probe. When a sample of the emulsion was drawn into the probe, polymerisation occurred thus encapsulating each of the droplets in a polymer film. The sample was then placed on a dish and photographed, the photographs being analysed on a Zeiss TGZ3 particle size analyser. One drawback of this technique is that the organic phase has to be chosen to be compatible with the monomer used for encapsulations, which itself may affect the droplet size.

2) Photomicroscopy

This technique was used by Tsukiyama and Takamura[29] due to the smaller drop sizes encountered when emulsifying agents (surfactants) are present. Scant details of the technique they used are available. Essentially, samples of the emulsion, removed from the parent

emulsion, were photographed under a microscope. The resulting photographs were analysed and the data was manipulated by computer.

3) Coulter Counter

The basic Coulter Counter is a device which measures droplet diameters by sensing the change in electrical resistance to the flow of current between two electrodes in an electrolyte when particles are drawn through a fine orifice through which the current is passing.

Rowe[44] used the Coulter Counter successfully for studies on the effect of an emulsifier on droplet size. As it is necessary to use only very dilute emulsions, Rowe diluted his samples in a two stage process. Firstly, two cubic centimetres of the sample were diluted to one cubic decimetre with a standard conductivity vehicle (0.9% sodiumchloride solution) then fifteen cubic centimetres of this solution were again diluted to one cubic decimetre. Solvation of the organic (mineral oil) was assumed to be negligible.

Sprow[49] also used a Coulter Counter in his studies of surfactant free emulsions. Again samples removed from the parent population were diluted, in this case with a salt water and glycerine mixture, where the glycerine was present to stabilise the drops. The final concentration of dispersed phase was between 0.05% and 0.5% on a volume basis.

4) Soap titration

This method was used by Nomura et al[28] in their studies on a styrene/S.L.S. solution system. The concentration of the soap was measured by means of the "Eptom method", the reference for which proved to be incorrect. As the initial concentration of the soap was known, the difference between the measured soap concentration and the initial concentration was due to adsorption of soap onto the interfacial area. Since soap molecules tend to each occupy a specific area, the total interfacial area may be calculated. This method

obviously relies heavily on accurate knowledge of the specific surface area of the molecules of the particular soap being used.

2.2.6. Reproducibility of Results

It was common to find in the literature covering all the technique of droplet size measurement mentioned references to the difficulty encountered in reproducing results. Vermeulen et al[41], for instance, noted that results were more easily reproduced if the materials used were not changed between experiments, and concluded that this was due to the difficulty of ensuring the total exclusion of, or the introduction of identical traces of, impurities into each fresh charge. Calderbank[47] also encountered this problem but discovered that the use of tap water, rather than distilled water, as the continuous phase gave more consistent results. He attributed this to the relatively large concentration of ions present in the tap water which would swamp any effects due to random trace impurities. He observed similar results when electrolytes were added deliberately. The problem was tackled differently by Roger et al[42] who included the term (t/t_o) in their final correlation to allow for the effects of random trace impurities. (See section 2·2·2)

In addition to the difficulties related to the systems used, some of the analytical techniques also suffered difficulties. Vermeulen et al's[41] light transmission technique, for example, yielded results with a mean deviation of about ±20% and a maximum deviation of about 50%. Weinstein and Treybal[30], using a similar analysis technique to Vermeulen et al[41] reported average deviations of the order of 10% with maximum deviations of 50%. Calderbank[47], using a light transmission technique which he claimed was an improvement over Vermeulen et al's[41] technique, found a mean deviation of the order of 10% and a maximum deviation of 50%, results which in fact show no

greater accuracy than those of Weinstein and Treybal[30].

Results obtained using in situ photography show no greater accuracy than the light transmission techniques. Chen and Middleman[46], for example, observed results of some 10% deviation, again with a maximum deviation of 50%. Mlynek and Resnek[49], however, using the technique of polymer encapsulation and photography reported maximum deviations of only 20%, although it must be stated that this referred only to the deviation of mean dropsize as measured on different photographs taken in the same location and under identical conditions. The overall deviation of data from their correlation was not discussed.

The scatter of the data obtained using other methods of analysis were not discussed by the authors of the appropriate papers[50][28]. Visual observation of graphical results would indicate that scatter was very low, but as the quantity of data presented was generally small, it would be unwise to make any comment on the accuracy of the results or the techniques employed to obtain them.

2.2.7. Power Input

In section 2.2.1., it was shown that theoretical correlations for droplet size predictions normally include an energy term. It is obvious, therefore, that power input relationships should be closely allied to droplet size correlations.

In the field of power input, unbaffled vessels have received some attention. Hixson and Baum[51] presented a correlation for power input in an unbaffled vessel agitated by a four bladed turbine for turbulent conditions where the Reynolds number exceeded 10^5. The measurement of the torque reaction of the motor was carried out by mounting the motor on a turntable and loading an attached scale pan with suitable weights. The correlation presented was,

$$P = \text{const} \cdot N^{2.77} \cdot D^{4.54} \cdot \rho^{0.77} \mu^{0.23} \qquad (2.41)$$

Rushton et al[52] using a similar technique obtained results of an extensive study of power input in mixing systems. A wide range of vessel sizes, impeller types and diameters and fluid systems were studied. The findings of their work on baffled vessels were used by Shinnar and Church[34] in the development of the special case equations for the prediction of droplet sizes presented here as equations 2.22 and 2.23.

Rushton et al[52], however, also studied unbaffled systems where a vortex was present, and correlated power input in a dimensionless form.

$$N_p = \text{Const} \cdot Re^m Fr^n \qquad (2.42)$$

where N_p = power number = $\dfrac{P}{\rho N^3 D^2}$

Fr = Froude number = $\dfrac{N^2 D}{g}$

Re = Reynolds number = $\dfrac{ND^2 \rho}{\mu}$

This is normally expressed graphically as a plot of power function ($\Phi = N_p/Fr^n$) against Reynolds number, a typical example is shown in figure 2.6.

For systems where no vortex was present, that is, at Reynolds numbers less than 100, m becomes -1 and n becomes zero. Above a Reynolds number of 100, both m and n vary, n being a function of Reynolds number. In the turbulent regime at Reynolds numbers greater than 10^4, m becomes constant with a small negative value, but n remains a function of the Reynolds number. Rushton expressed the functional dependence of n on the Reynolds number by the following expression:

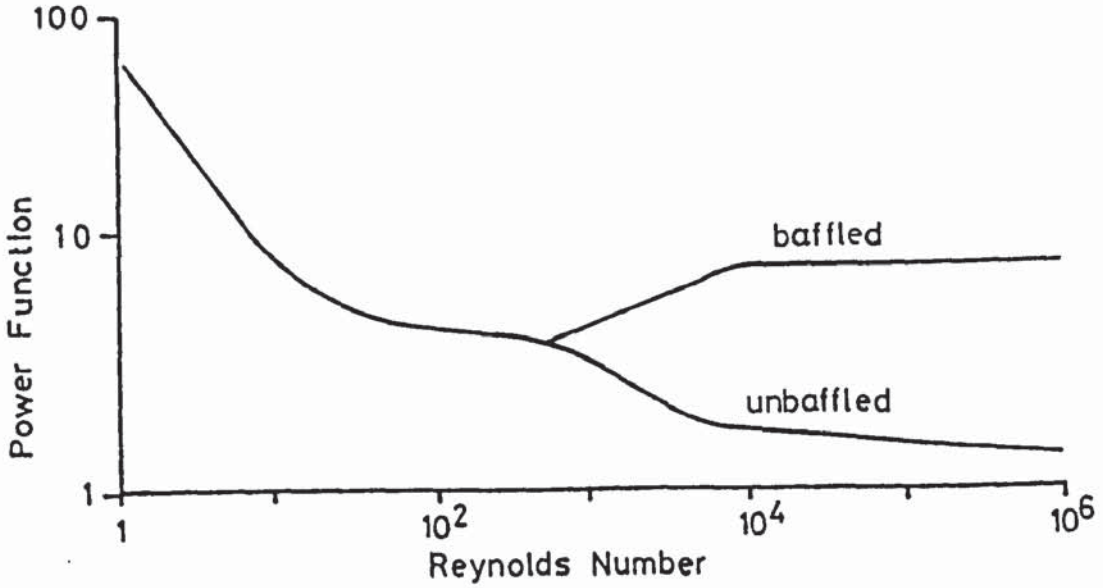

Fig 2·6 A typical logarithmic plot of Power function (Np/Fr^{-n}) against Reynolds number. Turbine impeller, 6 blades, $D/D_t = 1/3$ (After Rushton et al)

$$n = \left(\frac{a - \log Re}{b}\right) \qquad (2.43)$$

where a and b are constants dependent on the impeller used.

Power input in agitated systems has never been studied so comprehensively since Rushton et al[40] and certainly unbaffled vortexing systems have been left by the wayside.

Of course the expressions for power input relate to the total power dissipated within the total volume, although generally the energy term in droplet size correlations is represented in terms of energy dissipated per unit mass. A simple solution is to assume homogeneous energy dissipation throughout the liquid volume and to divide the total power input by the mass of fluid in the vessel, as was done by Shinnar and Church[34], giving the average energy dissipated per unit mass of fluid. The validity of this assumption, however, must be questioned. Metzner[39] using a photographic tracer technique to study flow regimes in stirred tanks, showed that it was possible to have both turbulent and laminar flow conditions occurring simultaneously

in the same vessel. He concluded that power dissipation was greater near the impeller, and fell off rapdily on moving away from the impeller. Park and Blair[53], Coulaglou[37] and Sprow[56] all produced results that supported Metzner's[39] conclusions. They showed that the drop size varied with position in the vessel for systems in which coalescence played an important role. Sprow[50] particularly noticed that it was possible to describe the droplet size near the impeller by a correlation relating to droplet breakup and the drop size in the rest of the fluid by a correlation based on droplet coalescence.

2.3 Scale-up

A full review of the subject of scale-up clearly could cover a vast range of topics and approaches which it is felt is outside the scope of this study. Even a full scale-up study of batch emulsion polymerisation must encompass heat transfer, mass transfer, mixing times, power input, shear rates and dispersion and it is certain that the simultaneous scale-up of each of these factors would lead to problems of incompatibility of the scale-up equations[54].

The major characteristic of the latex that it was required to reproduce upon scale-up in the current study was latex particle size and there is some evidence that the major factor affecting this is the degree of dispersion of the monomer. By choice, therefore, the subject for scale-up of interest to this project is that of equivalent dispersion and it is on this that this survey was concentrated. However, it is of useful background interest to introduce some of the fundamental concepts relating to scale-up in general.

The concept of similarity is of prime importance in any study of scale-up. There are three definitions of similarity[40][55]; geometric

kinematic and dynamic.

Geometric similarity is defined as the maintenance of a constant ratio of characteristic dimensions of the vessels under consideration, e.g. maintain constant the ratio of impeller diameter to vessel diameter.

Kinematic similarity is the similarity of motion and is observed if the ratio of velocities at corresponding points in geometrically similar vessels are equal.

Dynamic similarity is the similarity of masses and forces. Dynamic similarity is observed if in addition to kinematic similarity, the ratio of forces at corresponding points are also equal.

Considering the factors to be taken into account in analysis of a stirred reactor, there are four forces involved[55]; the inertia force from the agitator, the fluid force associated with viscosity, surface tension and gravitational forces. Nagata[55] observed that it is impossible to maintain constant the ratio of each of these individual fluid forces during scale-up unless the fluid properties are changed. It is often necessary however to carry out pilot plant trials on the same fluids that are intended for use in the full scale plant. As it is not possible to retain similarity in all force terms it is obviously necessary to select for similarity those forces which are of the greatest importance to the particular system being studied. Further to this, Rushton[40] has shown that it is theoretically and experimentally impossible to achieve complete dynamic similarity on scaling-up an unbaffled system where a vortex is present.

A limited number of papers pertinent to scale-up in emulsion polymerisation and scale-up to maintain equivalent dispersion have been published, and these are reviewed in the following sections.

2.3.1. Scale-up of emulsion polymerisation

The specific subject of scale-up of emulsion polymerisation has

received scant attention in the literature. Those scale-up techniques that have been published have generally involved arbitrary changes in the physical and chemical characteristics of the system to achieve the desired effects. Walker[56], for instance, described the technique employed at Uniroyal Limited. Recipes were first tested in bottle polymerisation units testing up to twenty four formulations simultaneously. Successful formulations were then tested in 20 gallon (76 dm^3) reactors where the impeller speed was adjusted by 'trial and error' to produce reaction times similar to those experienced by formulations that were already in full scale production. The formulation was further tested in a 500 gallon (1892 dm^3) vessel before finally moving on to full scale vessels. At each stage in the scale-up procedure adjustments were made to the formulations to achieve successful scale-up through the range of reactors. These reactors, however, were not geometrically similar. This is obviously not in agreement with the scientific approach to scale-up that demands geometrically similar vessels.

The only other reference of direct interest to the scale-up of emulsion polymerisation batch reactors appears to be a passing reference to levels of shear in scale-up of emulsion polymerisation made by Nagata[57] in his book. He suggested that care should be taken to avoid exceeding on scale-up the level of shear that would induce coagulation of the latex being produced. This is a logical development of the results presented by Nomura et al[24], which showed that the polymer particle population reduced if stirring speeds above a certain level were employed. The reduction in the polymer population was attributed to coagulation of polymer particles under the influence of excessively high shear.

2.3.2. Scale-up for equivalent dispersion

Baffled Vessels

The general principle for scaling-up on the basis of equivalent dispersion in baffled vessels was presented by Scully[58] in his paper on scale-up in suspension polymerisation. The equation governing the scale-up was derived from Vermeulen et al's[41] equation for predicting droplet diameter in baffled vessels.

$$\bar{d}_s = f(\phi) \left(\frac{N^2 D^3 \rho}{\sigma}\right)^{-0.6} \tag{2.44}$$

For equivalent dispersion, therefore

$$D_1 f(\phi) \left(\frac{N_1^2 D_1^3 \rho}{\sigma}\right)^{-0.6} = D_2 f(\phi) \left(\frac{N_2^2 D_2^2 \rho}{\sigma}\right)^{-0.6} \tag{2.45}$$

On simplifying equation 2.45 reduced to

$$N^3 D^2 = \text{constant} \tag{2.46}$$

The term $N^3 D^2$ was shown in section 2.2 to be representative of power input per unit volume for $Re > 10^4$. Thus to maintain equivalent dispersion on scale-up in baffled vessels, equivalent power input per unit volume must be maintained.

Unbaffled Vessels

With the exception of Rushton's[40] reference to the inability to naintain on scale-up both dynamic and kinematic similarity in unbaffled vessels with a vortex present no further papers on scale-up under such conditions appear to have been published.

3.0 EXPERIMENTAL EQUIPMENT AND TECHNIQUES

3.0 EXPERIMENTAL EQUIPMENT AND TECHNIQUES

The nature of this investigation required the design and operation of two series of rigs, one series to study the characteristics of liquid-liquid dispersion in a stirred batch reactor and the other to study the effects of agitation on emulsion polymerisation also in a stirred batch reactor. It was also necessary that some dispersion experiments should be performed in the latter rig.

A number of constraints were imposed upon the flexibility of the design of the reactor vessels, upon the choice of chemical systems used and upon the mode of operation of the polymerisation reactor. The project was one of scale-up and information was sought regarding the techniques required in scaling-up a process, which was in existence in small and intermediate size pilot units, to full production size. Clearly if the data from this project were to be comparable with data from these pilot units it was essential that the equipment geometry, chemical system and operation should also be comparable. Accordingly all vessels constructed for use in this project, were, as far as possible, made geometrically similar to the pilot scale reactors already in existence,but some twenty times smaller.

Similarly, the chemical system used for the polymerisation experiments was chosen to be representative of that system used in these pilot scale tests. In the dispersion experiments, however, more flexibility was possible and a simplified chemical system was studied in the interests of safety and ease of analysis.

Analysis techniques were developed to measure mean droplet size in the dispersion studies and mean polymer particle size in the polymerisation studies.

The experimental programme was structured such that the bulk of the dispersion experiments were completed before the polymerisation

experiments were conducted. Thus, this chapter describes the rigs and their operation, the chemical systems and the analysis techniques in approximate chronological order, i.e. the dispersion experiments first followed by the polymerisation experiments.

3.1 Dispersion vessel design

Three geometrically similar vessels of nominal bore 6, 9 and 12 inches (152, 229, 305 mm) were designed and constructed for use in the investigation of the effects of vessel size, impeller speed and other relevant factors, on the size distribution of droplets of an organic liquid in an emulsion with an aqueous soap solution as the continuous phase. The obvious choices for the parallel walled sections of these vessels were Q.V.F. glass pipe sections available from stock in convenient nominal bores and lengths. Each test vessel, therefore, was constructed from a section of the appropriate bore glass pipe section and to this was bolted a dished base.

The design for the dispersion vessels and thus for the dished bases was governed by the fact that the tests to be carried out were intended for comparison with an existing series of reactor vessels. Dished bases were not readily available and so the base for each vessel was fabricated from glass reinforced plastic (G.R.P.) formed over specially prepared plaster moulds. A simple wooden flange was used to provide structural integrity and the sealing of the joint was made by means of a standard Q.V.F. rubber gasket. (See Figure 3.1)

A scale was attached to the side of each vessel to allow easy observation of the liquid level in the vessel.

The vessels did not have any type of lid fitted nor were there any baffles in agreement with the existing reactor vessel design.

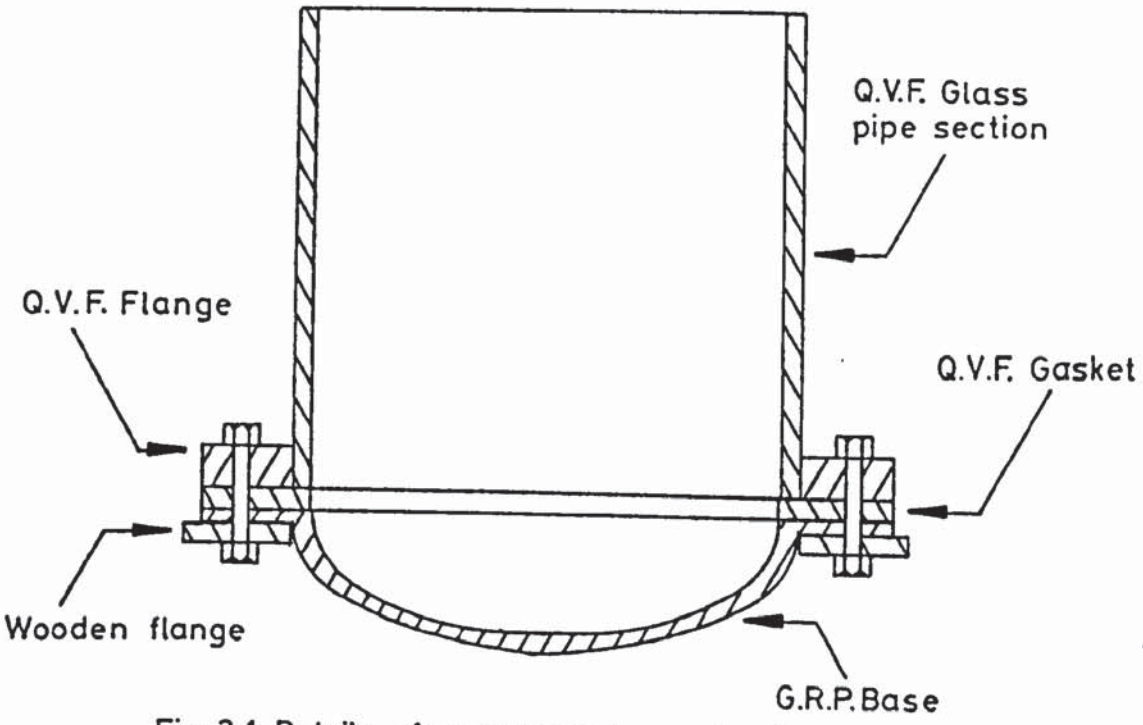

Fig 3·1 Details of open vessel construction
For vessel parameters see table 3·2

The initial design of the existing reactors used flat bladed turbine type impellers with six blades and thus this constraint in impeller design was initially placed upon the models. Figure 3.2 shows a photograph of the impellers. The impeller boss and blades were constructed from stainless steel, the boss being secured to a stainless steel shaft by a socket head grub screw and each of the blades being fastened to the boss with two socket head screws and nuts. All the screws and nuts used were of stainless steel.

The impeller shaft was supported at its upper end by two bearings (Figure 3.3) and driven, via a Bowden cable, by a direct current constant speed motor. The motor, a 0.25 KW G.E.C. Gemini, could be set at any speed desired between zero and 1,000 r.p.m. As the motors

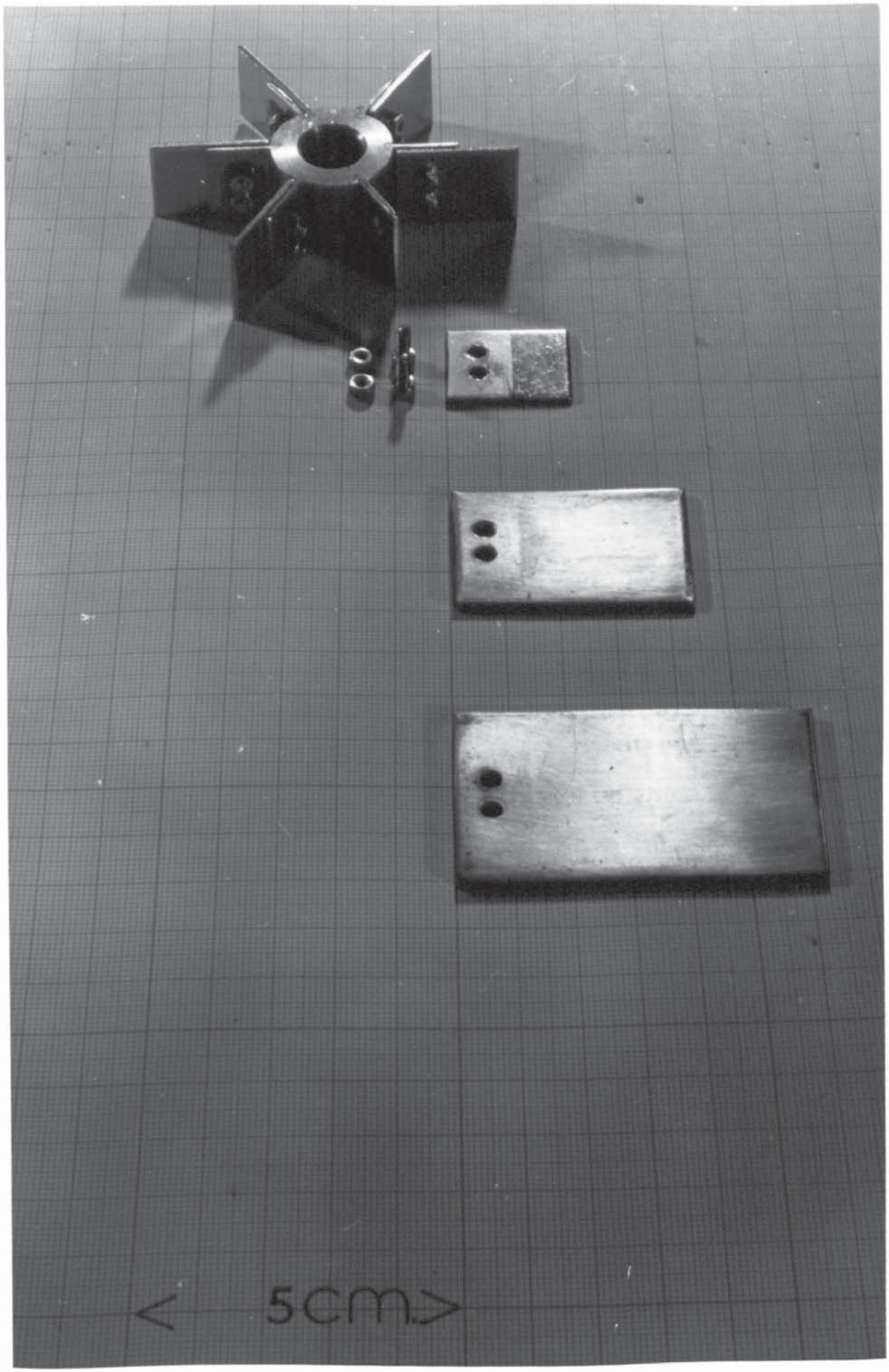

Fig 3·2 Impeller system.

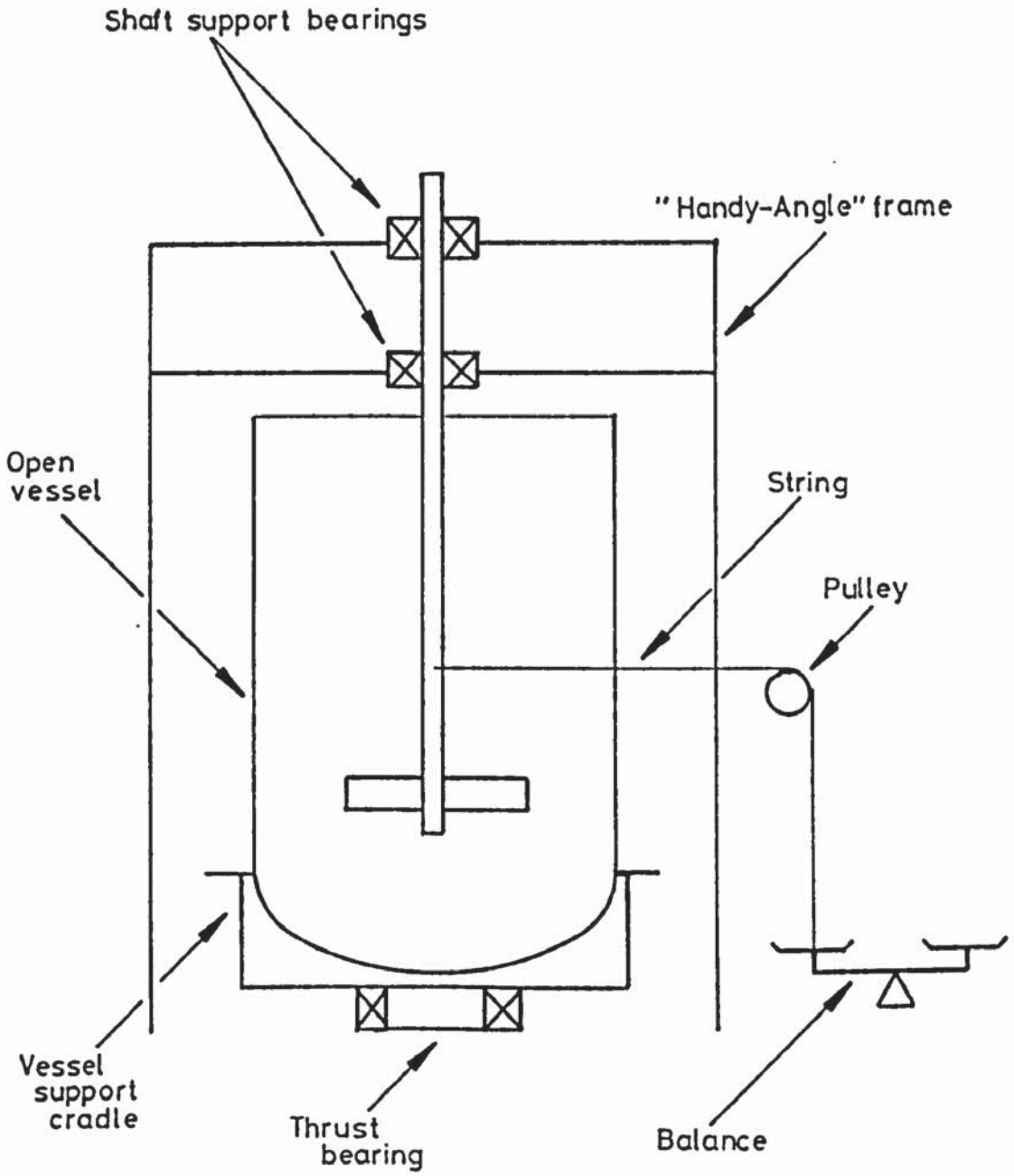

Fig 3·3 Diagram of open vessel arrangement showing balance for measuring the torque transmitted by the impeller

speed was proportional to the voltage applied, a voltmeter was calibrated so that the motor speed could be readily obtained.

As well as allowing droplet size analysis it was also intended that these vessels should be used in order to estimate the power input by the impeller during the dispersion operation. To allow this, a facility was designed whereby the vessels could be mounted on a turn-table which pivoted on a thrust bearing (a lightly oiled ball race). A beam balance was attached via a pulley to the vessel in order to measure the torque imparted to the vessel by the impeller. Figure 3.3 shows this arrangement.

3.2 Chemical systems used in dispersion studies

The chemical system involved in emulsion polymerisation involves essentially four ingredients, an organic monomer, water, a surfactant and a mixture of water soluble electrolytes including an initiator. Obviously in a study of the emulsification of the monomer, the system used would require, as a minimum, the presence of the first three ingredients. Quite clearly the presence of the initiator and other electrolytes may well have an effect on the dispersion in that the interfacial tension and stability of the dispersion may be affected by their presence. For this study, however, it was considered that the inclusion of these ingredients would make analysis of the problem more confused and it was thus decided that the dispersion systems would include the organic, the water and surfactant only.

The organic phase in the emulsion polymerisation of interest to this study was either pure styrene or a mixture of styrene and butadiene. Butadiene could, quite obviously, not be studied in an open vessel and even for styrene it was considered unwise due to the

health hazard involved and the quantities of monomer that would be required. Accordingly it was decided to carry out the dispersion experiments using an alternative organic phase. Analar grade toluene was chosen as this alternative as it has similar physical properties to styrene (see table 3.1). In addition it was easily reclaimed and recycled by firstly breaking the emulsion by addition of aluminium chloride and then distilling off the toluene as a toluene/water azeotrope boiling at 85°C. This on cooling separated into two distinct layers thus allowing the toluene layer to be run off.

For the majority of experiments, distilled water was used as the continuous phase as this was to be the continuous phase used in the polymerisation experiments. A few preliminary runs, however, employed Birmingham mains water.

		Toluene	Styrene
1)	Viscosity $mN.S.m^{-2}$	0.587	0.763
2)	Surface tension $mN.m^{-1}$	28.43	30.86
3)	Density $kg.m^{-3}$	866.94	905.9
4)	Boiling point °C	110.6	145.0
5)	Molecular Weight	92	104.14
6)	Formula	$C_6H_5CH_3$	$C_6H_5CH = CH_2$
7)	Solubility at 25°C % wt/vol	0.047	0.032

Table 3.1 Comparison of physical properties of toluene and styrene at 20°C.

The surfactant used was a commercial grade of sodiumdodecylbenzen-sulphonate (Nansa HS 85/S) which was supplied by the Marchon division of Albright and Wilson Limited. This particular soap was used as it was the specified constituent of the recipe for the emulsion polymerisations that were to be performed in later experiments. The physical properties of Nansa are shown in Appendix A.

The system studies in the open vessels was, therefore, toluene, water and Nansa. When later in the project a closed reactor vessel became available a number of dispersion runs were carried out using styrene, distilled water and Nansa in order to compare the results with the extensive data gathered using toluene.

3.3 Experimental procedures for the dispersion experiments

Essentially it was necessary to develop three distinct experimental procedures in the liquid/liquid dispersion investigation. The first procedure related to the use of the open vessels for dispersion experiments, whilst the second is appropriate to the use of the closed reactor vessel for dispersion experiments. The final procedure was developed to measure the power input by the impeller.

Descriptions of the various procedures employed are contained in the following sections.

3.3.1. Procedure for dispersion experiments using the open vessels

In order to carry out a dispersion experiment in each of the open vessels, the following procedure was adopted. The chosen vessel was first washed with a 1% weight/volume Nansa solution and then rinsed with distilled or mains water depending upon which of these was the intended continuous phase. If torque measurement was not intended, the vessel was merely centred around the shaft. If,

however, torque measurement was intended the vessel was placed on the turntable. The impeller and shaft were lowered into the vessel, the position of which was then adjusted such that the impeller shaft was axially central, with the vessel free to revolve about the axis of the shaft. The balance was connected to the vessel as indicated in figure 3.3.

The height of the impeller from the base of the vessel was set equal to half the vessel diameter in accordance with the practice adopted in the existing reactors. In order to investigate the possibility that the history of the emulsion, that is, for instance, the method of charging the liquids and the soap, might affect the degree of dispersion three different procedures were adopted and their resulting data were compared.

Procedure I

The vessel was charged firstly with the appropriate volume of water followed by the appropriate volume of toluene (see table 3.2) such that the liquid height was equal to the vessel diameter. No soap was added at this stage. Agitation was then applied at the lowest impeller speed selected for the experiment. After a period of twenty minutes (a period to allow for the attainment of steady state derived experimentally, see section 4.1.2.), a sample was removed, using a stainless steel tube fitted with a pipette filler. The sample was withdrawn from a position close to the vessel wall and at a height equivalent to two thirds of the vessel diameter from the base. This was done to ensure that samples were removed form the same region for each test in order to minimise the effect of any inhomogeneity that may have existed in the emulsion. This position was chosen as it was easy to reproduce in each vessel. It was, in fact, later

shown in experiments that the location of the sampling point did not have an effect on the dispersion data. After removal of the sample the impeller speed was increased and after a further twenty minutes a second sample was withdrawn. This procedure was repeated until the required range of impeller speeds had been covered. After the range of impeller speeds had been covered for zero soap concentration, the emulsion was allowed to break before a measured weight of Nansa was added in solid form and the above procedure repeated. After completion of the full impeller speed range at this soap level the emulsion was again allowed to break and a further soap charge added. This procedure was repeated and a total of four soap concentrations were studied in each vessel.

Samples withdrawn for droplet size analysis were treated according to the manner in which they were to be analysed. Analysis of the early runs was by photomicroscopy, whilst subsequent experiments were analysed on a Coulter Counter. Sample treatments for each of these techniques are described in section 3.4.

The temperature of each emulsion was monitored with a mercury in glass thermometer to ensure that all the experiments were carried out at the same ambient temperature.

Phase ratio (organic)	0·59	0·59	0·59
Vessel diameter D_t mm	152	229	305
Liquid volume dm^3	2.67	8.5	20.5
Impeller diameter D mm	75	114	152
D/D_t	0.49	0.50	0.50

Table 3.2 Vessel parameters

Procedure II

The second procedure was identical to the first except that instead of raising the impeller speed immediately after taking a sample, the impeller was stopped and the emulsion allowed to break before the impeller speed was set to its new, higher, value. The procedure for the incremental addition of soap (Nansa) was identical to Procedure I.

Procedure III

The third series of experiments involved a study of only two soap concentrations, both sufficiently large to prevent the emulsion from breaking. In this case a stock solution of Nansa was prepared. Charging of the vessel was in accordance with the following sequence: a measured volume of the stock Nansa solution was introduced into the vessel followed by the requisite amount of water required to make up the appropriate continuous phase volume, then the toluene was carefully poured down the outside of the impeller shaft to minimise premature mixing of the two phases. Agitation and sampling were then carried out as described in Procedure I.

3.3.2 Procedure for dispersion experiments using the closed vessel

A number of dispersion experiments were carried out in the closed reactor vessel in order to allow a comparison of the styrene data with the general conclusions drawn from the toluene tests performed in the open vessels. The charging procedure was similar to the open vessel Procedure III except that the organic (in this case styrene) was poured down the side of the vessel. Sampling was by means of a permanently fixed dip pipe, the vessel contents being forced out by a slight pressurisation of the vessel. The first few cubic centimetres of each sample were run off to waste in order to flush out the dip pipe.

Temperature control was possible on the reactor but due to the thermal inertia of the vessel it was found that fluid temperatures fluctuated less when no control was applied and thus these experiments were carried out at ambient temperature.

3.3.3 Procedure for measuring power input

During the early disperion experiments an approximate measurement of the power input by the impeller was carried out. The vessel was mounted on a turntable, as detailed in section 3.3.1, and connected to a balance via a pulley (see figure 3.3). The frictional drag of the turntable bearing was estimated before each experiment by loading the balance until the vessel, which was charged but was not being agitated, just revolved. When agitated, the vessel tended to revolve so as to oppose the pull of the balance. Estimates of the torque applied by the impeller were, therefore, obtained by loading the balance until the vessel became stationary with the balance at equilibrium.

3.4 Droplet size analysis

Two methods of droplet size analysis were employed in this study. Early experiments were analysed by means of a photomicrographic technique which proved to be very time consuming. Later experiments were, therefore, analysed using a Coulter Counter. The two techniques employed are discussed below.

3.4.1 Photomicrographic

This technique was applied largely to emulsions that exhibited a tendency to break if not agitated. To prevent this, all samples removed from the agitated vessel were placed into a 1% Nansa solution and gently shaken. This both stabilised the droplets and reduced their concentration. The reduction of the droplet concentration was necessary

as it was found that analysis of photographs of well spaced droplet was much easier than analysis of photographs of densely packed droplets.

A sample of the diluted emulsion, sufficient to wet a cover slip, was transferred to a dimpled microscope slide. It was observed in some samples, that droplets were coalescing whilst on the microscope slide. When this was observed, the sample was rejected, and a fresh slide was made up. Another occurrence was for the droplets to migrate to the circumferences of the dimple, forming swarms of drops. Coalescence did not appear to be a feature of this swarming effect and so these slides were not rejected. The slide was placed under the microscope and two photographs of different parts of the sample were taken under conditions of transmitted light using Kodak Tri-X film on an exposure time of 1/125 seconds. The camera used was a Miranda Sensorex 35 mm still camera. The prints were of 5¼ inch by 4 inch (133 mm x 102 mm) format, giving a final magnification factor of approximately 65. The exact magnification factors for these final prints of the photographs were measured from photographs of graticules, at least two of which were taken each time the microscope was set up. The exact magnification was measured for each set of prints as it varied slightly for different sets.

The prints were analysed using a Zeiss TG3 particle counter, hereafter referred to as the Zeiss. In this instrument, a spot of light was focussed onto the print, the diameter of this spot was then adjusted by means of an iris diaphragm so that it just covered the image of the droplet being counted. Depression of a foot pedal caused the droplet to be recorded in one of fortyeight digital registers. Each register represented a range of light spot diameters which could be calibrated to true droplet diameter using the appropriate magnification factor. Simultaneously with the count a needle pierced the photograph at the centre of the spot of light, thus marking that particular drop

and eliminating it from further counts.

In order to maintain consistency in the analysis of the photographs, the following practices were adhered to.

a) Each photograph was divided into zones by drawing a grid upon it. This made it easier to ensure that all droplets on the photograph were counted, thus preventing selective counting.

b) Droplets appeared on the photographs as light discs surrounded by a dark halo (figure 3.4). The spot of light was always adjusted to cover the entire drop including the halo. Fine focussing was necessary in each photograph to ensure that the sharp edge of the halo could be clearly seen.

c) All droplets in each zone of the photograph were counted and a minimum of 300 droplets per sample were required in order to allow confidence that the sample was representative of the parent population.[59]

Data from the Zeiss was input into a computer program, run on an IBM 1904S computer, which calculated the Sauter mean diameter for each dispersion.

3.4.2. Coulter Counter: Description

The Coulter Counter is an established piece of equipment which has been described many times in the literature[60][61][62]. Its major use has been the analysis of particle sizes of solid materials in the size range 2 to 300 μm but it has also been successfully used in the analysis of droplet dispersions. Figure 3.5 shows a simplified diagram of the test cell of the Coulter Counter. An electrolyte solution containing the particles or droplets to be analysed (A) has immersed in it a hollow glass probe (B) which is also filled with the electrolyte. The only contact between the electrolyte volumes inside and outside the probe is through an orifice of known diameter in the

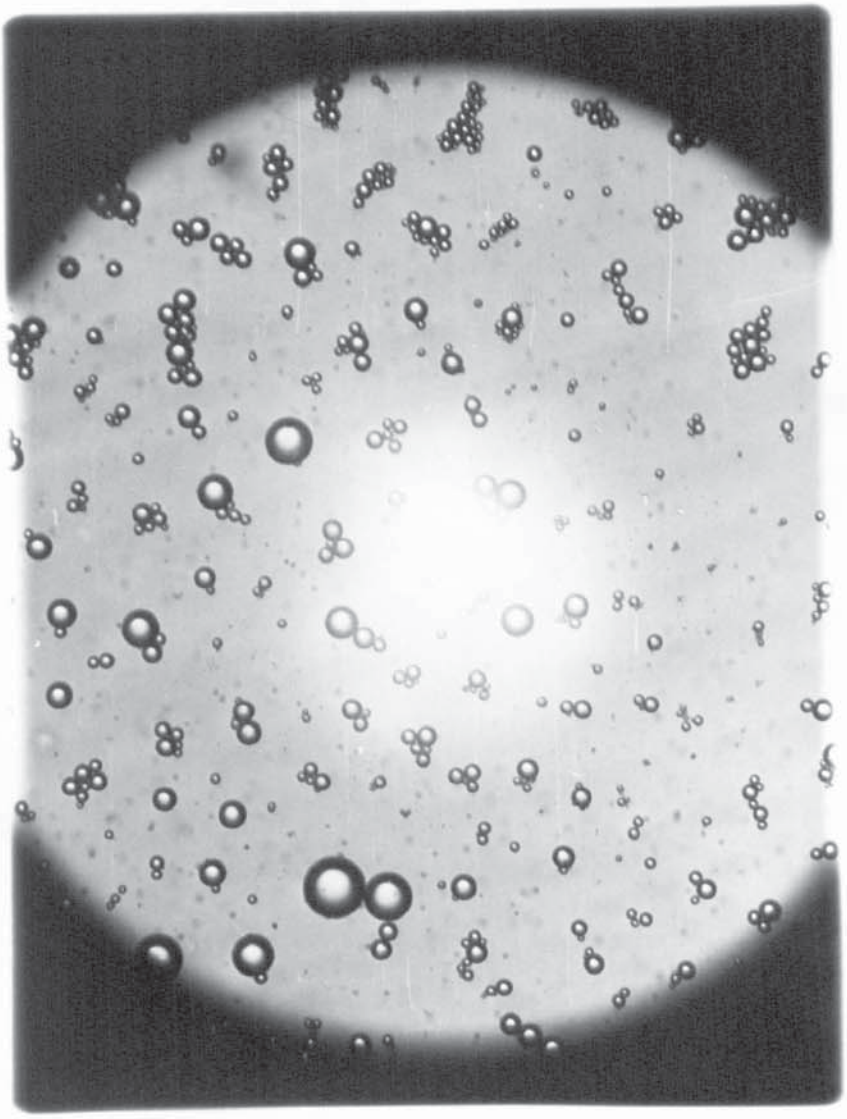

Fig 3·4 A typical photograph used in the low magnification factor photomicrographic analysis.
(magnification factor = 66)

wall of the probe. An electric current is passed between two electrodes (C), one in the outer electrolyte volume and one in the electrolyte inside the probe. The manometer arrangement (D) draws a given volume of electrolyte solution through the orifice. As droplets, dispersed in the solution, pass through the orifice, the resistance between the electrodes varies according to the size of the droplets. The electrical signal resulting from the resistance fluctuations is fed into the electronic section of the Coulter Counter where it is decoded. A threshold setting is manually selected which relates to a given particle size. All signals relating to particles above that given size are counted. Thus a cumulative oversize size distribution may be obtained by successively lowering the threshold setting and taking a count at each setting. In practice, several counts are made on each setting and then averaged.

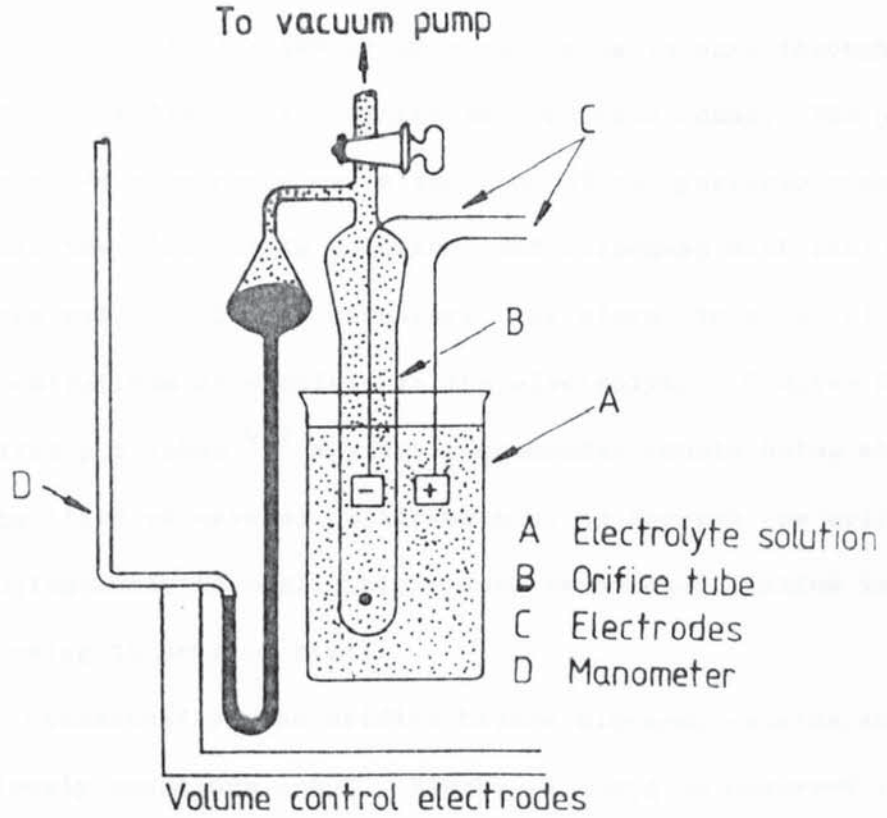

Fig 3·5 Coulter Counter test cell.

The Coulter Counter is sensitive to particle sizes in a range of 20% to 40% of the orifice diameter. Hence a range of orifices is available allowing particles in the size range 1 micrometre to 225 micrometres diameter to be analysed.

3.4.2.1. General precautions

When using the Coulter Counter three general precautions were found to be necessary:

1) Electrolyte filtration

Obviously, as the Coulter Counter counts all particles suspended in the electrolyte solution, some care was necessary to avoid the presence of extraneous particles. Careful filtration through a suitable membrane filter was, therefore, necessary.

2) Particle concentration

The Coulter Counter counted a particle each time the electrical resistance between the electrodes varied. Obviously, it was possible for two or more particles to pass through the orifice simultaneously causing an erroneous count. The probability of such an occurrence was a function of the particle concentration within the electrolyte solution, and increased with increasing concentration. It was necessary, therefore, to avoid high concentrations of droplets in the electrolyte. Coulter Counter Limited published[63] maximum recommended counts below which the probability of several particles passing through the orifice simultaneously is negligible. Such recommended maxima vary according to orifice size.

3) Occasionally, the orifice became blocked, causing an obviously anomalous count. Blockages could be observed through the attached microscope and they could be cleared by careful brushing. The problem of blockage was largely overcome by

careful filtration, however the smaller orifices remained susceptible to blockage.

3.4.2.2. Sample preparation

Two methods of sample preparation were used for the Coulter Counter analysis and may be categorised as (1) open vessel runs, and (2) reactor dispersion runs.

1) Open vessel runs.

Samples of a known volume (approximately 3 cm^3) were removed from the parent emulsion. These samples then underwent a two stage dilution to reduce the droplet concentration to a suitable level for use in the Coulter Counter. The first dilution involved mixing the whole 3 cm^3 of the emulsion sample with 80 cm^3 of 1% Nansa solution. This was necessary in order to ensure that the soap level would remain sufficiently high during the dilution process to ensure that the emulsion retained its stability. Three cm^3 of this dilute emulsion were then transferred into 320 cm^3 of electrolyte solution (0.9% sodium chloride solution). The Nansa solution and the electrolyte solution were, of course, filtered through a 0.45 μm filter immediately before use.

2) Reactor dispersion runs

The dispersion study was aimed at supplying data for the emulsion polymerisation studies which were to be carried out in a six inch (152 mm) diameter reactor. This reactor differed from the open vessels in that it had a lid. Dispersion runs were carried out in the reactor to allow comparison with data from the open vessels and also to allow collection of data for the hazardous styrene dispersion.

When sampling from the reactor, samples of various unknown volumes within the range 5 to 10 cm^3 were obtained. It was found that if one

drop of the dispersion removed from the reactor was added directly to 230 cm^3 of electrolyte solution, the resulting dilute emulsion was suitable for analysis in the Coulter Counter. This method bypassed diluting the sample emulsion with soap solution where the new soap could have solubilised some of the organic in the emulsion. As above, the electrolyte solution was filtered through a 0.45 µm filter immediately before use.

3.4.2.3. Analysis of samples

Before the samples could be analysed on the Coulter Counter it was necessary to select the appropriate size of orifice. Photomicrographic analysis of early runs indicated that the droplets in the emulsion were in the size range 5.6 to 112 µm, a range for which a 280 µm orifice was recommended for greatest accuracy. It was found from experience during the Coulter Counter analysis, however, that the dispersions produced did not contain measurable numbers of droplets above 56 µm diameter and thus a 140 µm orifice, sensitive to droplets in the size range 2,6 µm to 56 µm diameter, was more suitable.

After selection of the appropriate orifice size, the Coulter Counter was set up in accordance with the manufacturers operating instructions[63] and the electrolyte, containing the diluted dispersion was introduced into the test cell. One of two modes of analysis were employed as indicated below:

a) Analysis in descending order of size

The threshold setting of droplet diameter was firstly set at a level at the upper end of the range and the droplets in this range were counted first. The threshold was then reduced sequentially until the full range had been covered.

b) Analysis in ascending order of size

The threshold settings were sequentially raised from the minimum in the range.

Both methods of analysis resulted in a cumulative oversize distribution which was converted to a differential distribution by taking the difference between successive counts. A sample table of results is shown in Appendix B. The Sauter mean droplet diameter was calculated from;

$$\bar{d}_s = \frac{\Sigma n_i \, d_i^3}{\Sigma n_i \, d_i^2} \qquad (3.1)$$

Particular problems encountered in using the Coulter Counter with regard to the reproducibility and interpretation of the results are detailed in section 4.3.

3.5 Design of the polymerisation reactor

The experimental programme required the construction of a jacketed pressure vessel suitable for the batch production of styrene and styrene/butadiene (S.B.R.) latices via an emulsion polymerisation. The design of the polymerisation reactor was influenced by a number of factors;

1) The major constraint was that the performance of and product from this reactor were to be compared with those of existing large-scale reactors in order to examine the effects of scale-up. It was essential, therefore, that this vessel and its internals should be geometrically similar to those of the existing vessels.

2) The volume of the reactor should be relatively small so that the use of large quantities of chemicals was not necessary, and thus the running costs could be maintained as low as possible.

3) It was considered from analysis of earlier work that the effect of the impeller speed on the progress of the polymerisation was of prime importance and thus the reactor would have to be fitted with a variable speed impeller system to allow investigation of this.

4) . As the procedure adopted in the existing plant included sequential soap additions then it was essential that a facility for sequential soap addition should be included in the design.

5) The vessel should be designed for safe and reliable operation.

6) A reactor suitable for general use in future projects was desirable.

With these considerations in mind, a reactor was designed.

The VESSEL was fabricated from a section of stainless steel (type 316) pipe of six inch (152 mm) bore and wall thickness 6.5 mm to which a stainless steel end cap conforming to British standard pressure vessel dished-end configuration (B.S. 1966) was welded. Design calculations[64] using a weld factor of 0.6 showed that a vessel constructed of this wall thickness and diameter would be capable of a working pressure of 70 bar, a pressure considerably greater than the immediate requirements.

The vessel was secured to its lid by means of a FLANGE which was again of stainless steel and its dimensions were chosen from B.S. 10 table E. (See figure 3.6).

The vessel LID was constructed from a mild steel blind flange conforming to B.S. 10 table E. The lid was secured to the vessel with eight 3/4 inch B.S.W. mild steel bolts. Initially the lid was rated for a working pressure of14.8 bar, however as it was necessary to drill several holes in the lid (see figure 3.7) to allow for sample probe, impeller shaft, etc., the final maximum working pressure was estimated to be approximately 10 bar. The inner face of the lid was lined with a thin sheet of stainless steel to ensure that the vessel contents came into contact only with stainless steel.

The seal between the vessel and lid was effected by the use of a Fluorlion envelope GASKET which consists of compressed asbestos fibre enveloped with P.T.F.E.

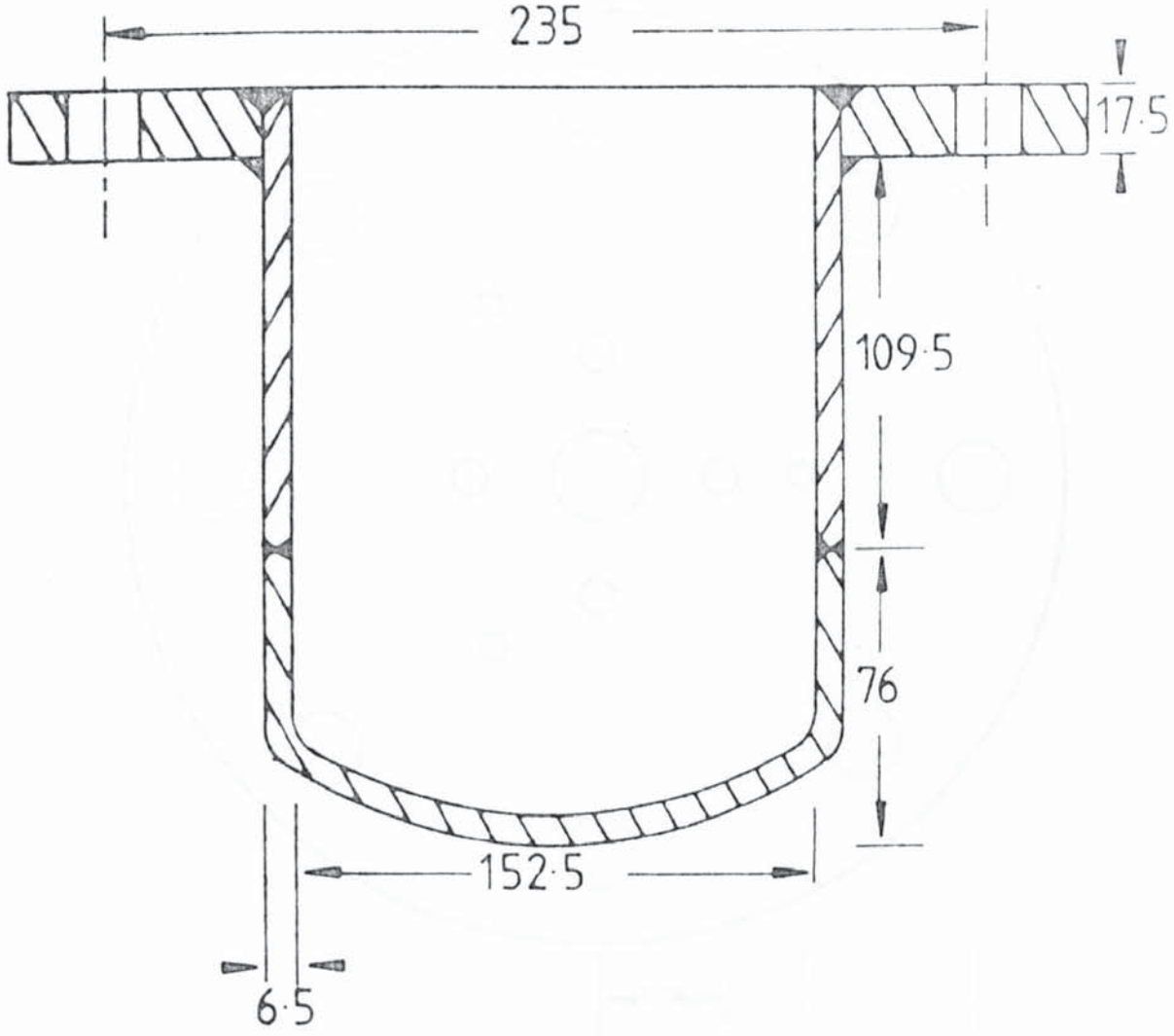

Fig 3·6 Details of reactor vessel construction. Dimensions in millimetres.

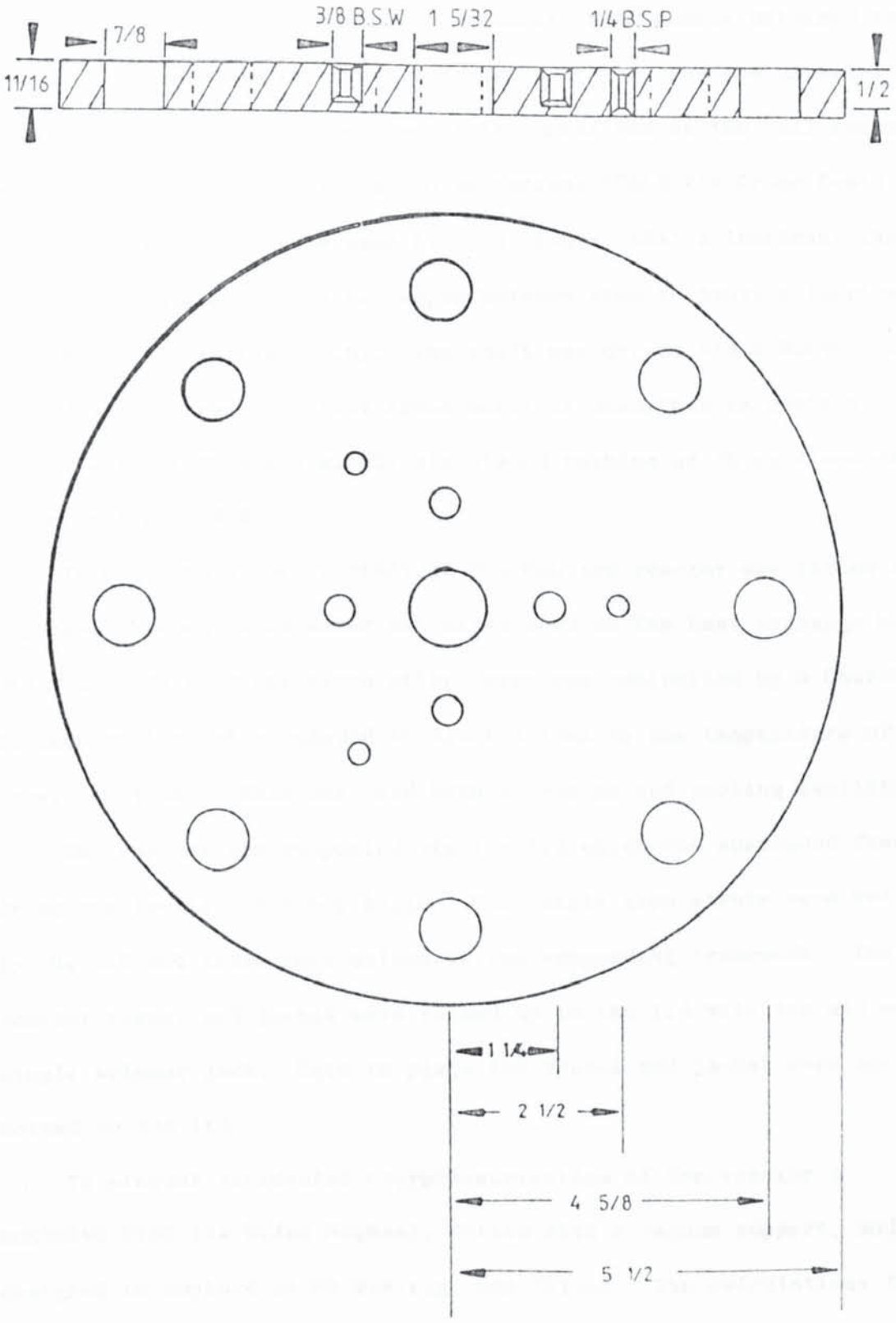

Fig 3·7 Details of reactor lid construction. Dimensions in inches

The IMPELLER SHAFT diameter was dictated by the size of bearings and seals available, of which the smallest, most easily obtained were for a half inch diameter shaft. Accordingly this was the diameter chosen. The shaft was supported at its upper end by two ball races, and it entered the vessel via two mechanical SEALS (Ex Crane Seals Limited). Two seals were used back to back so that a lubricant (an oil/water emulsion) could be pumped between them to provide lubrication and cooling (see figure 3.8). The shaft was driven via a Bowden cable, by a direct current constant speed motor as described in section 3.1.

The IMPELLER was a simple six bladed turbine of 75 mm diameter as shown in figure 3.2.

In order to allow TEMPERATURE CONTROL the reactor was fitted with a jacket through which water was circulated as the heat exchange medium. The temperature of the circulating water was controlled by a Churchill Captain unit which responded to fluctuations in the temperature of the vessel contents. This unit had both a heating and cooling facility.

The reactor was supported via the lid which was suspended from a frame constructed of Handy Angle. Four angle iron struts were welded to the lid and these were bolted to the suspending framework. The reactor vessel and jacket were raised up to the lid with the aid of a simple scissor jack. Once in place the vessel and jacket were securely bolted to the lid.

To prevent accidental overpressurisation of the reactor a BURSTING DISC (ex Elfab Hughes), fitted with a vacuum support, and designed to rupture at 60 p.s.i.g. was fitted. The calculations for the cross sectional area of the bursting disc vent were based on a pressure rise due to a runaway reaction, i.e. a relatively slow pressure rise. The discharge line from the bursting disc was fed into a five litre dump tank.

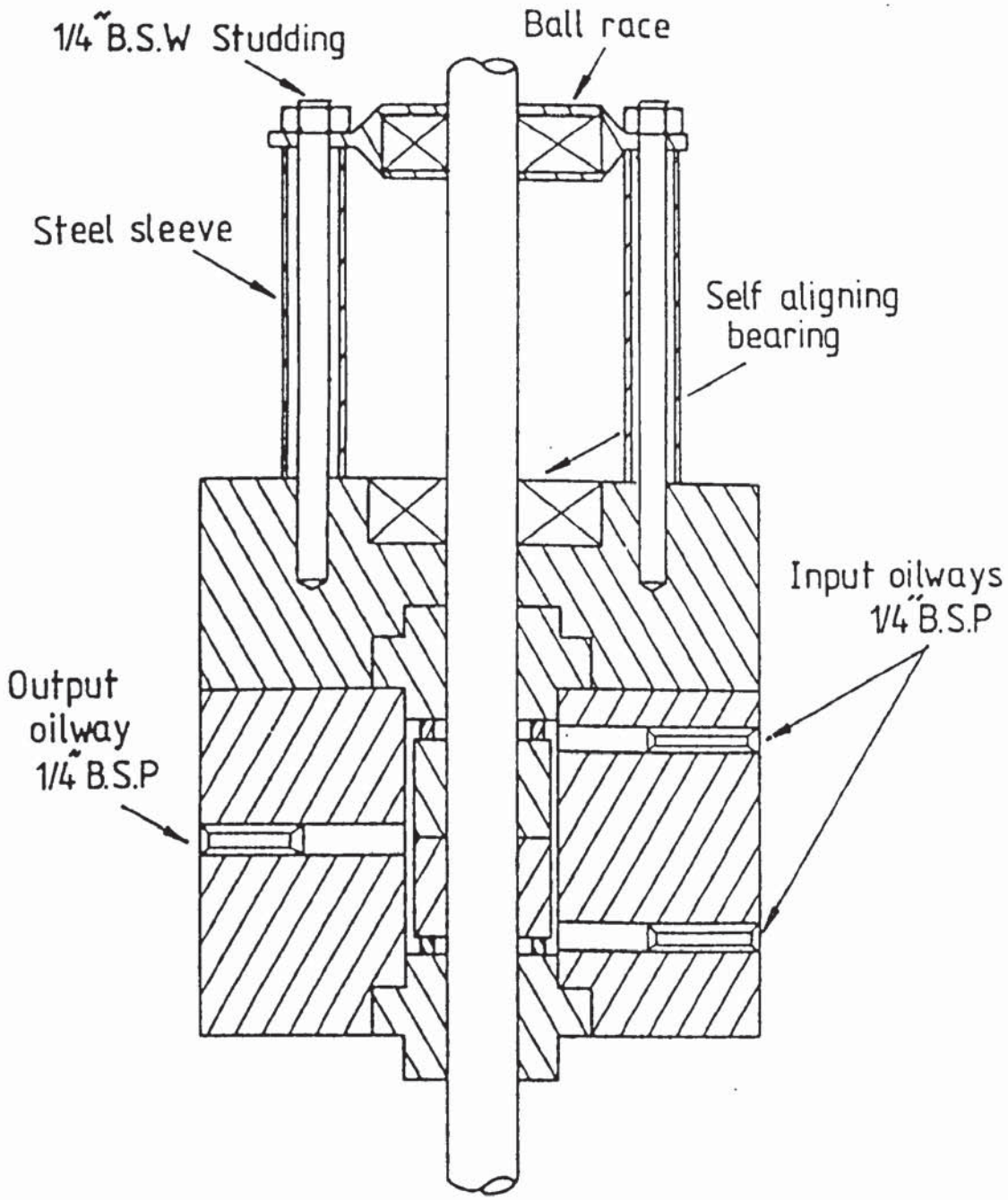

Fig 3·8 Diagram of seal and bearing housing.

In order to contain any leakage of styrene vapour or butadiene gas the reactor vessel was surrounded by an enclosure which was connected to a fume extraction fan. The enclosure consisted of a Handy Angle frame covered with polythene sheet. A door of reinforced Perspex was also fitted on the front of the enclosure to provide added protection to the operator.

As a further safety precaution, the reactor was fitted with a manual vent valve which discharged directly into the fume extraction duct.

A diagram of the reactor and its services is shown in figure 3.9, whilst a photograph is shown in figure 3.10.

In order to facilitate the addition of sequential soap, a CHARGE BOMB was constructed of stainless steel. The bomb was fitted with two diaphragm valves, one at each end, and a length of nylon tube to enable the bomb to be connected to the reactor. The nominal capacity of the bomb was 500 cm^3, and the design pressure was 10 bar. The bomb is shown in figure 3.11.

3.6 Polymerisation recipe

The aim of the project was to investigate the procedures for scaling-up an emulsion polymerisation plant. Data from two existing large scale plant operating on a specific S.B.R. recipe were available and thus it was sensible that that recipe should be used in this project to allow comparisons to be made.

In the preliminary work, however, the polymerisations were to be used to identify the factors that generally affected the progress of the polymerisation and its product latex and thus adherence to the specific recipe was not essential. It was decided that a simpler recipe using

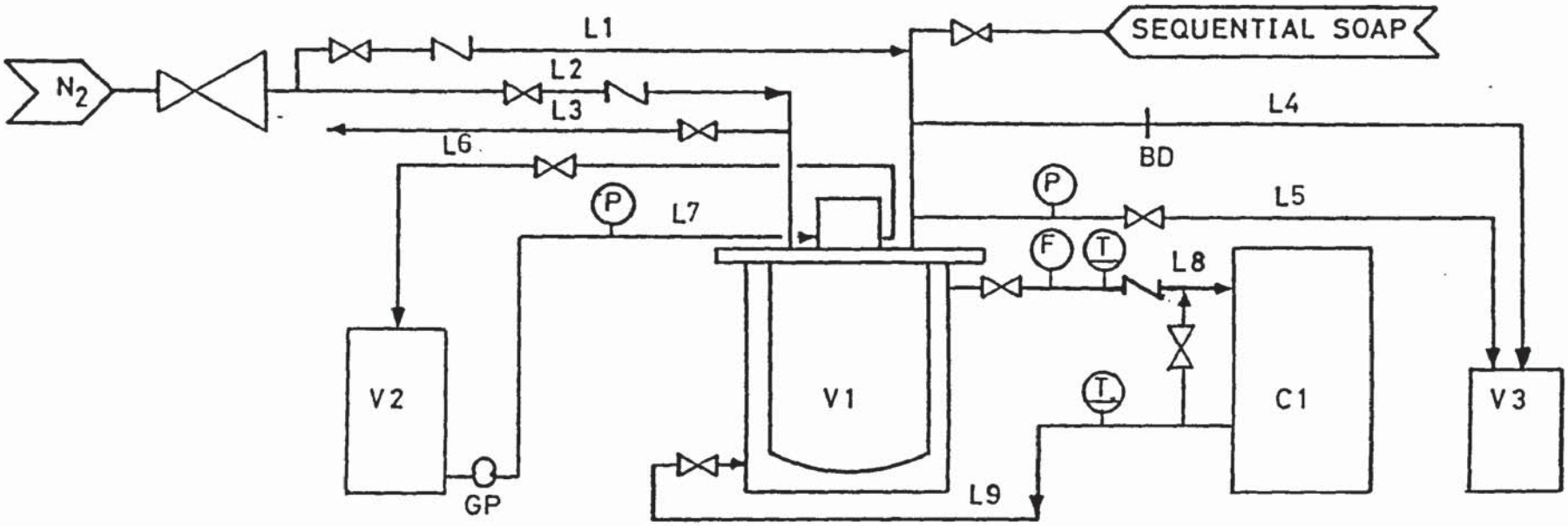

V1 Reactor

V2 Lubricant reservoir

V3 Dump vessel

BD Bursting disc

GP Gear pump

L1 Pressurisation line

L2 Purge line

L3 Sample line

L4 Overpressure vent line

L5 Manual vent line

L6,L7 Seal lubricant lines

L8,L9 Heat exchange fluid lines

C1 Churchill temperature controller

Fig 3·9 Diagram of polymerisation rig

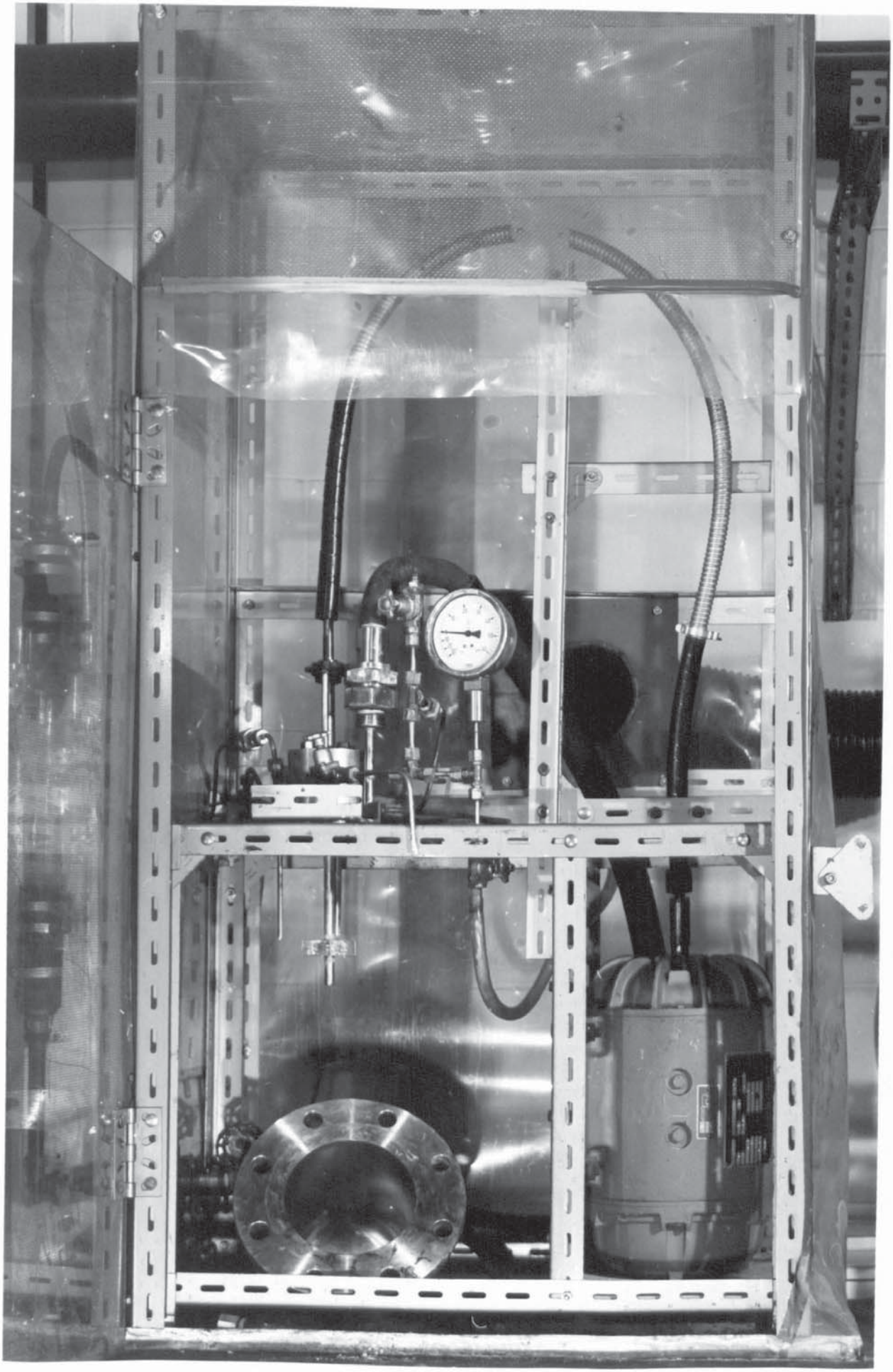

Fig 3·10 Polymerisation reactor.

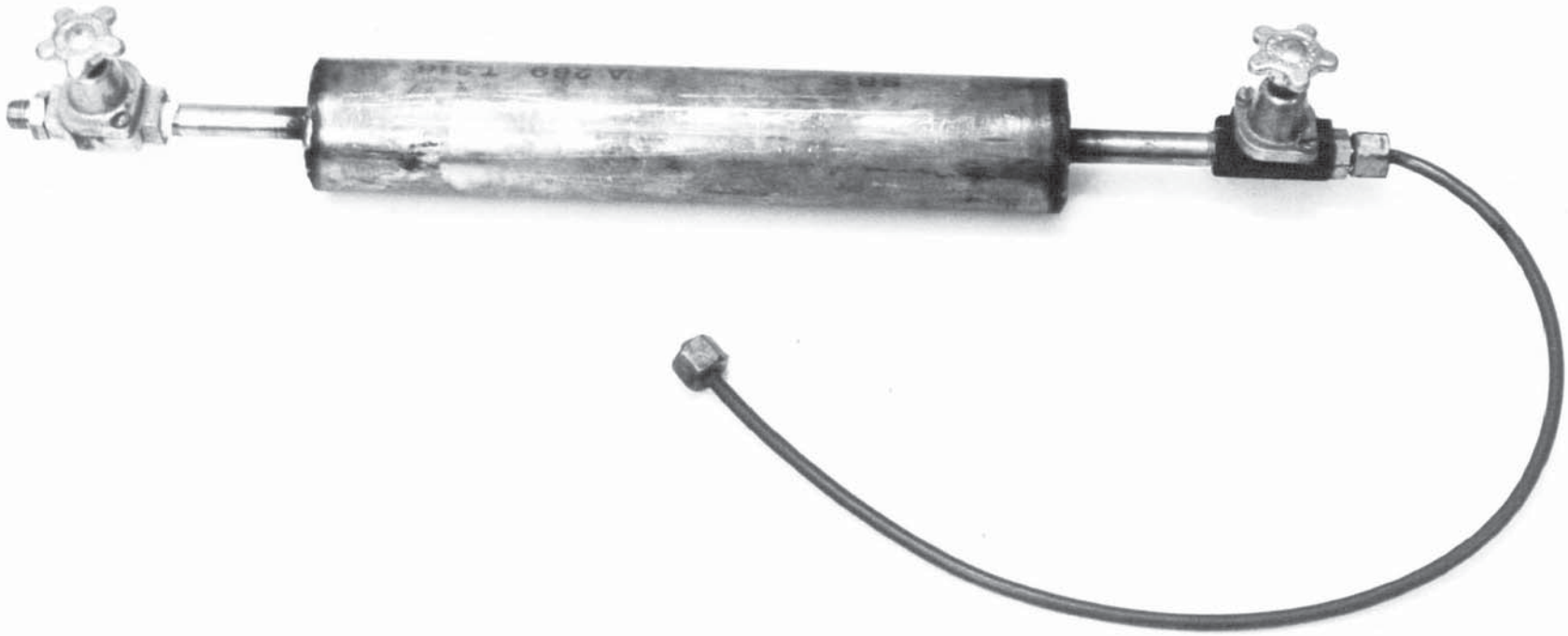

Fig 3·11 Charge bomb.

only styrene and avoiding the problematical butadiene should be used. However, the mixture of electrolytes and surfactants was retained as in the existing process. It was decided that the only chemical variable should be the soap concentration, a limited range of which was studied.

A few runs were attempted using the exact styrene/butadiene monomer recipe in order to allow comparison with the large scale runs carried out. These runs were, however, unsuccessful and thus no results are presented.

The basic recipe is shown in table 3.3

Component	Parts by weight	Typical charge (g)
Styrene	100	1268
Water	70	900
Nansa (soap)	1 - 0.3	12.8 - 4
Potassium persulphate (initiator)	0.2	2.57
Electrolytes	0.55	6.98
Soap) 1st addition	0.99	12.57
Water)	9.46	120
Soap) 2nd addition	1.25	15.91
Water)	11.74	148.82

Table 3.3 Basic emulsion polymerisation recipe

3.7 Polymerisation experiments - experimental technique

Polymerisation experiments were conducted covering a range of variables. Whilst the basic technique was similar throughout, a number of refinements were adopted to cope with specific problems encountered during the tests. These are detailed in the text. The basic experi-

mental procedure may conveniently be divided into three sections; vessel preparation, vessel charging, and rig operation.

3.7.1. Vessel preparation

Prior to a polymerisation run, the reactor vessel and all the reactor internals were thoroughly cleaned. The cleaning involved scouring with an abrasive cloth or brushing with a wire brush, then washing with a 1% Nansa solution and thoroughly rinsing.

3.7.2. Vessel charging

Vessel charging was carried out before the vessel was bolted to the reactor lid. For all the early polymerisation experiments (up to P5) the following procedure was followed. The electrolytes and initiator, in solid form, were weighed out and charged into the vessel. A measured volume (200 cm^3) of a stock Nansa solution was then added followed by a measured volume of water (700 cm^3). Finally a measured volume (1400 cm^3) of styrene was charged into the vessel. For later runs (from P6 onwards) the method was changed slightly to improve the consistency of the vessel charges. Rather than measure the volumes of the styrene, soap and water, weighed amounts of these materials were used, as it was easier to reproduce weights of large quantities rather than volumes.

Conversely, the electrolytes, with the exception of the initiator (potassium persulphate) were made up into standard solutions. In this case it was more accurate to weigh out the relatively large quantities required to make up standard solutions. Use of a pipette allowed accurate measurement of the volumes of electrolyte solution required.

The charging sequence was similar to that of the previous runs, i.e. firstly the electrolyte solutions were charged followed by the initiator in solid form, followed by the soap, water and finally the monomer.

3.7.3. Rig Operation

After the vessel had been charged, it was, together with its jacket, bolted to the reactor lid. The temperature control jacket was connected via flexible hoses to the Churchill temperature control unit. The temperature at which the reaction was to be performed (i.e. 50°C) was selected on the Churchill unit and the unit activated.

Oxygen is widely reported to act as an inhibitor of polymerisation and in order to avoid this problem the contents of the reactor vessel were purged with nitrogen (white spot grade) by successively pressurising the reactor to approximately 3 bar and then venting to atmospheric pressure. This was performed five times. On the fifth venting the vessel was vented down to about 1.5 bar, the operating pressure. After completion of purging the agitation was commenced.

The progress of the reaction was monitored by measuring the solids content at half hourly intervals until the sequential soaps had been added and thereafter at one hourly intervals.

The samples for solids content analysis were drawn off through the dip pipe. When the valve was opened the excess pressure in the vessel drove a sample out of the vessel for collection. At each sampling a quantity of the latex was firstly run off as waste to ensure that the dead volume within the dip pipe had been flushed out. A small sample of latex, usually less than 30 cm^3, was then run into a 150 cm^3 Winchester bottle. A drop of short stop (5% sodium dimethyldithiocarbamate) was added to halt the polymerisation. Both the waste latex and the sample were weighed. At the time each sample was removed, the reactor temperature and pressure were recorded.

Where sequential soap addition was necessary the soap was introdused by means of a pressurised charge bomb. (see figure 3.11). The necessary weight of soap solution was poured into the bomb via a funnel,

the bomb was then purged with nitrogen before being pressurised, again with nitrogen, to about 3.5 bar. The bomb was connected to the vessel charge port via a translucent nylon tube. Firstly the bomb valve and then the vessel valve were opened and the soap charge was driven under pressure into the vessel. The point when all the soap had entered the vessel could be clearly observed through the nylon pipe. The valves were then closed and the residual pressure in the bomb released.

The sequential soaps were either added when previously, arbitrarily decided levels of total solids content (T.S.C.) were reached or when a sample indicated that soap addition was necessary in order to alleviate a tendency to instability of the monomer emulsion. This tendency to instability was clearly indicated by the samples, as on withdrawal the monomer would settle out as a clear upper layer if the free soap concentration was falling too low. The severity of this instability was indicated by how rapidly this clear layer formed. Experience allowed an estimate of the T.S.C. values at which instability of the monomer dispersion was likely to become a problem and it became possible, therefore, to decide beforehand at which values of T.S.C. extra stabilising soap should be added in order to prevent instability and coalescence. In gaining experience, however, some experiments had to be aborted due to excessive coagulation. (see figure 3.12).

Early experiments were run to completion (approximately 50% T.S.C.) before a final sample for particle size analysis was removed. However, as the actual final degree of conversion was found to vary, it was decided for consistency to stop the reaction at a given total solids content of 35%. Accordingly, samples for particle size analysis were thereafter removed at a total solids content of as close to 35% as it was possible to estimate. Although short stop was added to these samples, in practice it was found that a T.S.C. increase of up to 10% was possible

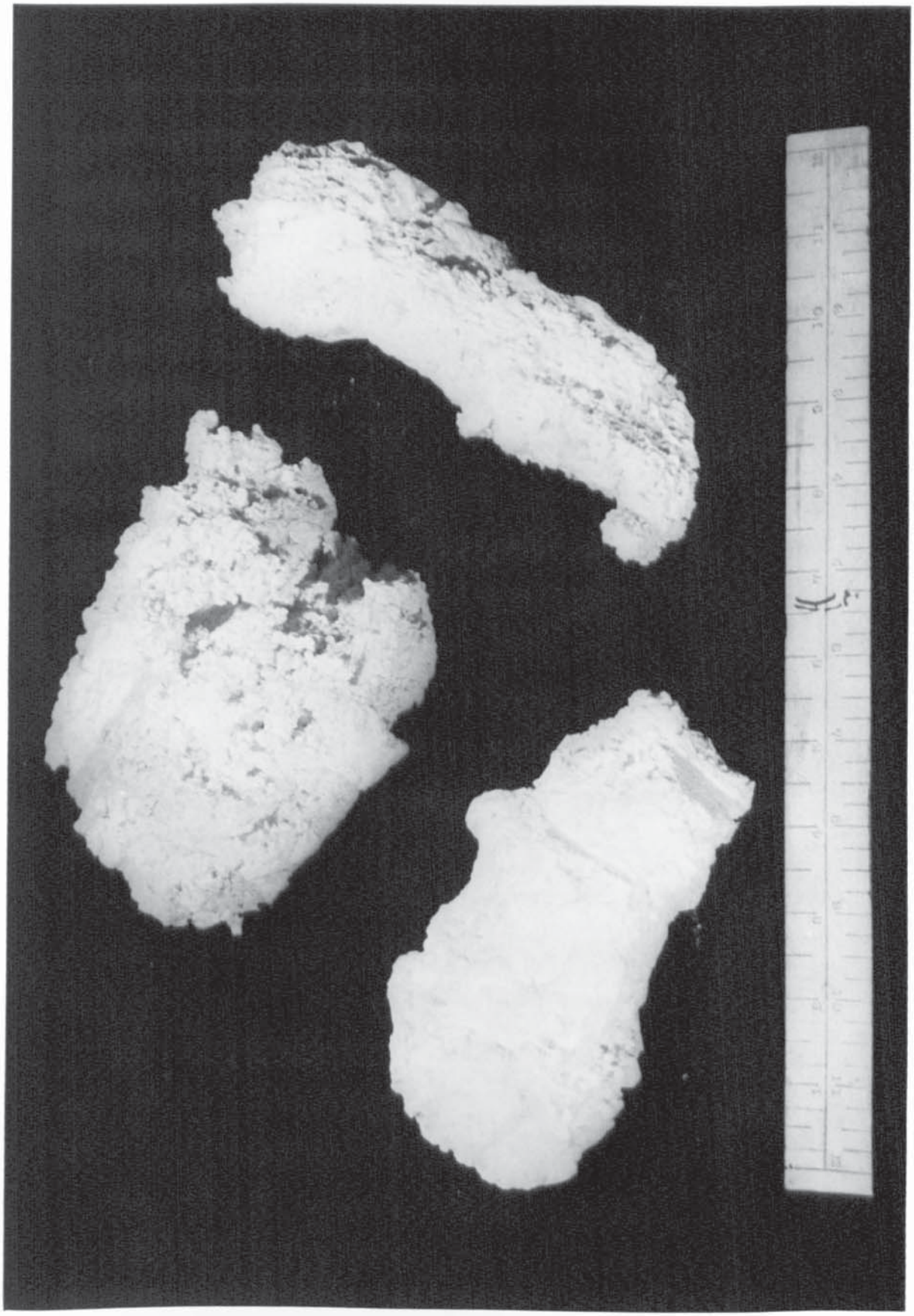

Fig 3·12 Assorted coagulum. Ruler (12 inch = 305mm) shows scale.

within the sample bottles. This led to difficulties in particle size analysis which are discussed in section 5.2.

3.7.4. Monitoring of reaction

The progress of each reaction was monitored by measuring the total solids content of samples removed from the bulk latex at regular intervals as detailed in the previous section. The T.S.C. was determined by weighing a small sample of the latex then drying to constant weight by heating the sample in a stream of hot air. The dried sample was re-weighed and the total solids content calculated thus,

$$\text{T.S.C.} = \frac{\text{Dry sample weight}}{\text{Wet sample weight}} \times 100\% \qquad (3.2)$$

It should be noted that there was a base solids content (approximately 1%) due to the soap, both initial and sequential, and electrolytes present. Thus the polymer solids content (P.S.C.) is given by

$$\text{P.S.C.} = \text{T.S.C.} - \text{base solids} \qquad (3.3)$$

Generally, however, T.S.C. values were sufficiently accurate for monitoring the progress of a reaction and it was not necessary to correct the P.S.C.

3.8 Latex particle size analysis

Four techniques for the measurement of submicronic particle sizes are prominent in the literature[25]. The techniques are; electron microscopy, soap titration, light scattering and light transmission. Details of these techniques may be found in section 2.2.5. Of the four options, light transmission was chosen as the most logical technique for this project, as suitable equipment was readily available and a

basic method was described in the literature[22]. Although electron microscope facilities were available, electron microscopy was dismissed as unsuitable as it was anticipated that a large number of micrographs would have been needed for a full analysis.

Of the other available techniques, soap titration was dismissed because the soap used in the recipe for the polymerisation was of a commercial grade, which although primarily consisting of sodium-dodecylebenzenesulphonate also contained a mixture of other surfactant molecules. This meant that accurate data regarding the specific area of the soap was not easily obtained. In addition, the technique of measuring surface area by soap titration promised to be tedious.

Finally, light scattering was not considered as an appropriate techniques for measuring the final particle size for the purely practical reason that suitable equipment was not available.

3.8.1. Latex particle size analysis by light transmission

Two methods of analysis using light transmission have been described in the literature. Both techniques involve measuring the turbidity of a diluted latex at a number of wavelengths of light. The method described by Bateman et al[22] required knowledge of the polymer particle concentration whilst that of Barnes et al[23] offered a means of calculating both particle size and concentration and would have been the obvious choice for this project. This latter technique, however, involved the superposition of the maxima of the experimentally determined light transmission spectra onto the maxima of the theoretically calculated spectrum. It was observed, however, in a preliminary check that a smooth transmission curve, without any identifiable maxima was obtained for a polystyrene latex and thus it would have proved impossible to locate with confidence the corresponding range on the theoretical curves.

The choice of latex particle size analysis technique was therefore restricted to the method which Bateman et al[27] had developed for polystyrene latices. Essentially this method involved measuring the turbidity of a dilute polystyrene latex and then calculating the value of a parameter K/α, from equation 3.4.

$$K/\alpha = \frac{0.4887\ \rho_p E}{(n/\lambda)\ c.l.} \qquad (3.4)$$

where

K = the extinction coefficient (cm^{-1})

ρ_p = the density of a polymer particle ($g.cm^{-3}$)

c = the mass concentration of polymer per cm^3 of fluid ($g.cm^{-3}$)

l = the cell length (cm)

λ = the wavelength of light in air (cm)

E = $\log I/I_o$

I_o = incident light intensity

I = transmitted light intensity

n = $a + \frac{b}{\lambda_o^2}$ = refractive index of particles

For polystyrene $a = 1.5683$ $b = 10.087 \times 10^{-11}$

For water $a = 1.324$ $b = 3.046 \times 10^{-11}$

α = $2.\pi.r.n/\lambda$

r = particle radius

Bateman et al[27] have published tables of theoretically determined values of K appropriate to given wavelengths and particle radii. A value of the particle radius could thus be obtained by interpolation, where necessary, from this table (table 3.4). Values of r could be obtained from turbidity tests at a number of wavelengths and the mean value taken as the particle radius of the four latices studied by Bateman et al[27], results obtained by light transmission in three cases were within 1% of the results obtained from electron microscopy.

r(nm) / λ_o(nm)	80	132	1940	255.5	3300	407	500	585.5	700
370	0.232	0.802	1.703	2.595	3.438	3.743	3.352	2.637	1.863
430	0.144	0.526	1.185	1.945	2.792	3.450	3.723	3.458	2.710
500	0.0891	0.333	0.809	1.387	2.147	2.864	3.466	3.698	3.494
560	0.0614	0.232	0.611	1.084	1.730	2.400	3.084	3.500	3.691
650	0.0360	0.153	0.416	0.767	1.275	1.843	2.515	3.031	3.520
750	0.0211	0.102	0.276	0.543	0.935	1.400	1.986	2.506	3.090

Table 3.4 Values of the light extinction coefficient K.

After Bateman et al

3.8.2 Equipment for turbidity measurement

A Pye Unicam SP 1800 ultraviolet spectrophotometer was available for the measurement of the light attenuation. Sample cells of one, two and four centimetre length were available and a wavelength range of between 200 nm and 700 nm could be used.

A value of $\log(I_o/I)(E)$ was directly read on the meter of the spectrophotometer.

3.8.3 Preparation of the sample for analysis

The latex was optically too dense to allow direct turbidity measurement. It was necessary, therefore to dilute the latex. The dilution was carried out in two stages. Firstly approximately one gram of the latex was weighed into a tared 150 cm^3 bottle. Distilled water was added to give a total sample weight of approximately 100 grams. Further dilution was then performed by again weighing out approximately one gram of the first dilute sample and making up to 100 grams with

distilled water. This final dilute sample was then of a suitable concentration for analysis in the spectrophotometer.

3.8.4. Test procedure

Glass cells of one centimetre length were used for the analysis although in order to check the effect of cell length on the results one latex was analysed using cells of one, two and four centimetre lengths. A slit width of 6.5 nm was set before two cells containing distilled water were positioned so that the spectrophotometer could be set to zero. One cell was then removed and rinsed twice with the intended sample before being filled with the sample and repositioned in the spectrophotometer. A direct reading of E was obtained at five wavelengths (370, 430, 500, 560, 650 nm).

The results of this analysis are shown in section 5,2

4.0 RESULTS OF DISPERSION EXPERIMENTS

4.1 Sampling

4.2 Photomicrographic analysis

4.3 Coulter Counter analysis

4.4 Power input data

4.0 RESULTS OF DISPERSION EXPERIMENTS

The investigation of the factors influencing the monomer dispersion stage of emulsion polymerisation involved a range of experiments. These experiments were designed to study the relationship betweem the mean droplet size of the dispersed monomer and the impeller diameter and the impeller speed. The experiments involved the use of a series of unbaffled vessels covering the diameter range 152 mm to 305 mm of which three were open and one was closed, two different analysis techniques and a number of soap concentrations.

Although the analytical techniques used encountered some problems, and some of the data suffered high levels of scatter, some definite trends were discernible. These trends led to the proposal of a relationship between the mean droplet diameter and the impeller diameter and speed.

4.1 Sampling

The analysis of droplet size in the dispersion required the withdrawing of samples of the dispersion from a point source in the mixing vessel and as Sprow[50] had indicated that the location of withdrawal had a significant effect upon the measured droplet size of his dispersions, it was felt necessary to carry out preliminary checks on the effect of sampling position on the mean droplet size data. Similarly it was appreciated that the attainment of the final steady state doplet dispersion was not instantaneous and a preliminary investigation was carried out to determine a suitable time period in which to allow the emulsion to come to equilibrium before sampling.

4.1.1. Sampling location

An experiment was conducted where a toluene/water emulsion was

formed at 300 r.p.m., for which an initial soap concentration of 12.8 $g.dm^{-3}$ was employed. The organic/aqueous phase ratio was 0.59. The vessel diameter was 152 mm (6 inches). Samples were taken from three positions close to the vessel wall as shown in figure 4.1.

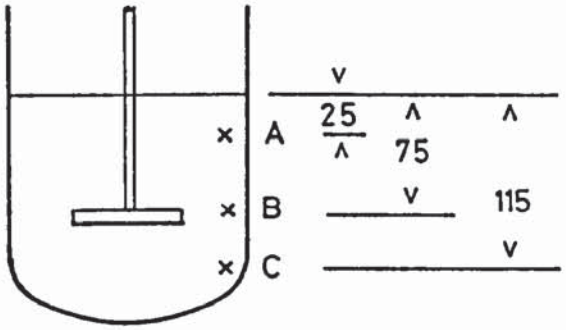

Fig 4·1 Sampling positions.
Dimensions in millimetres.

Photomicrographic analysis according to the technique described in section 3.4.1 was carried out on the samples, and a final magnification factor of approximately 550 was achieved. The results are shown in figure 4.2 as a plot of size distributions.

It may be seen from figure 4.2 that there was little difference between the distributions. The modes of all three distributions are coincident. The Sauter mean diameters obtained at positions A, B and C were, respectively, 14.88 μm, 13.66 μm and 13.77 μm. Obviously there is no significant difference between the Sauter mean diameters obtained at sample positions B and C. The Sauter mean diameter obtained at position A is approximately 8% greater than the other two, and this may be an effect of coalescence. If this were the case, however, it would be expected that the whole size distribution would show a shift towards larger droplets. This was not the case and it appears, therefore, that, despite its high dispersed phase fraction,

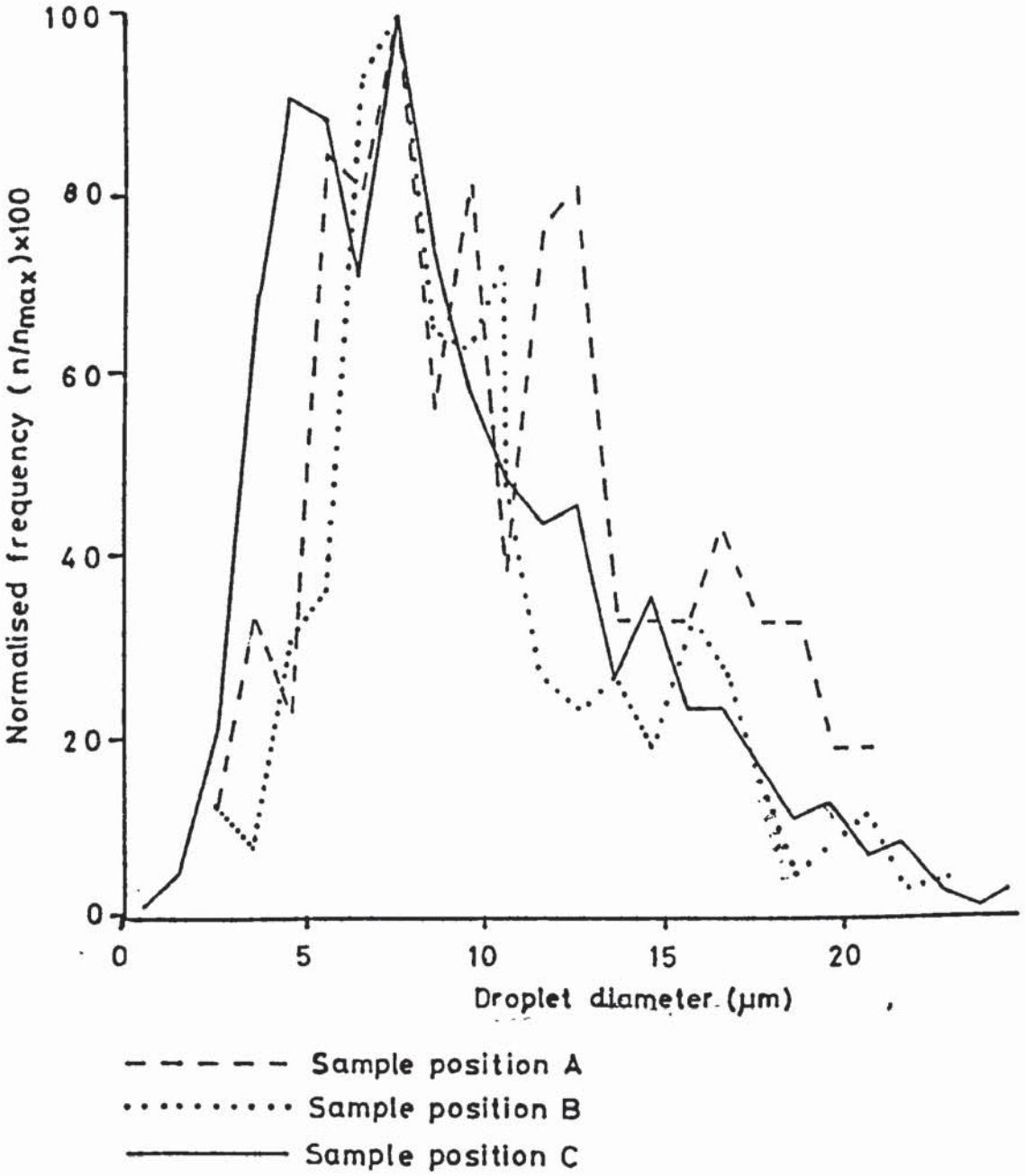

Fig 4·2 Droplet size distributions obtained at sample positions A, B and C. $\phi = 0{\cdot}59$, $S = 12{\cdot}8 g.dm^{-3}$, D = 75mm, N = 300 r.p.m.

this emulsion when stabilised by a soap displays a reasonable degree of homogeneity in terms of both the spacial droplet size distribution and the spacial mean droplet size distribution. This suggests that the results of the studies of the dependence of droplet size on impeller speed may be taken to be insensitive to the location of the sample removal point. Sampling during these experiments was, however, carried out at the same relative positions to ensure that any possible inhomogeneity had the minimum effect on the comparison of results.

It is of interest to compare these results with those of Sprow[50] who found during his studies of the effect of the sampling location on the mean droplet size, for strongly coalescing systems there was a definite difference between mean droplet size near the impeller and that near the surface of the liquid (approximately 30%). His studies, however, of non-coalescing systems[65], achieved by the use of very low dispersed phase fractions, showed no discernible variation in mean droplet size with sampling location. This would suggest that the addition of surfactant induces these non coalescing properties even at the high dispersed phase fractions found in the current study.

4.1.2 Timing of sampling

In order to ensure that the time interval between setting the impeller speed and taking a sample was adequate to allow steady state to be achieved, a simple experiment was conducted. The 152mm diameter closed vessel was charged with toluene, water and soap (Nansa) to give an organic phase fraction of 0.59 and an initial soap concentration of 8.0 $g.dm^{-3}$. An impeller speed was selected and samples were taken at regular intervals after agitation had commenced. Analysis was carried out using the Coulter Counter. The results, shown in figure 4.3, show little change in the droplet diameter beyond 20 minutes. Accordingly this was chosen as the minimum stirring time before sampling in all of the dispersion experiments.

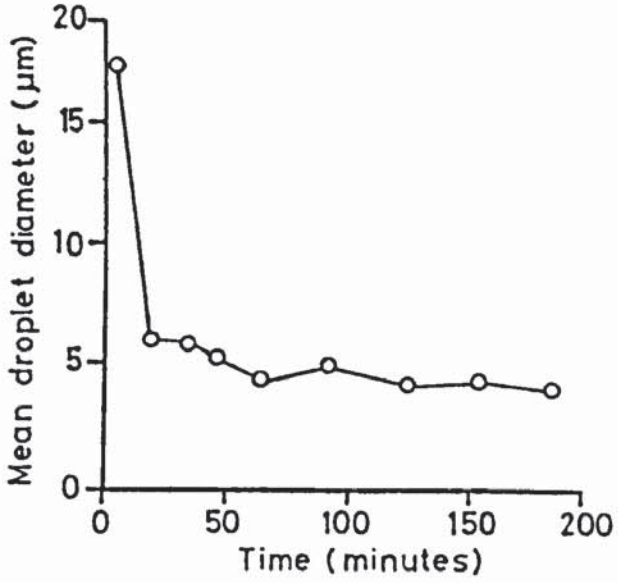

Fig 4·3 Plot of mean droplet diameter against time. $\phi = 0{\cdot}59, S = 8{\cdot}0\ g.dm^{-3}$, D=75mm, N=520r.p.m.

4.2 Photomicrographic analysis

The droplet dispersion data presented below was gained using two techniques of photomicrographic analysis; the first allowing a final magnification factor of 65 and the second allowing a factor of 550. Figure 4.4 shows a comparison of photographs of similar samples at the two magnification factors. The lower magnification factor did not allow a complete and accurate analysis of the dispersions and the data obtained showed a considerable degree of scatter. The results from this first analysis, therefore, are presented as a preliminary study only but they are results which show some interesting and useful trends. The data collected at 550 x magnification did not cover a wide range of experimental variables. They were collected, however, to allow comparison with and a check of the calibration of the Coulter Counter data.

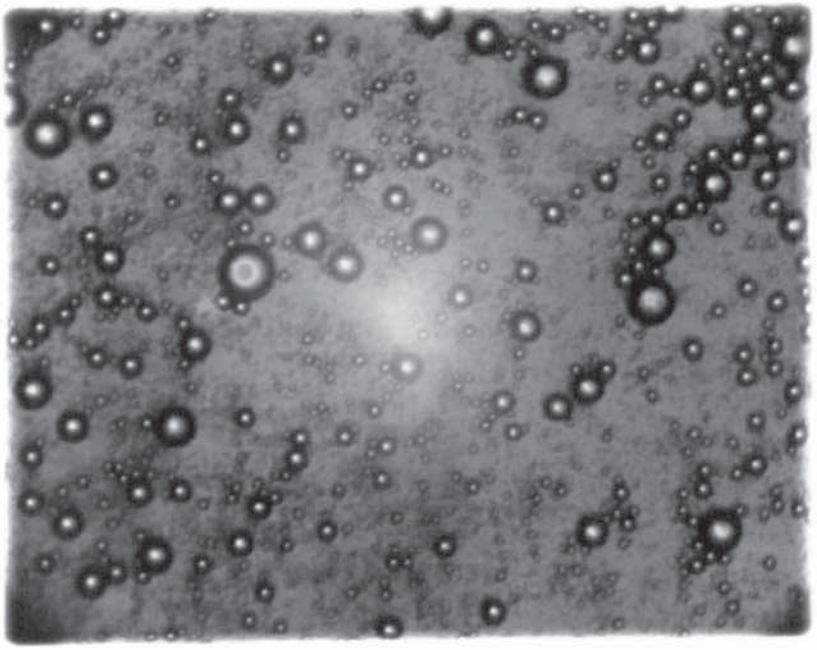

a) Magnification factor = 65

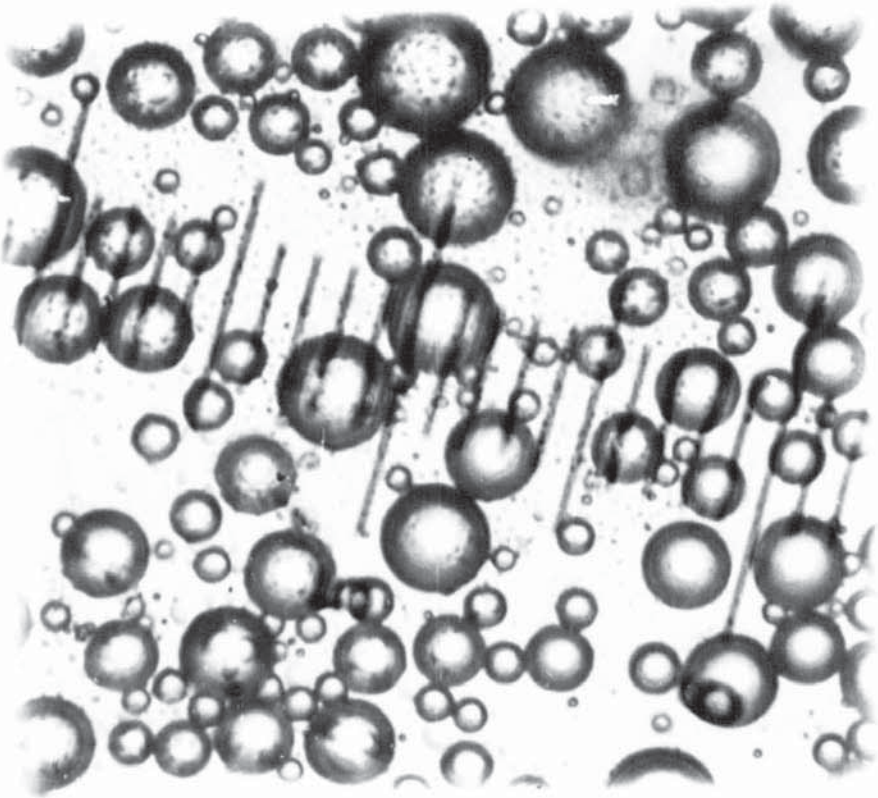

b) Magnification factor = 550

Fig 4·4 Comparison of photographs used in photomicrographic analysis.

The photomicrographic analysis of this first series of dispersion experiments, using a magnification factor of 65 x, was carried out using Birmingham mains water and a range of soap concentrations, impeller speeds and vessel sizes. The results are shown in figures 4.5 to 4.7 and in Appendix C (table C1). The most striking feature of this set of graphs is the high level of scatter in the data. Indeed the scatter of the data is sufficient to prevent use of this data to correlate a scale-up equation for equal dispersion. Closer inspection of the graphs, however, reveals that the scatter of the data tends to progressively worsen as the vessel size increases, although this may be due to the fact that fewer data points were obtained for the two larger vessels.

These data were obtained during a series of experiments for which the impeller speed was progressively increased between sampling without returning the impeller speed to zero. In order to check the effect of this procedure on the data a second technique was adopted for which, in fact, the impeller was stopped after each sampling and the dispersion allowed to break before setting the impeller speed at the next test value. The results of one of these experiments (D13) is shown in comparison with the results of experiment D2 in figure 4.8. These results do not appear to be any better than the previous experiments (D1 - D12) in that they show no less scatter. Nor, as far as may be judged through this scatter, do they show any significant effect on the Sauter mean droplet diameter of the differing procedures.

Probably the most signficant factor concerning the scatter of the data obtained at the lower soap concentration ($S < 1.0$ g.dm^{-3}) was the stability of the emulsion. For example, it was observed that at the lower soap concentrations, the emulsions tended to break into two

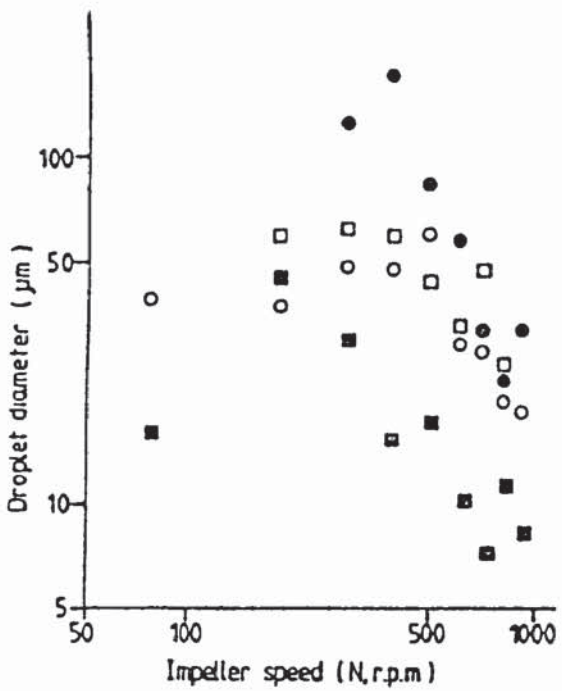

Fig 4·5 Logarithmic plot of Sauter mean droplet diameter against impeller speed. Photomicrographic analysis, open vessel, D=75mm, ϕ = 0·59, toluene. Temp = 50°C.

- ● S = 0 g.dm^{-3} = soap conc.
- □ S = 0·093 g.dm^{-3}
- ○ S = 0·44 g.dm^{-3}
- ■ S = 9·06 g.dm^{-3}

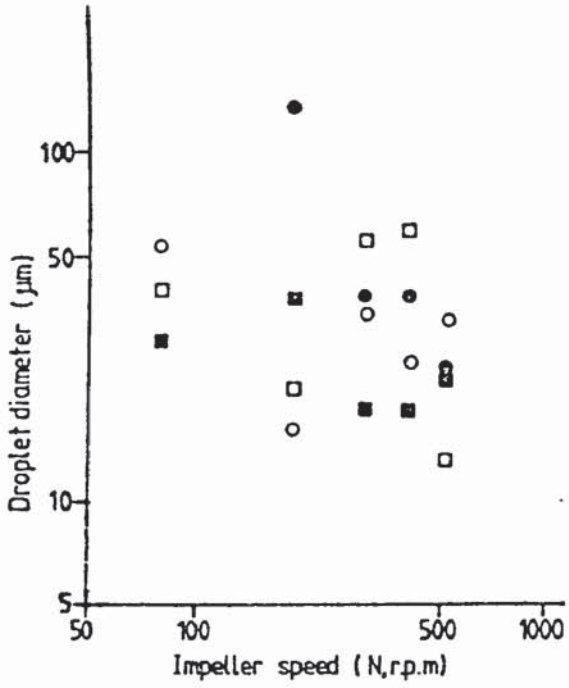

Fig 4·6 Logarithmic plot of Sauter mean droplet diameter against impeller speed. Photomicrographic analysis, open vessel, D=114 mm, ϕ = 0·59, toluene. Temp = 50°C.

- ● S = 0 g.dm^{-3} = soap conc.
- □ S = 0·086 g.dm^{-3}
- ○ S = 0·39 g.dm^{-3}
- ■ S = 9·10 g.dm^{-3}

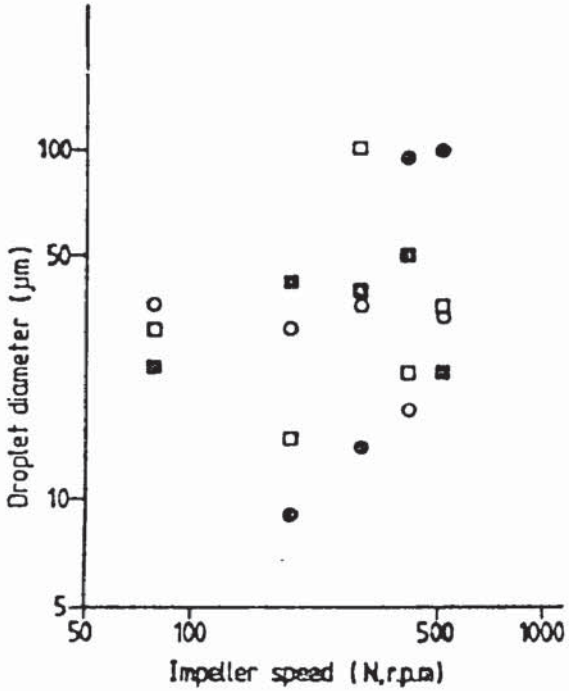

Fig 4·7 Logarithmic plot of Sauter mean droplet diameter against impeller speed. Photomicrographic analysis, open vessel, D=152mm, ϕ = 0·59, toluene. Temp = 50°C.

- ● S = 0 g.dm^{-3} = soap conc.
- □ S = 0·095 g.dm^{-3}
- ○ S = 0·041 g.dm^{-3}
- ■ S = 8·84 g.dm^{-3}

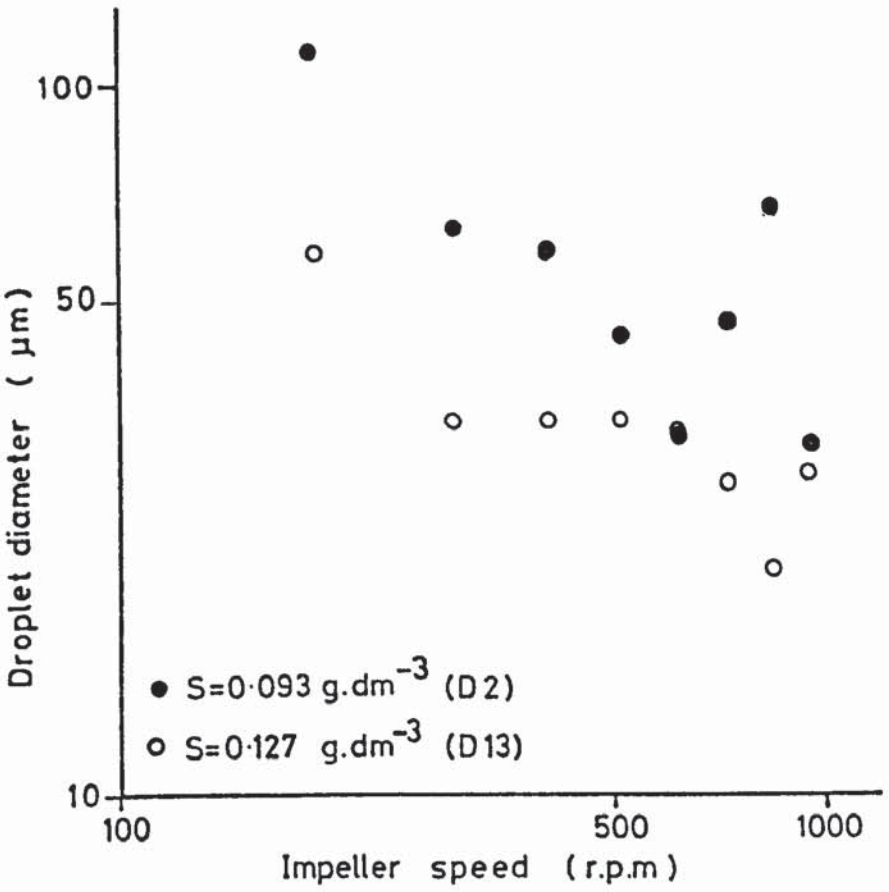

Fig 4·8 Sauter mean droplet diameter vs. impeller speed.
152mm diameter open vessel.75mm impeller diameter.
ϕ=0·59, toluene.

distinct layers within a few hours of the agitation ceasing. In the case of zero soap, this time reduced to a few minutes. This suggests that the emulsion formed at the lower soap levels were relatively unstable in the absence of agitation. In order to overcome the problem of instability the samples for analysis were dispersed into a soap solution of concentration 10 g.dm^{-3} in order to stabilise them but it is possible that some coalescence could have occurred during transfer of the sample from the bulk emulsion to the diluting soap solution. Such assumptions, however, are less likely to be valid for the emulsions formed at the higher soap concentrations (S ≈ 9.0 g.dm^{-3}).

In the light of the scatter of the data, it is probably only worth discussing figure 4.5 in any greater detail. In this figure, a general trend may be distinguished. As the soap concentration increases, the Sauter mean drop diameter for a given impeller speed may be seen to decrease. This is the expected trend.

It is, however, of interest to note that each data set exhibited a maximum which was not expected, but may be explained in terms of incomplete dispersion of the organic phase[66]. If a proportion of the organic phase remains undispersed, this would effectively reduce the apparent organic phase holdup in the aqueous phase and a low holdup is, of course, consistent with a reduced droplet size. Further experiments to test this theory were not performed as emulsion polymerisation demands complete dispersion of the monomer. It was considered necessary, therefore, only to ensure that further experiments were carried out in such an impeller speed range as to avoid incomplete dispersion.

One further observation may be made. In figure 4.5 the data points for the high soap run ($S = 9.06\ g.dm^{-3}$) all, with the exception of the 80 r.p.m. point, lie around a regression line with a slope of -1.10. The significance of this is that the gradient of -1.10 is of a similar order as the gradient of -1.20 derived from equations for predicting droplet diameter where droplet breakup is predominant, i.e.

$$\frac{\bar{d}s}{D} = f(\emptyset)\ \left(\frac{N^2 D^3 \rho}{\sigma}\right)^{-0.6} \qquad (4.1)$$

Despite the excessive scatter of the data, the earlier experiments usefully indicated a suitable range of impeller speed with which to work in later experiments.

4.3 Coulter Counter analysis

Measuring and counting the large numbers of droplet images required by photomicrographic analysis proved to be both time consuming and tedious. In addition, the results did not appear to be particularly accurate. An alternative analysis technique was, therefore, sought.

The Coulter Counter promised to provide a rapid and convenient method of analysing the droplet size distribution of a large number of emulsions. This technique, however, although considerably more rapid than photomicrographic analysis suffered from a few problems mainly stemming from the disappearance of emulsion droplets from the electrolyte vehicle in which they were suspended. These difficulties are indicated together with the techniques adopted to overcome them.

4.3.1 Coulter Counter: Droplet disappearance

The major problem encountered in using the Coulter Counter was the apparent disappearance of droplets from the electrolyte solution during the test. This problem first became apparent when using a descending order analysis technique, (a size distribution being obtained by successively reducing the threshold level. See section 3.4.5). The Coulter Counter results are readily presented as a cumulative oversize distribution and figure 4.9 shows typical results that would be expected for a cumulative oversize distribution, compared with a typical result experienced in these tests. As may be seen the experimental count fell off at the smaller diameters, (corresponding to low threshold levels) indicating that total droplet numbers were reducing. Three possible causes of this apparent disappearance of droplets were considered, these being coalescence, dissolution and evaporation. There is, however, evidence that neither coalescence nor dissolution were significant factors in the disappearance of the droplets. Figure 4.10 shows the results of an analysis for which the threshold setting of the Coulter

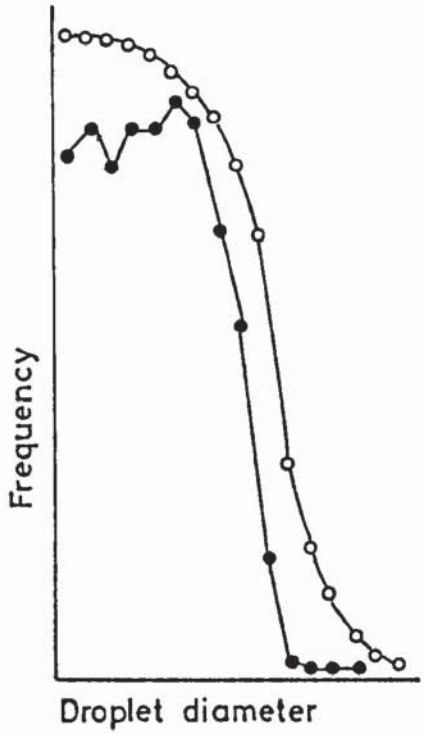

Fig 4·9 Diagram of the expected type of cumulative oversize distibution curve (o) from Coulter Counter analysis compared with actual result (•).

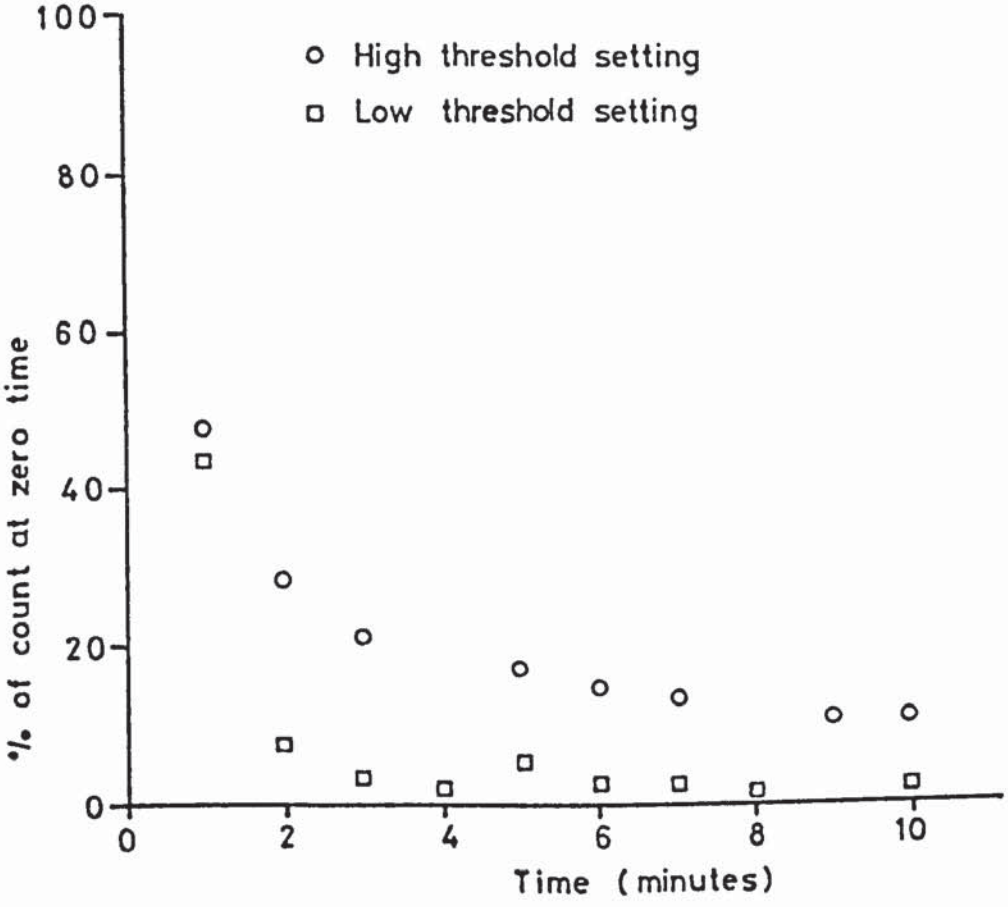

Fig 4·10 Particle frequency in a sample under analysis vs time as measured with a Coulter Counter.

Counter was maintained at a constant setting and counts were made over a period of time. The electrolyte solution used had been pre-saturated with toluene thus eliminating the possibility of dissolution and as may be seen the number of droplets counted reduced over a period of time. If coalescence was occurring, the droplet count would not be expected to fall as droplets previously below the threshold size, and thus not counted, would coalesce into droplets large enough to be counted.

This test clearly suggests that the disappearance of droplets could be identified with evaporation of organic from the surface of the dispersion. To tackle the problem of evaporation it would have been necessary to have saturated the vapour space above the electrolyte solution with the organic vapour. Due to the flammable nature of the organics used, and the fact that the Coulter Counter incorporated an agitator driven by a non flame proof electric motor, saturation of the vapour space above the electrolyte solution was not considered practicable.

4.3.2 Comparison of photomicrographic and Coulter Counter dispersion data

Because of the difficulties experienced with the Coulter Counter, it was thought prudent to compare results obtained from the Coulter Counter with results obtained with another analysis technique such as photomicroscopy. Results obtained by photomicrographic analysis of a sample emulsion using the more sensitive magnification factor (i.e. 550x) were, therefore, compared with results obtained using a full combination of ascending order analysis, descending order analysis, the 140 μm orifice and the 280 μm orifice. The results are shown in figures 4.11 amd 4.12, from which a number of observations may be made.

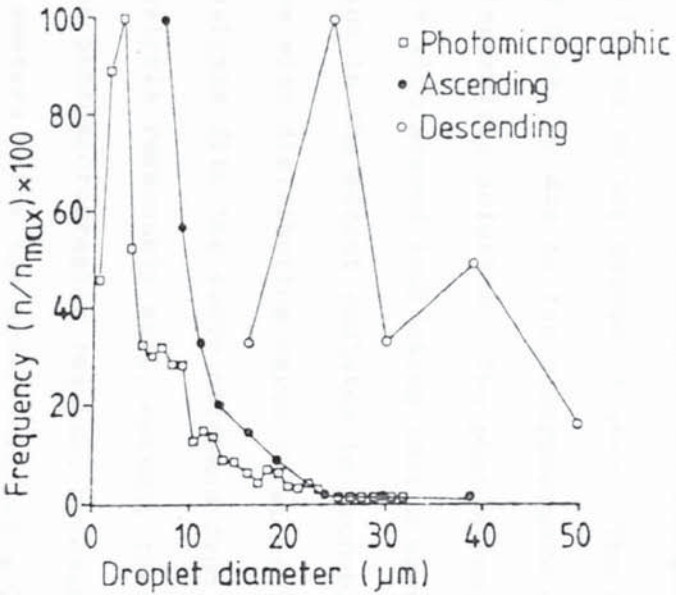

Fig 4·11 Comparison of photomicrographic analysis with Coulter Counter analysis using a 280μm orifice. S=8·0 g.dm^{-3}, N=300 r.p.m.

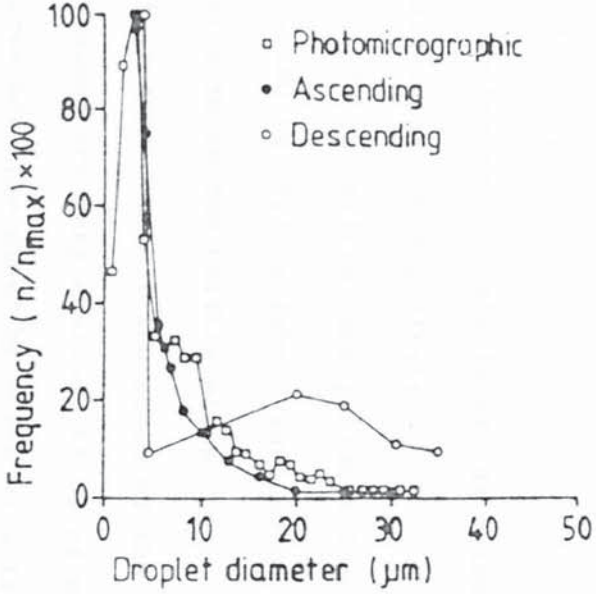

Fig 4·12 Comparison of photomicrographic analysis with Coulter Counter analysis using a 140μm orifice. S=8·0 g.dm^{-3}, N=300 r.p.m.

1) The size distributions obtained using ascending order analysis are much less scattered than those obtained using descending order analysis.

2) Ascending order analysis yields a lower mean drop size than descending order analysis.

3) The 140 μm orifice tube yields a lower mean drop size than the 280 μm orifice tube. When comparing the results obtained using these two orifice sizes under ascending order analysis, it is apparent that the shape of the size distribution curves obtained are very similar, it being possible to transpose one curve onto the other by means of a lateral shift along the ordinate.

4) The size distribution curves resulting from ascending order analysis are skewed to the point where the maximum frequency occurs for the smallest droplet size counted whilst the results of the descending analysis are too poor to make any observations relating to the degree of skew. The skew of the curves may, in part, be due to the disappearance of droplets from the electrolyte solution. The photomicrographic results, however, are also skewed indicating that a skewed droplet size distribution in the parent emulsion is probable.

5) The size distribution curve obtained from the photomicrographic analysis fits the curve obtained from the 140 μm ascending order analysis reasonably well, notably the maxima virtually coincide. The photomicrographic results, however, reveal droplets of diameters below the sensitivity of a Coulter Counter fitted with a 140 μm orifice. Obviously, a 50 μm orifice could be used but that would exclude droplets greater than 20 μm diameter, the presence of a number of which are shown by the photomicro-

graphic curve. The frequency of large drops is greater on the photomicrographic curve than on the 140 μm ascending curve. This, presumably, is because the droplet population in the electrolyte had fallen considerably by the time counts of larger drops were made. A consequence of this is that the Sauter mean drop diameters as determined from the photomicrographic analysis is considerably larger than that obtained from the Coulter Counter 140 μm ascending order analysis, as the Sauter mean is particularly sensitive to changes in the population of larger drops.

As data obtained using the 140 μm orifice with ascending order analysis appeared to be in best agreement with the direct visual analysis of photomicrographic technique it was decided to base the data on the data on the results obtained using this technique.

4.3.3. Results of Coulter Counter analysis

Two series of analysis were carried out with the Coulter Counter, one series on samples taken from open vessels and the other on samples taken from the closed vessel. The results of these two series of analysis are shown below.

4.3.3.1. Open Vessels

The poor data resulting from photomicrographic analysis demanded further investigation of the dispersion characteristics in open vessels. In this case analysis was carried out using a Coulter Counter which thus allowed a large number of droplets to be sized in a short time. Three vessel sizes were used in this study but nominally only one soap concentration was studied (S = 2.0 $g.dm^{-3}$ ± 1%).

The results of this series of experiments designated D15 to D23, are shown as plots of Sauter mean drop diameter against impeller speeds in figures 4.13 to 4.15 and in table 4.1. The data is

Expt.	D15	D23	D16	D20	D21	D18	D19
S ($g.dm^{-3}$)	9.10	9.03	9.03	9.03	9.03	8.98	8.98
D mm	75		114			152	
N rpm							
190	-	-	-	-	-	9.48	9.24
217	-	-	-	-	-	7.94	9.05
245	-	-	5.74	7.29	7.47	6.62	7.47
272	-	-	-	6.5	5.67	6.73	7.03
300	5.80	7.03	5.58	6.35	4.82	3.83	6.83
327	-	6.53	-	4.23	5.69	5.37	-
355	-	6.40	4.88	-	5.43	-	5.43
382	-	5.28	-	-	-	-	-
410	5.24	-	4.23	-	-	-	-
465	-	-	3.72	-	-	-	-
520	3.90	-	-	-	-	-	-
630	2.67	-	-	-	-	-	-
740	2.10	-	-	-	-	-	-

Table 4.1 Sauter mean droplet diameters (μm)

Open vessels, Coulter Counter analysis.

markedly less scattered than corresponding data from the photomicrographic analysis. The gradients and the 95% confidence limits of the least mean squares regression lines are shown in table 4.2.

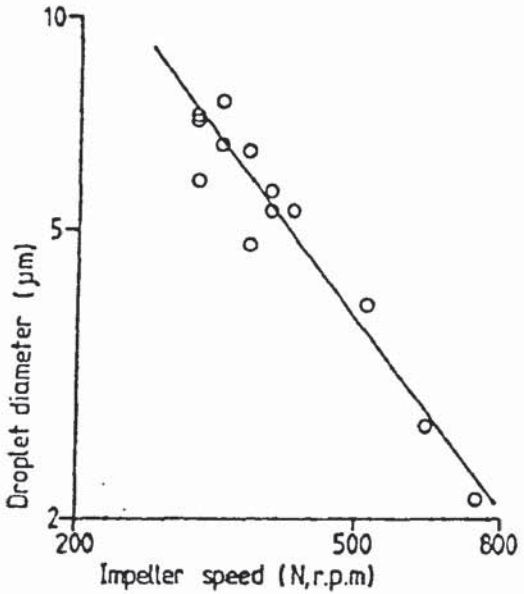

Fig 4·13 Logarithmic plot of Sauter mean droplet diameter against impeller speed. Coulter Counter analysis, open vessel, D=75mm, S∼9 g.dm^{-3}, ϕ=0·59, toluene.

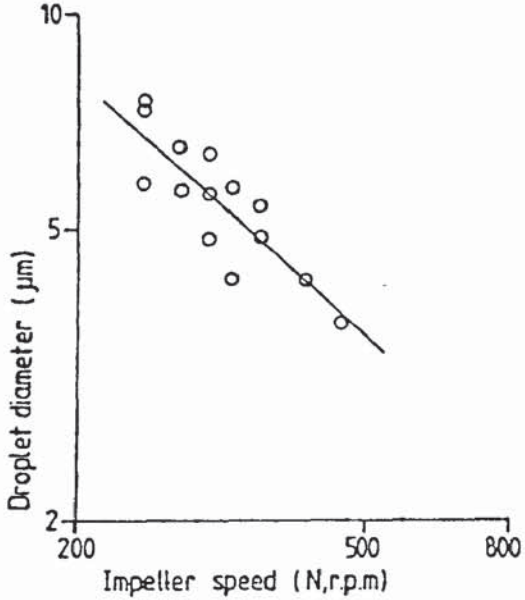

Fig 4·14 Logarithmic plot of Sauter mean droplet diameter against impeller speed. Coulter Counter analysis, open vessel, D=114mm, S∼9 g.dm^{-3}, ϕ=0·59, toluene.

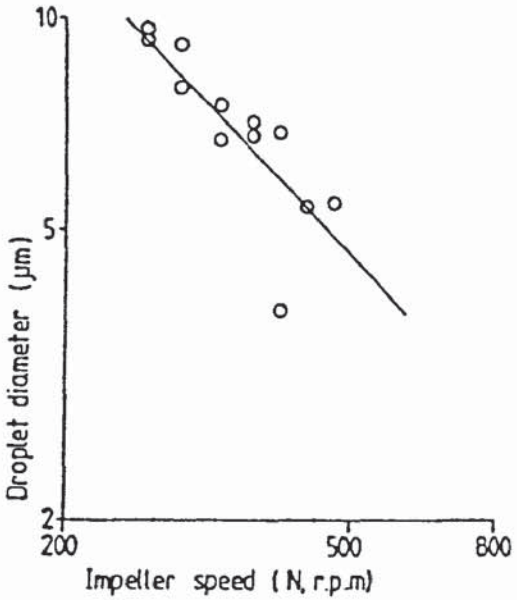

Fig 4·15 Logarithmic plot of Sauter mean droplet diameter against impeller speed. Coulter Counter analysis, open vessel, D=152mm, S∼9 g.dm^{-3}, ϕ=0·59, toluene.

Vessel diameter mm	Gradient	95% confidence limits		Number of data points	Average deviation %	Max. deviation
		lower	upper			
152	-1.227	-1.024	-1.530	13	7.49	19.05
229	-0.895	-0.540	-1.250	14	8.55	18.34
305	-1.056	-0.545	-1.567	12	8.81	33.97

Table 4.2 Gradients of regression for open vessel data

It is evident from the graphs and regression analysis that, at a given impeller diameter and soap concentration, the Sauter mean droplet diameter is inversely proportional to some power of the impeller speed, thus

$$\bar{d}_s \propto N^{-x} \qquad (4.3)$$

For baffled vessels, the literature[41][42][45] points out that x is not a function of vessel/impeller size and although the values for x gained experimentally for the three vessel sizes studied are not identical, examination of the 95% confidence limits shows an area of overlap between the confidence limits on the three experimentally determined values of x. A proposal could be made that the differences are solely through random experimental scatter around a probable value of x which lies in the range 1.024 to 1.250.

As the objective of the overall project was to study scale-up of emulsion polymerisation and the part played by dispersion within it, it was obviously important to relate droplet size to impeller diameter. To this end, the data presented in figures 4.13 to 4.15 was processed through a multiple regression analysis program, MULGREG, on a Hewlet Packard HP 2000 computer. Regression of all the results for the three vessel sizes showed the mean droplet diameter of the toluene emulsions

to be the following function of impeller speed and diameter.

$$\bar{d}_s \propto N^{-1.080}\ D^{-0.185} \qquad (4.4)$$

The data is plotted on these axes in figure 4.16. The exponents of this equation are not in agreement with those of the equations generally applicable to baffled vessel systems. i.e. For baffled vessels in which droplet breakup controls the droplet size,

$$\bar{d}_s \propto N^{-1.2}\ D^{-0.8} \qquad (4.5)$$

$$(Re > 10^4)$$

This is equivalent to

$$\bar{d}_s \propto (N^3D^2)^{-0.4} \qquad (4.6)$$

The alternative condition applicable to baffled vessels is the case where droplet coalescence controls the mean droplet size, where

$$\bar{d}_s \propto N^{-0.75}\ D^{-0.5} \qquad (4.7)$$

$$(Re > 10^4)$$

This is equivalent to

$$\bar{d}_s \propto (N^3D^2)^{-0.25} \qquad (4.8)$$

Both of these theoretical equations simplify to forms which include the term (N^3D^2), a term which is common to equations which include a power disipation per unit volume approach. To allow comparison of the current data with relationships of this type, the experimental values of $\bar{d}_s$ were plotted against N^3D^2 as shown in figure 4.17.

As would be expected, the data deviated less from the empirical regression function, i.e. figure 4.16 than it did from the theoretical function for baffled vessels, i.e. figure 4.17 The mean deviations were, respectively, 9.47% amd 16.63%. The experimental data from unbaffled vessels is unlikely to conform to the theoretical correlation for baffled vessels for two reasons;

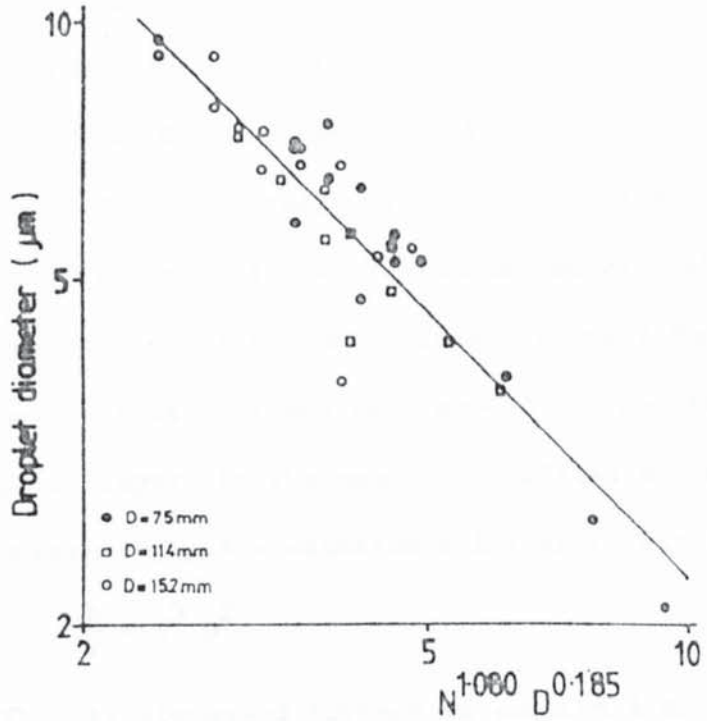

Fig 4·16 Logarithmic plot of Sauter mean droplet diameter against $N^{1\cdot080}\ D^{0\cdot185}$. Coulter Counter analysis, open vessels, $S = 12{\cdot}8\ g.dm^{-3}$, $\phi = 0{\cdot}59$, toluene.

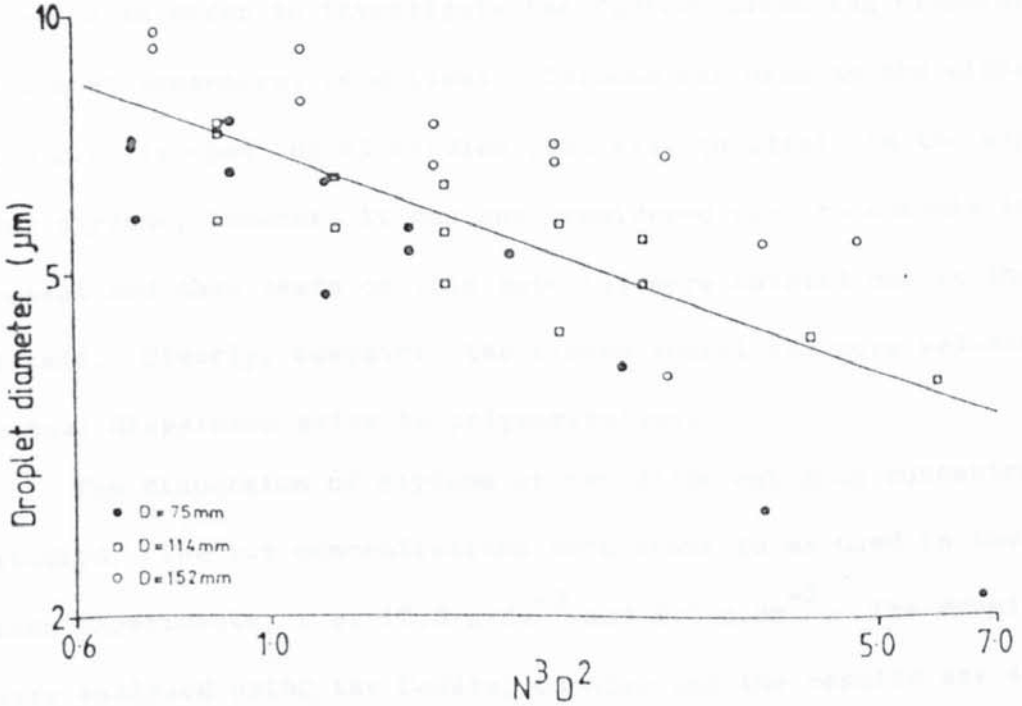

Fig 4·17 Logarithmic plot of Sauter mean droplet diameter against $N^3\ D^2$. Coulter Counter analysis, open vessels, $S = 12{\cdot}8\ g.dm^{-3}$, $\phi = 0{\cdot}59$, toluene.

1) The Reynolds numbers relating to the experimental studies were in the range $1x10^2$ to $2x10^4$, that is, the bulk of the experimental data was for conditions where the Reynolds number was less than 1×10^4, the lower limit of the application of the baffled vessel equations (equation 4.5 and 4.8).

2) Basic theoretical considerations suggest that in unbaffled vessels, droplet size is likely to be a function of specific power input. It has been shown[52], however, that specific power input, in the case of unbaffled vessels, cannot be expressed by the equation relating to baffled vessels, i.e.

$$\frac{P}{V} \propto N^3 D^2 \qquad (4.9)$$

This is discussed further in section 4.4.

4.3.4.2 Closed vessel

The open vessel studies on dispersion were carried out as preliminary studies in order to investigate the factors affecting dispersion under the most convenient conditions. Toluene was used as the dispersed phase and clearly open vessel studies gave rise to little in the way of hazards. For styrene, however, it was not considered wise to operate in an open vessel and thus tests on this material were carried out in the reactor itself. Clearly, moreover, the closed vessel was more relevant to the actual dispersion prior to polymerisation.

The dispersion of styrene at two different soap concentrations were studied. The two concentrations were those to be used in the polymerisation experiments, i.e. 12.8 $g.dm^{-3}$ and 8.0 $g.dm^{-3}$. The droplet sizes were analysed using the Coulter Counter and the results are shown in figure 4.18 and in the appendix (Appendix C, table C3). Table 4.3 shows the gradients and 95% confidence limits for the closed vessel data.

As may be seen from figure 4.18 and table 4.3, both sets of styrene data give reasonably parallel lines with slopes of a similar order to

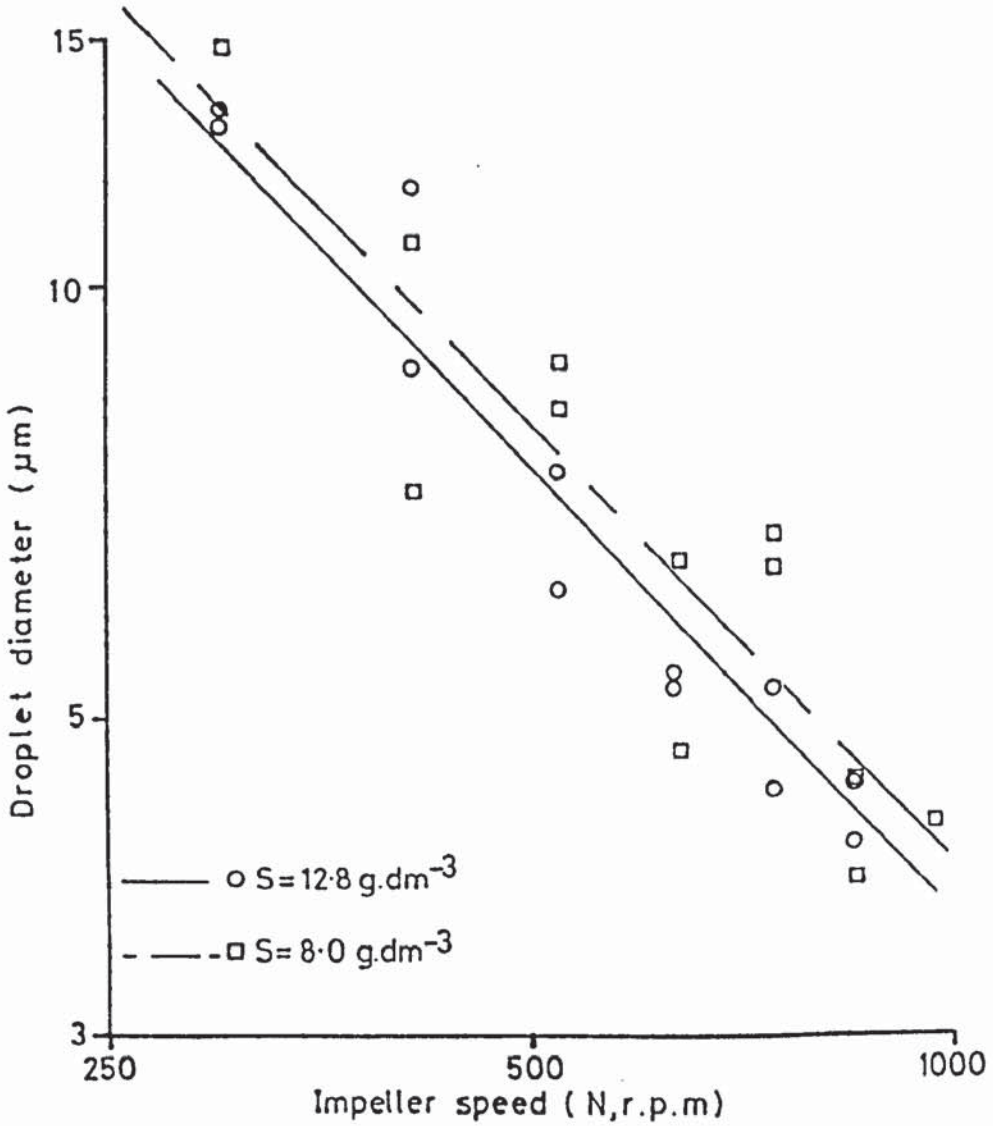

Fig 4.18 Logarithmic plot of Sauter mean droplet diameter against impeller speed. Closed vessel, D = 75mm, styrene.

the open vessel data.

The difference in the location of lines may be attributed to the difference in the physical properties of the toluene (open vessel) system and the styrene (closed vessel) system. A difference of interfacial tension, viscosity or density will all affect the droplet size. Indeed this is highlighted by the fact that the two lines through the styrene data are parallel and not coincident. This is most likely due to the effect of the two different soap concentrations, and as such would be consistent with Nomura et al's[24] observations for styrene dispersion in baffled vessels.

It appears therefore that for the two soap concentrations considered, the dispersion of styrene in a closed vessel follows the behaviour described by equation 4.4 which was formulated from the results of studies of the dispersion of toluene in open vessels.

As a check with the more general correlation relating droplet size to both impeller diameter and impeller speed (i.e. equation 4.4) the closed vessel data was plotted against $N^{1.08}\ D^{0.185}$ together with the regression line through the open vessel data. This may be seen in figure 4.19 whilst the gradients are shown in table 4.4.

Clearly the closed vessel data is in reasonable agreement with the open vessel data in terms of slope. This is a most important comparison as it is the slope that describes the change in droplet size with a change in the impeller parameters, and this is interdependent of the physical properties of the system if the exponents of N and D are independent of Reynolds number as is assumed here. The fact that the regression line through the open vessel data and those through the closed vessel data are not coincident is not surprising.

Dispersed phase	Soap concentration $g.dm^{-3}$	Slope	95% confidence limits		Number of data point	Average deviation %	Max. deviation
			lower	upper			
Styrene	12.8	-1.051	-1.219	-0.883	14	8.3	21.1
Styrene	8.0	-1.022	-1.372	-0.672	12	6.7	26.8

Table 4.3 Gradients of regression lines for closed vessel data

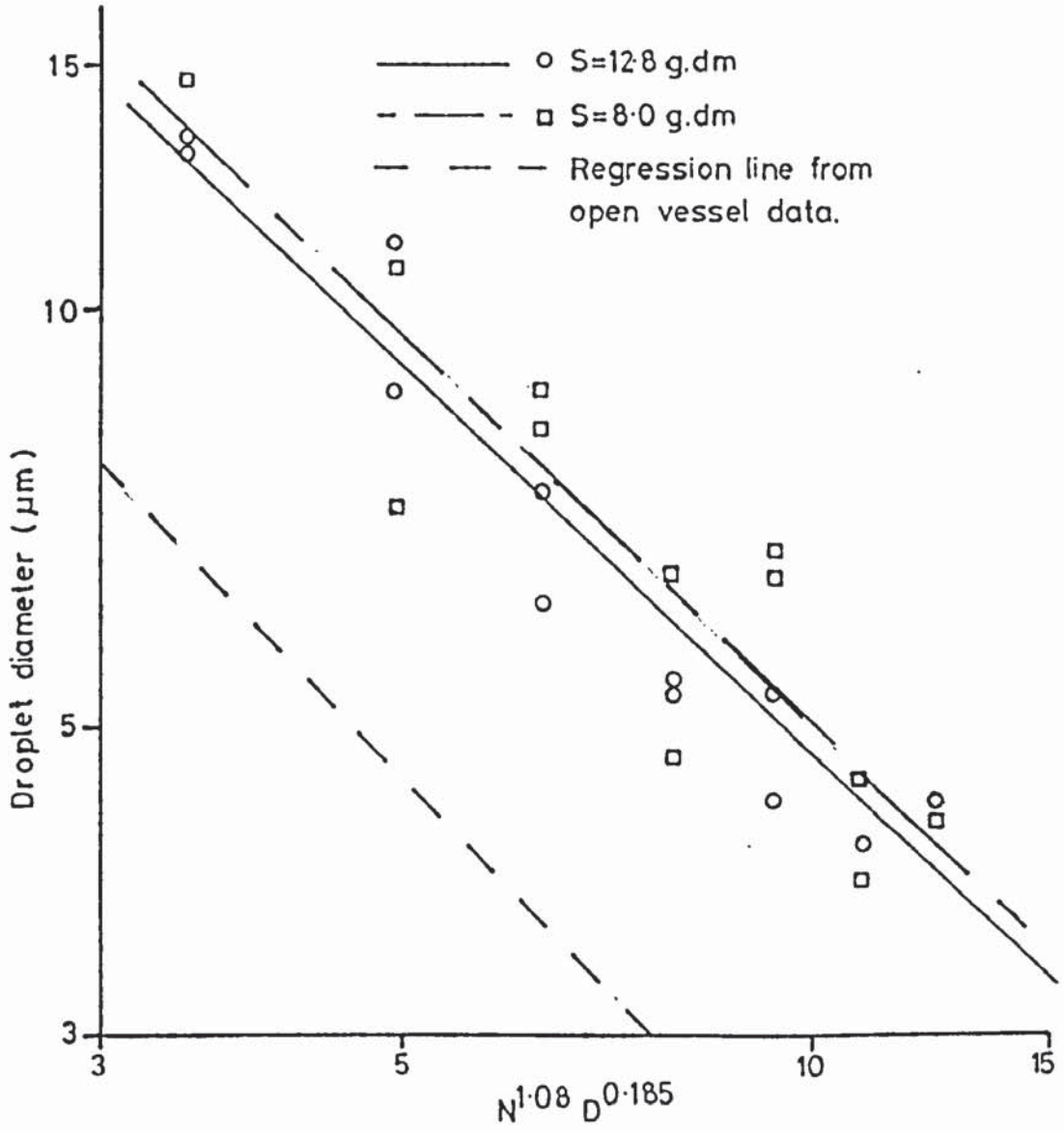

Fig 4·19 Logarithmic plot of Sauter mean droplet diameter against $N^{1·08}\,D^{0·185}$ for styrene. Closed vessel, D=0·075mm.

Vessels	Dispersed phase	Soap concentration $g.dm^{-3}$	Slope
Open	toluene	9 ± 1%	-1.01
Closed	styrene	12.8	-0.93
Closed	styrene	8.0	-0.93

Table 4.4 Gradients of regression lines

4.4 Power input data

Collection of the basic data of power input via the impeller was effected by measuring the torque transmitted from the impeller to the vessel wall (section 3.3.3). The power input by the impeller was calculated by the simple relationship

$$P = \frac{D_{TO}}{2} \cdot g \cdot \frac{N}{60} \cdot m \cdot 2\pi \qquad (4.10)$$

where P = power

D_{TO} = outside diameter of vessel

g = acceleration due to gravity

N = angular impeller speed (r.p.m.)

m = balance reading

The power input per unit volume of emulsion in the vessel was then calculated simply by dividing the power input by the appropriate volume of emulsion. The data for power input is tabulated in table 4.5

4.4.1 Data treatment

The governing equation relating power input to impeller speed, impeller dimensions and system physical properties is, according to Rushton et al[52];

Expt	D1	D2	D3	D4	D5	D6	D7	D8	D9	D10	D11	D12
S ($g.dm^{-3}$)	0	0.093	0.44	9.06	0	0.086	0.39	9.1	0	0.095	0.41	8.84
D mm	75				114				152			
N rpm												
80	0.14	-	-	-	0.09	0.09	0.09	0.17	0.21	0.21	0.41	0.41
135	-	-	-	-	-	-	-	-	-	0.82	0.82	1.23
190	0.05	0.05	0.03	0.16	0.77	0.69	0.69	0.86	1.03	1.64	1.85	1.85
245	-	-	-	-	-	-	-	-	-	3.49	2.26	4.51
300	0.14	0.14	0.08	0.41	1.81	1.63	1.89	2.67	4.72	6.56	6.15	6.97
355	-	-	-	-	-	-	-	-	-	6.56	5.95	7.59
410	0.32	0.38	0.24	0.70	3.96	3.70	3.78	4.99	11.69	7.59	6.36	10.25
520	0.54	0.51	1.00	1.30	7.22	7.48	7.31	-	19.07	18.25	19.68	19.07
630	0.68	1.03	0.89	2.11	-	-	-	-	-	-	-	-
740	1.84	1.78	1.00	3.70	-	-	-	-	-	-	-	-
850	2.43	2.46	2.40	5.75	-	-	-	-	-	-	-	-
960	2.67	2.75	2.86	8.15	-	-	-	-	-	-	-	-

Table 4.5 Power input data (Watts)

$$\frac{Np}{Fr} = \Phi \propto Re^{m} \qquad (4.11)$$

The major problem in dealing with power input data using this equation lies in the complex nature of the Froude group exponent n and to come extent the nature of the Reynolds group exponent m. For baffled vessels, n approaches zero for Reynolds numbers greater than 10^4, thus the effect of Fr becomes insignificant. For unbaffled vessels, n is finite and in fact has been shown[52] to be a function of the Reynolds number, of the type;

$$n = a + b \ln Re \qquad (4.12)$$

In order to fit the collected data to an equation of the type shown above (equation 4.11), the character of n needs to be assessed. There are three possible ways to treat the data obtained from the power input measurements, each one differing with regard to the approach made to estimate n. Having found a value for n they all allow an estimation of m by plotting ln Φ against ln Re.

1) The assumption that the Froude number is insignificant, and may therefore be neglected, may be made. In this case, the power number may be plotted against the Reynolds number as shown in figure 4.20. This approach is only really valid for baffled vessels but may be a valid approximation for unbaffled vessels. The scatter of data in the current study, for instance, is not unreasonable as may be seen by the data presented in figure 4.20 which exhibits a mean deviation of 15.4% and a maximum deviation of 46.7%.

   The correlation is:

$$Np \propto Re^{-0.79} \qquad (4.13)$$

2) It may be assumed that the exponents on the Froude number and Reynolds number are constant. This assumption of constant

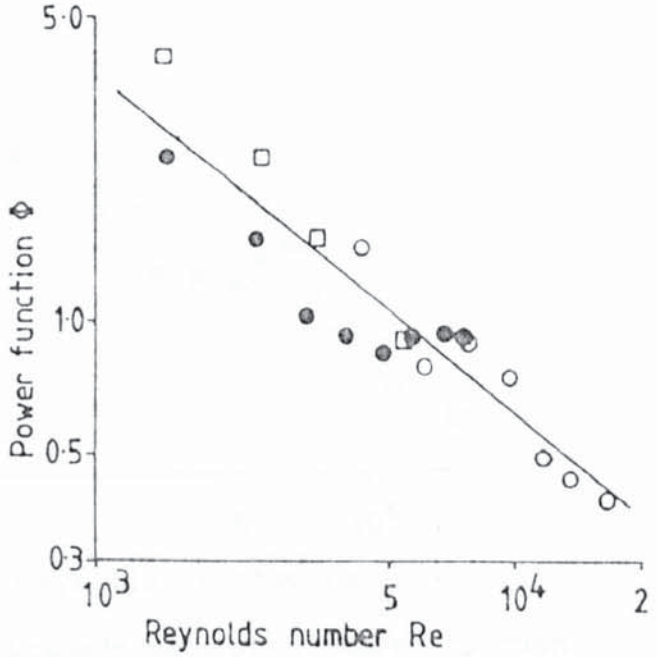

Fig 4.20 Logarithmic plot of Power function against Reynolds number $\Phi = Np$

- ● D=75 mm
- □ D=114 mm
- ○ D=152 mm

m is valid for unbaffled vessels if the range of Reynolds number studied is not too wide. The assumption of a constant value for n is more likely to lead to error. In this case, linear multiple regression of the collected data yields the following expression:

$$\Phi = \frac{Np}{Fr^{-0.12}} \propto Re^{-0.62} \qquad (4.14)$$

This is plotted in figure 4.21 in comparison with the actual data. The mean deviation from the regression line is 12.1% with a maximum of 40.7%, a slight improvement over the previous assumption.

3) The final way in which the data may be treated is to accept that the Froude number exponent is a function of the Reynolds

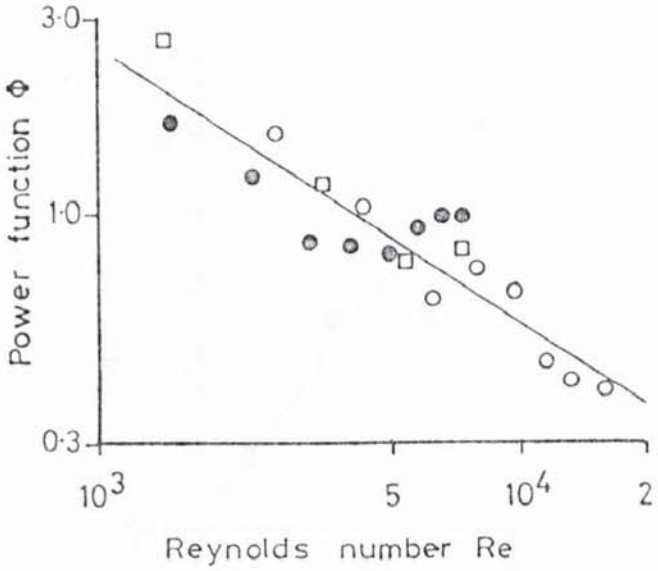

Fig 4·21 Logarithmic plot of Power function against Reynolds number. $\Phi = Np/Fr^{-0.12}$

● D= 75mm
□ D= 114mm
○ D= 152mm

number and to attempt to define this dependence. In order to evaluate this function it is necessary to calculate the slopes of logarithmic plots of power number against Froude number at constant Reynolds numbers. The data available was limited, but it was possible to calculate four slopes from nine pieces of data. It was assumed that at constant Reynolds number, the power number was a linear function of the Froude number. It was also necessary, as experiments were not conducted at constant Reynolds numbers, to take pairs of data at similar Reynolds numbers. Average Reynolds numbers were used for the plot of slopes against the logarithm of Reynolds number, shown in figure 4.22.

Using this technique and linear regression the Froude number exponent was found to be the following function of

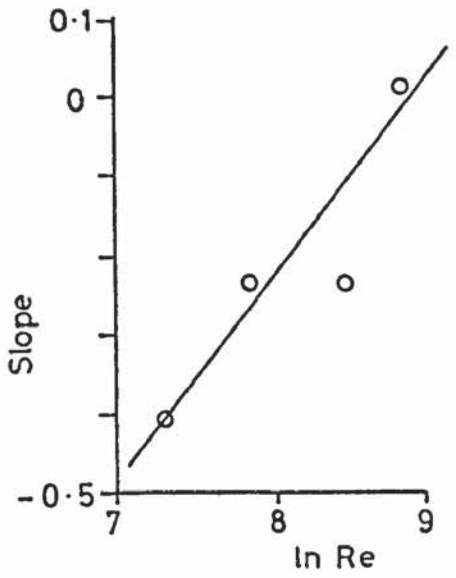

Fig 4·22 Plot of the slopes, from plots of Power number against Froude number at constant Reynolds number, against log of Reynolds number.

Reynolds number:

$$n = -2.07 + 0.23 \ln Re \qquad (4.15)$$

The appropriate power function plot is shown in figure 4.23. It can be seen that above a Reynolds number of 10^4, the power function appears to decrease rapidly in value. A curve could be fitted to this line and in fact a curve would be expected if comparison is made with the work of Rushton et al[52]. For simplicity, however, linearity was assumed over two clearly separate ranges of Reynolds number, in order to facilitate the calculations of constant values of the Reynolds number exponent, m, over two Reynolds number ranges. Thus two regression lines were fitted to the data:

$$\frac{Np}{Fr^{(-2.07 + 0.23 \ln Re)}} = \phi \propto Re^{-0.03} \qquad (4.16)$$

$$Re < 8 \times 10^3$$

$$\frac{Np}{Fr^{(-2.07 + 0.23 \ln Re)}} = \Phi \propto Re^{-1.21} \qquad (4.17)$$

$$Re > 8 \times 10^3$$

The mean deviation from these regression lines is 5.9% with a maximum deviation of 21.4%. It is apparent from these results that the power input per unit volume is dependent on the Reynolds number as would be expected by comparison with the work of Rushton et al[52].

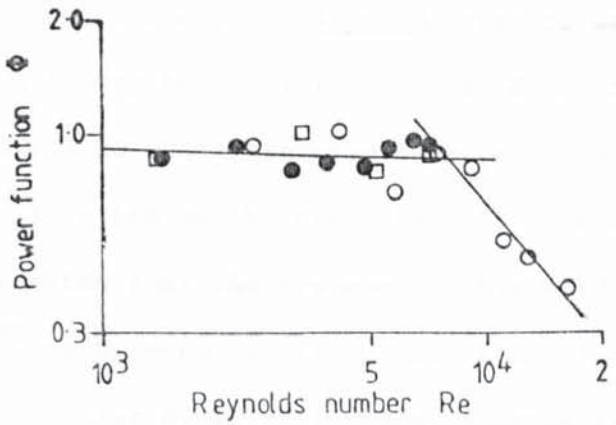

Fig 4.23 Logarithmic plot of power function against Reynolds number. $\Phi = Np/Fr^n$, $n = -2.07 + 0.23 \ln Re$.

- ● D=75mm
- □ D=114mm
- ○ D=152mm

The clear emergence of a Reynolds number dependent exponent for the Froude group leads to two conclusions.

a) It is confirmed that it is invalid to assume a constant value of the Froude group exponent over anything but a very small range of Reynolds numbers.

b) Comparison of figure 4.23 with Rushton et al's[52] data (figure 4.24) suggests, by virtue of the correspondence of the

discontinuity in the curves, that the systems investigated in the current study were being operated mainly in region A, a region common to both baffled and unbaffled vessels. This conclusion does not in fact concur with that drawn from observation of the corresponding Reynolds number ranges as a Reynolds number range of 1,500 to 17,000 is indicated, by figure 4.24, to signify that the systems were operated in region B. No obvious significance may be proposed for this disagreement although it should be noted that little data was gathered in the current study for Reynolds numbers greater than 8×10^3, and thus it may be possible that the data shown in this region in figure 4.23 (data gathered from only one vessel) is in error and the location of the discontinuity is spurious. It should also be noted that the systems of this study and of Rushton et al's[52] study were not truly comparable in that their data was for an impeller diameter to tank diameter ratio of 1/3. The corresponding ratio used in this study was 1/2.

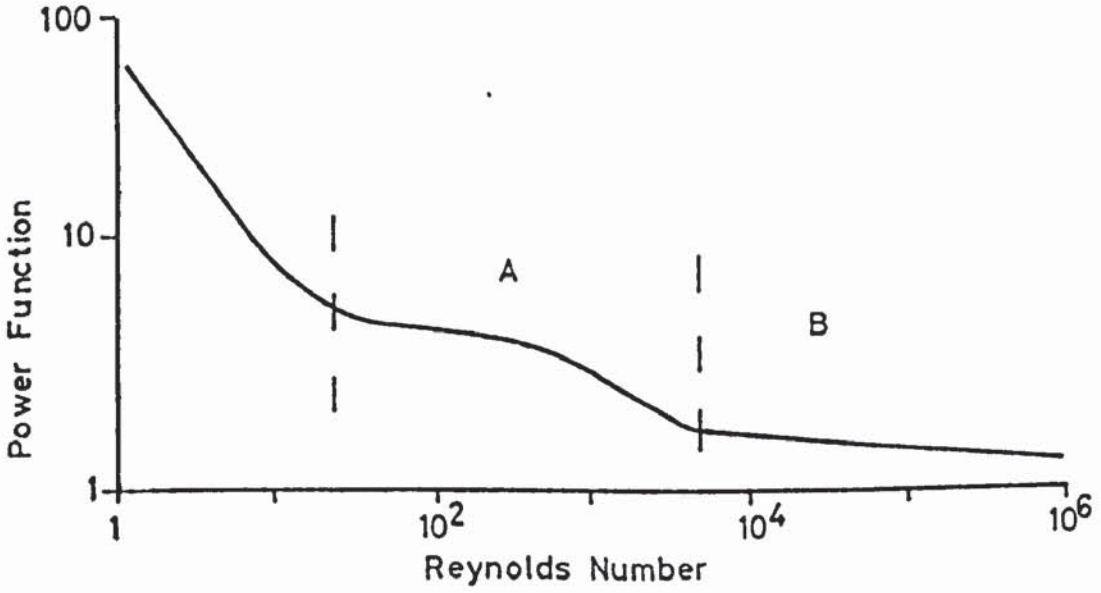

Fig 4·24 A typical logarithmic plot of Power function against Reynolds number for unbaffled vessels.Turbine impeller,6 blades, D/D =1/3.(After Rushton et al)

Overall there is insufficient data to draw hard conclusions. Whilst the point outlined above must be borne in mind, further experimentation over a wider range of vessel size and conditions obviously would be desirable to clarify these points.

4.4.2 Power input results applied to droplet size prediction

According to most theoretically based models for dispersion the degree of dispersion is a function of specific power input. It should therefore be possible to identify a mathematical relationship between the degree of dispersion and the specific power input by plotting mean droplet size against the specific power input. This has been done for experimental values of power input, and the results are shown in figure 4.25. The regressed function is:

$$\bar{d}_s = 2.81\ (P/V)^{-0.52} \qquad (4.18)$$

As can be seen, there is a degree of scatter, the mean deviation from the regression line being 6.9%. The maximum deviation is 38.7%.

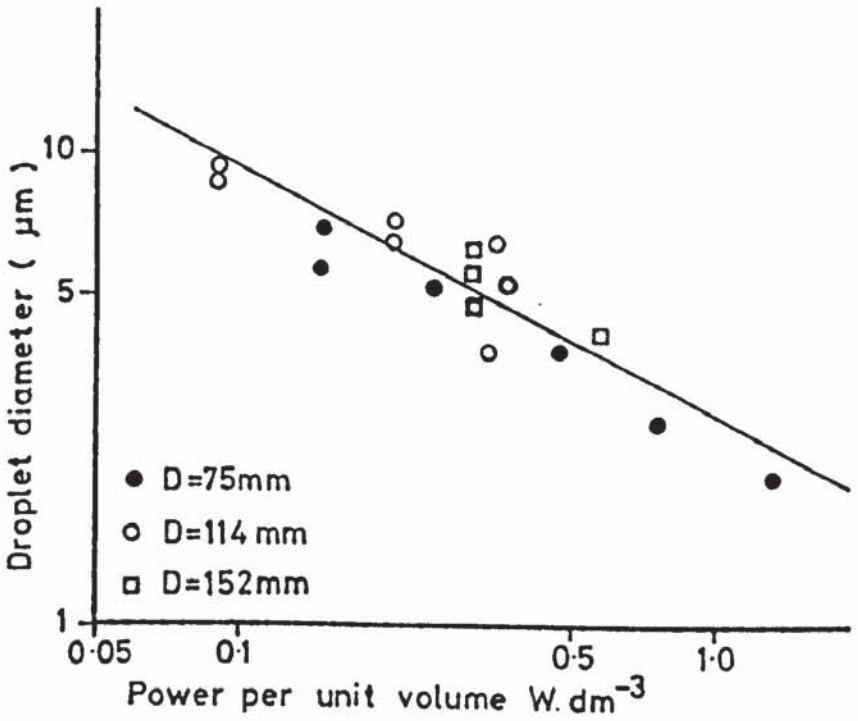

Fig 4·25 Logarithmic plot of droplet diameter against specific power input.

For scale-up the most useful relationship for droplet size prediction is of the type relating average droplet diameter to impeller speed and impeller diameter. To transform equation 4.18 to this form, a relationship between the power input and impeller speed and diameter is needed. The various empirical relationships of equations 4.13, 4.14, 4.15 and 4.16 may be rearranged to give a relationship betweem P/V, N and D thus:

From equation 4.13

$$P/V \propto N^3 D^2 (ND^2)^{-0.79} \tag{4.19}$$

From equation 4.14

$$P/V \propto N^3 D^2 (ND^2)^{-0.62} (N^2D)^{-0.12} \tag{4.20}$$

From equation 4.16

$$(P/V) \propto N^3 D^2 (ND^2)^{-0.03} (N^2D)^{-2.07 + 0.23 \ln Re} \tag{4.21}$$

From equation 4.17

$$(P/V) \propto N^3 D^2 (ND^2)^{-1.21} (N^2D)^{-2.07 + 0.23 \ln Re} \tag{4.22}$$

Combining equation 4.18 with the above equations individually yields:

With equation 4.19 which assumes the effect of the Froude group to be negligible,

$$\bar{d}_s \propto N^{-1.15} D^{-0.22} \tag{4.23}$$

With equation 4.20 which assumes both n and m are constant,

$$\bar{d}_s \propto N^{-1.11} D^{-0.33} \tag{4.24}$$

With equation 4.21 which assumes the Froude exponent, n, to be a function of Reynolds number and m to be a constant for $Re < 8 \times 10^3$,

$$\bar{d}_s \propto N^{0.61 - 0.24 \ln Re} D^{0.07 - 0.12 \ln Re} \tag{4.25}$$

With equation 4.22 which assumes n to be a function of Reynolds number and m to be a constant for $Re > 8 \times 10^3$,

$$\bar{d}_s \propto N^{1.22 - 0.24 \ln Re} D^{1.28 - 0.12 \ln Re} \tag{4.26}$$

The empirical relationship relating the mean drop size to the impeller speed and diameter, derived in section 4.4 is

$$\bar{d}_s \propto N^{-1.08} D^{-0.185} \qquad (4.4)$$

Direct comparisons with this empirical relationship and equations 4.23 and 4.24 are possible as they all assume constant exponents of N and D over the full range of Reynolds numbers. Equation 4.4 is in reasonable agreement with equation 4.24 which assumes the exponent of the Froude group to be finite and constant. Reasonable agreement is also shown between equation 4.4 and equation 4.23, where it is assumed that the exponent of the Froude group is negligible. This is consistent with a system operating in region A of the power function versus Reynolds number relationship shown in figure 4.24.

Comparison of equation 4.25 and equation 4.26 with equation 4.4 is difficult due to the functional exponents in the former. However, for the case where $Re < 8 \times 10^3$ the values of the N and D exponents over the range of Reynolds number studied can be compared with equation 4.4.

For N, the exponent is in the range -1.14 to -1.55 whilst for D it is in the range -0.81 to -1.01. In this case, it can be seen that the N exponent range is in reasonable agreement with the N exponent in equation 4.4. The D exponent range, however, is considerably larger than the value in equation 4.4. It is interesting to note that the approximate ratio of N to D exponents in equation 4.25 is 3:2, indicating that:-

$$P/V \propto (N^3 D^2)^Z \qquad (4.27)$$

Equation 4.27 supports the suggestion that the operational range of the experiments was range A in figure 4·24.

The data from which equation 4.26 was determined is so limited that comparison of this equation with equation 4.4 is difficult and any

conclusions drawn must be viewed with some reserve. As a general observation, however, it may be noted that the exponents calculated for Re=22000 , (N; -1.18, D; -0.01) do indicate a move away from the N:D ratio of 3:2. This obviously suggests that the simple relationship of Sauter mean emulsion droplet diameter with power per unit volume, as is the case in a baffled vessel operating in a Reynolds number range in excess of 10^4, does not apply in this case.

Obviously, if the degree of dispersion is a function of the specific power input, and this in turn is a complex function of the Reynolds number and Froude number, it would indicate that any empirical relationship such as equation 4.4 which presents the exponents of N and D as constants is not valid. In deriving equation 4.4, however, only small ranges of Reynolds number and Froude numbers were investigated, and it is reasonable to suggest that the empirical equation is an acceptable approximation over this range, (i.e. $1.5 \times 10^3 < Re < 1.7 \times 10^4$, $0.08 < Fr < 1.16$). It would not, however, be valid to extend its use beyond the range studied. An equation, or more likely a family of equations, of a type that recognises that the N and D exponents are a function of the Reynolds number potentially offer a better guide to scale-up. Equations 4.25 and 4.26, however, were developed over only a small range of variables and until this range is extended by further experimentation it would be unwise to apply these equations in conditions where the Reynolds number is outside the range studied.

Further work is clearly necessary to expand the range over which the degree of dispersion may be predicted.

5.0 POLYMERISATION RESULTS

5.1 Kinetic data

5.2 Latex particle size

5.0 POLYMERISATION RESULTS

A programme of polymerisation experiments was carried out using the recipe for polystyrene production shown in section 3.6.

Theory suggests that the alteration of either the soap concentration or the impeller speed should have a similar effect on the reaction rate, and indeed on the final latex particle size, of an emulsion polymerisation reaction. These effects were therefore studied and the results of this programme of experiments are presented in the following sections of this chapter.

The results presented for the final latex particle size were obtained by use of the basic analytical technique described in chaper 3.8. Specific problems were encountered in applying the technique to this study and these are discussed in this chapter.

In addition to the styrene polymerisations, one successful styrene/ butadiene copolymerisation was carried out. It is only possible, however, to record the reaction rate in this instance as the technique used for particle size analysis could not be extended for use with an S.B.R. copolymer.

5.1 Kinetic data

Conversion rate data was gathered from a total of 23 styrene polymerisations over a range of impeller speeds and soap concentrations, and one S.B.R. polymerisation. The degree of conversion as a function of time is presented in Appendix D for each of these tests and a few typical examples are shown in figures 5.1 to 5.4.

According to the classical Smith and Ewart kinetic model (see section 2.1.3) reaction rate curves for emulsion polymerisation should, after an initial period of accelerating conversion rate, (stage I)

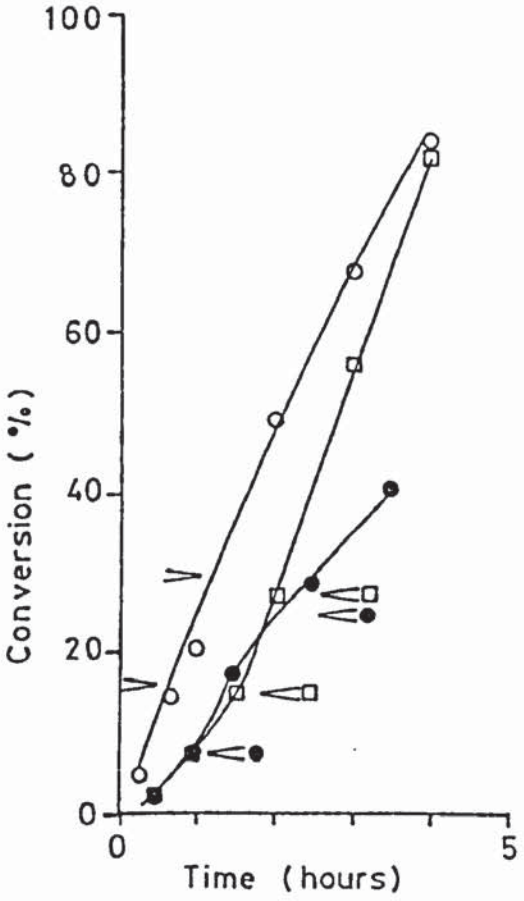

Fig 5·1 Reaction rate curves.
N=190 r.p.m, S=12·8 g.dm^{-3}.

o P2

□ P2/1

● P2/2

< Soap addition

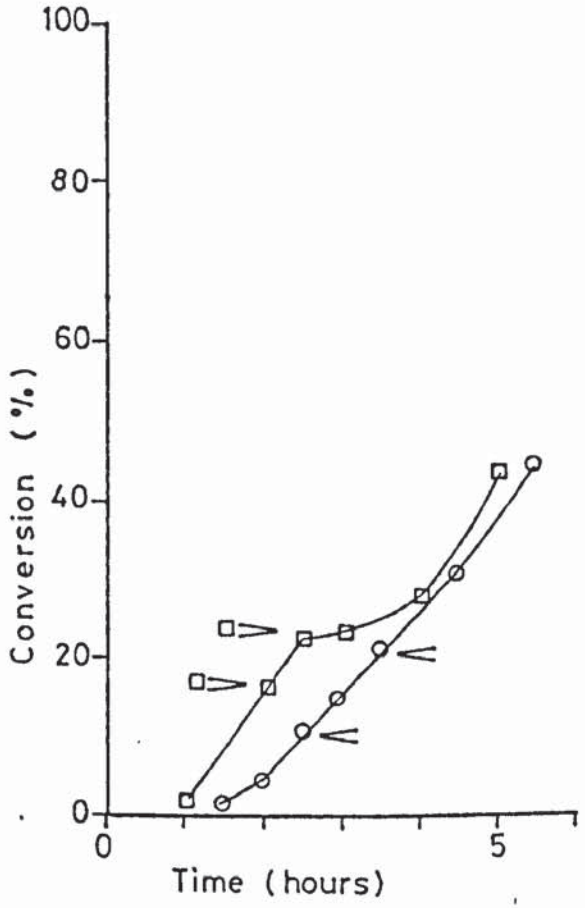

Fig 5·2 Reaction rate curves
N=435 r.p.m, S=8·0 g.dm^{-3}.

o P7

□ P7/1

< Soap addition

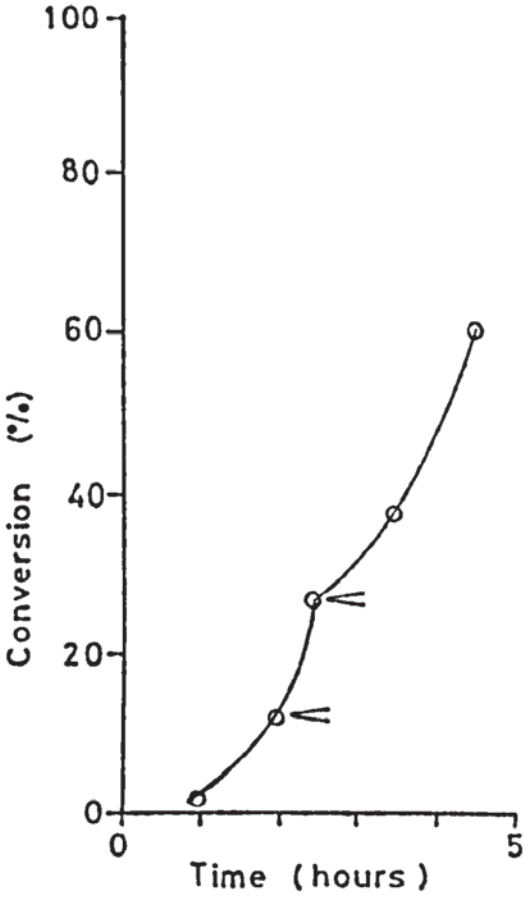

Fig 5·3 Reaction rate curve
N = 600 r.p.m, S = 8·0 g.dm^{-3}, P9
⩤ Soap addition

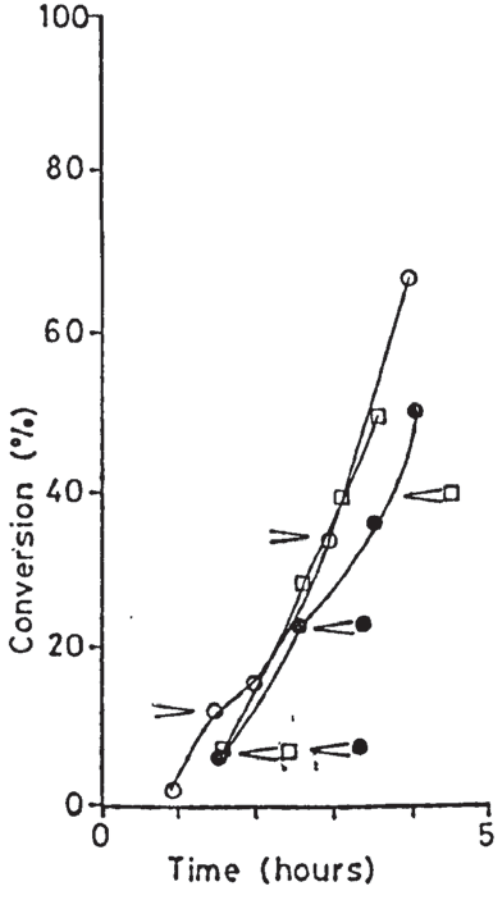

Fig 5·4 Reaction rate curves.
N = 960 r.p.m, S = 4·0 g.dm^{-3}
o P20
□ P21
● P22
⩤ Soap addition

settle down to exhibit a constant rate period, (stage II) and to a large extent this was found to be the case. To compare different tests therefore, this constant rate was determined for each test. The constant rate was well established in all cases by 30% conversion and so the reaction rates at 30% conversion were calculated and the values are shown in table 5.1.

According to the simple Smith and Ewart model this constant rate during stage II should not be a function of impeller speed. The model being tested in this study, however, suggests that because of the dependence of monomer dispersion area on impeller speed, the reaction rate during stage II should increase with decreased impeller speed. in stage I.
It was hoped, therefore, to use comparisons of this reaction rate in order to observe the validity of this model. Examination of the results shown in table 5.1, however, reveals that it was not possible to recognise such a trend from the experimental data. In fact, because of the scatter in the data it was not possible to recognise any trend with confidence. The reason for this scatter was the very poor reproducibility between runs. Experiments carried out under seemingly identical conditions, for instance, yielded different reaction rate curves. This is clearly shown in figure 5.1 and figure 5.2. The reason for this did not lie in the accuracy of the analysis techniques which was a simple timed solids content analysis. The source of the lack of reproducibility, therefore, must have lain in inconsistencies within the reaction system.

The possibility of inadvertently imposing different conditions on otherwise similar runs was recognised in the effect of reaction inhibition The conditions that may be inadvertently varied are the level of oxygen contamination present, the concentrations of inhibitor in the initial monomer charge or the timing of the sequential soap addition. Obviously any permutation of the above effects may apply to a given experiment.

Time h^{-1} / Run	0·3	0·5	0·6	1	1·5	2	2·5	3	3·5	4	4·5	5	5·5	N r.p.m	Rate %.h^{-1}	S g.dm^{-3}
P2	4·5	-	14·3	20·6	-	49·5	-	67·8	-	86·4	-	-	-	190	27·6	12·8
P3	1·1	-	0·7	14·4	-	37·1	-	62·3	-	84·2	-	-	-	410	23·3	12·8
P4	-	1·1	-	6·6	19·9	30·1	-	70·7	-	86·1	-	-	-	600	31·3	12·8
P5	-	0·7	-	6·9	18·8	-	48·6	-	75·8	-	-	-	-	820	28·7	12·8
P2/1	-	1·1	-	7·7	17·5	-	28·9	-	40·7	-	-	-	-	190	13·2	12·8
P2/2	-	1·1	-	5·7	13·7	26·5	-	55·7	-	81·6	-	-	-	190	27·6	12·8
P7	-	0	-	0	1·1	4·7	10·4	14·3	21·0	-	31·2	-	44·8	435	10·2	8·0
P8	-	-	-	0·4	-	9·5	15·1	27·2	-	42·8	-	60·1	-	960	18·0	8·0
P9 :	-	-	-	1·1	-	11·8	26·4	-	37·9	-	59·9	-	-	600	-	8·0
P7/1	-	-	-	1·6	-	15·1	22·0	22·4	-	37·5	-	53·0	-	435	-	8·0
P10	-	-	-	2·7	9·8	20·8	-	45·8	-	63·4	-	-	-	410	24·0	8·0
P11	-	-	-	2·0	7·3	17·2	-	43·4	-	66·2	-	-	-	960	22·8	8·0
P12	-	-	-	2·0	7·8	17·9	-	46·9	-	63·3	-	-	-	575	29·0	8·0
P13	-	-	-	0·4	5·5	13·5	26·2	-	55·9	-	-	-	-	740	28·0	8·0
P14	-	-	-	2·4	11·3	22·5	-	58·4	-	-	-	-	-	410	35·9	12·8
P15	-	-	-	4·7	16·3	-	51·4	-	-	-	-	-	-	740	35·1	12·8
P16	-	-	-	8·6	18·2	33·7	-	75·5	-	-	-	-	-	410	41·8	8·0
P17	-	-	-	9·9	19·6	-	55·3	-	-	-	-	-	-	575	35·7	12·8
P18	-	-	-	9·3	25·2	-	63·7	-	-	-	-	-	-	960	36·3	12·8
P19	-	-	-	1·3	4·7	15	-	42·0	-	69·7	-	-	-	575	27·1	4·0
P20	-	-	-	1·1	11·8	14·4	-	33·8	-	67·6	-	-	-	960	-	4·0
P21	-	-	-	-	6·9	-	27·9	39·0	49·0	-	-	-	-	960	-	4·0
P22	-	-	-	-	4·7	-	21·5	-	34·2	49·9	-	-	-	960	-	4·0

Table 5·1 Conversion data for polymerisation experiments. (% monomer)

Each individual effect is discussed below together with the possibility of the presence of polymer in the initial monomer charge.

5.1.1 Oxygen contamination

The inhibiting effect of oxygen contamination on polymerisation has been recognised and discussed in the literature (see section 2.1.6). Nomura et al[24] observed for instance that oxygen inhibition is characterised by an induction period during which no observable reaction occurs, this induction period is followed by a constant reaction rate period, the rate of which is increased in direct proportion to the length of induction period. Thus for two experiments, identical except that one suffered oxygen contamination, the oxygen free reaction would commence more rapidly than the contaminated one although the latter would exhibit the faster stage II reaction rate. Some evidence of this can be seen in figure 5.1. Although rigorous purging was carried out, and the nitrogen used was of the same nominal purity (i.e. 99.9% pure) the curves A and B exhibit different reaction rates.

The possibility of oxygen contamination is not confined to the initial charging of the vessel. There is also a possibility that, despite rigorous nitrogen purging, the additon of sequential soap could also have introduced oxygen thus causing a reduction in the reaction rate. Evidence of this occurrence may be seen in figure 5.2 and figure 5.3.

5.1.2 Inhibitor

One of the aims of this project was to simulate a specific commercial polymerisation process, the styrene was not, therefore, washed or distilled before an experiment. Commercial styrene always contains an inhibitor in order to inhibit polymerisation during storage. The styrene used in this project was ordered (ex Fisons) in ten litre batches consisting of 4 x 2.5 litre Winchester bottles. The concentration of the

inhibitor (tert butyl catechol) was specified as 10-15 p.p.m., but as the inhibitor concentration reduces over a period of time in storage it is unlikely that a uniform concentration was present throughout the course of the experiments.

The specific polymerisation recipe studied included sodium hydroxide which was thought[67] to remove the inhibitor. This, however, is unlikely to be an instantaneous process, and, therefore, variable induction times may result from variable inhibitor concentrations.

5.1.3 Sequential soap additions

Soap is generally required to be added to the reactor, to maintain stability, at times which are dependent upon the progress of the reaction. As the progress of the reaction was monitored by measuring the solids content, it was desirable to relate soap addition to a given solids content in order to maintain a reproducable experimental technique. This would, however, have required continuous monitoring of the solids content, a course of action that was not possible. A technique of adding soap when routine solid content analysis indicated that the critical solids content had been exceeded, was adopted. This obviously meant that it was difficult to ensure that two experiments would have involved the soap additions being made at identical solids contents, and sometimes this led to problems due to the soap being added too late.

As the sequential soap is required to stabilise growing polymer particles, the late addition of soap would clearly allow some coagulation to occur. This could lead to further problems in the reaction. The impact of coagulation on the reaction kinetics, however, would depend on the scale of such coagulation, which may not even be detectable or at the other extreme may be so massive as to prevent further agitation (see figure 3.12), and thus effectively stop the reaction.

5.1.4 Secondary particle generation

If at any time after the end of stage I the soap concentration is increased beyond c.m.c. then it is possible that further particles may be generated. It was thought possible that such secondary initiation could have occurred due to over large or early sequential soap addition. The series of experiments P20 to P22 were conducted to investigate this.

Calculations of the new soap concentration after soap additions did not lead to the expectation that c.m.c. will be exceeded and as can be seen from figure 5.4 there is not kinetic evidence of this occurring. The curves representing the high and low levels of sequential soaps (experiments P20 and P22 respectively) show a reduction in the reaction rate after the first soap addition whereas secondary particle generation should lead to an increase. This reduction is a phenomenon which has been discussed in relation to oxygen contamination being introduced with the additional soap. The curve representing the intermediate additional soap level shows no unusual behaviour. These data all lead to support for the suggestion that the sequential soap concentrations, and their timing, were unlikely to instigate secondary particle generation, the observed effects being more likely attributable to oxygen contamination.

5.1.5 Polymer contamination of monomer

It is obvious from the need to add inhibitor to styrene monomer that, potentially, polymerisation may occur during storage, a fact illustrated by a batch of styrene observed during this study which, on prolonged storage became viscous to the point where pouring became difficult thus indicating that polymerisation had occurred. Needless to say, this styrene was not used in the experimental programme.

There may well be, therefore, some polymer in the styrene charged to the reactor but the effect of these polymer molecules on the

kinetic behaviour of a polymerisation is unclear. There appears to be no reason why molecules of polymer present in the original monomer charge should affect the reaction kinetics at all.

It should be pointed out that none of the monomer used in this project contained any measurable quantities of polymer solids.

5.1.6 Concluding remarks

It is obvious from this programme of experiments that reaction rates are difficult to reproduce under the experimental conditions employed. The two most likely sources of inconsistency may be proposed as oxygen contamination and the presence of inhibitor, either of which would not be uniform across the whole series of runs. Obviously it would be desirable to eliminate or at least maintain constant these two factors. For this a full study of the problems of inhibition would be required and this would have to establish a distinction between inhibition due to the presence of inhibitor and inhibition due to oxygen contamination.

The inconsistent induction times and reaction rate results experienced during this programme of experiments suggest that the process under study, as it stands, is likely to encounter problems in reproducibility even on this small scale. The reproduction of reaction rates upon scale-up is, therefore, equally likely to meet with difficulty.

5.2 Latex particle size

The final latex particle size was measured using the light transmission technique of Bateman et al[22]. Some problems were encountered in applying the technique, to a large extent however, these problems were overcome. The problems encountered, and a comparison of the results obtained by the light transmission technique with results obtained

using electron microscopy, are discussed in the following sections.

5.2.1 Data treatment

A method based on that described by Bateman et al[22] using light extinction was employed for particle analysis. This technique involved measuring the turbidity of a diluted latex and then calculating the parameter k/α according to equation 3.4, reproduced below.

$$k/\alpha = \frac{0.4887\ \rho_p\ E}{(n/\lambda_o)\ c.l} \qquad (5.1)$$

The calculated value of k/α could then be compared with a published table of values of k/α and particle radii. Thus the particle radii could be obtained for five values of k/α, calculated at different wavelengths of light. The mean value was than taken as the actual value of the particle radius.

The first problem to arise was that the calculated values of k/α arising from the analysis were below the range of the published values. Insufficient data were available to calculate exact theoretical values of k/α, but an equation, the Rayleigh-Gans-Debye[68] formula allowed calculation of values of k/α for the range $\alpha \leqslant 2.65$.

The Rayleigh-Gans-Debye formula is:-

$$k = (m-1)^2 \left[\frac{5}{2} + 2\alpha^2 - \frac{\sin 4\alpha}{4\alpha} - \frac{7}{16\alpha^2}(1 - \cos 4\alpha) \right.$$

$$\left. + \frac{1}{2\alpha^2} - 2 \sum_{n=1}^{\infty} (-1)^{n+1} \frac{(4\alpha)^{2n}}{(2n)\ 2n} \right] \qquad (5.2)$$

From equation 5.2 a number of values of k/α were calculated, and these are shown graphically, as plots of k/α against particle diameter, in figure 5.5.

Because of the time required for each polymerisation to reach 100% conversion it was intended in this study to halt the reaction at some convenient common level of conversion and to compare particle size at

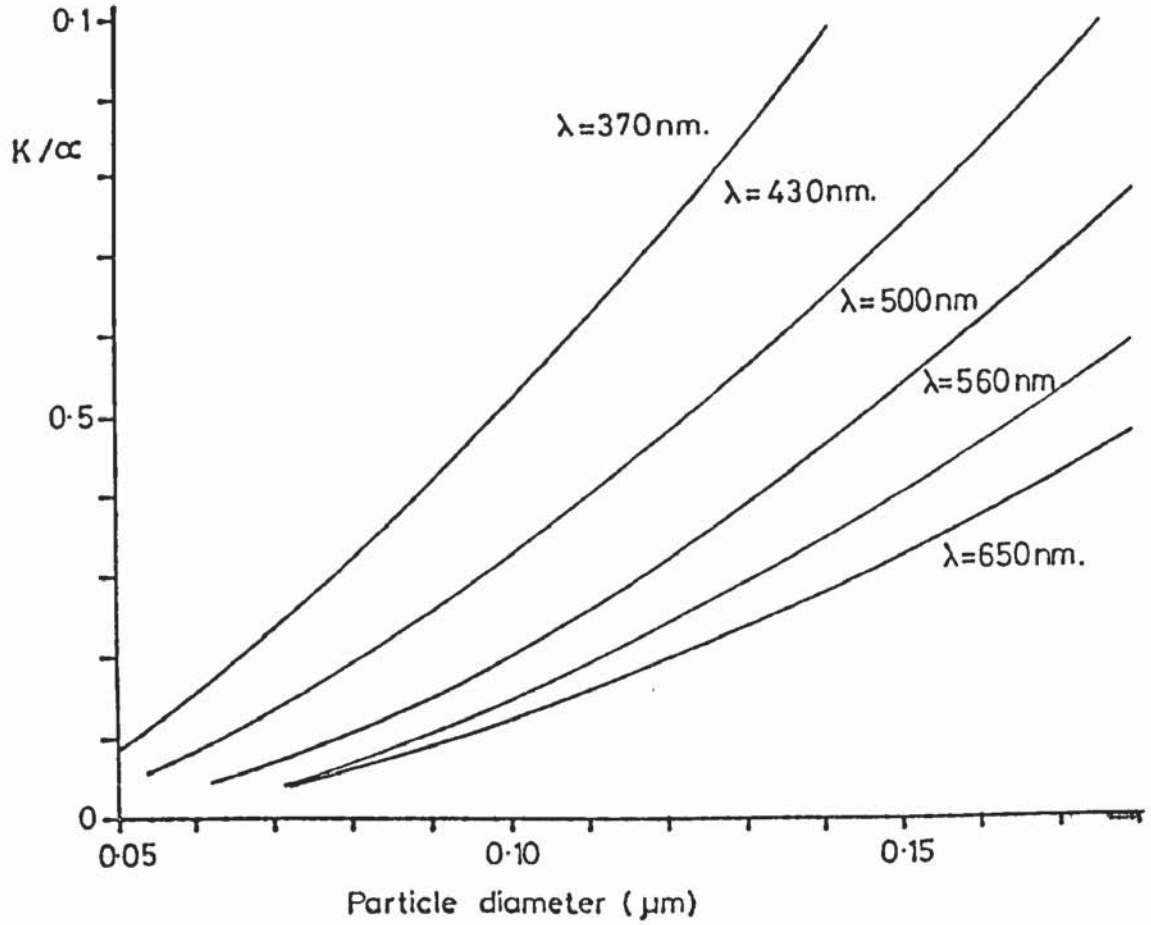

Fig 5·5 Plot of K/α against particle diameter. Curves predicted by the Rayleigh-Gans-Debye formula.

this point rather than at total conversion. It proved impossible, however, to ensure that each sample used in the particle size analysis was at the same given conversion, and this would clearly lead to inconsistency in the results. Two corrections to the apparent latex size were, therefore, necessitated. The calculations relating to polymer concentration and particle density were, therefore, carried out with the aim of compensating for variable amounts of monomer present in the particles. In addition, the results were corrected to 100% conversion to allow comparison between experiments. The following set of calculations were developed.

1) Calculation of the particle mass concentration in the final dilute sample was amended to allow for dissolution of unreacted monomer into the aqueous phase at high dilutions. The equations developed were as follows.

Weight of polymer in sample $= W_p = W_D \cdot (MPC - MSC + TSC)$ (5.3)

Weight of styrene in sample $= W_s = (MSC - TSC) \cdot W_D$ (5.4)

Weight of water in sample $= W_A =$ Total sample weight $- (W_D \cdot MSC)$ (5.5)

Weight of styrene in aqueous phase $= W_{SA} = \dfrac{M \cdot W_A \cdot W_S}{W_P + M \cdot W_A}$ (5.6)

Weight of styrene in polymer particles $= W_{SP} = W_S - W_{SA}$ (5.7)

Polymer particle mass concentration $= C = \left(\dfrac{W_P + W_{SP}}{W_A}\right) \cdot \rho_{H_2}$ (5.8)

Where W_D = weight of sample taken from first dilution

M = partition coefficient $= \dfrac{C_A}{C_P} = 2.2393 \times 10^{-4}$

C_A = The concentration of styrene in aqueous phase

C_P = The concentration of styrene in polymer particles

Both the above values were assumed to be those at saturation.

2) The particle density cannot be assumed to be that of pure polystyrene, as it will contain a proportion of the monomer. An expression for estimating the density of the particles was derived, based upon the parameters calculated in the calculations for particle concentration.

To estimate a density for polymer particles that contained less than saturation concentration of monomer required the assumption that the particles contained two distinct components. One component was polymer that was saturated with monomer, the other component was pure polystyrene. The density of the particles was calculated as the mean of the densities of these two components, thus:-

$$\rho = \left(\frac{W_{SP}}{W_{SP} + W_P} \cdot \frac{1}{\phi_V}\right) \rho_{SWP} + \left(1 - \left(\frac{W_{SP}}{W_{SP} + W_P} \cdot \frac{1}{\phi_V}\right)\right) \rho_P \qquad (5.9)$$

which condenses to

$$\rho = \rho_P + \left(\frac{W_{SP}}{W_{SP} + W_P} \cdot \frac{1}{\phi_V}\right) \left(\rho_{SWP} - \rho_P \right) \qquad (5.10)$$

where ρ = particle density

ρ_P = density of polystyrene

ρ_{SWP} = density of monomer swollen polymer at saturation

ϕ_V = volume fraction of monomer dissolved in polymer at saturation.

The value of ρ_{SWP} was calculated from

$$\rho_{SWP} = \frac{W_{SS}}{Q_W} \qquad (5.11)$$

Where W_{SS} is the mass of styrene dissolved in a unit volume of

polymer particle at saturation, the value of which was taken from Nomura et al's paper[28] as 0.570 $g.cm^{-3}$.

3) Normalising the results to a consistent level of conversion, (100%) was carried out in order to allow comparison between experiments. The normalisation equation was developed as follows.

The mass of a single particle in the second dilute sample (W_1) is given by

$$W_1 = (\frac{\pi\ dp^3}{6}) \cdot \rho \qquad (5.12)$$

The mass of styrene dissolved in the aqueous phase that was previously dissolved in the particle (W_2) is given by

$$W_2 = \frac{W_1}{(W_P + W_{SP})} \cdot W_{SA} \qquad (5.13)$$

Hence the mass of a polymer particle in the undiluted latex (W_3) is

$$W_3 = W_1 + W_2 = (\frac{\pi.dp^3}{6})\ (1 + \frac{W_{SA}}{W_P + W_{SP}})\ \rho \qquad (5.14)$$

The volume of a particle in the undiluted latex at 100% conversion is, therefore,

$$\frac{\pi\ dp^3_{100}}{6} = \frac{\pi\ dp^3}{6}\ (1 + \frac{W_{SA}}{W_P + W_{SP}})\ \rho/\rho_p \qquad (5.15)$$

Therefore

$$dp_{100} = (dp^3\ (1 + \frac{W_{SA}}{W_P + W_{SP}})\ \rho/\rho_{pol})^{1/3} \qquad (5.16)$$

5.2.2 The effect of particle concentration and cell length

One latex sample was chosen to investigate the possible effect of both spectrophotometer sample cell length and the polymer concentration of the diluted latex on the analysis results.

The results of this analysis are shown in table 5.2.

Cell length mm / Conc $\bar{n}$ g x 10^5	10	20	40
9.93	0.13	0.13	0.12
3.90	0.13	0.13	0.13
1.86	0.12	0.13	0.12

Table 5.2 Mean latex particle size as measured for a range of c and l. Polymer sample P12. (see table 5.1).

As can be seen from table 5.2, no discernible trend is shown to suggest that either cell length or particle concentration would affect the results to any great extent. This conclusion is further supported by the work of Cao[69] who has carried out a number of latex particle size analysis at varying concentrations of polymer and has shown that at dilutions of above 20,000 x, as in these analyses, and particularly at conversions above 20% solids (i.e. > 40% conversion) the measured particle size was not a function of polymer concentration.

5.2.3 Error analysis

An error analysis was carried out to find the typical error that may be expected in the final value of the latex particle diameter due to round off error in the calculation. A typical set of calculations for the analysis of particle size of a sample from experiment P12 were subject to the error analysis.

The error generated in a particular calculation step was estimated thus;

If $Z = f(X, Y, ...)$ (5.17)

Then the error in Z, S_Z, is given by

$$S_Z^2 = \left(\frac{\partial Z}{\partial X}\right)^2 S_X^2 + \left(\frac{\partial Z}{\partial Y}\right)^2 S_Y^2 + \ldots\ldots \quad (5.18)$$

For the case where

$$Z = X + Y \quad (5.19)$$

The error, E_Z, was estimated as

$$Z \pm E_Z = X + Y \pm (E_X + E_Y) \quad (5.20)$$

The final error analysis revealed a probable error of approximately 1.5% in the final particle size, due to round off in the calculations.

It should also be pointed out that the published and estimated values of k/α are for pure polystyrene. The samples analysed contained a small proportion of styrene monomer, and it would therefore be expected that some error could arise from this.

Cao's[69] work, however, appears to show that at the relatively high degree of conversion in the latex samples, the influence of the monomer present is negligible and the error is therefore not significant.

5.2.4 Comparison of light transmission analysis results with electron micrographic analysis results

Because of the possible sources of error in the turbidity technique of particle size analysis it was clearly necessary to check the effect of these factors by comparison with particle size data from an alternative technique. Four latex samples were analysed for particle size, therefore, using electron microscopy. Micrographs of the samples were taken on a stereoscan type of electron microscope. The diameters of 35 particles were measured and the mean was then calculated. This work was carried out by Ministry of Defence personnel at P.E.R.M.E. Waltham Abbey.

Results of this analysis and the results of the corresponding light extinction analysis are shown in table 5.3.

Sample	Particle diameter (μm)	
	Electron microscope	Light extinction
P16	0.14	0.11
P12	0.15	0.13
P13	0.16	0.14
P11	0.15	0.15

Table 5.3 Comparison of measured particle diameters

This comparison shows that the results obtained from turbidity measurements are of a similar order as those obtained by electron microscopy. In addition, similar trends are shown by both sets of results. Thus, the validity of the light extinction technique of particle size analysis appears, in this case, to be supported by the results obtained by electron microscopy.

5.2.5 Variation of experimental latex particle size with impeller speed

Polymerisations were carried out over an impeller speed range of 410 r.p.m. to 960 r.p.m. and at three initial soap concentrations. Of the 23 styrene polymerisations performed only 12 were fully analysed for particle size as the technique for particle size analysis was not fully developed until a number of experiments were completed. The results for these are tabulated in table 5.4 and shown graphically in figure 5.6.

The results are presented as final latex particle size against impeller speed for these different soap levels. The model under test predicts that the particle size will become more sensitive to variations in impeller speed at low initial soap concentrations. It can clearly be seen that the results from the high soap experiments (12.8 $g.dm^{-3}$) show no significant change in particle size with variation of impeller

Soap concentration g . dm^{-3}	12.8	8.0	4.0
Impeller speed r.p.m.			
410	0.12	0.11	-
575	0.11	0.13	0.13
740	0.12	0.14	-
960	0.11	0.15	0.14

Table 5.4 Final latex particle diameters (μm)

speed. The medium soap (8 g.dm^{-3}) runs, however, show a marked trend towards the formation of larger particles at higher impeller speeds. The data for the low soap runs, although limited, also support this trend. Such a trend is consistent with the theory that the degree of monomer dispersion can influence the final particle size via its effect on the micelle population, this effect becoming more marked as the soap concentration is reduced. This agrees with the results of Nomura et al[28].

The effect of the soap concentration, at a constant impeller speed, on the final particle size can be clearly seen in figure 5.6. As would be expected, the particle size increases with decreasing soap concentration.

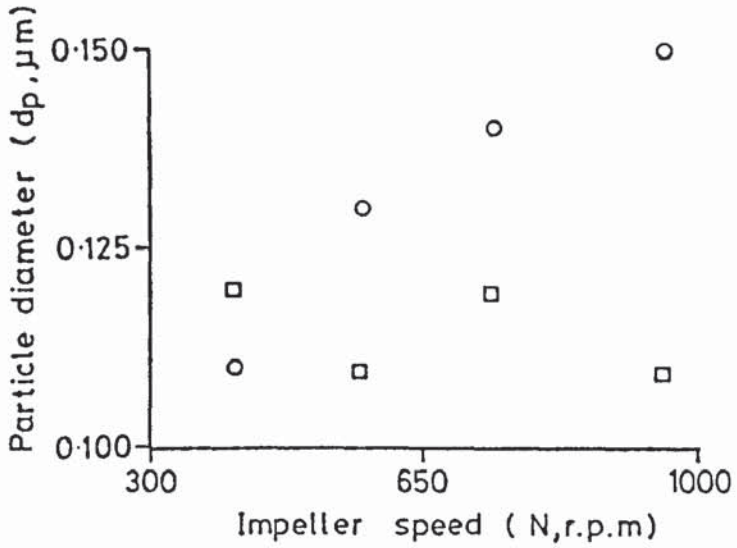

Fig 5·6 Final particle diameter against impeller speed

□ S= 12·8 g.dm^{-3}

o S= 8·0 g.dm^{-3}

6.0 MATHEMATICAL MODELLING OF EMULSION POLYMERISATION

6.1 A numerical model of emulsion polymerisation

6.2 Programming of a model

6.3 Program input parameters

6.4 Program results

6.0 MATHEMATICAL MODELLING OF EMULSION POLYMERISATION

A number of mathematical models of emulsion polymerisation have been published but many of these may be recognised as modifications of the first model published, that is the model of Smith and Ewart[5]. Some of the models are exceedingly complex, for example the comprehensive model of Min and Ray[8]. They all, however, ignore the effect of monomer dispersion characteristics on the reaction kinetics.

It is a basic assumption of mathematical models based upon the micellar theory of particle generation that the number of particles formed is a function of the micelle population. In general, current models relate the micelle population directly to the total initial soap concentration and ignore the fact that some of the soap will not be available to form micelles, this being a proportion of the soap equal to the c.m.c. and a proportion of the soap adsorbed onto the monomer droplet surface. It is, however, clearly incorrect to assume that either of these, but more particularly, that soap adsorption may be neglected when modelling the reactions. Equally and, more importantly for this study, if the dependence of the reaction on soap adsorption and thus on the degree of dispersion is accepted it is clearly necessary in any procedure for scale-up to assume reproducibility of this degree of dispersion.

It was thought useful, therefore, to develop a mathematical model of emulsion polymerisation that took into account the effect of c.m.c. and the degree of monomer dispersion on the amount of soap available to form micelles. In addition, it was considered that prediction of particle size should also be included in the model.

6.1 A numerical model of emulsion polymerisation

At the heart of any model of polymerisation are the kinetic equations. Kinetic models may be developed during the research programme

or use may be made of existing, published kinetic models. As this project did not involve fundamental study of the reaction kinetics of emulsion polymerisation, the latter course of action was adopted.

The kinetic equations chosen as the base for the new model were those of Smith and Ewart[5].

As always, when trying to model a physical process, it is necessary to make a number of assumptions. The two most basic assumptions in this case are;

1) The assumption that the micellar theory for particle generation is valid. Although there is continuing debate on the subject of the trueloci of particle generation, the micellar theory is the oldestand best developed theory at the present time. It is partially for this reason that the micellar theory was assumed. A further argument in its favour of particular relevance to this project is that the micellar theory gives a simple explanation for the effect that the degree of monomer dispersion has upon the final particle size of the latex.

2) The assumption that the Smith and Ewart kinetic model was suitable to form the basis of the new model. In this case, the Smith and Ewart model was undoubtedly the simplest kinetic model with which to work. It is also the best established model and it has been shown to give reasonable results.

On the basis of these two assumptions a new model was, therefore, founded. The structure of this new model may be divided into a number of subsections, and a basic flow chart showing these can be seen in figure 6.1. The individual subsections are described below.

6.1.1 Degree of dispersion

This section of the model deals with all the parameters related to the degree of dispersion, i.e. the mean droplet diameter, the

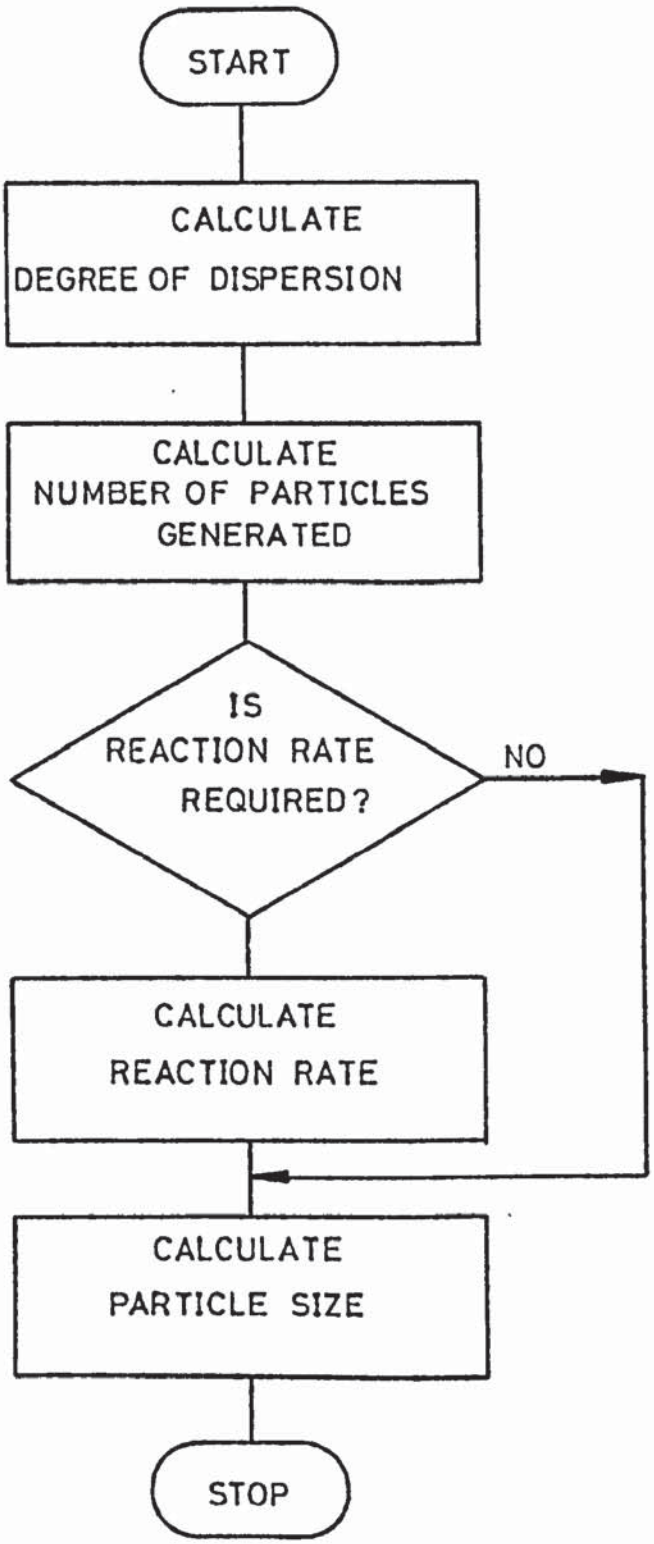

Fig 6·1 Flowchart showing basic structure of author's model

number of droplets, the interfacial area of the droplets, the total interfacial area and the surface areas presented by the micelles.

Mean droplet diameter

Calculation of the droplet diameter is based upon the empirical relationship presented in section 4.4. Reference values of the impeller parameters (speed, N_o; diameter, D_o) and a corresponding reference value of the mean droplet diameter $\bar{d}_{so}$ were used enabling the value of the mean droplet size, $\bar{d}_s$, at a given impeller speed, N, and diameter, D, to be estimated by the following expression;

$$\bar{d}_s = \bar{d}_{so} \left(\frac{N}{N_o}\right)^X \left(\frac{D}{D_o}\right)^Y \qquad (6.1)$$

Where X = empirical exponent (estimated in this study to be -1.08)

Y = empirical exponent (estimated in this study to be -0.185).

Droplet numbers and surface area

The number of droplets is simply calculated from a knowledge of the initial volume of monomer and the droplet diameter. This assumes, in fact, that there is a monodispersion which is clearly not the case but as the important characteristic in this study is the total surface area of the dispersion, this will lead to no error.

$$N_d = \frac{6\ V'}{\pi(\bar{d}_s)^3} \qquad (6.2)$$

Where N_d = number of droplets per unit volume of aqueous phase

V_{do} = initial volume of monomer per unit volume of aqueous phase.

The initial interfacial area of the drops, A_{do}, is then calculated from;

$$A_{do} = \frac{6\ V_{do}}{\bar{d}_s} \qquad (6.3)$$

It is an assumption of the new model that the number of monomer droplets calculated remains constant until all the monomer is transferred to polymer particles.

Total interfacial area and the surface area of the micelles

The classical micellar theory assumes that soap molecules are found in three physical states, i.e. those in free solution, those forming micelles and those adsorbed onto the droplet and particle interfaces. A fundamental assumption of the Smith and Ewart physical model is that each molecule of soap adsorbed onto a surface or forming a micelle, presents a specific area to the aqueous phase, the initial total interfacial area is simply calculated thus;

$$A = (S_i - S_{cmc})\ a_s \qquad (6.4)$$

Where A = total interfacial area

S_i = initial number of soap molecules

S_{cmc} = soap molecules in free solution

a_s = specific area of a soap molecule.

The surface area of the micelles, a_m, is calculated from;

$$a_m = A - A_d \qquad (6.5)$$

6.1.2 Number of polymer particles generated

The basic kinetic equation used to predict the number of polymer particles generated during Stage I of the reaction was the second idealised situation of the Case 2 solution of the Smith and Ewart model. This assumes that radical capture is a function of the rate of radical generation and of the total surface area of the micelles, i.e.

$$N_p = 0.37 \left(\frac{\rho'}{\mu}\right)^{2/5} (a_s\ S)^{3/5} \qquad (6.6)$$

Where N_p = the number of particles generated.

This basic equation was modified in two ways, a simple modification of the equation as it stands and a more complex modification which involved amendment of the fundamental derivation of the equation from which equation 6.6 was developed.

Simple modification

This merely involved altering the soap term in equation 6.6 from S, the total initial soap to S_m, the soap available to form micelles. It is assumed that soap in free solution and soap adsorbed onto the droplet surface is not available for micelle formation. The value of S_m is thus calculated from,

$$S_m = S - S_{cmc} - \frac{A_d}{a_s} \qquad (6.7)$$

Complex modification

If stage I of emulsion polymerisation is pictured (see section 2.1.1) according to the Harkins physical model[4] it is easy to see that the number of soap molecules available to form micelles reduces throughout stage I as more soap is adsorbed onto the increasing interfacial area of the emergent polymer particles. In opposition to this, the surface of droplets will reduce as the reaction proceeds and thus will release soap for micelle formation. The simple modification to equation 6.6 does not take this latter point into account and indeed no previous models have attempted to do so. To include this effect, it was necessary to examine the fundamental equation from which equation 6.6 was derived by Smith and Ewart, i.e.

$$\frac{dN_p}{dt} = \frac{\rho A_m}{A} \qquad (6.8)$$

Where A = the total interfacial area of the micelles and polymer particles.

It is necessary, in order to develop the new model to redefine the term A in equation 6.8. The new definition is; A is the total interfacial area of the micelles, polymer particles and monomer droplets, and it has a constant value determined by the soap concentration, provided all interfaces are saturated with soap.

Equation 6.8 must be integrated between time t = 0, and t = t_I the time at which the micelles cease to exist, in order to obtain a value of N_p. Expressing A_m as a function of time leads to the following expansion of equation 6.8:

$$N_p = \rho' \int_0^{t_I} \left(1 - \frac{A_p + A_d}{a_s (S - S_{cmc})}\right) dt \qquad (6.9)$$

Where $A_p = \rho' \int_0^t (t_I - t)^{2/3} \left(\frac{dN}{dt}\right) dt$

$$A_d = (N_d.\pi)^{1/3} (6(Vd_o - (\rho_{swp}/\rho_m) Vp)$$

$$Vp = \mu \int_0^t (t_I - t) \left(\frac{dN_p}{dt}\right) dt$$

A full development of this equation is to be found in Appendix E. The obvious way to solve equation 6.9 is to apply numerical techniques with the aid of a computer. The way in which this was done is discussed in section 6.2.

6.1.3 Stage II and Stage III reaction rates

Stage II of the reaction was assumed to occur in the manner described by the Smith and Ewart case 2 solution, and hence their kinetic equation was used as part of the new model to describe stage II. The equation used, was therefore;

$$Vm_{II} = \frac{N_p.K_p.\emptyset_v}{2.N_A} (t_{II} - t_I) \qquad (6.10)$$

Where $\emptyset_v$ = volume fraction of monomer in particles at satuation

K_p = propagation constant

N_A = Avagadro's number

t_{II} = time at which all the monomer droplets disappear.

Stage III required a modification to equation 6.10 as the monomer concentration in the polymer particles could no longer be treated as a constant. Hence an incremental solution was required, i.e.,

$$V_{III} = \sum_{\emptyset'_{v,t}=\emptyset}^{\emptyset'_{v,t}=0} \frac{N_p k_p \emptyset'_{v,t}}{2N_A} \Delta t \qquad (6.11)$$

Where $\emptyset'_{v,t}$ = volume fraction of monomer in the polymer particles at time t.

Δt = incremental time steps.

In using equation 6.11 as part of the new model it was assumed that termination remained instantaneous during stage III. As discussed in section 2.1.3.3 this appears to be unlikely, especially in the case of large particles. However, use of equation 6.11 for this initial development of the new model is thought to be justified as a great deal more kinetic data than is currently available would be required to allow use of an equation that did not assume instant termination.

6.1.4 Calculation of final particle size

Given that the density of a polymer is greater than that of the corresponding monomer, calculation of the final polymer particle diameter is simple, i.e.

$$dp = \left(\frac{6 \cdot Vd_o \rho_m}{N_p \pi \cdot \rho_p}\right)^{1/3} \qquad (6.12)$$

Where ρ_m = monomer density

ρ_p = polymer density

dp = particle diameter

Here it is assumed that polymer particles are smooth solid spheres.

6.2 Programming of model

The basic model as described in the previous section would have been laborious to solve by hand due to the need to use numerical methods to predict the number of particles generated. It was obviously beneficial

to program the model for solution on a computer. Accordingly a program was written for solution on Aston University's I.C.L. 1904S computer in the FORTRAN language. A full program listing and flowcharts are shown in Appendix E.

6.2.1 Structure of program

The program consists of a master program that calls a number of subroutines. This structure is analogous to the structure of the model as previously described. The purpose of each routine is described below.

Master

The basic function of the program master is; to read the appropriate input data; to convert the values into suitable units for use in the program, to calculate the degree of dispersion and to feed this data into the appropriate subroutines and to call the subroutines required to calculate the final particle size or the reaction rate for the course of a polymerisation.

SMITHE

The object of this subroutine is to calculate the number of particles generated using both of the Smith and Ewart case 2 solutions and to calculate the time length of the particle generation period for the case where all the radicals formed enter micelles.

STAGE 1

This subroutine calculates the number of particles generated in Stage I of a reaction. The basis of this subroutine is equation 6.9 which for the purpose of programming was adapted into an algorithm to allow the application of a numerical solution. The set of equations forming the algorithm are shown in table 6.1.

STAGE 2

This subroutine deals with the constant rate period, stage III, of the emulsion polymerisation reaction.

The basis of this routine is the rate equation, equation 6.10.

Number of particles generated in a set time interval	$\Delta Np_n = \rho' \, Am_{n-1} \Delta t / A$
The total number of particles formed up to time t_n	$Np_n = \sum_{t=t_o}^{t=t_n} \Delta Np_n$
Total particle volume at time t_n	$Vp_n = Vp_{n-1} + Np_n \cdot \mu \cdot \Delta t$
Total particle surface area at time t_n	$Ap_n = \theta . \Delta t^{2/3} \sum_{i=0}^{i=n} n^{2/3} \Delta Np_{n+1-i}$
Total volume of monomer droplets at time t_n	$Vd_n = Vd_o - \sum_{o}^{n} (Vp_n \cdot \rho_{swp} / \rho_m)$
Total area of monomer droplets at time t_n	$Ad_n = (6 \, Vd_n)^{2/3} \cdot (N_d \pi)^{1/3}$
Surface area of micelles at time t_n	$Am_n = A - Ad_n - Ap_n$

Table 6.1 Basic algorithm for the solution of the equation predicting the number of particles generated in stage I of an emulsion polymerisation.

Obviously there is no immediate need to carry out incremental calculations in order to solve this equation. An incremental solution, however, allows values of the degree of conversion and particle size to be calculated at various times during stage II. It may also be a more suitable form of programming if the program is to be developed further to include, for example, the possibility of droplet polymerisation.

The basic algorithm for stage II is shown in table 6.2. This section is deemed to be complete when the volume of the droplets falls to zero.

STAGE III

This routine simulates stage III of an emulsion polymerisation.

The basis of this subroutine is again the rate equation, equation 6.10. This time, however, an incremental solution is required as the monomer concentration within the polymer droplets continuously falls. The algorithm is shown in table 6.3.

In this case, the volume of monomer reacted in each given time increment varies for each increment due to the changing value of the monomer concentration in the polymer particles. The degree of conversion is also calculated and when this reaches 90% the subroutine returns to the master, indicating the end of the reaction simulation. The use of 100% as the termination condition would have required an uneconomic use of computer time.

PARSIZE

This routine calculates the polymer particle diameter at 100% conversion. The algorithm used is simply;

$$dp = \left(\frac{Vd_o \cdot \rho_m \cdot 6}{N_p \cdot \pi \cdot \rho_p}\right)^{1/3} \qquad (6.13)$$

This is the last subroutine to be called by the master program.

6.2.2 Program Options

It was decided to program into the computer model three options;

The volume of monomer reacted in a given time increment	$Vm_n = \frac{N_p K_p \phi_v}{2 . N_A} . \Delta t$
Correction factor to allow for the change in volume when monomer is absorbed into polymer	$Z = (\frac{1}{\phi_v} + \frac{\rho_m}{\rho_{swp}} - 1)/(\frac{1}{\phi_v} - 1)$
Total volume of monomer droplets at time t_n	$Vd_n = Vd_{n-1} - Z. \sum_{t=t_{n-1}}^{t=t_n} Vm_n (\frac{1}{\phi_v} + \frac{\rho_m}{\rho_{swp}} - 1)/(\frac{1}{\phi_v} - 1)$
Total volume of polymer particles at time t_n	$Vp_n = Vp_I + \sum_{t=t_I}^{t=t_n} Vm_n (Z - 1 + \rho_m/\rho_{swp})$
Total surface area of monomer droplets at time t_n	$Ad_n = (6\ Vd_n)^{2/3} . (N_d\ \pi)^{1/3}$
Total surface area of polymer particles at time t_n	$Ap_n = (6\ Vp_n)^{2/3}\ (N_p\ \pi)^{1/3}$
Particle diameter at time t_n	$dp_n = 6 . Vp_n/Ap_n$

Table 6.2 Algorithm for simulation of stage II of an emulsion polymerisation

Volume of monomer reacted in a given time increment	$Vm_n = \frac{Np \cdot Kp\ Vmp_{n-1}}{2\ NA\ Vp}\ \Delta t$
Volume of monomer in the polymer particles at time t_n	$Vmp_n = Vmp_o - \sum_{n=o}^{n=n} Vm_n$
Volume of polymer particles at time t_n	$Vp_n = Vp_{II} - \sum_{n=o}^{n=n} Vm_n\ (1 - \frac{\rho_{swp}}{\rho_p})/\phi_v$
Surface area of polymer particles at time t_n	$Ap_n = (N_p)^{1/3} \cdot (6\ Vp)^{2/3}$
Particle diameter at time t_n	$dp_n = 6Vp/Ap$

Table 6.3 Algorithm to simulate stage III of an emulsion polymerisation

1) A full simultation of a reaction can be obtained listing the degree of conversion and particle size at simulated thirty minute intervals. This option is selected by setting the control parameter MODE to zero.

2) Final particle size and number can be calculated using the subroutine stage I. This option is selected by setting the control parameter MODE to 1.

3) Final particle size and number can be obtained using the subroutine SMITHE with a modified soap parameter to account for the effect of monomer dispersion on the amount of soap available to form micelles. Set the control parameter MODE1 to 1 to select this option.

6.3 Program input parameters

The input parameters for the computer model can be classified into three groups; the truly independent variables such as impeller speed, impeller diameter, phase ratio, soap concentration and temperature values, all of which were chosen on the basis of experience in operating the reactor; the dependent variables, such as the mean droplet diameter of the monomer dispersion, for which values were determined experimentally and finally, the physical and kinetic data for the system under study for which values were normally obtained from the literature. All values of input parameters used for the purpose of this project were for the emulsion polymerisation of styrene.

Table 6.4 shows a list of the input parameters and the values used.

6.3.1 Truely independent variables

The input parameters for which values were chosen are, the initial

	Input parameter	Input value
AS	Adsorption area of a soap molecule (a_s)	5.2×10^{-15} cm^2 . $molecule^{-1}$
CONST	Propagation constant (kp)	$0.127 \times 10^8 cm^3$. $Mole^{-1}$. min^{-1}
D	Impeller diameter (D)	7.5 cm
DBARI	Reference Sauter mean droplet size of emulsion	0.0128 cm
DENMON	Monomer density at 50°C (ρ_m)	0.879 $g.dm^{-3}$
DENPOL	Polymer density at 50°C (ρ_p)	1.049 $g.dm^{-3}$
DENSWP	Density of monomer swollen polymer at 50°C (ρ_{swp})	0.934 $g.dm^{-3}$
DI	Reference impeller diameter	7.5 cm
FI	Volume fraction of monomer in polymer at saturation ($\emptyset_v$)	0.65
GROW	Volumetric growth rate of a polymer particle (μ)	cm^3 . $particle^{-1}$. min^{-1}
RAD	Rate of radical generation (ρ')	5.93×10^{14} radicals . min^{-1}
REV	Impeller speed (N)	410/575/740/960 r.p.m.
REVI	Reference impeller speed	410 r.p.m.
S	Total soap concentration (S)	0.004/0.008/0.00128 $g.cm^{-3}$
SA	Critical micelle concentration (c.m.c.)	0.000105 $g.cm^{-3}$
VDI	Initial monomer volumer per unit volume of aqueous phase (Vd_o)	1.35 cm^3 . cm^{-3}
X	Impeller speed exponent	- 1.08
Y	Impeller diameter exponent	- 0.185

Table 6.4 Program input parameters

monomer volume, VDI, the total initial soap concentration, S, and the reference values of the impeller speed, REVI, and diameter, DI, and the actual values of impeller speed, REV, and size, D.

The values of VDI and S were chosen to be the same as values used in the polymerisation experiments as were the values of REV and D. The choice of values of REVI and DI, although independent, was based on experience gained in the dispersion experiments (Chapter 4.0).

6.3.2 Experimentally determined variables

The experimentally determined variables were; the number of soap molecules initially in free aqueous solution equivalent to the c.m.c. of the soap, SA, the reference value of the mean droplet diameter, DBARI, and the exponents X and Y in the dispersion equation.

Although values of the c.m.c. of the soap (sodiumdodecylebenzene-sulphonate) used in the system studied in this project are available in the literature[70], such values do not account for the effect of electrolytes on the c.m.c. As the recipe studied included electrolytes it was necessary to determine experimentally the c.m.c. of the soap under such conditions. The value determined for the c.m.c. of Nansa under these conditions is

$$c.m.c. = 0.105\ g.dm^{-3} \text{ at } 20^{o}C.$$

Details of the experimental determination may be found in Appendix A.

The value of DBARI, i.e. the reference value of the mean droplet diameter, was taken from the experimental data obtained during the dispersion experiments and the values of X and Y were derived from the correlation of results of those experiments (Chapter 4.0).

6.3.3 Variable values obtained from the literature

The parameters for which values were abstracted from the literature are; the specific surface area of a soap molecule, AS, the propagation constant, CONST, the rate of radical generation, RAD, the volumetric

growth rate of a polymer particle, GROW, the monomer density, DENMON, the polymer density, DENPOL, the density of the monomer swollen polymer and the volume fraction of monomer dissolved in polymer at saturation, FI.

Specific surface area of a soap molecule

The value of the specific area of a soap molecule was taken directly from the Polymer Handbook[71] for sodiumdodecylbenzenesulphonate. The abstracted value was

$$AS = 5.2 \times 10^{-15} \text{ cm}^2 \text{ . molecule}^{-1}$$

Propagation constant

The Polymer Handbook[72] listed six values for the propagation constant for styrene polymerisation at a temperature of 50°C. These are shown in table 6.5 together with the value determined by Harada et al[13]. As can be seen there is considerable disagreement although the values centre around a value of about 200 $\text{dm}^3 \text{ . mole}^{-1} \text{ . s}^{-1}$. Possible reasons for this disagreement may be suggested. The values of kp listed were obtained from reaction rate data for experimental emulsion polymerisations. The values of kp were then calculated on the basis of the Smith and Ewart model (the exception to this was the value presented by Harada et al[13] which was calculated using a technique based on their own model, this technique did not require knowledge of the number of particles formed). It is apparent that any value of kp obtained from experimental emulsion polymerisation rates relies upon the consistent behaviour of such polymerisation for its accuracy, and indeed upon the validity of the model used in the calculations and the accuracy of input variables. As has been shown in this thesis (Chapter 4.0) and as discussed by Nomura et al[24], emulsion polymerisation reactions are subject to non ideal behaviour which would clearly affect the validity of any estimate of kp obtained from

Propagation constants at 50°C

kp . (l/mol . s)	Source	Method
390	Polymer Handbook[72]	Emulsion polymerisation
209	" "	" "
123	" "	Rotating sector
223	" "	Emulsion polymerisation
206	" "	" "
300	" "	" "
212	Harada et al[13]	" "
200	Polymer Handbook[72]	Ahrenius plot through all data

Table 6.5 Propagation constants for the polymerisation of styrene at 50°C

emulsion polymerisation. Using experimental data and a mathematical model in order to estimate kp clearly concentrates into the value of kp the cumulative discrepancies of the experimentation and of the model. The inconsistency of kp values is a further indication of the difficulty in achieving consistency in the emulsion polymerisation reaction.

Obviously, however, a value of kp, for use in the program, had to be chosen. The value presented by Harada et al[13] was taken as it was estimated from data obtained from relatively high organic phase ratio emulsion polymerisations, and these conditions were the closest approach to the conditions employed in experiments carried out during this study.

An obvious alternative to this was of course to calculate a value of kp from the experimental data available from the current study. Experimental results yielded, however, a range of values for kp, as shown in table 6.6 again presenting the problem of selecting the most appropriate value. It was also thought desirable to use an independently

N r.p.m.	S $g.dm^{-3}$	dp μm	Np $\times 10^{-15}.cm^{-3}$	$\frac{dXm}{dt}$ $\%.h^{-1}$	kp $dm^3.mole^{-1}.S^{-1}$
410	12.8	0.13	0.98	35.9	201
575	12.8	0.12	1.25	35.7	157
740	12.8	0.12	1.25	35.1	154
960	12.8	0.12	1.25	36.3	159
410	8.0	0.12	1.25	41.8	183
575	8.0	0.13	0.98	29.0	162
740	8.0	0.14	0.79	28.0	194
960	8.0	0.15	0.64	22.8	195

Table 6.6 Calculated values of the propagation constant, kp, based on experimental observations

derived value of kp as it was considered that the aim of modelling any reaction should be to predict its behaviour without it being necessary to actually perform the reaction.

Monomer and polymer densities

The polymer density was taken from The Polymer Handbook[74] whilst the monomer density was taken from The Encyclopedia of Chemical Technology[73]. The values obtained for the reaction temperature, i.e. 50°C, are:

DENMON = 0.879 $g.dm^{-3}$

DENPOL = 1.049 $g.dm^{-3}$

Volume fraction of monomer in polymer

The volume fraction of monomer in polymer at saturation was calculated from the weight fraction and molar concentration of monomer in the polymer particles at saturation, both taken from Nomura et al[2], and the monomer density in the following way.

Assuming unit volume of polymer particles the volume of monomer present, Vm, is given by

$$Vm = \frac{Mp \cdot Mw}{\rho_m} \qquad (6.14)$$

Where Mw = molecular weight of monomer

ρ_m density of monomer.

The volume fraction, FI, is therefore given by

$$FI = \frac{Vm}{1} \qquad (6.15)$$

For styrene/polystyrene the value of FI was calculated to be 0.65.

Density of monomer swollen polymer

The density of monomer swollen polymer is determined from the molar concentration of monomer in polymer and the corresponding monomer weight fraction ϕ_w, which is calculated from an expression presented by Nomura et al, i.e.

$$\phi_w = \frac{1}{1 + \frac{10^3 \rho_p}{Mp \cdot Mw} \cdot - \frac{\rho_p}{\rho_m}} = 0.61 \qquad (6.16)$$

Assuming a unit volume of polymer particles saturated with monomer, the density, therefore, is given by;

$$DENSWP = \frac{Mp \cdot Mw}{\phi_w \cdot 1} = 0.934 \qquad (6.17)$$

Volumetric growth rate of a polymer particle

An expression for GROW was given by Gardon[11] as

$$\mu = \frac{kp}{N_A} \cdot \frac{\rho_m}{\rho_p} \cdot \frac{\phi m}{(1-\phi m)} \qquad (6.18$$

Where ϕm = volume fraction of monomer in emulsion. Solution of equation 6.18 gives the value for GROW as 3.29×10^{-17} $cm^3 \cdot particle^{-1} \cdot min^{-1}$.

Rate of radical generation

The rate of radical generation is given by Gardon as;

$$\rho = 2 \cdot N_A \cdot k_d [I] \qquad (6.19)$$

Where [I] = initiator concentration (8.64×10^{-6} mole . cm^{-3})

k_d = the rate constant for dissociation of the initator ($9.5 \times 10^{-7} \cdot s^{-1}$)

The solution to equation 6.19 gives;

ρ = RAD = 5.93×10^{14} . radicals . min^{-1}

The value of k_d was obtained from The Polymer Handbook[74]. The best value available was for the dissociation of potassiumpersulphate in a 0.1M sodium hydroxide solution at 50°C, whereas the solution used in the current polymerisation experiment was 0.07M.

6.4 Program results

The results of the polymerisation experiments were divided into two sections, these being particle size and reaction rate. Similiarly, the predicted results also fall into these two divisions and are presented accordingly.

6.4.1 Particle size results

The program afforded two routes for calculating the final particle size, a simple modification of the Smith and Ewart model, the modification being an allowance for the effect on the micelle population of the soap adsorbed onto the monomer interface; and a more complex model that takes into consideration the desorption of soap from the monomer interface as the monomer volume decreases. The results for both of these models are shown in figure 6.2 which allows comparison of the predictions of the two models with the predictions of the unaltered Smith and Ewart model and with the experimental results.

As may be seen predictions of the two modified forms of the Smith and Ewart model are very similar to each other, with the more complex

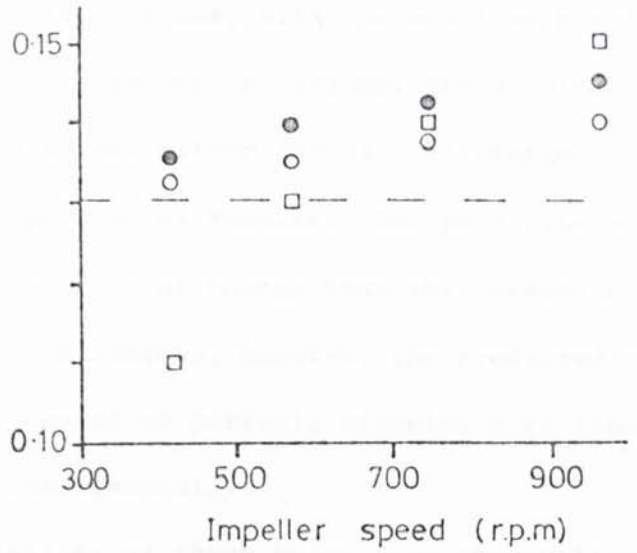

Fig 6·2a $S = 8{\cdot}0\ g.dm^{-3}$

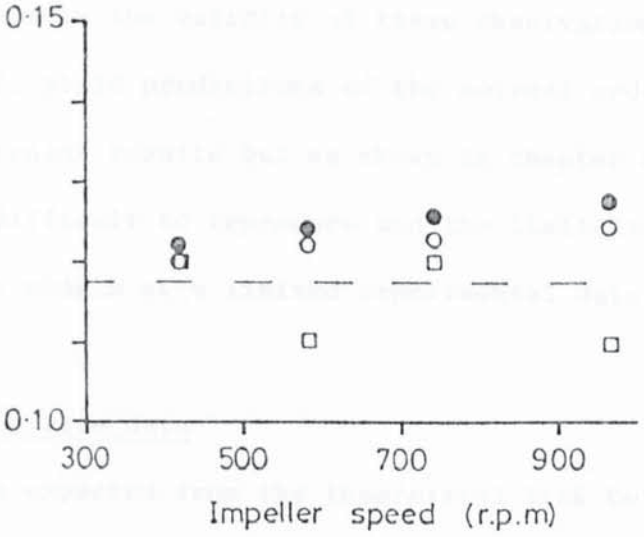

Fig 6·2b $S = 12{\cdot}8\ g.dm^{-3}$

Fig 6·2 Plot of predicted and experimental particle diameters against impeller diameter.

o Simple modification ● Complex modificaion

— — Smith and Ewart □ Experimental

model predicting slightly larger particle diameters. The agreement of all three mathematical models, however, is within 14% agreement with experimental particle sizes, with the modified models being within 8%. At the 8.0 $g.dm^{-3}$ soap concentrations, the predicted results of both modified models do not mirror the rate of change in particle diameter shown by the experimental results. The predictions, in this case, indicate a slower rate of change than that observed. In the case of the higher soap concentrations, however, the predicted results indicate a faster rate of change of particle diameter with impeller speed, than that observed experimentally.

The possibility of these being true observations can not be neglected, but without substantially more experimental data, it is difficult to assess the validity of these observations. It is obvious that the models yield predictions of the correct order, as indicated by the experimental results but as shown in chapter 5 experimental results were difficult to reproduce and the limitations of any comparison of the models with limited experimental data should not be overlooked.

6.4.2 Reaction rate data

As may be expected from the theoretical link between reaction rate and particle concentration, the reaction rate predictions of the two modified Smith and Ewart models do not differ widely. The results are shown in table 6.7 together with the comparable experimental observations. As may be seen, reasonable agreement between predicted and experimental results can, in the main, be claimed.

Graphs showing the predicted reaction rate curves at the extremes of impeller speed employed in this study, and the comparable experimental results are shown in figure 6.3.

N r.p.m.	410			575			740			960		
S . g.dm^{-3}	A	B	C	A	B	C	A	B	C	A	B	C
4.0	-	15.2	16.8	27.1	13.3	15.7	-	11.4	14.1	-	8.7	11.9
8.0	41.8	26.7	27.9	29.0	25.2	27.0	28.0	23.8	26.0	22.8	21.8	24.6
12.8	35.9	37.3	38.2	35.7	36.0	37.5	35.1	34.8	36.6	36.3	33.0	35.5

A = Experimental results

B = Numerical model results

C = Simply modified Smith and Ewart model results

Table 6.7 Stage II reaction rates

Clearly, the major deviations between predicted and observed results are the times at which polymerisation commences, the model cannot predict induction times which are, by their nature, functions of unpredictable inhibitor concentrations. In figure 6.4 the predicted curves have been transposed along the time axis by one hour, the approximate induction time shown by the experimental data. It can be seen that there is good agreement between predicted and experimental results up to approximately 40% conversion. Beyond this point, i.e. in stage III, some divergence is observed. The inability of these models to model stage III of the reaction probably lies in the fundamental assumptions, that is, it was assumed that stage II kinetics could be applied to stage III with only the monomer concentration modified on an incremental basis. In fact, it would appear unlikely that this is the case. The possibility of slow termination was discussed in section 2.1.3.3, and this would appear to offer an improvement to the modelling of emulsion polymerisation reactions.

6.4.3 Concluding remarks

The two modifications to the Smith and Ewart model yield similar results. In analysing the relative success or advantages of each model it is worth noting that one of the models involves simple calculations which may be performed without the aid of a computer, the other model, however, due to its incremental nature requires a computer for solution. The latter model may be one step closer to modelling the real situation, but the simpler model yields results that bear comparison with experimental results that are themselves difficult to reproduce with any degree of consistency. An inevitable question must be; does the prediction of particle diameters and reaction rates of minimally greater accuracy warrant the extra complexity and subsequent computer usage required in the more rigorous model? This question can only be answered

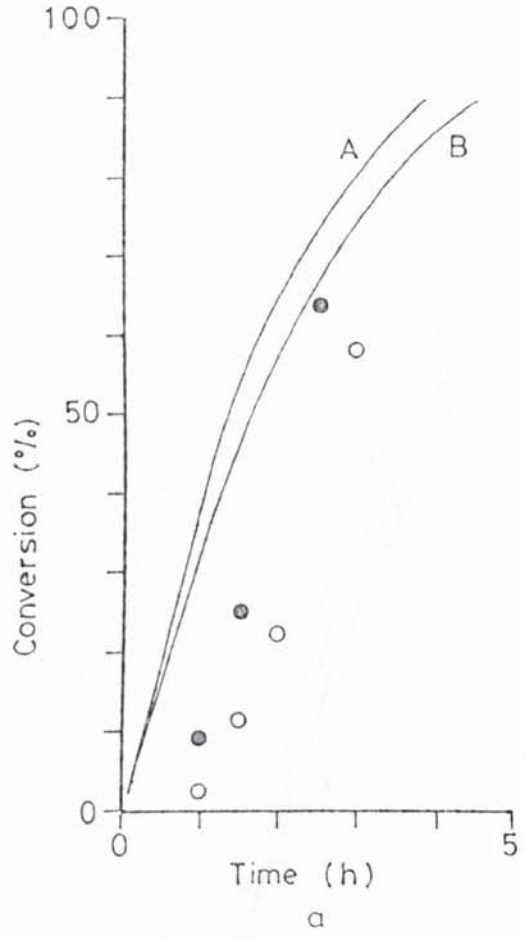

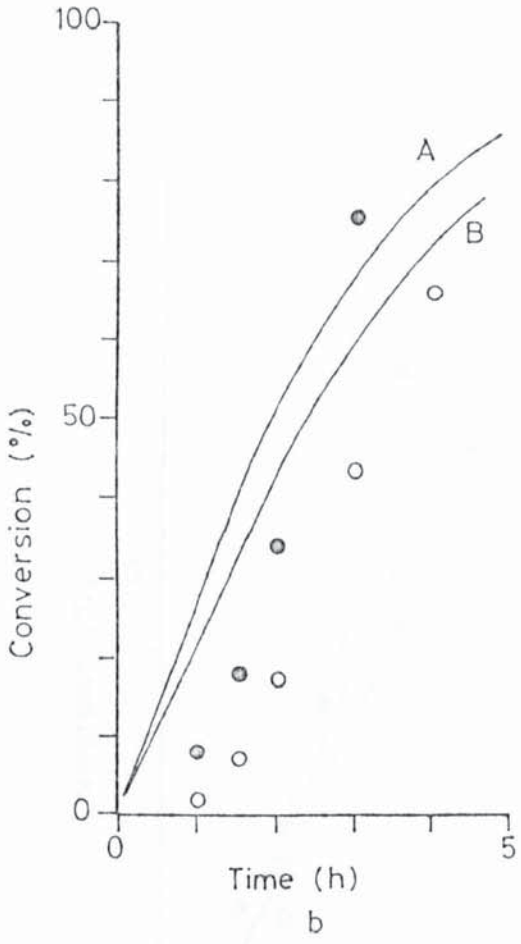

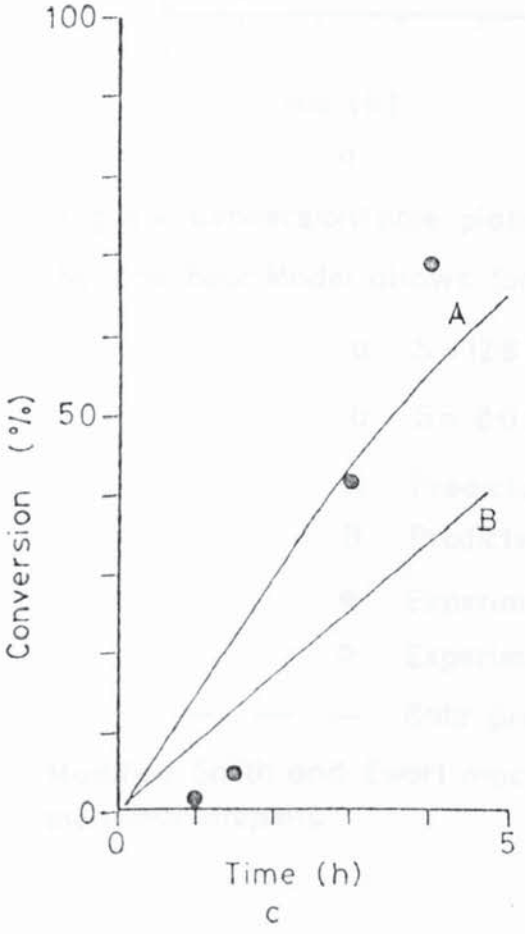

Fig 6·3 Conversion/time plots

a S = 12·8 g.dm^{-3}

b S = 8·0 g.dm^{-3}

c S = 4·0 g.dm^{-3}

A Predicted curve, N=410rpm

B Predicted curve, N=960rpm

● Experimental, N=410rpm

○ Experimental N=960rpm

Modified Smith and Ewart model allowing for soap desorption from monomer droplets.

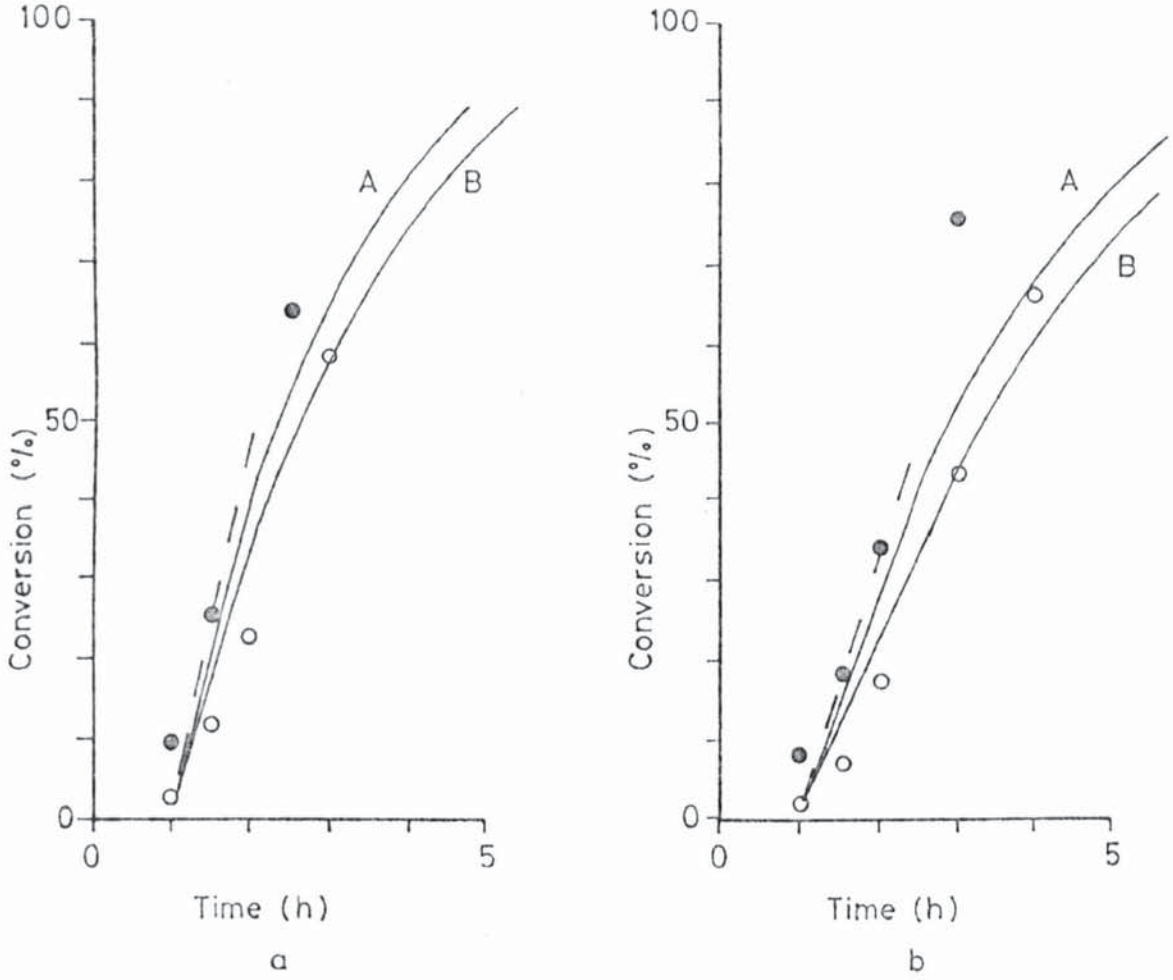

Fig 6·4 Conversion/time plots showing the predicted curves transposed by one hour. Model allows for soap desorption from monomer droplets.

a $S = 12{\cdot}8\ g.dm^{-3}$

b $S = 8{\cdot}0\ g.dm^{-3}$

A Predicted curve, N = 410 r.p.m

B Predicted curve, N = 960 r.p.m

● Experimental, N = 410 r.p.m

○ Experimental, N = 960 r.p.m

— — — Rate predicted by Smith and Ewart model.

Modified Smith and Ewart model allowing for soap desorption from monomer droplets.

in the light of the computer facilities available to the user, and indeed the establishment of whether or not the more complex model is truely more accurate than the simple model.

7.0 SCALE-UP

7.1 Scale-up equations for constant monomer dispersion

7.2 Limitations to scale-up

7.3 Scale-up diagram

7.0 SCALE-UP

The particular aspect of scale-up in emulsion polymerisation that has been the subject of this project has been the retention on scale-up. of the initial degree of dispersion of the monomer. The data of Nomura et al[28] indicated that the final particle size and the reaction rate were functions of the impeller speed. This, they recognised to be associated with the adsorption of soap onto the interface of the monomer dispersion and, of course, the more soap that is adsorbed onto the monomer, the less is available for micelle formation and thus, the number of particles formed is lower. This phenomenon is expected to be of greater significance for low soap systems with a relatively high monomer/ aqueous phase ratio, and as this project was particularly concerned with such systems it is apparent that a dependence on impeller speed should be expected here.

Introduction of the effect of soap adsorption into the Smith and Ewart model for emulsion polymerisation indicates that, it should, in fact, be expected that a close relationship between the initial degree of monomer dispersion and the final particle size exists, and clearly the experimental results for emulsion polymerisation (see chapter 5) confirm this relationship.

The conclusion to these considerations, therefore, is that the final particle size is dependent upon the initial monomer dispersion. Hence, it is implied that if a given latex particle size, or reaction rate is desired, then scale-up to retain these would equally demand retention, on scale-up, of the initial degree of monomer dispersion. The route adopted to develop guideline equations for the retention of the degree of dispersion on scale-up involved the investigation of the effect of impeller size and speed on the size of the monomer droplets.

Guideline scale-up equations were developed.

7.1 Scale-up equations for constant monomer dispersion

From chapter 4, it may be seen that two forms of equation relating droplet size to the impeller parameters have been developed in this study:

1) Equation 7.1 which was empirically derived using multiple linear regression. This equation is,

$$\bar{d}_s \propto N^{-1.08}\, D^{-0.185} \tag{7.1}$$

If the pilot scale is denoted by the subscript 2, and the scaled-up plant is denoted by the subscript 1, then for equivalent droplet diameter, the following is obtained.

$$N_1^{-1.08}\, D_1^{-0.185} = N_2^{-1.08}\, D_2^{-0.185} \tag{7.2}$$

Thus on scale-up, the impeller speed is indicated by;

$$N_1 = N_2 \left(\frac{D_2}{D_1}\right)^{0.1713} \tag{7.3}$$

2) The droplet size was related to the impeller parameters via the power input and two equations were developed in this case.

For $Re < 8 \times 10^3$

$$\bar{d}_s \propto N^{0.61-0.24 \ln Re}\, D^{0.07-0.12 \ln Re} \tag{7.4}$$

For $Re > 8 \times 10^3$

$$\bar{d}_s \propto N^{1.22-0.24 \ln Re}\, D^{1.19-0.12 \ln Re} \tag{7.5}$$

These equations may be represented by the general form;

$$\bar{d}_s \propto N^{x-0.24 \ln Re}\, D^{y-0.12 \ln Re} \tag{7.6}$$

Using the same subscripts as previously, the following quadratic equation may be developed;

$$a_1(\ln N_1)^2 + b_1 \ln N_1 + (c_1 - a_2(\ln N_2)^2 - b_2 \ln N_2 - c_2) = 0 \tag{7.7}$$

where $a = -0.24$ (7.8)

$$b = x - 0.24 \ln \left(\frac{D^2\rho}{\mu}\right) - 0.12 \ln D \quad (7.9)$$

$$c = \left(y - 0.12 \ln \frac{D^2\rho}{\mu}\right) \ln D \quad (7.10)$$

A full development is shown in Appendix F.

7.2 Limitations to scale-up

When scale-up in an unbaffled vessel is carried out, it is impossible to maintain both dynamic and kinematic similarity[40], a normal requirement of scale-up. This immediately highlights the empirical nature of the project, it also serves as a reminder that there are limitations to the scale-up equations developed. For example, the two equations relating droplet size to impeller parameters via power input, equation 7.4 and equation 7.5, relate to Reynolds numbers of less than 8×10^3 and greater than 8×10^3 respectively. The overall range of Reynolds numbers studied in this project was 1500 to 17000. These Reynolds numbers are, therefore, the limits to which the scale-up equations presented here may be applied with any confidence. Similarly, the Froude number range was 0.007 - 2.1, and again these are limiting factors.

A further complication arises from Nomura et al's[28] observation that at higher impeller speeds, excessive levels of shear are responsible for coagulation of polymer particles, and therefore it is inadvisable to employ impeller parameters that create excessive shear. Thus shear, which may be related to impeller diameter and speed by equation 7.11 becomes another limiting factor if a constant impeller speed is to be maintained for the duration of a reaction.

$$\text{Shear} \propto N^2 D^2 \quad (7.11)$$

7.3 Scale-up diagram

The easiest way to show the effect of the limiting factors to scale-up is in the form of a diagram relating impeller speed to impeller diameter. Two such diagrams are presented here, one for equation 7.3 and one for the pair of equations 7.4 and 7.5. Each diagram covers an impeller diameter range from 0.075m, which is the datum, to an impeller diameter of 1m. This represents an increase in volume from about 2.5 dm^3 to about 6300 dm^3.

The scale-up diagrams should be used in the following manner.

1) Establish a datum point. This obviously involves determining which impeller speed is required to obtain a suitable degree of monomer dispersion in the pilot scale reactor.
2) Follow the line that passes through the datum point and represents scale-up for constant emulsion droplet size.
3) If this line intersects a Reynolds number limit, then change to the appropriate scale-up line in the new regime.
4) When the scale-up line intersects the line representing the new impeller diameter the new speed may be read off. If the scale-up line intersects a limiting line before the desired impeller diameter is reached then it should be considered that the existing data does not permit scale-up to such an impeller diameter with any confidence.

Obviously, the data presented in this thesis are of a limited nature and it is, therefore, desirable for a greater range of conditions to be studied in order to expand the usefulness of the scale-up diagrams.

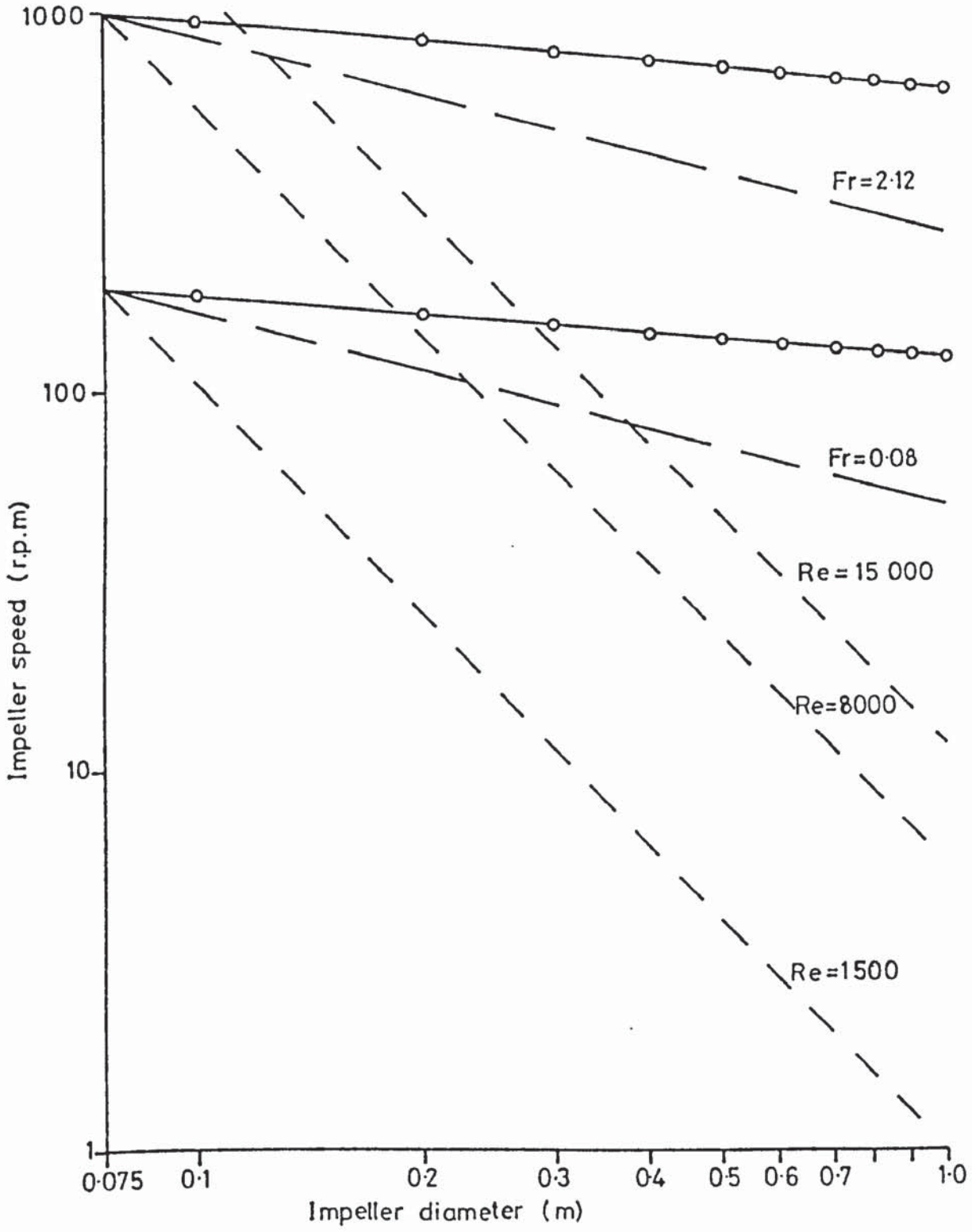

Fig 7·1 Scale-up plot. Logarithmic plot showing the limiting values of Fr and Re studied. Scale-up equation:

o—o $N_1 = N_2 \times (D_2/D_1)^{0.1713}$

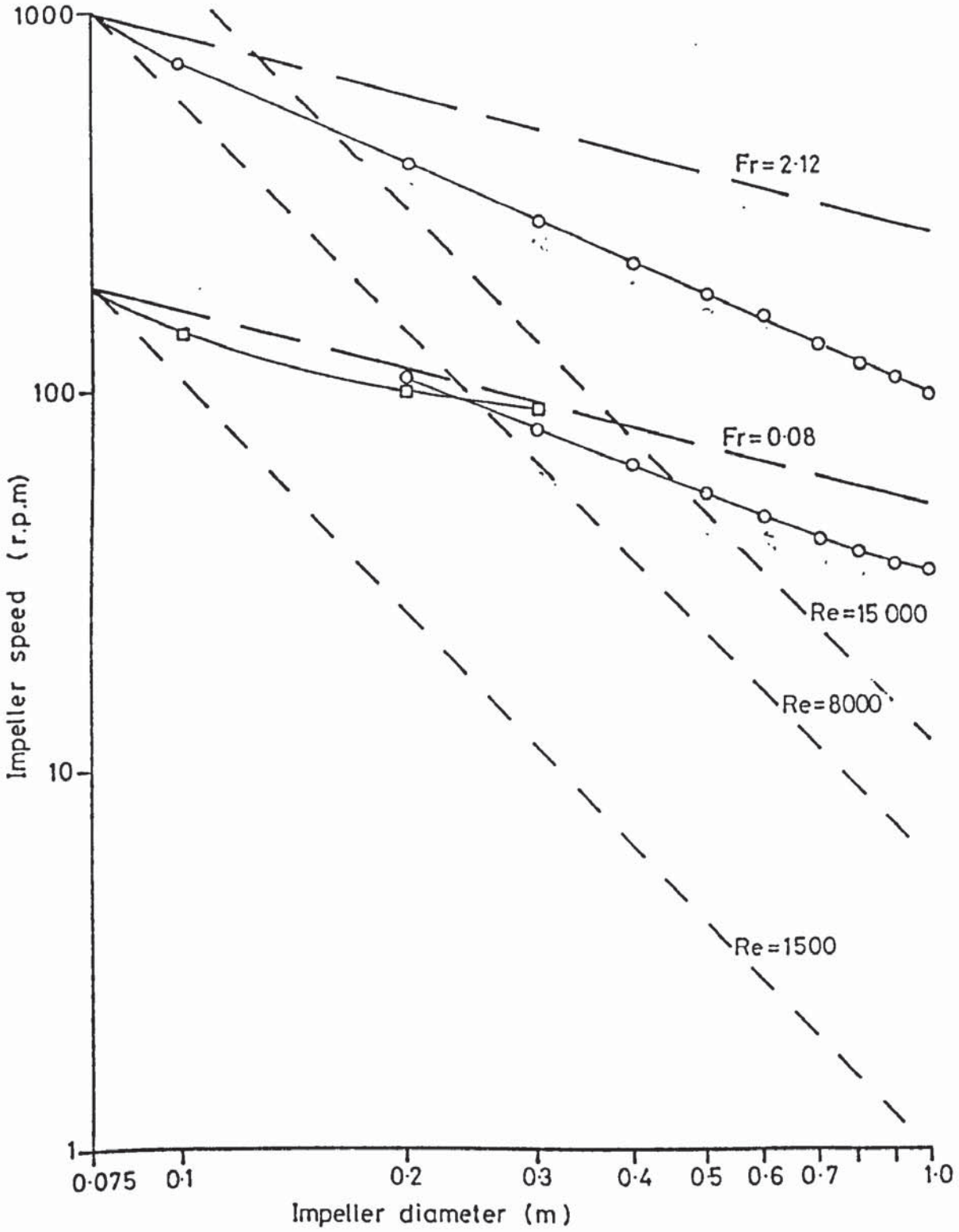

Fig 7·2 Scale-up plot. Logarithmic plot showing the limiting values of Fr and Re studied. Scale-up equation:

$$a_1 (\ln.N_1)^2 + b_1 \ln.N_1 + (c_1 - a_2 (\ln.N_2)^2 - b_2 \ln.N_2 - c_2) = 0$$

$a = -0{\cdot}24$, $b = x - 0{\cdot}24.\ln.(D^2\rho/\mu) - 0{\cdot}12.\ln.D$, $c = (y - 0{\cdot}12.\ln(D^2\rho/\mu)).\ln.D$

$Re < 8000$ □—□ $x = 0{\cdot}61, y = 0{\cdot}07$; $Re > 8000$ ○—○ $x = 1{\cdot}22, y = 1{\cdot}19$.

8.0 CONCLUSIONS

8.1 Major conclusions

8.2 Further conclusions

8.0 CONCLUSIONS

This chapter has been divided into two sections; major conclusions, which arise from the objective study, and further conclusions, which are drawn from practical experience relating to techniques used in the study.

8.1 Major conclusions

1) The final particle size in a latex produced by emulsion polymerisation is, for a given initial soap concentration, a function of the initial degree of monomer dispersion and thus of impeller speed.

2) The dependence of final latex particle size and impeller speed becomes increasingly significant as the level of initial soap is reduced. The amount of soap adsorbed onto the monomer droplet surface accounts for a greater proportion of total soap under these low initial soap conditions. This dependence is also of greater significance in systems of high organic/aqueous phase ratio.

3) Scale-up to reproduce a specific latex particle size requires a scale-up procedure that maintains the initial monomer dispersion constant between the small-scale and large-scale plant.

4) There is no simple scale-up equation which is universally appropriate to scale-up for an equivalent degree of monomer dispersion in unbaffled reactors. Scale-up to achieve equivalent dispersion may certainly be accomplished but it is inconsistent with the requirement to retain constant all other parameters such as Reynolds number, Froude number, shear and specific power input. These inconsistencies mean that any simple scale-up equation produced will have a limited

range of application beyond which its use would lead to increasing error. The following forms of governing equation relating impeller speed and impeller diameter are, however, recommended for use over the ranges indicated.

For $Re < 8 \times 10^3$

$$N^{0.61-0.24 \ln Re} D^{0.07-0.12 \ln Re} = \text{const} \qquad (8.1)$$

For $Re > 8 \times 10^3$

$$N^{1.22-0.24 \ln Re} D^{1.19-0.12 \ln Re} = \text{const} \qquad (8.2)$$

5) Further work is required to extend the range over which scale-up with respect to maintaining constant the degree of monomer dispersion may be confidently executed. The work carried out in this study involves only a narrow range of parameters such as Reynolds number, Froude number and particularly vessel size. In addition, the physical properties of the system were constant for the entire study, and, therefore, the scale-up recommendations contained in this thesis apply specifically to the limited system studied and should only be extrapolated beyond the range covered in this study, or applied to other systems, with caution.

6) Maintenance of an equivalent degree of monomer dispersion will not guarantee successful scale-up of any emulsion polymerisation. Inconsistencies in results in the small scale polymerisations performed in this study suggest that inconsistencies will undoubtedly be encountered on a large scale.

In these larger scale plant, the balance of factors affecting the inconsistencies in conversion rate and particle size may alter and thus prevent succesful scale-up. It is apparent that a full study involving the use of a family of different sized reactors is necessary to clarify these points.

8.2 Further conclusions

Measurement Techniques

1) A light extinction technique has been developed which provides a suitable method for measuring the particle size of polystyrene latices. The basic technique of Bateman et al[22] has been extended in this study, in that the manner in which the polymer concentration was calculated has been developed to allow for unreacted styrene monomer in the latex.

2) Accurate measurement of the mean diameter of monomer emulsion droplets proved difficult and tedious. Although careful photomicrographic analysis using high quality equipment can yield good results it is a very time consuming technique. A faster technique, that using a Coulter Counter, however, encountered severe practical problems. The dispersion droplets were found to be disappearing from the electrolytic vehicle. Presaturation of the electrolyte with the organic used in the dispersion tests, to prevent dissolution of the droplets, failed to alleviate this problem. Neither did coalescence appear to be the cause of this problem. It can only be summised that evaporation of the organic was the cause of the disappearance of the droplets, and this may only be overcome by saturating the vapour space above the dispersion with the organic phase. This was not a practical solution in this study.

Practical operation of emulsion polymerisation plant

1) Reproduction of consistent reaction rate data was difficult with the emulsion polymerisation system studied. This reaction system used commercial grade chemicals, in common with the procedures used on the parent plant. As a result of this, individual monomer charges inevitably contained inconsistent quantities of the inhibitor, added to commercial grade styrene to prevent polymerisation in

storage. In addition, there were indications of contamination by another inhibiting influence, probably oxygen, in some, but not all, of the experiments. It is certain that in normal industrial practise this would continue to give rise to inconsistency in reaction performance.

2) Formation of excessive coagulum could be controlled by the addition of soap to the reactor during the reaction. The timing of these soap additions, however, is critical. A slightly early addition of soap will have no apparent effect on the reaction. Failure to introduce soap at the appropriate time may allow coagulation to occur and this process cannot be reversed by subsequent soap addition. Late addition of soap must therefore be avoided. Although the timing of the soap addition will vary according to the system being used, and therefore will have to be determined experimentally, a good 'rule of thumb' appears to be to add soap when a sample removed from the reactor shows even the slightest sign of rapidly separating into two distinct phases.

Correlation of data

1) Emulsion droplet diameter, in an unbaffled vessel, may be empirically related to impeller parameters. Two types of correlation were considered; a straightforward multiple linear regression of the data relating the droplet size to impeller speed and diameter, and a correlation involving relating the droplet diameter to the power input. The latter type of correlation is better suited to extension over a wider range of parameters. The following correlations were developed.

Multiple linear regression

$$\bar{d}_s \propto N^{-1.08} D^{-0.185} \qquad (8.3)$$

Power input measurements

$$\bar{d}_s \propto 2.81(P/V)^{-0.52} \qquad (8.4)$$

Mathematical model

1) The Smith and Ewart model amended to take account of adsorption of soap on the monomer will predict with reasonable accuracy the final latex particle size. The normal Smith and Ewart model ignores the effect of degree of monomer dispersion on the final latex particle size or on the reaction rate. If instead of using a total soap parameter, as previously used in the Smith and Ewart model, the soap input term is adjusted to allow for the quantity of soap not present in micellar form, i.e. soap adsorbed onto the monomer/aqueous interface, the Smith and Ewart model will produce results that vary for identical total soap concentrations in line with experimental observations, i.e. high impeller speed leads to a larger final latex particle.

2) The modified Smith and Ewart model that considers both soap adsorption and desorption during stage I also gives reasonable results. This model considers the effects on the micelle population of soap released from the decreasing monomer droplet surface area. The results were similar to those obtained from the former Smith and Ewart model although the final particle sizes predicted by the latter model were all slightly larger.

3) The model that allows for the changing micelle population, i.e. the latter model, is best suited for solution by computer. A computer program allowing the solution of both models was written and successfully run.

9.0 RECOMMENDATIONS FOR FURTHER WORK

9.1 Scale-up

9.2 Dispersion

9.3 Polymerisation

9.4 Model

9.0 RECOMMENDATIONS FOR FURTHER WORK

The current study has answered a number of questions, some of specific interest to a particular scale-up problem and others of general interest in the field of dispersion and emulsion polymerisation. There are, inevitably however, gaps in the knowledge and understanding of these processes which need to be filled in order to allow full confidence in modelling and scale-up procedures for emulsion polymerisation.

Areas for further study which the author feels would help to close these gaps are presented below under their appropriate headings.

9.1 Scale-up

The following points are particularly relevant if successful scale-up of emulsion polymerisation, over a wide range, is to be achieved.

1) A comparison of polymerisations carried out in a number of different sized geometrically similar reactors is necessary to test the ultimate validity of applying the scale-up procedure to emulsion polymerisation.

2) Heat transfer. No investigation of the heat transfer was made in this study and it must be stressed that a knowledge of the characteristics of heat transfer and the way in which heat transfer behaves on scale-up will be necessary when specifying plant. It is apparent from consideration of the heat transfer processes that scale-up to achieve reproducible monomer dispersion will not be consistent with reproducible heat tranfer per unit volume of charge, and effects of other amendments to the heat transfer technique must be clarified.

3) The accuracy of the scale-up equations clearly depend upon the accuracy of the correlations between dispersion droplet diameter, impeller speed, impeller diameter and power input. In order to improve the scale-up equations it would be valuable to extend

the study to gather further data on the dispersion and power input relationship. Similarly it would be necessary to improve the technique for measuring the power input. Either an improvement in the bearing arrangement, for example, use of an air bearing to reduce the frictional losses, or the use of a strain gauge type of torque transducer on the impeller shaft.

4) The limit of shear that may be endured by a latex would warrant further study. The literature suggests that shear may induce coagulation of polymer particles, and although this study indicates that on scale-up over a limited range the level of shear will not vary much, this parameter may impose a limit to the validity of the scale-up procedure. If latices are shear sensitive, then the development of a method to establish the maximum shear tolerable and relate it to the agitation parameters would be highly desirable.

9.2 Dispersion

Because of the complex form of the governing equations for dispersion in unbaffled vessels it is difficult to extrapolate the current findings beyond a limited range of vessel size and systems. A greater range of variables should be studied in order to extend the study, paying particular interest to the following points.

1) The range of size over which studies are made should be extended in order to extend the range of the equations developed.

2) The effect on the effectiveness of emulsifications of impeller type, the numbers of impellers and impeller locations, should be examined in depth.

3) The effect of system physical properties on the dispersion characteristics should be studied together with the effects on these properties of the various additives to the emulsion

polymerisation system such as soaps, electrolytes, and the addition of a second organic phase as is the case in co-polymerisation.

4) The effect on the swirl pattern and turbulence (and thus on dispersion) of the height of the vessel lid from the surface of the vessel charge would be a valuable study. The swirl pattern in an unbaffled reactor is characterised by a parabolic shaped surface. The outer edge of this rises above the original liquid level and at high impeller speeds may well impinge on the undersurface of the vessel lid. This must have consequences upon the pattern of turbulence and thus on the degree of dispersion.

9.3 Polymerisation

It would be desirable, in order to gain a complete picture of the emulsion polymerisation process, for further study to be performed in the following areas.

1) The cause of inhibition. Inhibition has remained, as for many previous workers, a source of inconsistency in the polymerisation reactions in this work. With such inconsistency present, successful scale-up will be impossible to guarantee and it is therefore necessary to establish the cause of inhibition so that it may either be eliminated or reproduced.

2) The effect of foam formation on the micelle population, and thus on the reaction rate. An agitated soap solution will foam, and it is obvious that soap molecules will be present in this foam. What is not clear is whether the presence of soap in the foam reduces the number of micelles available for particle generation to any significant extent.

3) The method of agitation. The possibility that different stages

of the emulsion polymerisation process may benefit from different degrees of agitation (i.e. different impeller speeds) does not appear to have been studied previously. Such a study would appear to be attractive especially as it may lead to a reduction in the total power requirements of the process.

4) For soap starved systems the stabilities of the monomer dispersion and of the latex are sensitive to the timing of the soap additions. It would be of considerable value to develop a continuous monitoring technique to indicate the timing of the sequential soap additions. Such a method could possibly be based on monitoring the electrical conductivity of the emulsion, as this property varies with the free soap concentration.

9.4 Model

There is scope for further development of the model and program, and in particular in the following areas.

1) The inclusion in the program of the facility to simulate sequential soap additions, temperature variations and the heat generated. The latter two would obviously require simulation of the heat exchange facilities available on the reactor system to be used.

2) It would be desirable to have a more comprehensive range of reliable kinetic and physical data available for use in the model. For example, the rate of radical generation under varying concentrations of soap and electrolytes.

3) The inclusion in the model of a facility to model the reaction when conditions of slow termination prevail. This would allow a more accurate prediction of stage III of the reaction.

4) A facility to model inhibition and thus to predict inhibition

times would be a most useful addition to the model.

5) Possibly the ultimate aim of developing a model of emulsion polymerisation is to aid scale-up. A subroutine that applied the scale-up procedure to the simulation, and indicated any possible faults would obviously be of considerable value.

APPENDICES

APPENDIX A

PHYSICAL AND CHEMICAL PROPERTIES OF

NANSA HS 85/S

A1 Properties of Nansa HS 85/S

Nansa is a commercial detergent which is a mixture of sodium alkyl benzene sulphonates. The main constituent is Sodiumdodecylbenzenesulphonate. The physical properties of Nansa are shown in table A1.

Property	Value	Source
Active matter %	85 ± 3	(1)
Water content %	3 max	(1)
pH (1% aqueous solution)	9 - 11	(1)
mol wt. (main component)	348	(2)
Specific surface area of molecule (cm^2)	52×10^{-16}	(2)
c.m.c. ($g.dm^{-3}$)	0.4	(2)
c.m.c. ($g.dm^{-3}$) reaction conditions	0.104	(3)

1) Albright and Wilson data sheet[75]

2) Polymer Handbook[70]

3) Measured value, see A2

Table A1 Properties of Nansa HS 85/5

A2 Determination of the c.m.c. of Nansa in aqueous soluting in the presence of electrolytes

Procedure

Two solutions of electrolytes were made up and Nansa was dissolved in one of these solutions. Samples were prepared by mixing the two solutions in differing proportions. These samples were stored in glass bottles for 24 hours. Surface tension measurement were carried out with a Du Noy ring surface tension balance. The results were plotted on a linear/log plot of surface tension against concentration of Nansa, as shown in figure A1, and two least mean squares regression lines were placed through the data. The intersection of the two regression lines

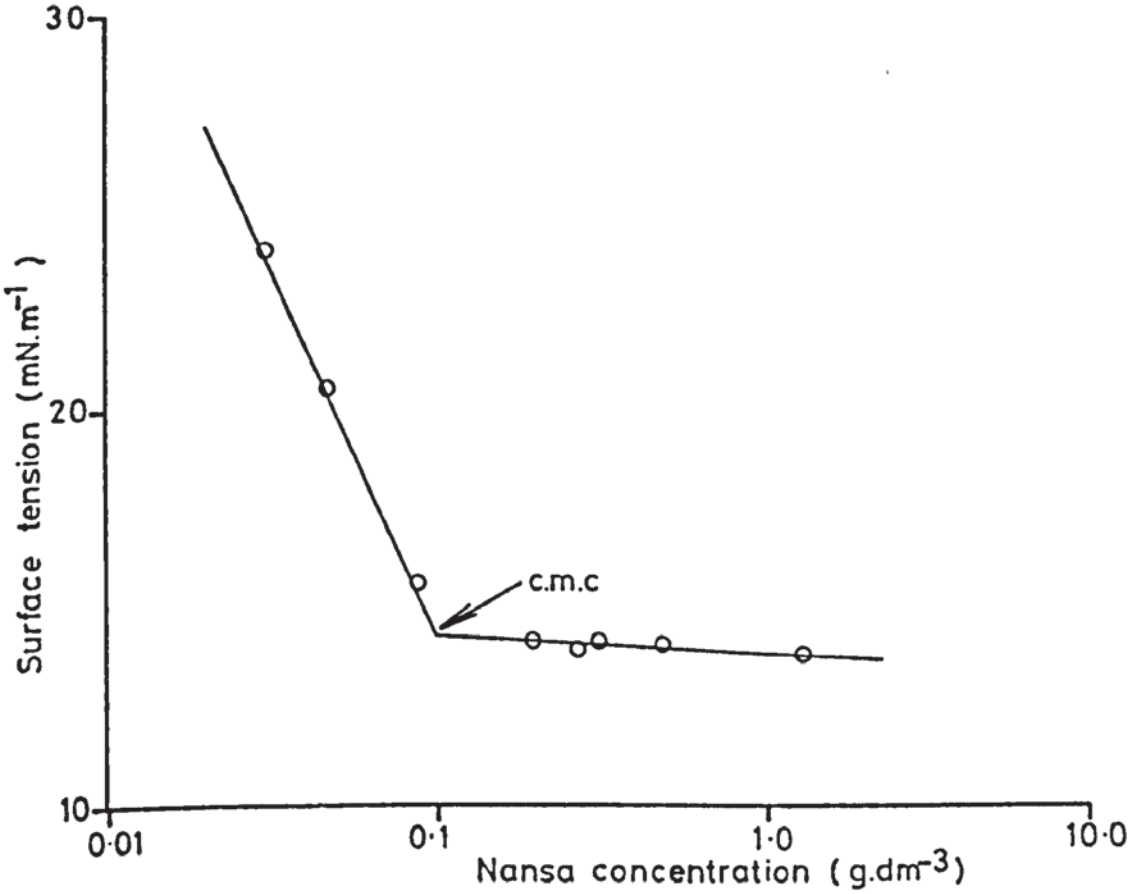

Fig A1 Linear/log plot of surface tension against soap concentration, to determin c.m.c.

indicates the critical micelle concentration.

Result

The value of the c.m.c. of Nansa in an aqueous solution containing electrolytes as specified in the polymerisation recipe is 0.104 $g.dm^{-3}$.

APPENDIX B

SAMPLE COULTER COUNTER CALCULATION TABLE

B1 Sample Coulter Counter calculation table

Table B1 shows sample calculation table for a dispersion experiment carried out with an impeller diameter of 152 mm, an impeller speed of 300 rpm and a soap concentration of 8.98 $g.dm^{-3}$.

The threshold setting on the Coulter Counter is indicated by t', whilst the current is indicated by I. The calibration factors are listed under F. A correction factor is added to the mean particle count to allow for the simultaneous passage of more than one particle through the counting head (n") and the number of particles counted in the blank electrolyte (✓) is subtracted. The threshold diameters below which particles are not counted are shown in column d. The differential size distribution is shown in columns Δn and $\bar{d}$.

The final mean particle size is calculated thus,

$$\bar{d}_s = \frac{\Sigma\ (\Delta n)_i\ \bar{d}_i^{\,3}}{\Sigma\ (\Delta n)_i\ \bar{d}_i^{\,2}} \quad . \tag{B1}$$

Sample D17/60, tube aperture = 280 µm

t'	I	F	n'		$\bar{n}'$	$n'' = p(\bar{n}')^2$	✓	$n = \bar{n}' + n'' - ✓$	d	Δn	$\bar{d}$
300	1	1.0	2	1	1	-	2	-	239	-	225.5
210	1	1.0	2	1	2	-	2	-	212	-	201.0
150	1	1.0	2	1	2	-	2	-	190	-	175.0
90	1	1.0	2	1	2	-	2	-	160	1	150.0
60	1	1.0	4	2	3	-	2	1	140	4	125.5
60	2	0.501	8	8	8	-	2	5	111	162	99.5
60	3	0.250	161	172	167	2	2	167	88	458	79.0
60	4	0.126	624	589	607	20	2	625	70	359	63.0
60	5	0.0643	974	902	938	48	2	984	56	361	50.0
60	6	0.0312	1282	1242	1262	87	4	1345	44	225	39.5
60	7	0.0157	1440	1476	1458	117	5	1570	35	225	31.5
60	8	0.00804	1708	1639	1674	154	6	1822	28	281	25.5
60	9	0.00446	1816	2010	1913	201	11	2103	23	309	21.0
60	10	0.00251	1971	2361	2166	257	11	2412	19	28	17.0
30	10	0.00251	2204	2197	2201	266	27	2440	15	291	13.0
15	10	0.00251	2410	2468	2439	326	34	2731	11		

Table B1 Typical Coulter Counter calculation table

APPENDIX C

DISPERSION EXPERIMENTAL RESULTS

TABLES OF SAUTER MEAN DROPLET DIAMETERS

Expt.	D1	D2	D3	D4	D5	D6	D7	D8	D9	D10	D11	D12	D13	D14
S ($g.dm^{-3}$)	0	0.093	0.44	9.06	0	0.086	0.39	9.1	0	0.095	0.41	8.84	0.127	0.409
D mm	75				114				152				75	
N rpm														
80	-	-	39	16	-	40	54	29	-	31	36	24	-	-
190	-	58	37	45	136	22	16	38	9	15	31	42	112	35
300	128	62	48	29	38	55	35	18	14	101	36	40	34	79
410	170	58	47	15	38	59	25	18	96	23	18	50	35	44
520	84	44	59	17	24	13	33	22	100	36	33	23	34	41
630	57	32	28	10	-	-	-	-	-	-	-	-	33	21
740	31	46	27	7	-	-	-	-	-	-	-	-	28	46
850	24	68	19	11	-	-	-	-	-	-	-	-	21	35
960	31	31	18	8	-	-	-	-	-	-	-	-	29	44

Table C1 Sauter mean droplet diameters (μm). Open vessels, photomicrographic analysis

Expt.	D15	D23	D16	D20	D21	D18	D19
S ($g.dm^{-3}$)	9.10	9.03	9.03	9.03	9.03	8.98	8.98
D mm	75		114			152	
N rpm							
190	-	-	-	-	-	9.48	9.24
217	-	-	-	-	-	7.94	9.05
245	-	-	5.74	7.29	7.47	6.62	7.47
272	-	-	-	6.5	5.67	6.73	7.03
300	5.80	7.03	5.58	6.35	4.82	3.83	6.83
327	-	6.53	-	4.23	5.69	5.37	-
355	-	6.40	4.88	-	5.43	-	5.43
382	-	5.28	-	-	-	-	-
410	5.24	-	4.23	-	-	-	-
465	-	-	3.72	-	-	-	-
520	3.90	-	-	-	-	-	-
630	2.67	-	-	-	-	-	-
740	2.10	-	-	-	-	-	-

Table C2 Sauter mean droplet diameters (μm)

Open vessels, Coulter Counter analysis,

Expt.	S1	S2	S3	S4	S5
S ($g.dm^{-3}$)	12.8	12.8	12.8	8.0	8.0
N					
300	13.0	13.24	-	14.76	-
410	-	11.19	8.73	10.82	7.18
520	-	6.15	7.38	8.16	8.77
630	-	5.29	5.37	6.48	4.72
740	5.29	5.29	4.43	6.72	6.36
850	4.51	-	4.10	4.55	3.85
960	4.38	-	-	4.22	-

Table C3 Sauter mean droplet diameters.

Closed vessel, Coulter Counter analysis, D = 75 mm

APPENDIX D

GRAPHS SHOWING MONOMER CONVERSION (%)

PLOTTED AGAINST TIME

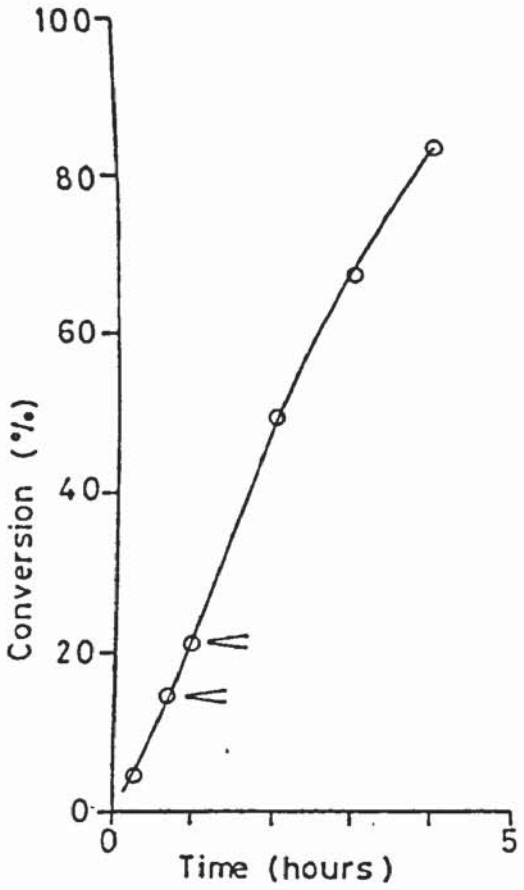

P2, N=190, S=12·8g.dm^{-3}

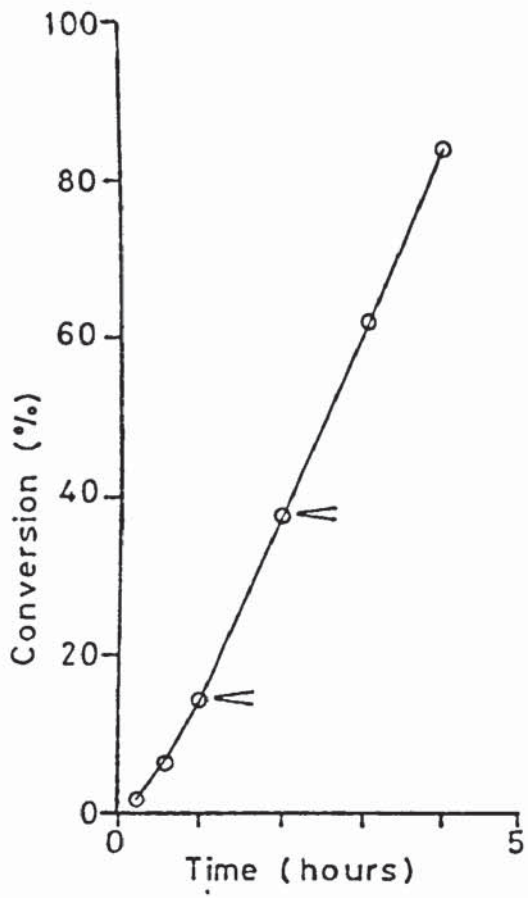

P3, N=410r.p.m, S=12·8g.dm^{-3}

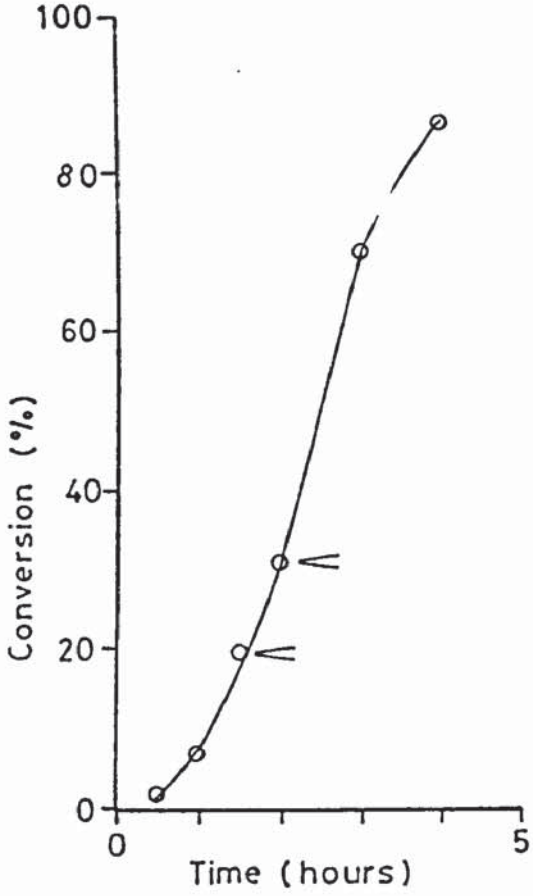

P4, N=600, S=12·8g.dm^{-3}

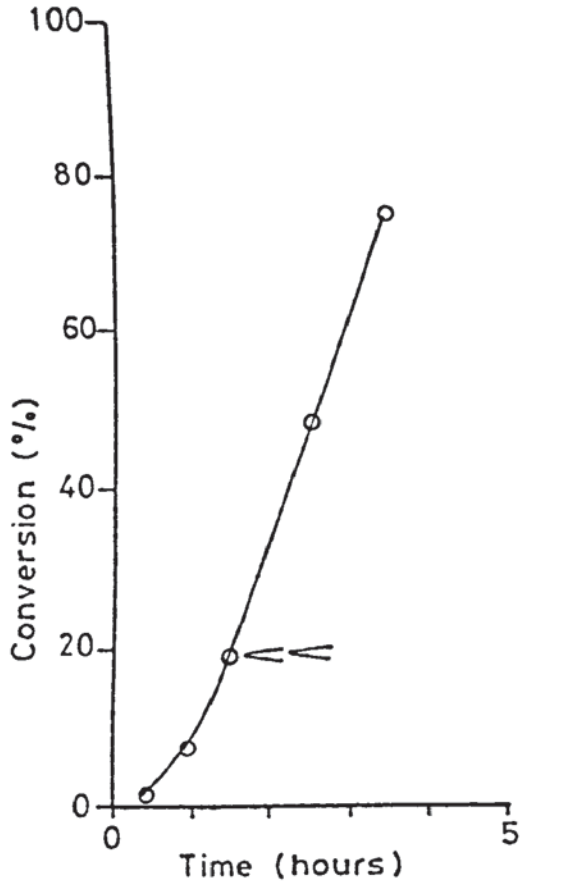

P5, N= 820 r.p.m, S=12·8 g.dm^{-3}

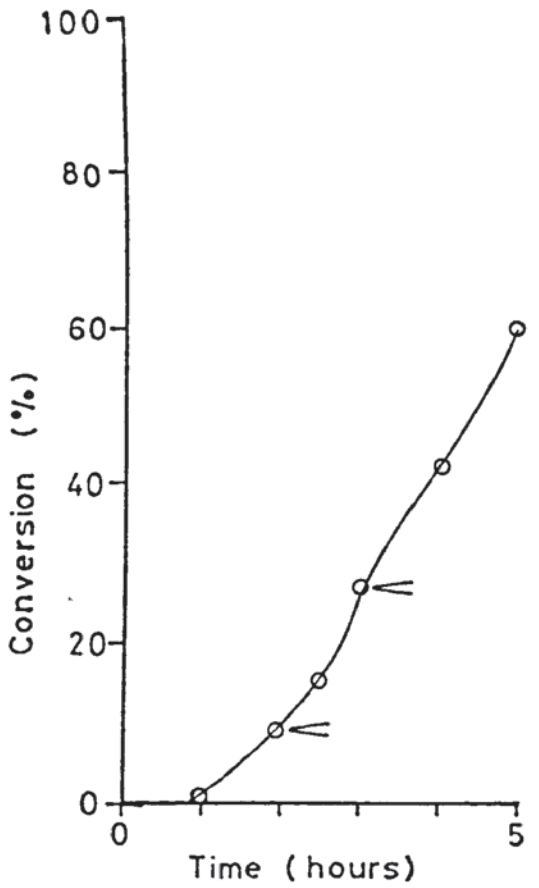

P8, N= 960 r.p.m, S=8·0 g.dm^{-3}

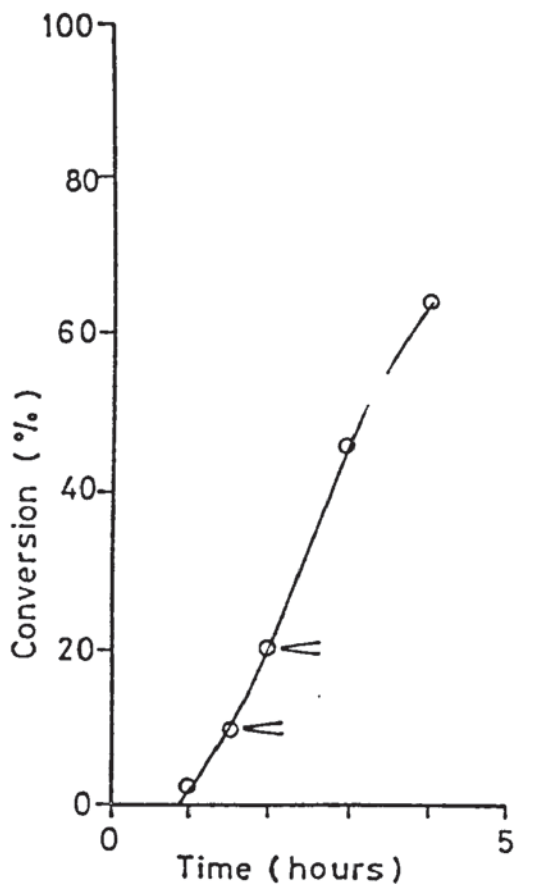

P10, N=410 r.p.m, S= 8·0 g.dm^{-3}

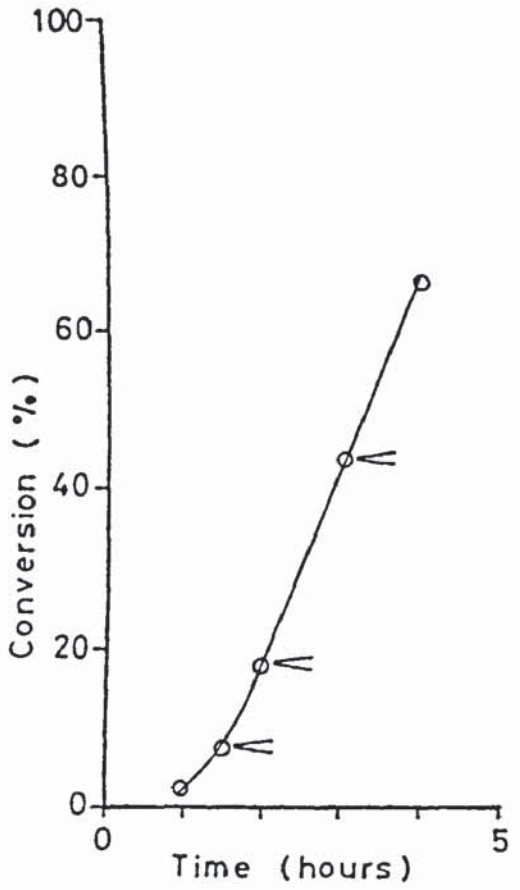

P11, N=960r.p.m, S=8·0g.dm^{-3}

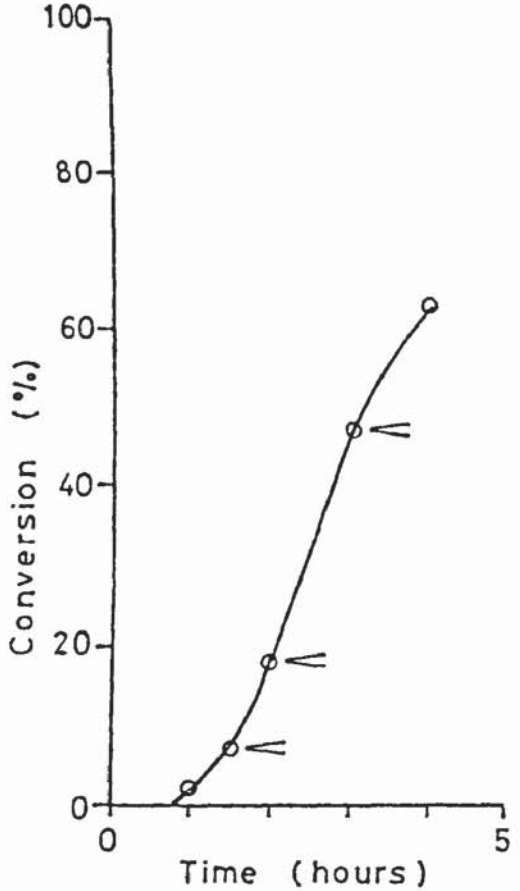

P12, N=575r.p.m, S=8·0g.dm^{-3}

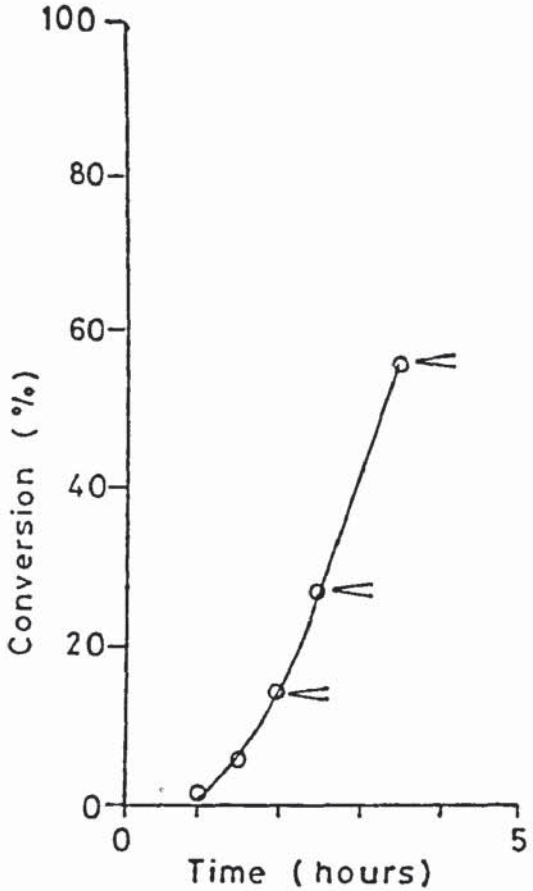

P13, N=740r.p.m, S=8·0g.dm^{-3}

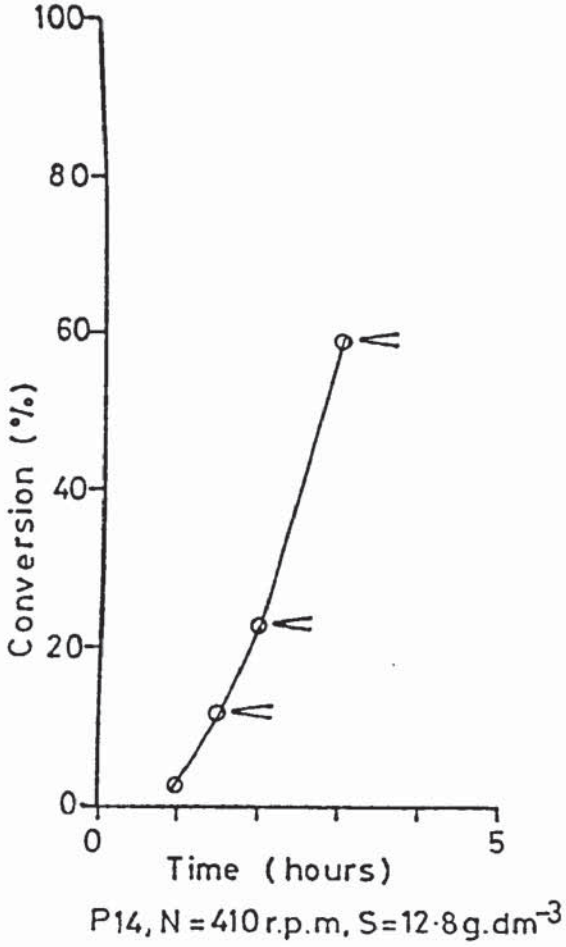

P14, N = 410 r.p.m, S = 12·8 g.dm^{-3}

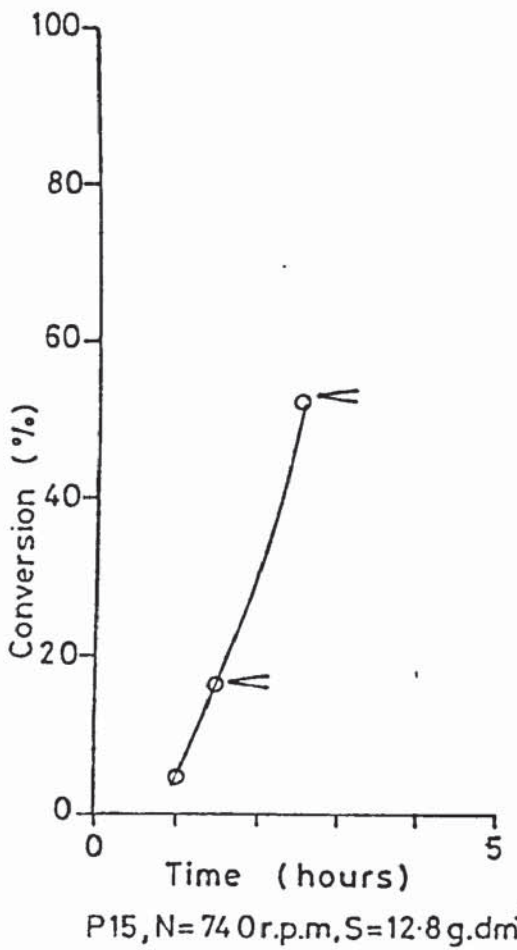

P15, N = 740 r.p.m, S = 12·8 g.dm^{-3}

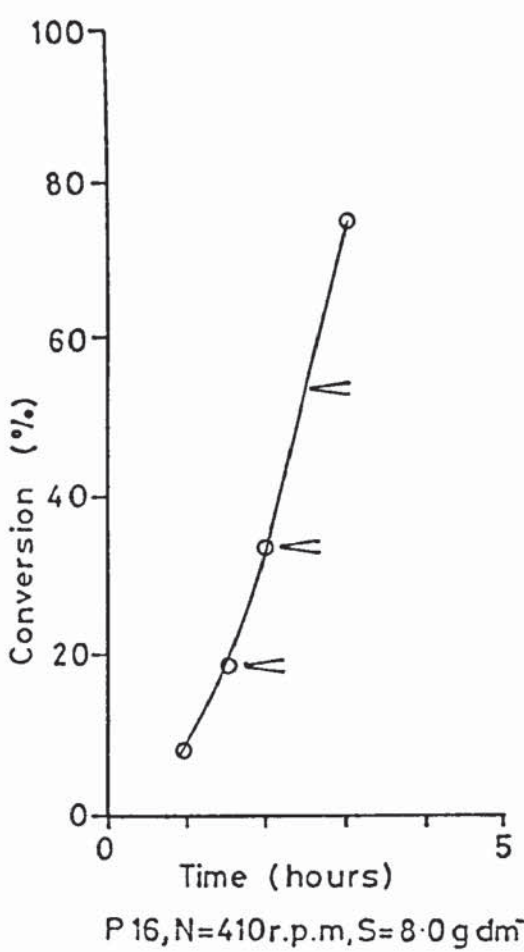

P 16, N = 410 r.p.m, S = 8·0 g dm^{-3}

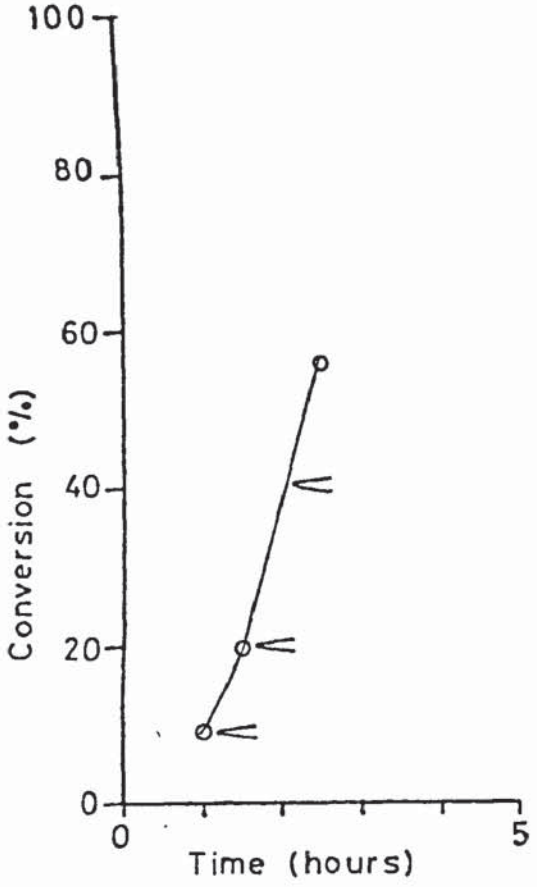

P17, N=575 r.p.m, S=12·8 g.dm^{-3}

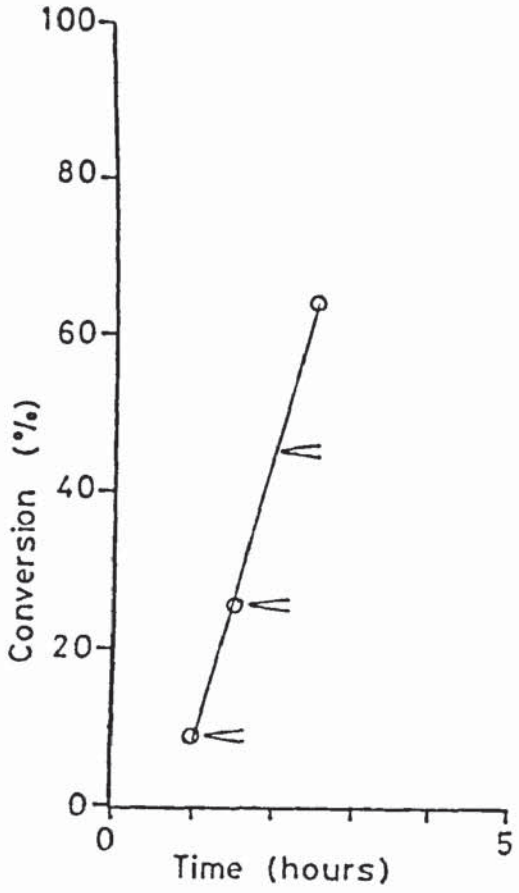

P18, N=960 r.p.m, S=12·8 g.dm^{-3}

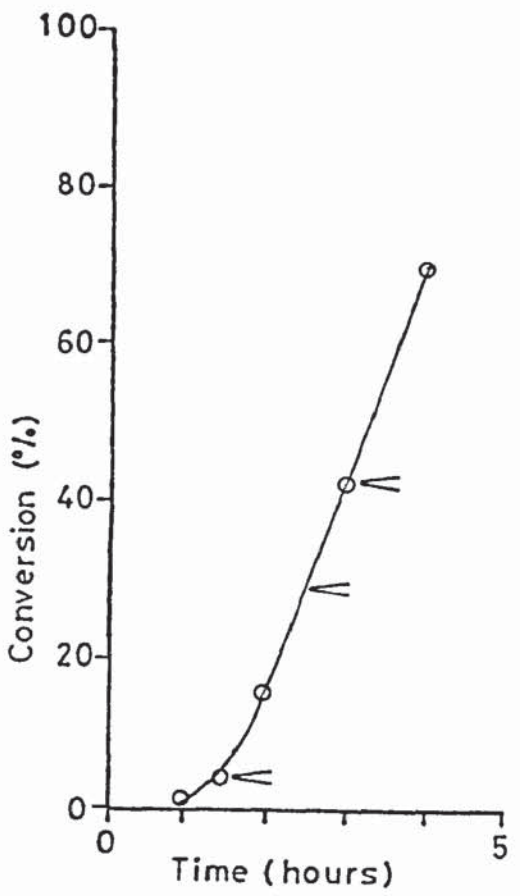

P19, N=575 r.p.m, S=4·0 g.dm^{-3}

APPENDIX E

DEVELOPMENT OF THE MATHEMATICAL MODELS OF EMULSION POLYMERISION AND PROGRAM FLOWCHARTS AND LISTING

E1 Development of mathematical models

E1.1 Smith and Ewart equations

Fundamental to this development is the assumption that the area occupied by a soap molecule is constant, i.e.

$$\frac{A}{S} = \frac{A_m}{S_m} = \frac{A_p}{S_p} = a_s \qquad \text{(E1)}$$

First idealised situation

Here it is assumed that all radicals produced generate polymer particles, i.e.

$$\frac{dN_p}{dt} = \rho' \qquad \text{(E2)}$$

The number of particles formed is found by integrating equation E2 to time t_I, at which time the total area of the particles, A_p, is equal to the total area of the soap, $a_s S$.

The volume $V_{T,t}$ at time t, of a particle formed at time τ is given by-

$$V_{T,\,t} = \mu(t - T) \qquad \text{(E3)}$$

The area $a_{T,\,t}$ is given by;

$$a_{T,\,t} = \theta(t - T)^{2/3} \qquad \text{(E4)}$$

Where $\theta = (4\pi)^{1/2} \cdot (3\,\mu)^{2/3}$

The total area of the particles is therefore given by;

$$A_p = \rho\theta \int_0^t (t - T)^{2/3} \cdot dt$$

$$= (3/5)\ \rho'\,\theta\, t^{5/3} \qquad \text{(E5)}$$

As at time t_I, $a_s S = A_p$, the following may be written;

$$t_I = (5\ a_s S/3\rho'\theta)^{3/5} \qquad \text{(E6)}$$

Hence the number of particles generated is given by;

$$N_p = \rho' t_I = \rho'^{2/5} \cdot (5a_s S/3\theta)^{3/5}$$

$$= 0.53\ (\rho'/\mu)^{2/5}\ (a_s S)^{3/5} \qquad \text{(E7)}$$

Second idealised situation

This assumes that the micelle surface has to compete with the particle surface for radical capture.

The basic equation is;

$$\frac{dN_p}{dt} = \rho'\ A_m/A \qquad \text{(E8)}$$

Where $A = A_m + A_p$ (E9)

Combination of equation E8, E9 and E1 yields;

$$\frac{dN_p}{dt} = \rho'\ (1 - A_p/a_s S) \qquad \text{(E10)}$$

The total area of the particles at time t is, in this case, given by;

$$A_p = \theta \int_0^t (t - T)^{2/3} \left(\frac{dN_p}{dT}\right) dT \qquad \text{(E11)}$$

Thus equation E10 may be written as

$$\frac{dN_p}{dt} = \rho' - (\rho'\theta/a_s S) \int_0^t (t - T)^{2/3} \left(\frac{dN_p}{dT}\right) dT \qquad \text{(E12)}$$

On solution of equation E12 for the condition $\frac{dN_p}{dt} = 0$, the following is obtained;

$$N = 0.37\ (\rho'/\mu)^{2/5}\ (a_s S)^{3/5} \qquad \text{(E13)}$$

The reader is referred to the original paper for details of the solution.

E1.2 New Model for predicting the number of particles generated

The equation that is the fundamental base of this model is identical to the fundamental equation of the second idealised situation of Smith and Ewart, i.e. equation E8. The definition of A, however, differs. In

this case A is defined thus;

$$A = A_m + A_p + A_d \tag{E14}$$

The total interfacial area is also related to the soap concentration thus

$$\frac{A}{(S-S_{cmc})} = \frac{A_m}{S_m} = \frac{A_d}{S_d} = \frac{A_p}{S_p} = a_s \tag{E15}$$

Thus by combination of equation E14 with equation E15, the following may be derived;

$$A_m = a_s \left(S - S_{cmc} - \frac{A_p}{a_s} - \frac{A_d}{a_s}\right) \tag{E16}$$

The number of particles generated is, therefore, given by;

$$N_p = \rho \int_o^{t_I} \left(1 - \frac{A_p + A_d}{a_s (S-S_{cmc})}\right) dt \tag{E17}$$

The surface area of the particles is calculated by the same equation as used in the Smith and Ewart solution, i.e. equation E12.

The surface area of the droplets at time t is given by;

$$Ad_t = (6\ Vd_t)^{2/3}\ (Nd\ \pi)^{1/3} \tag{E18}$$

Where

$$Vd_t = Vd_o - Vp_t$$

$$= Vd_o - \frac{\rho_{swp}}{\rho_m} \cdot \mu \cdot \int_o^t (t - T) \frac{dN}{dT} \cdot dT \tag{E19}$$

Solution of equation E17 requires the application of numerical methods.

E2 Program Flowcharts

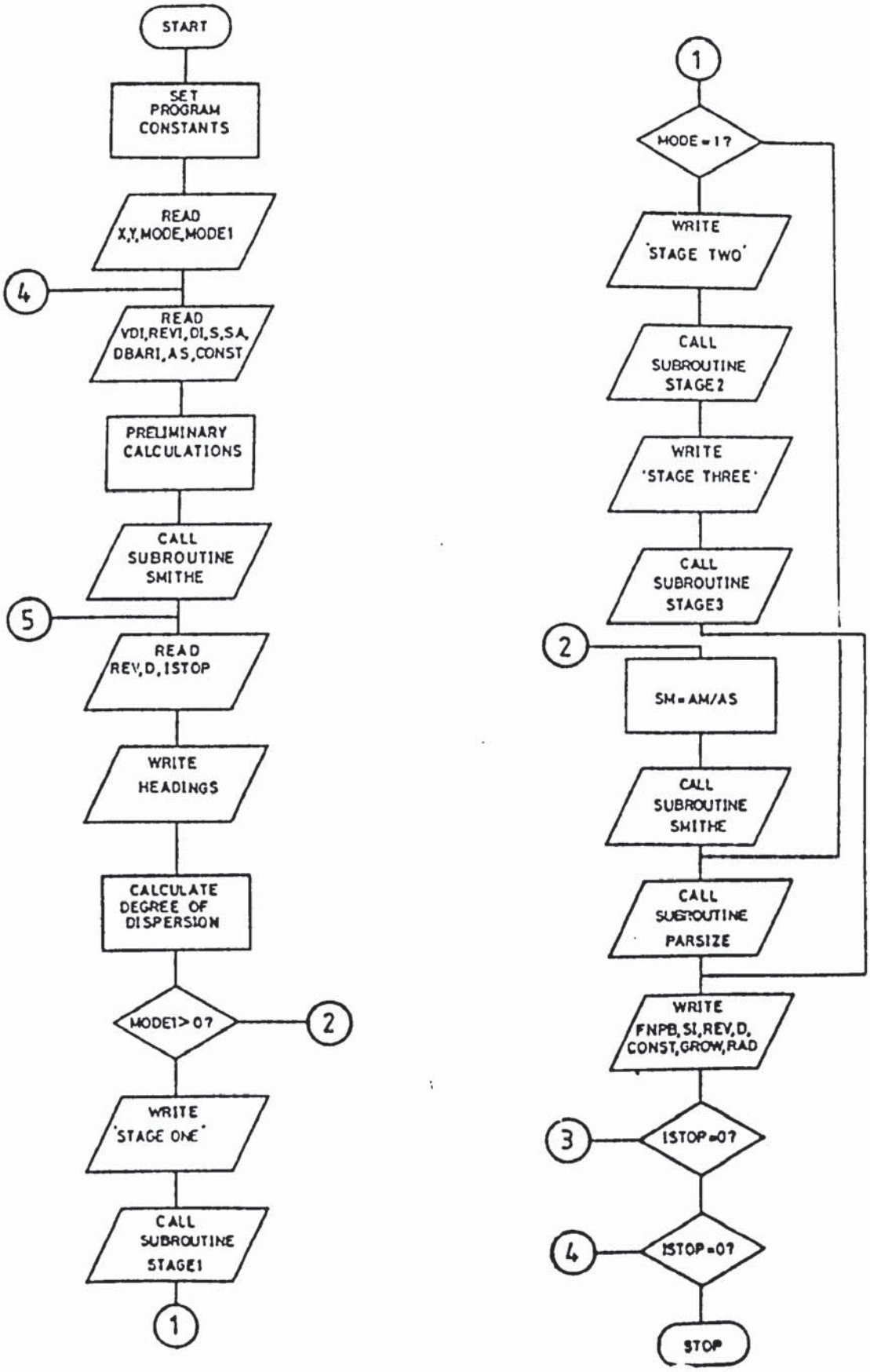

Fig E1 Program master.

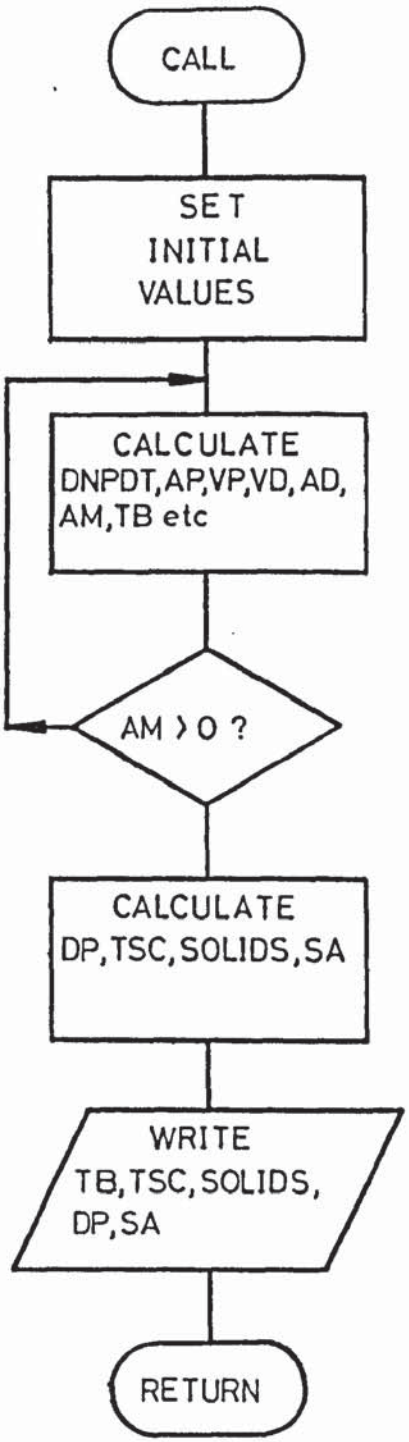

Fig E2 SUBROUTINE STAGE1

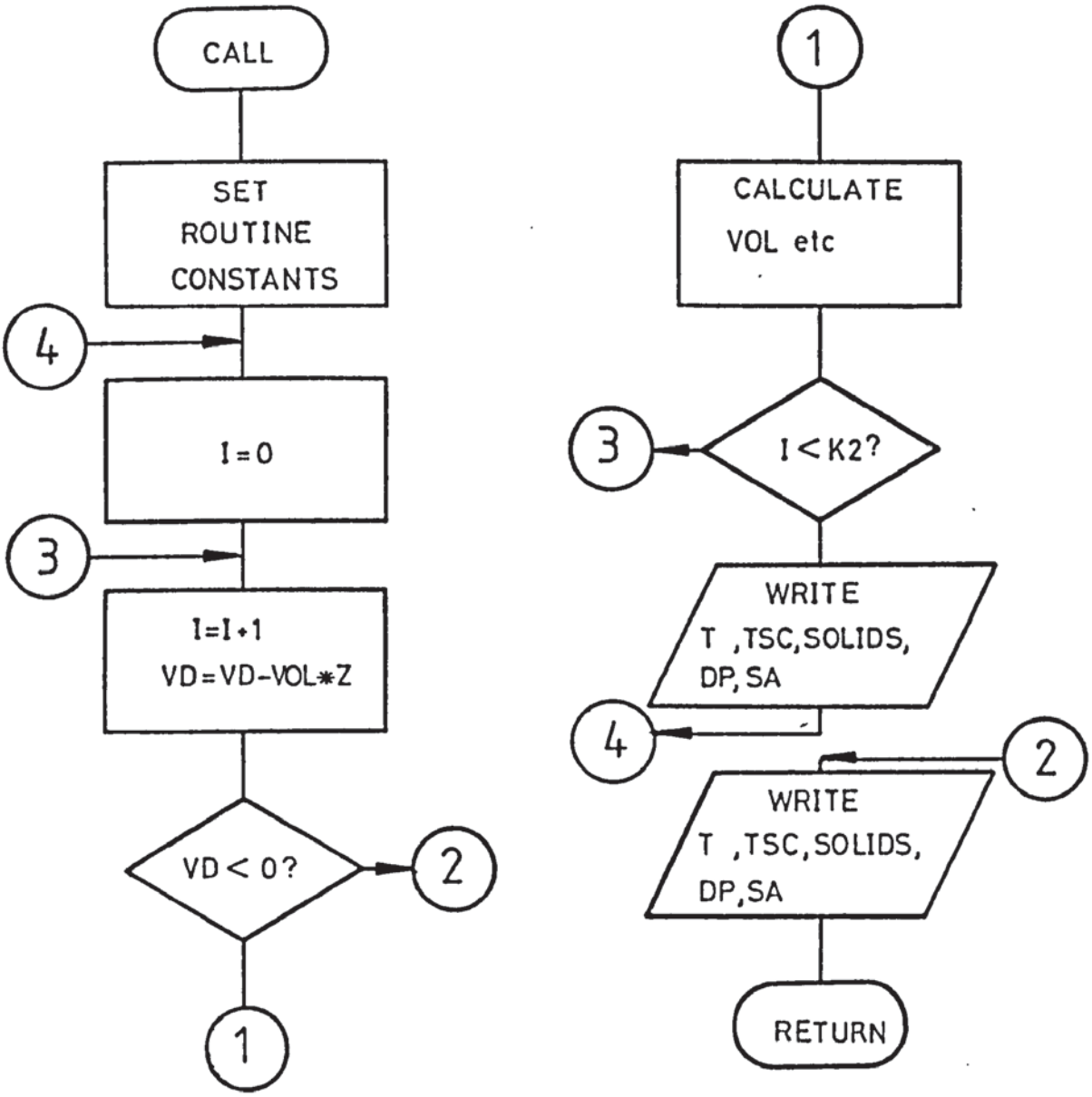

Fig E3 SUBROUTINE STAGE2

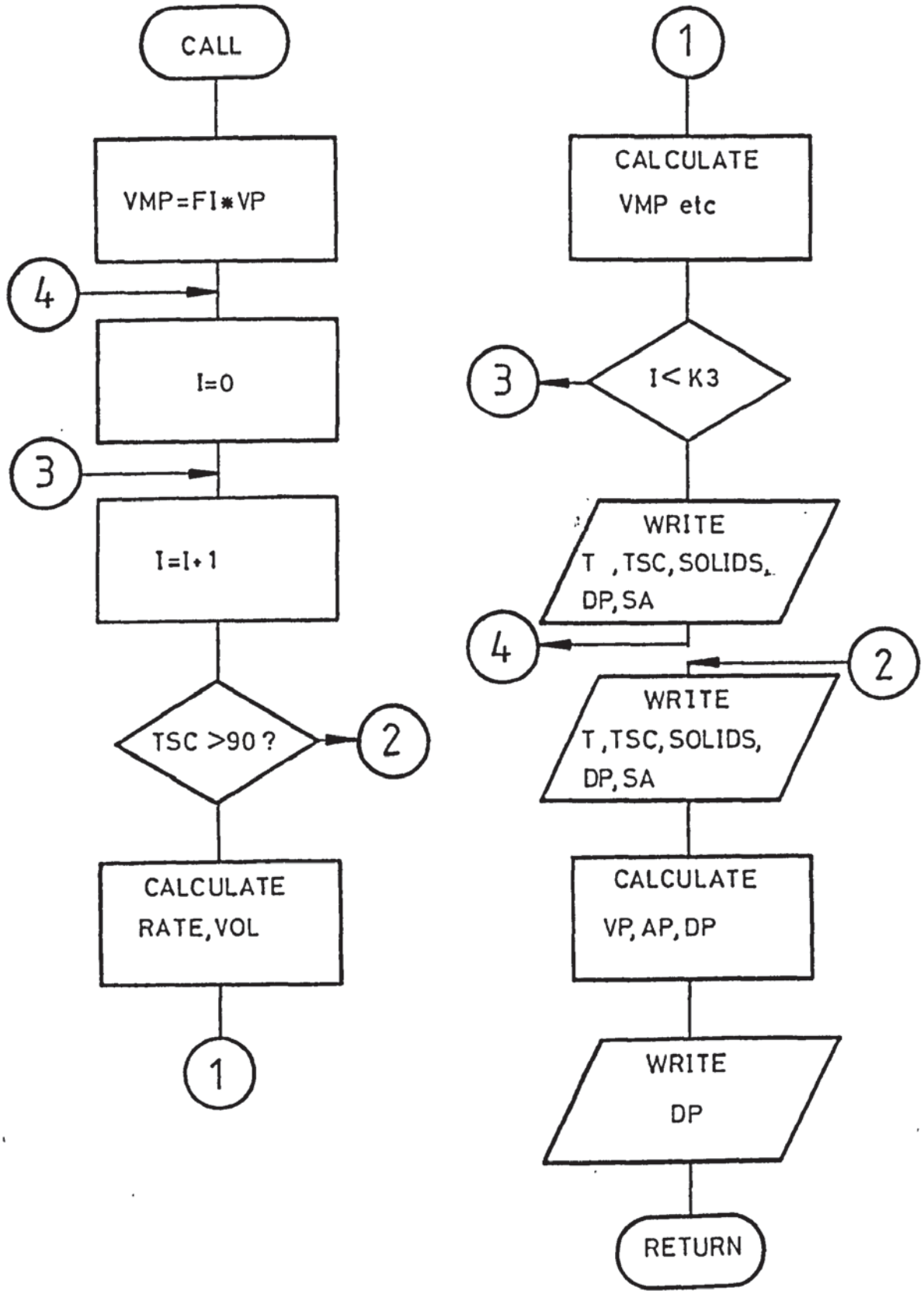

Fig E4 SUBROUTINE STAGE3

E3 Program Listing

```
      MASTER EPOL
C THIS PROGRAM SIMULATES EMULSION POLYMERISATION OF STYRENE
C EITHER CONVERSION OR FINAL PARTICLE SIZE MAY BE PREDICTED
C SET MODE = 1 FOR FINAL PARTICLE SIZE
C SET MODE = 0 FOR CONVERSION
C SET MODE1 = 1FOR SMITH EWART SOLUTION
C
      COMMON FNPB,VDI,DENMON,DENPOL,RAD,GROW,PS,S,T,P1,P2,
     1P3,VP,VD,FND,CONST,AVOGAD,CONFAC,DENSWP,FI,A,SA,TSC
C
C SET PROGRAM CONSTANTS
      DATA T2,T3,K2,K3/1.0,1.0,30,30/
      AVOGAD=0.6023 24
      RAD=5.93 E 14
      FI=0.65
      GROW=3.29 E-17
      DENMON=0.879
      DENPOL=1.049
       DENSWP=0.9
      P1=1.0/3.0
      P2=2.0/3.0
      P3=1.0/3.0
C
C READ DATA
      READ(1,500)X,Y,MODE,MODE1
    5 READ(1,1000)VDI,REV,DI,S,SA,DBARI,AS,CONST
C
C PRELIMINARY CALCULATIONS
      SI=S
      S=S*0.6023 24/348
      SA=SA*0.6023 24/348
      SCMC=SA
      CONFAC=(VDI+1)/(DENMON*VDI)
C
C SMITH AND EWART SOLUTION
      CALL SMITHE
C
C READ IMPELLER SPEED (REV),IMPELLER DIAMETER (D),
C DATA TERMINATOR (ISTOP)
   20 READ(1,2000)REV,D,ISTOP
C
C WRITE HEADINGS
   10 WRITE(2,5900)
C
C CALCULATE DEGREE OF DISPERTION
      DBA =DBARI*((REV/REVI)**X)*((D/DI)**Y)
      FND=6*VDA/(3.14159*(DBA**3))*0.1E 13
      ADI=VDI*6*UCI/DBA
      A=(C-SCMC)*C
      AN=A-ADI
C
      IF(MODE1.GT.0)GOTO 26
C
C CALCULATE PROGRESS OF REACTION
C
      WRITE(2,5100)
   21 CALL GET GEI(...,N)
C
```

```
   25 IF(MODE.EQ.1)GOTO 30
C
      WRITE(2,6200)
      CALL STAGE2(T2,K2)
C
      WRITE(2,6300)
      CALL STAGE3(T3,K3)
      GOTO 40
C
C CALCULATE NUMBER OF PARTICLES GENERATED BY SMITH EWART
C WITH MODIFIED SOAP CONCENTRATION
   28 S=AM/AS
      CALL SMITHE
C
C CALCULATE FINAL PARTICLE SIZE
   30 CALL PARSIZ
C
C PRINT SELECTED INPUT DATA
   40 WRITE(2,6500)FNPB,SI,REV,D,CONST,GROW,RAD
C
C TEST FOR MORE DATA
      IF(ISTOP.EQ.0)GOTO 20
      IF(ISTOP.EQ.1)GOTO 5
C
C FORMATS
  500 FORMAT(2F10.5,5I1)
 1000 FORMAT(6F10.5,2E10.3)
 2000 FORMAT(2F10.5,I1)
 2500 FORMAT(2F5.2)
 5900 FORMAT(/,2X,'TIME MIN     CONV PC     SOLIDS P',3X,
     1'DIA MICRN   SOAP MOLCS')
 6000 FORMAT(/,4(2X,F10.3),2X,1PE10.3)
 6100 FORMAT(/,5X,'STAGE ONE')
 6200 FORMAT(/,5X,'STAGE TWO')
 6300 FORMAT(/,5X,'STAGE THREE')
 6500 FORMAT(//,2X,'NUMBER OF PARTICLES (1/CC)  ',  E10.3,
     1' INITIAL SOAP (G/CC)       ',F10.3,/2X,'IMPELLER',
     2' SPEED (RPM)',8X,F10.3,' IMPELLER DIAMETER (CM)  ',
     3F10.3,/,2X,' RATE CONSTANT (CC/MOLE.MIN) ',E10.3,
     4' GROWTH RATE (CC/CC.MIN) ',E10.3,/,'   RATE OF ',
     5'RADICAL GENERATION (1/CC,MIN) ',E10.3)
      STOP
      END
      SUBROUTINE STAGE1(AM,X)
C THIS ROUTINE SIMULATES STAGE ONE  CALULATIONS ARE ITERATIVE
      COMMON FNPB,VDT,DENMON,DENPOL,RAD,GROW,AS,S,TB,P1,P2,
     1P3,VP,VD,FND,CONST,AVOGAD,CONFAC,DENSWP,FI,R,SA,TSC
      DIMENSION DELTAN(1000)
C
C SET LOOP CONSTANTS AND INITIAL VALUES
      I=1
      THET=(1.33*GROW)**2
   20 AP=0
      TB=0
      H=0.01
      VP=0
      FNP=0
C
```

```
C INCREMENTAL CALCULATIONS FOR PARTICLE VOLUME (VP),AREA (AP)
C NUMBER (ENPB),DROPLET VOLUME (VD),AREA (AD)
   40 DELTAN(I)=A*D*AM*H/A
      FNPB=FNPB+DELTAN(I)
      VP=VP+FNPB*GROW*H
      Z=0
      DO 30 J=1,I
   30 Z=Z+J**P2*DELTAN(I+1-J)
      AP=THETH**P2*Z
      VD=VDI-VP*(DENSWP/DENMON)
      AD=(6*VD)**(P2 )*(FND*3.14159)**(P3)
      AM=A-AD-AP
      TB=TB+H
      I=I+1
C
      IF(AM.GT.0)GOTO 40
C
C CALCULATE PARTICLE DIAMETER (DP),CONVERSION (TSC),SOLIDS
C CONTENT (SOLIDS)
 9000 DP=(VP/AP)*SLOOO
   75 TSC=VP*DENSWP/(VDI*DENMON)*(1-FI)*100
   80 SOLIDS=TSC/CONFAC
      SA=S-(AP+AD)/AS
C
   90 WRITE(2,6000)TB,TSC,SOLIDS,DP,SA
C
 6000 FORMAT(/,4(2X,F10.3),2X,1PE10.3)
 9999 RETURN
      END
      SUBROUTINE STAGE2(T2,K2)
C THIS ROUTINE SIMULATES STAGE TWO
      COMMON FNPB,VDI,DENMON,DENPOL,RAD,GROW,AS,S,T,P1,P2,
     1P3,VP,VD,FND,CONST,AVOGAD,CONFAC,DENSWP,FI,A,SA,TSC
C
C SET ROUTINE CONSTANTS
      RATE=FNPB*CONST*FI/(2*AVOGAD)
      VOL=RATE*T2
      Z=((1/FI)+(DENMON/DENSWP)-1)/((1/FI)-1)
C
C SET INITIAL VALUES
    5 I=0
   10 I=I+1
      VD=VD-VOL*Z
C
C TEST FOR DISAPPEARANCE OF MONOMER DROPLETS
      IF(VD.LE.0)GOTO 9999
C
C CALCULATE PARTICLE VOLUME (VP),AREA (AP),DIAMETER (DP)
C DROPLET VOLUME (VD),AREA (AD),CONVERSION (TSC),SOLIDS
C CONTENT (SOLIDS),NUMBER OF FREE SOAP MOLECULES (SA)
   45 T=T+T2
      VP=VP+VOL*(Z-1+(DENMON/DENSWP))
C
      AD=(6*VD)**(P2 )*(FND*3.14159)**(P3)
      AP=((FND*3.1415)**P3)*((6*VP)**P2)
      DP=(VP/AP)*3.000
      SA=S-(AP+AD)/AS
      TSC=VP*DENSWP/(VDI*DENMON)*(1-FI)*100
      SOLIDS=TSC/CONFAC
C
```

```
C
C TEST FOR PRINT-OUT
   20 IF(I.LT.K2)GOTO 10
C
      WRITE(2,6000)T,TSC,SOLIDS,DP,SA
      GOTO 5
C
 9999 WRITE(2,6000)T,TSC,SOLIDS,DP,SA
C
 6000 FORMAT(/,4(2X,F10.3),2X,1PE10.3)
      RETURN
      END
      SUBROUTINE STAGE3(T3,K3)
C THIS ROUTINE SIMULATES STAGE THREE
      COMMON FNPB,VDI,DENMON,DENPOL,RAD,GROW,AS,S,T,P1,P2,
     1P3,VP,VD,FND,CONST,AVOGAD,CONFAC,DENSWP,FI,A,SA,TSC
C
C SET INITIAL VALUE OF MONOMER IN POLYMER (VMP)
      VMP=FI*VP
    5 I=0
   10 I=I+1
C
C TEST FOR COMPLETION OF REACTION
      IF(TSC.GE.90.0)GOTO 9999
C
C CALCULATE REACTION RATE (RATE),VOLUME REACTED IN
C TIME INCREMENT (VOL)
      RATE=FNPB*CONST*VMP/(2*VP*AVOGAD)
      VOL=RATE*T3
C
C CALCULATE VOLUME OF MONOMER IN POLYMER (VMP),
C PARTICLE VOLUME (VP),AREA (AP),DIAMETER (DP)
C NUMBER OF FREE SOAP MOLECULES (SA)
C CALCULATE CONVERSION (TSC),SOLIDS CONTENT (SOLIDS),TIME (T)
   20 VMP=VMP-VOL
      VP=VP-VOL*(1-(DENSWP/DENPOL))/FI
      AP=((FNPB*3.1416)**P3)*((6*VP)**P2)
      DP=(VP/AP)*6000
      SA=S-AP/AS
   30 TSC=(1-VMP/VDI)*100
   40 SOLIDS=TSC/CONFAC
      T=T+T3
C
C TEST FOR PRINT-OUT
      IF(I.LT.K3)GOTO 10
C
      WRITE(2,6000)T,TSC,SOLIDS,DP,SA
      GOTO 5
C
 9999 WRITE(2,6000)T,TSC,SOLIDS,DP,SA
C
C CALCULATE PARTICLE DIAMETER AT TOTAL CONVERSION
      VP=VP-VMP*(1-(DENSWP/DENPOL))/FI
      AP=((FNPB*3.1416)**P3)*((6*VP)**P2)
      DP=(VP/AP)*6000
C
```

```
C
      WRITE(2,7000)DP
C
 7000 FORMAT(/'  PARTICLE SIZE AT TOTAL CONVERSION  ',F6.3)
 6000 FORMAT(/,4(2X,F10.3),2X,1PE10.3)
      RETURN
      END
      SUBROUTINE SMITHE
C THIS ROUTINE SOLVES SMITH EWART KINETICS FOR STAGE ONE
      COMMON FNPBS,VOI,DENMON,DENPOL, RAD,GROW,AS,S,TAS
      X=(RAD/GROW)**(2.0/5.0)*(AS*S)**(3.0/5.0)
      FNPAS=0.53*X
      FNPBS=0.37*X
      TAS=FNPAS/ROOT
      WRITE(2,7000)FNPAS,TAS,FNPBS
 7000 FORMAT(//,2X,'SMITH AND EWART SOLUTIONS   CASE A : NP= '
     1,E10.3,'  TIME ',F10.3,//,30X,'CASE B : NP= ',E10.3)
      RETURN
      END
      SUBROUTINE PARSIZE
C THIS ROUTINE CALCULATES FINAL PARTICLE DIAMETER
      COMMON FNPB ,VOI,DENMON,DENPOL, RAD,GROW,AS,S,T,P1,P2,P3
      DP=10000*(VOI*DENMON*6/(FNPB*3.14159*DENPOL))**P3
      WRITE (2,1000)DP
 1000 FORMAT(/,' FINAL PARTICLE SIZE (MICRONS)',F6.3)
      RETURN
      END
      FINISH
```

APPENDIX F

DEVELOPMENT OF SCALE-UP EQUATIONS

F1 Development of scale-up equations

A scale-up equation may be developed from the general form of the equation relating droplet size to power input, i.e.

$$\bar{d}_s \propto N^{x - 0.24 \ln Re} D^{y - 0.12 \ln Re} \tag{F1}$$

Using the subscripts 1 to indicate the large scale plant and 2 to indicate the small scale plant, for equivalent droplet diameter then;

$$N_1^{x - 0.24 \ln Re_1} D_1^{y - 0.12 \ln Re_1} = N_2^{x - 0.24 \ln Re_2} D_2^{y - 0.12 \ln Re_2} \tag{F2}$$

Taking logs;

$$(x - 0.24 \ln Re_1) \ln N_1 + (y - 0.12 \ln Re_1) \ln D_1 = (x - 0.24 \ln Re_2) \ln N_2 + (y - 0.12 \ln Re_2) \ln D_2 \tag{F3}$$

Expanding equation F3 gives

$$x_1 \ln N_1 - 0.24 \ln N_1 \cdot \ln \left(\frac{D_1^2 N_1 \rho}{\mu}\right) + y \cdot \ln D_1 - 0.12 \ln D_1 \cdot \ln \left(\frac{D_1^2 N_1 \rho}{\mu}\right) = x \ln N_2 - 0.24 \ln N_2 \ln \left(\frac{D_2^2 N_2 \rho}{\mu}\right) + y \ln D_2 - 0.12 \cdot \ln D_2 \cdot \ln \left(\frac{D_2^2 N_2 \rho}{\mu}\right) \tag{F4}$$

Further expansion and collection of terms gives;

$$- 0.24 (\ln N_1)^2 + \left(x - 0.24 \ln \left(\frac{D_1^2 \rho}{\mu}\right) - 0.12 \ln D_1\right) N_1 + \left(y - 0.12 \ln \frac{D_1^2 \rho}{\mu}\right)\right) \ln D_1 = -0.24 (\ln N_2^2) + \left(x - 0.24 \ln \left(\frac{D_2^2 \rho}{\mu}\right) - 0.12 \ln D_2\right) \ln N_2 + \left(y - 0.12 \ln \left(\frac{D_2^2 \rho}{\mu}\right)\right) \ln D_2. \tag{F5}$$

The following substitutions may be made.

$$a = - 0.24 \tag{F6}$$

$$b = \left(x - 0.24 \ln \left(\frac{D^2 \rho}{\mu}\right) = 0.12 \ln D\right) \tag{F7}$$

$$c = (y - 0.12 \ln \frac{D^2 \rho}{\mu})) \ln D. \quad \text{(F8)}$$

Thus, equation F5 reduces to

$$+ a_1(\ln N_1)^2 + b_1 \ln N_1 + C_1 = + a_2 (\ln N_2)^2 + b_2 \ln N_2 + C_2 \quad \text{(F9)}$$

Which on rearrangement gives the following quadratic equation where N_1 is the unknown;

$$a_1 (\ln N_1)^2 + b_1 \ln N_1 \; 1 \; (C_1 - a_2 (\ln N_2)^2 - b_2 \ln N_2 - C_2) = 0 \quad \text{(F10)}$$

NOMENCLATURE

A	Total interfacial area per unit volume of aqueous phase.	($cm^2 . cm^{-3}$)
a	Specific interfacial area of an emulsion.	($cm^2 . cm^{-3}$)
A_d	Surface area of emulsion droplets per unit volume of aqueous phase.	($cm^2 . cm^{-3}$)
A_m	Surface area of micelles per unit volume of aqueous phase.	($cm^2 . cm^{-3}$)
A_p	Surface area of polymer particles per unit volume of aqueous phase.	($cm^2 . cm^{-3}$)
a_s	Specific adsorption area of a soap molecule.	($cm^2 . molecule^{-1}$)
c	Polymer particle weight concentration.	($g . cm^{-3}$)
D	Impeller diameter.	(mm)
d	Particle or droplet diameter.	(μm)
dp	Mean particle diameter.	(μm)
$\bar{dp}_L$	Linear mean particle diameter.	(μm)
$\bar{dp}_{r.m.s.}$	Root mean square particle diameter.	(μm)
$\bar{dp}_v$	Volume mean particle diameter.	(μm)
$\bar{d}_s$	Surface mean (Sauter mean) droplet diameter.	(μm)
D_T	Internal vessel diameter.	(mm)
D_{To}	External vessel diameter.	(m)
E	$k_2 M_m/k_1$	
g	Acceleration due to gravity.	($m . s^{-2}$)
$[I]$	Initiator concentration in aqueous phase.	($mole . cm^{-3}$)
I	Transmitted light intensity.	

I_o	Incident light intensity.	
K	Theoretical light scattering coefficient.	
k_d	Rate constant for dissociation of initiator.	
k_H	$\frac{k_p M_{pc} M_w}{M_o N_A}$	
k_p	Propagation constant.	($dm^3 . mole^{-1} . S^{-1}$)
k_t	Termination rate constant.	
k_v	$[36 \pi/(1 - \phi_w)^2 a_s^3 \rho_p^2]^{1/3}$	
l	Optical path length.	(cm)
M	Partition coefficient.	
M_m	Micelle agregation number.	(-)
M_o	Initial monomer concentration.	(moles . dm^{-3})
M_p	Monomer concentration at reaction site.	(moles . dm^{-3})
M_{pc}	Concentration of monomer in polymer particles at saturation.	(moles . dm^{-3})
M.P.C.	Maximum polymer content.	(% . wt)
M.S.C.	Maximum solids content.	(% . wt)
M_w	Molecular weight of monomer.	
N	Impeller speed.	(r.p.m.)
n	Particle number concentration.	(cm^{-3})
N_A	Avagadro's number.	(molecules . $mole^{-1}$)
N_d	Number of droplets per unit volume of aqueous phase.	(cm^{-3})
n_i	Number of droplets of diameter d_i.	
N_p	Number of particles per unit volume of aqueous phase.	(cm^{-3})
p	Power dissipated by impeller.	(W)

Q	Average number of radicales per particle.	(-)
r	Particle radius.	(m)
S	Total soap concentration per unit volume of aqueous phase.	($g \cdot dm^{-3}$)
S_d	Soap adsorbed onto the droplet surface in a unit volume of aqueous phase.	($g \cdot dm^{-3}$)
S_m	Soap forming micelles in a unit volume of aqueous phase.	($g \cdot dm^{-3}$)
S_p	Soap adsorbed onto the particle surface in a unit volume of aqueous phase.	($g \cdot dm^{-3}$)
t	Time.	(h)
t_I	Time at end of stage I of reaction.	(h)
t_{II}	Time at end of stage II of reaction.	(h)
Vd	Volume of droplets per unit volume of aqueous phase.	($cm^3 \cdot cm^{-3}$)
Vp	Volume of particles per unit volume of aqueous phase.	($cm^3 \cdot cm^{-3}$)
V_T	Volume of vessel.	(dm^{-3})
W_A	Weight of water in sample for particle size analysis.	(g)
W_p	Weight of polymer in sample for particle size analysis.	(g)
W_S	Weight of styrene in sample for particle size analysis.	(g)
W_{SA}	Weight of styrene in aqueous phase of sample for particle size analysis.	(g)
W_{SP}	Weight of styrene in the polymer particles in sample for particle size analysis.	(g)

W_{SS}	Weight of styrene dissolved in a unit volume of polymer particle at saturation.	($g \cdot cm^{-3}$)
α	$2\pi r/\lambda$	(-)
ε	Local energy dissipation per unit mass of fluid.	($W \cdot kg^{-1}$)
$\bar{\varepsilon}$	Mean energy dissipation per unit mass of fluid.	($W \cdot kg^{-1}$)
λ	Wavelength of light.	(nm)
η	Microscale of turbulence.	(nm)
ϕ_m	Volume fraction of monomer in emulsion.	(-)
ϕ_v	Volume fraction of monomer in polymer particles.	(-)
ϕ_w	Weight fraction of monomer in polymer particles.	(-)
σ_i	Interfacial tension.	($mN \cdot m^{-1}$)
μ	Dynamic viscosity.	$N \cdot S \cdot m^{-2}$
μ	Volumetric growth rate of a polymer particle.	($cm^3 \cdot S^{-1} \cdot$ particle)
ν	Kinematic viscosity.	($m^2\ S^{-1}$)
ρ'	Rate of radical generation per unit volume of water.	($S^{-1} \cdot cm^{-3}$)
ρ_m	Density of monomer.	($g \cdot cm^{-3}$)
ρ_p	Density of polymer.	($g \cdot cm^{-3}$)
ρ_{swp}	Density of monomer swollen polymer.	($g \cdot cm^{-3}$)

Dimensionless groups

$$Fr = \left(\frac{DN^2}{g}\right)$$ Froude group

$$Re = \left(\frac{ND^2\rho}{\mu}\right)$$ Reynolds number

$$Np = \left(\frac{P}{\rho N^3 D^5}\right)$$ Power number

$$\Phi = \left(\frac{Np}{Fr^n}\right)$$ Power function

REFERENCES

1) Blackly, D.,C. "Emulsion Polymerisation, Theory and Practise" Page 3, Applied Science Publishers Ltd. London (1975).

2) Bovey, F.,A.; Kolthoff, I.,M.; Medalia, A.,I. and Mechan, E.,J. "High Polymer Vol. IX "Emulsion Polymerisation" Page 31 John Wiley and Sons (1965).

3) Hohenstein, W.,P. and Mark, H. "Polymerisation of Olefins and Diolefins in Suspension and Emulsion" J.Polym.Sci. 1 127-145 (1946).

4) Harkins, W.,D. "General Theory of Mechanisms of Emulsion Polymerisation" J.Amr.Chem.Soc. 69 1428-1444 (1947).

5) Smith, W.,V. and Ewart. R.,H. "Kinetics of Emulsion Polymerisation" J.Chem.Phys. 16 592-599 (1945)

6) Bovey, F.,A.; Kolthoff, I.,M., Medalia, A.,I. and Mechan, E.,J. "High Polymer Vol. IX Emulsion Polymerisation" Page 22 John Wiley and Sons (1965).

7) Elworthy, P.,H. "The increasingly clever micelle" Pharm.J. 217 566-570 (1976).

8) Min, K.,W. and Ray, W.,E. "On the mathematical modelling of emulsion polymerisation reactors" Reviews in Macromolecular Chemistry 12 177-255 (1975).

9) Roe, C.,P. "Surface chemistry aspects of emulsion polymerisation" Ind.Eng.Chem. 60 20-33 (1968).

10) Goodhall, A.,B.; Wilkinson, M.,C. and Hearn, J. "Mechanism of emulsion polymerisation of styrene in soap free systems" J.Polym. Sci.Poly.Chem.ed. 15 2193-2218 (1977).

11) Gardon, J.,L. "Emulsion Polymerisation I. Recalculation and extension of the Smith-Ewart theory" J.Polym.Sci.PT.A1 6 623-640 (1968).

12) Gardon, J.,L. "Emulsion polymerisation II.Review of experimental data in the context of the revised Smith-Ewart theory" ibid. 643-664.

13) Harada, M.; Nomura, M.; Kojima, H.; Eguchi, W. and Nagata, S. "Rate of emulsion polymerisation of styrene" J.Appl.Polym.Sci. 16 811-833 (1972).

14) Smith, W.,V. "The kinetics of styrene emulsion polymerisation" J.Am.Chem.Soc. 70 3695-3702 (1948).

15) Bovey, F.,A.; Kolthoff, I.,M.; Medalia, A.,I. and Mechan, E.,J. "High Polymers Vol. IX Emulsion Polymerisation" Page 179 John Wiley and Sons (1965).

16) Van der Hoff, B.,M.,E. "On the mechanism of emulsion polymerisation of styrene II. Polymerisation in soap solutions below and above critical micelle concentration and some remarks on the kinetics of emulsion polymerisation" J.Polym.Sci. 44 241-259 (1960).

17) Gardon, J.,L. "Emulsion polymerisation III. Theoretical prediction of the effects of slow termination rates within latex particles" J.Polym.Sci. PT.A1 6 665-685 (1968).

18) Hansen, F.,K.; Ofstad, E.,B. and Ugelstad, J. "Theory and Practise of emulsion technology" Ed. Smith A.,L. Page 13-21 Academic Press London (1976).

19) Ugelstad, J.; Hansen, F.,K. and Lange, S. "Emulsion polymerisation of styrene with sodium hexadecyl sulphate/hexadecanol mixtures as emulsifiers. Initiation in Monomer drops" Makromol Chem. 175 No. 2 507-521 (1974).

20) Bovey, F.,A.; Kolthoff, I.,M.; Medalia, A.,I. and Mechan, E.J. "High Polymers Vol. IX Emulsion Polymerisation" Page 290-296 John Wiley and Sons (1965).

21) Brown, W.,E. "Procedure for preparing latex samples for electron micrgraphs" J.App.Phys. 18 273 (1947).

22) Bateman, J.,B; Weneck, E.,J. and Eshter, D.,C. "Determination of particle size and concentration from spectrophotometric transmission" J.Colloid.Sci. 14 308-329 (1959).

23) Barnes, M.,D. and La Mer, V.,K. "Monodispersed hydrophobic colloidal dispersions and light scattering properties II. Total scattering from transmittance as a basis for the calculation of particle size and concentration" J.Colloid.Sci. 1 79-91 (1947).

24) Shunmukham, S.,R.; Hallenbeck, V.,L. and Guile, R.,L. "Emulsion polymerisation of styrene II. Effect of agitation". J.Polym.Sci. 6 691-698 (1951).

25) Schoot, C.,J.; Bakker, J. and Klaassens, K.,H. J.Polym.Sci. 7 657 (1951).

26) Evans, C.,P.; May, M.,P.; Marker, L.; Murray, R.,W; and Sweeting,O.,J. "Mechanism of emulsion polymerisation of vinylidine chloride III. Effects of stirring rate on kinetics" J.Appl.Polym.Sci. 5 39-47 (1961).

27) Omi, S.; Shiraishi, Y.; Sato, H. and Kubota, H. "The effect of agitation on the rate of emulsion polymerisation of styrene" J.Chem.Eng. Japan 2 64-70 (1969).

28) Nomura, M.; Harada, M.; Eguchi, W. and Nagata, S. "Effect of stirring on emulsion polymerisation of styrene" J.Appl.Polym.Sci. 16 835-847 (1972).

29) Tsukiyama, S. and Takamura, A. "Effect of the size of tank and impeller to the liquid-liquid dispersion on mechanical agitation" Chem.Pharm.Bull. 23 616-622 (1975).

30) Weinstein, B. and Treybal, R.,E. "Liquid-liquid contacting in unbaffled agitated vessels" A.I.Ch.E.J. 19 304-312 (1973).

31) Kolmogoroff, A.,N. Acad.Sci. URSS 30 301-305 (1941).

32) Kolmogoroff, A.,N. ibid. 32 16-18 (1941).

33) Batchelor, G.,K. "Kolmogoroffs theory of local isotropic turbulence" Proc.Camb.Phil.Soc. 43 533-559 (1947).

34) Shinnar, R. and Church, J.,M. "Statistical theories of turbulence in predicting particle size in agitated dispersions" Ind.Eng.Chem. 52 253-256 (1960).

35) Hinze, J.,O. "Fundamentals of the hydrodynamic mechanism of splitting in dispersion processes" A.I.Ch.E.J. 1 289 (1955).

36) Shinnar, R. "On the behaviour of liquid dispersions in mixing vessels" J.Fluid Mech. 10 259-275 (1961).

37) Coulaloglou, C.,A. and Taularides, L.,L. "Drop size distributions and coalescence frequencies of liquid-liquid dispersions in flow vessels". A.I.Ch.E.J. 22 289-297 (1976).

38) Cutter, L.,A. "Flow and turbulence in a stirred tank" A.I.Ch.E.J. 12 35-45 (1966).

39) Metzner, A.,B. and Taylor, J.,S. "Flow patterns in agitated vessels" A.I.Ch.E.J. 6 109-114 (1960).

40) Rushton, J.,H. "The use of pilot plant mixing data" Chem.Eng.Progr. 47 485-488 (1951).

41) Vermeulen, T.; Williams, G.,M. and Langlois, G.,E. "Interfacial area in liquid-liquid and gas-liquid agitation". Chem.Eng.Progr. 51 85F-94F (1955).

42) Roger, W.,A.; Trice, V.,G. and Rushton, J.,H. "Effect of fluid motion on interfacial area of dispersions", Chem.Eng.Progr. 52 515-520 (1956).

43) Laity, D.,S. and Treybal, R.,E. "Dynamics of liquid-liquid agitation in the absence of an air liquid interface" A.I.Ch.E.J. 3 176-180 (1957).

44) Rowe, E.,L. "The effect of emulsifier concentration and type on the particle size distribution of emulsions" J.Pharm.Sci. 54 260-264 (1965).

45) Brown, D.,E. and Pitt, K. "Drop break-up in a stirred liquid-liquid contactor" Chemca '70 Melbourn Sydney 83-98 (1970).

46) Chen, H.,T. and Middleman, S. "Drop size distributions in agitated liquid-liquid systems" A.I.Ch.E.J. 13 989-995 (1967).

47) Calderbank, P.,H. "Physical rate processes in industrial fermentation Part I. The interfacial area in gas-liquid contacting with mechanical agitation" Trans.Inst.Chem.Engr. 36 443-463 (1958).

48) Cauchy, A. C.R.Acad.Sci.Paris 13 1060 (1841).

49) Mlynek, Y. and Resnick, W. "Drop sizes in agitated liquid-liquid systems" A.I.Ch.E.J. 18 122-127 (1972).

50) Sprow, F.,B. "Drop size distribution in strongly coalescing agitated liquid-liquid systems" A.I.Ch.E.J. 13 995-995 (1967).

51) Hixson, A.,W. and Baum, S.,J. "Power requirements of turbine agitators" Ind.Eng.Chem. 34 194-208 (1942).

52) Rushton, J.,H.; Costich, E.,W. and Everett, M.,J. "Power Characteristics of mixing impellers" Chem.Eng.Prog. 46 395-404, 467-476 (1950).

53) Park, J.,Y. and Blair, L.,M. "The effect of coalescence on drop size distribution in an agitated liquid-liquid dispersion" Chem. Eng.Sci. 30 1057-1064 (1975).

54) Wilson, M.,P. and Merry, A.,J. "Emulsion polymerisation - problems in modelling and scale-up". I.ChemE. Symposium series No. 52

55) Nagata, S. "Mixing" Page 444-446 JohnWiley and Sons (1975).

56) Walker, J.,L. "Scale-up for SBR and nitrile latices" Rubber Industry 69-73 (1974).

57) Nagata, S. "Mixing" John Wiley and Sons (1975).

58) Scully, D.,B. "Scale-up in suspension polymerisation" J.App.Polym. Sci. 20 2299-2203 (1976).

59) Irani, R.,R. and Callis, C.,F. "Particle size: Measurement Interpretation and Application" Page 99 John Wiley and Sons (1963).

60) ibid. Page 134.

61) Allen, T. "Particle size measurement" 2nd edition, Chapman and Hall, London (1974).